Zebrafish as a model for regenerative studies - from dissecting the effects of cryoinjury to the cellular diversity of heart repair

Inaugural-Dissertation

to obtain the academic degree

Doctor rerum naturalium (Dr. rer. nat.)

submitted to the Department of Biology, Chemistry, Pharmacy

of Freie Universität Berlin

by

Sara Lelek-Greskovic

Berlin, 2022

I completed my doctorate studies from August 2018 to July 2022 under the supervision of Dr. Daniela Panáková and Prof. Dr. Simone Spuler at the Max Delbrück Center for Molecular Medicine in the Helmholtz Association, Berlin-Buch.

Primary Reviewer:	Dr. Daniela Panáková
Secondary Reviewer:	Prof. Dr. Simone Spuler
Date of Disputation:	02.08.2022

Statement of Authorship

Herewith I certify that I have prepared and written my thesis independently and that I have not used any sources and aids other than those indicated by me. I confirm that this work has not been submitted to any other university or examining body for a qualification of any kind.

Table of Contents

1. Summary

Zebrafish is an excellent model to study cardiac regeneration. This freshwater teleost fish can fully regenerate its heart after myocardial infarction (MI) within one to two months after the injury. Cryoinjury method is widely used to induce the injury in the zebrafish heart since it mimics the closest human MI.

Current protocols used in adult zebrafish, including cryoinjury method, do not involve any analgesia treatment and they do not take into consideration the adverse effects that can arise out of these techniques. Nociception is a basic response of the animal to harmful external or internal stimuli, which is essential for survival and adaptability to the environment. Fish can react to noxious stimuli, similarly to the higher vertebrates, which should be considered in the design of scientific experiments. In this study, I showed that cryoinjury is a noxious stimulus for zebrafish by assessing zebrafish behaviour Moreover, I showed that morphine treatment for 6h after the cryoinjury procedure, but not lidocaine, significantly improved zebrafish behaviour using swimming speed as a readout. Importantly, the morphine treatment for 6h did not impair regeneration based on histological analysis and did not affect regenerative capacities based on the transcriptome analysis using scRNA-seq and qPCR. We advise using morphine as the analgesic of choice to reduce adverse effects associated with the cryoinjury procedure in adult zebrafish.

The refinement of the current cryoinjury protocol allowed us to investigate cellular drivers of zebrafish heart repair with consideration of zebrafish welfare with the improved protocol. Several pro-regenerative factors and signalling pathways are known to be crucial for zebrafish heart regeneration, however, the cellular composition of the zebrafish regenerating heart and cell types involved in the process are still incompletely understood. To systematically investigate the diversity of activated cell states in the zebrafish regenerating heart, we used single cell transcriptomics and spatiotemporal analysis. We showed that upon the injury there is a significant induction of several cell states with fibroblasts characteristics and we confirmed the pro-regenerative role of transient *col12a1a*-expressing fibroblasts. To determine the origin of transient cell states, we performed Cre/lox lineage tracing, in order to understand the events leading to heart regeneration. We reported that transient fibroblasts can originate both from epicardium and endocardium, similarly to the development process. We also identified Wnt signalling as a key regulator of endocardial-derived fibroblasts, which was at least partially mediated by the impaired revascularization during regeneration. In this study, we identified the great diversity of specialized activated fibroblasts as one of the factors crucial for zebrafish heart regeneration, which gives us new possibilities towards improving mammalian heart repair.

2. Zusammenfassung

Der Zebrafisch ist ein hervorragendes Modell für die Untersuchung der Herzregeneration. Dieser Süßwasser-Teleostfisch kann sein Herz nach einem Myokardinfarkt (MI) innerhalb von ein bis zwei Monaten nach der Verletzung vollständig regenerieren. Die Kryo-Verletzungsmethode wird weitgehend verwendet, um die Schädigung des Zebrafischherzens herbeizuführen, da sie dem menschlichen MI am nächsten kommt.

Die derzeit bei erwachsenen Zebrafischen angewandten Protokolle, einschließlich der Kryoverletzungsmethode, beinhalten keine Analgetikabehandlung und berücksichtigen nicht die nachteiligen Auswirkungen, die sich aus diesen Techniken ergeben können. Die Nozizeption ist eine grundlegende Reaktion des Tieres auf schädliche äußere oder innere Reize, die für das Überleben und die Anpassungsfähigkeit an die Umwelt unverzichtbar ist. Fische können ähnlich wie die höheren Wirbeltiere auf schädliche Reize reagieren, was bei der Planung wissenschaftlicher Experimente berücksichtigt werden sollte. In dieser Studie konnte ich zeigen, dass die Kryoverletzung ein schädlicher Reiz für Zebrafische ist, indem ich das Verhalten der Zebrafische untersuchte. Darüber hinaus konnte ich zeigen, dass die Behandlung mit Morphin für 6 Stunden nach der Kryoverletzung, nicht aber mit Lidocain, das Verhalten der Zebrafische deutlich verbesserte, wobei die Schwimmgeschwindigkeit als Indikator verwendet wurde. Wichtig ist, dass die 6-stündige Morphin-Behandlung die Regeneration laut histologischer Analyse nicht beeinträchtigte und sich auch nicht auf die Regenerationsfähigkeit auswirkte, wie die Transkriptomanalyse mittels scRNA-seq und qPCR ergab. Wir empfehlen die Verwendung von Morphin als geeignetes Analgetikum, um unerwünschte Wirkungen im Zusammenhang mit der Kryoverletzung bei erwachsenen Zebrafischen zu vermindern.

Die Verfeinerung des aktuellen Kryo-Verletzungsprotokolls ermöglichte es uns, die zellulären Triebkräfte der Zebrafisch-Herzreparatur unter Berücksichtigung des Wohlergehens der Zebrafische mit dem verbesserten Protokoll zu untersuchen. Es ist bekannt, dass mehrere regenerationsfördernde Faktoren und Signalwege für die Regeneration des Zebrafischherzens von entscheidender Bedeutung sind. Die zelluläre Zusammensetzung des Zebrafischherzens und die Zelltypen, die an diesem Prozess beteiligt sind, sind jedoch noch unvollständig bekannt. Um die Vielfalt der aktivierten Zellzustände im regenerierenden Zebrafischherz systematisch zu untersuchen, haben wir Einzelzelltranskriptomik und raum-zeitliche Analysen eingesetzt. Wir konnten zeigen, dass nach der Verletzung eine signifikante Induktion verschiedener Zellzustände mit Fibroblastencharakteristika stattfindet, und wir bestätigten die pro-regenerative Rolle von transienten *col12a1a*-exprimierenden Fibroblasten. Wir identifizierten ebenso den Wnt-Signalweg als einen wichtigen Regulator der aus dem Endokard stammenden Fibroblasten, der zumindest teilweise durch die beeinträchtigte Revaskularisierung während der Regeneration vermittelt wurde. In dieser Studie haben wir die große Vielfalt an spezialisierten aktivierten Fibroblasten als einen der entscheidenden Faktoren für die Regeneration des Zebrafischherzens identifiziert, was uns neue Möglichkeiten zur Verbesserung der Herzreparatur bei Säugetieren eröffnet.

3. Introduction

3.1 Cardiovascular diseases and pathological remodelling in ischemic injury.

CVDs are a group of medical conditions that involve heart and blood vessels including coronary heart disease, cerebrovascular disease, rheumatic heart disease and other disorders. Cardiovascular diseases (CVDs) are a leading cause of death worldwide. Each year 17.9 million people die from cardiovascular diseases, which accounts for 32% of all global deaths. This number is expected to grow to 23.6 million per year by 2030. Over 80% CVD deaths are caused by either heart attack or a stroke (WHO, 2017).

Heart attack (myocardial infarction, MI) is an outcome of either acute or chronic myocardial ischemia. Myocardial ischemia is characterized by a lack of oxygen supply leading to cellular damage usually caused by a blood clot in the coronary artery (Meier and Oyman, 2009). The main problem after MI is pathological remodelling. After MI, up to 1 billion cardiac cells die in the result of ischemia (Talman and Ruskoaho, 2016). The adult mammalian heart has a very little regenerative capacity and the lost cells are replaced by a fibrotic scar. The pathological remodelling after fibrotic tissue formation involves changes in the left ventricular wall such as thickening (hypertrophy) and stiffening (fibrosis). (Talman and Ruskoaho, 2016). The outcomes of the pathological remodelling of a mammalian heart are changes in the heart size, mass, geometry, shape and function, which might eventually lead to heart failure (Azevedo *et al.*, 2016).

There are several risk factors, which can contribute to coronary heart disease such as hypertension, dyslipidemia, glucose imbalance, smoking and family history of coronary heart disease. In the observational study reported by Canto *et. al.*, 85.6% out of 2160671 patients presented with initial myocardial infarction had at least 1 out of 5 coronary disease risk factors (Canto *et al.*, 2015).

Nowadays, the guidelines for CVDs care contain reperfusion-based treatments and drug therapies mostly reducing the symptoms generated by cardiac functional deterioration.

Unfortunately, therapeutic concepts targeting favourable reparative myocardial remodelling remain challenging taking into consideration limited regenerative capacity of the mammalian heart.

Worth mentioning is also prevention and enhancement of cardiovascular health, which includes exercise and physical activity. Exercise was found to be an economical and effective cardioprotective factor in many studies (Xiao and Rosenzweig, 2021), so it is crucial to combine therapeutic approach with prevention in order to ensure the best outcome for patients.

Since CVDs are currently an urgent and worldwide problem, more studies and scientific effort are necessary to ensure improvement of the current treatments.

3.2 Zebrafish as a model for regeneration studies

The vertebrate tissues are able to replace their cells, which no longer perform their function, with new ones to maintain tissue homeostasis. However, this continuous tissue turnover is not possible for all cells and tissues. It is known that skin keratinocytes and gut enterocytes are able to renew (Young et al., 2014), but cells such as cardiomyocytes and neurons are infrequently replaced during adulthood (Lázár et al., 2017; Ernst et al. 2014). Another reason for cell renewal is tissue regeneration due to injury. Some of the organs are able to replace injured tissue in the regeneration process where new cells proliferate and/or differentiate into the same cell type and regain original function. In some cases, as in the case of MI, tissue is replaced by fibrotic tissue to overcome the injury. However, this process will not lead to the full recovery and regaining of the function.

The healing process involves distinct phases, which are preserved in most of the tissue injuries (Fig. 1). First, an immune response will take place during which immune cells will clear damaged tissue and will prevent possible infections. Next, an extracellular matrix (ECM) will be deposed, which provides support and structure for the injured tissue. This process can lead to formation of permanent fibrotic scar, which can cause changes in organ morphology and function. As an alternative, the injured area can be replaced by new tissue in a process involving dedifferentiation, proliferation and redifferentiation of existing cells leading to full regeneration. This process can be accompanied by transient fibrosis and scar resolution (Marques et al., 2019).

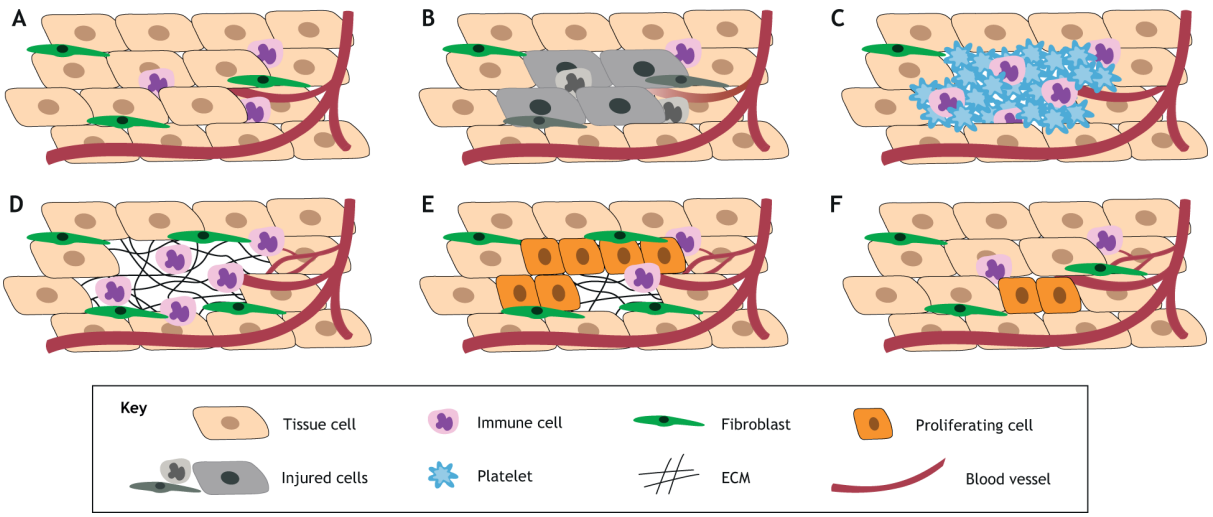

Figure 1: Phases of tissue regeneration. (A) Healthy tissue. (B) Tissue after the injury: injured area is depicted in grey, showing damaged and dead cells. Damaged blood vessels close to the injury area are shown in a light red. (C) Wound closure and immune response: lesion is infiltrated by platelets to stop the bleeding caused by the injury to the blood vessels in the damaged area. Simultaneously, the injury area is also infiltrated by immune cells. (D) Clearing of debris and deposition of extracellular matrix (ECM): the immune cells are responsible for cleaning the dead tissue and tissue debris caused by the injury. Fibroblasts proliferate and produce ECM that fill the cleared injury area. Generation of new blood vessels occurs (thinner red lines). (E) Resolution of ECM and cell proliferation: the ECM starts to be removed as the injury is repopulated by new cells by cell proliferation. (F) Regeneration: new cells repopulated the injury area and the tissue recovered to its homeostatic status. Cells enter cell cycle arrest and very few proliferating cells can be detected. Adapted from Marques et al. 2019.

Vertebrates differ in their regenerative capacity. Mammals exhibit very limited tissue regeneration, which is restricted either to the organ (liver and skin) or time of regeneration. For instance in mice, hearts are able to regenerate after injury only until postnatal day 7 as reported by Porrello et al. in 2011. Other vertebrates such as axolotls are able to regenerate multiple organs for example heart (Cano-Martínez et al., 2010) or the limbs (Simon and Tanaka 2012). Another example of a vertebrate able to regenerate most of its body parts is zebrafish (*Danio rerio*).

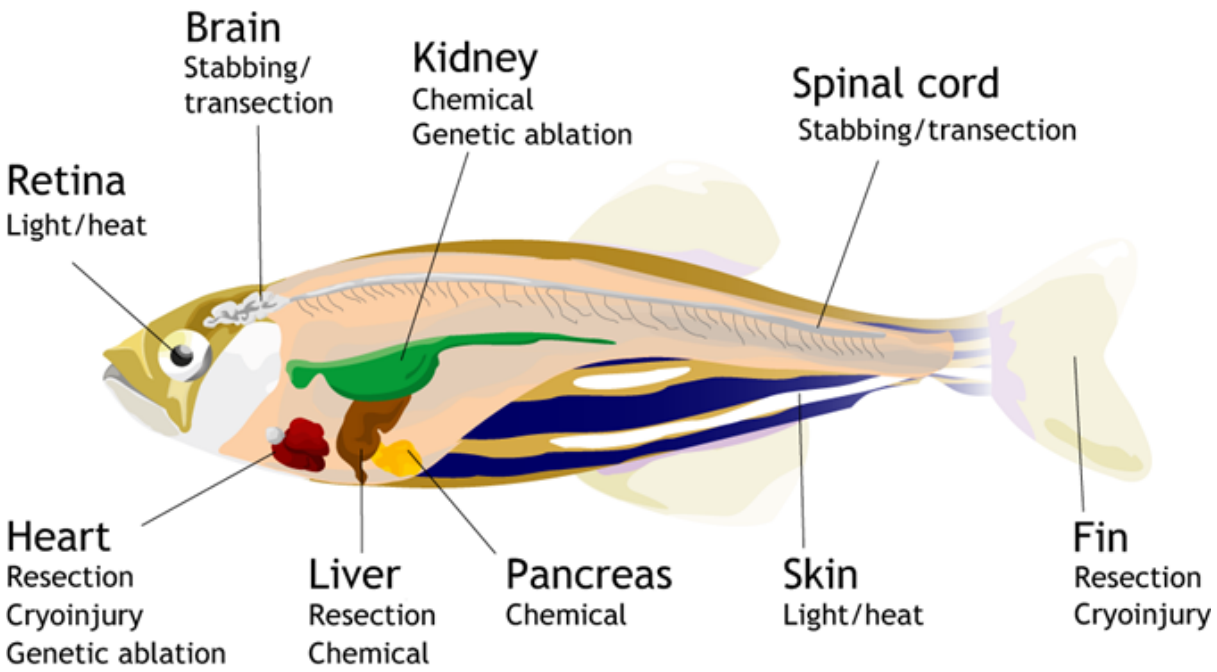

Figure 2: Organ regeneration in zebrafish. Zebrafish organs and tissues, which can be fully regenerated after the injury. From Marques et al. 2019.

Zebrafish is a 2-5 cm long freshwater teleost, which can regenerate most of its body parts (Fig. 2). Zebrafish was first established as a model to study development (Furutani-Seik et al., 1996; Singer, 1981) and it gained recognition as a model for regeneration shortly afterwards. Zebrafish is known to be used in regeneration research by studying multiple organs and tissues such as spinal cord (Becker et al., 1997), brain (Brand, 2011), retina (Vihtelic and Hyde, 2000), hair cells (Harris et al., 2003), heart (Poss et al., 2002), caudal fin (White et al., 1994), kidney (Reimschuesse, 2001) and liver (Burkhardt-Holm et al., 1999). One of the main advantages of using zebrafish in regeneration studies is the great availability of genetic tools such as transgenesis and genome-editing to generate loss-of-function mutations. Other advantages of the zebrafish model are accessibility for live imaging, drug screenings and platforms to share the obtained knowledge such as Zebrafish Information Network (www.zfin.org) or International Zebrafish Society (Marques et al. 2019).

3.2.1 Zebrafish heart regeneration

The zebrafish heart consists of a bulbus arteriosus, one atrium and one ventricle with ~1 mm3 volume (Fig 3.). Although mammalian hearts are bigger, the histological composition of zebrafish hearts is comparable to other vertebrates (González-Rosa et al., 2017). The ventricle of zebrafish comprises a trabecular myocardium and is surrounded by a thin layer of compact myocardium (Bise et al., 2020) (Fig. 3).

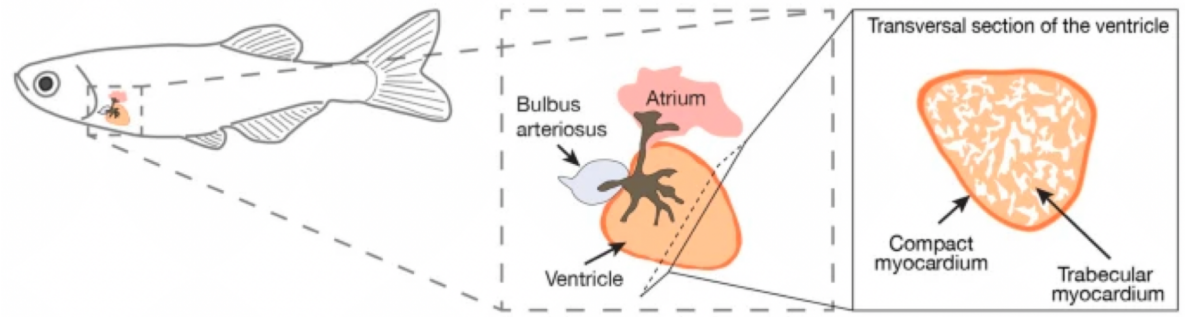

Figure 3: Zebrafish heart schematics. Illustration of zebrafish heart anatomy and histology. Adapted from Bise et al. 2020.

It was reported for the first time by Poss et al. (Poss et al., 2002) that zebrafish hearts can fully regenerate after amputation of up to 20% of the ventricle. After the resection, the heart bleeds profusely for a few seconds, however, the rapid formation of fibrin clot ensures the end of bleeding. Within a few weeks fibrin clot is replaced by new muscle and fish regains a completely functioning heart between 30 to 60 days after the amputation (Poss et al., 2002; González-Rosa et al., 2017).

Zebrafish heart regeneration is a very dynamic process and can be divided into three overlapping phases (inflammatory, reparative and regenerative) (Fig. 4), which were first described using histology (Chablais and Jaźwińska, 2012). The first phase after the injury is the inflammatory phase (day 0 to 4 after the injury). During this acute stage, massive death of cardiomyocytes starts an inflammatory response to clear the damaged tissue and prevent infection. In the course of the reparative phase (4 to 7 days after injury), non-myocytes including fibroblasts become activated and start accumulating at the injury site. These cells are responsible for the extracellular matrix (ECM) deposition and for the formation of the fibrotic scar.

In the last regenerative stage, the complete tissue and functional recovery takes place (day 7 to 60 after the injury). Fibrotic scar fully resolves as the cardiomyocytes first dedifferentiate, and then proliferate and redifferentiate to replace the scar with the healthy myocardium (Chablais and Jaźwińska, 2012).

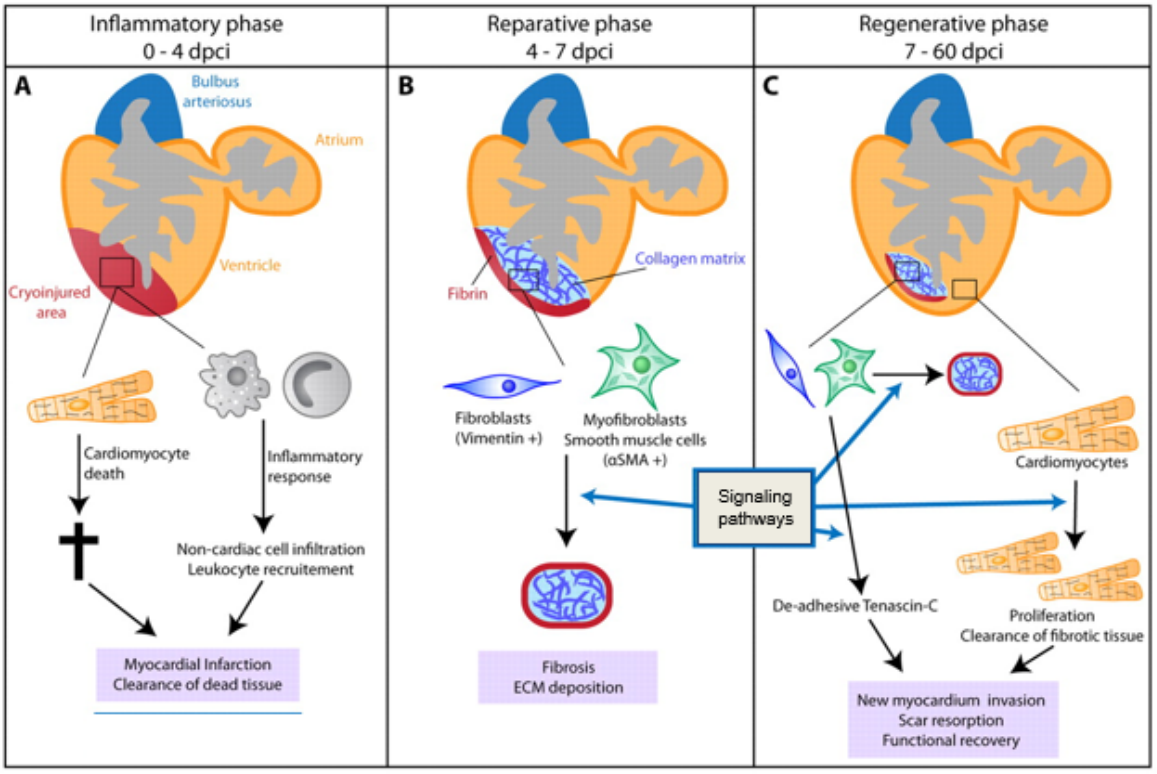

Figure 4: Phases of zebrafish heart regeneration. (A) Inflammatory phase with immune cell infiltration, (B) reparative phase with activation of fibroblasts and deposition of fibrotic scar, (C) regenerative phase with fully regenerated zebrafish heart due to cardiomyocytes dedifferentiation and fibrotic scar resolution. Adapted from Chablais et al. 2012.

3.2.2 Methods for heart injury in zebrafish

Currently, there are four different methods to injure zebrafish heart, namely amputation, cryoinjury, cardiomyocyte genetic ablation, hypoxia/reoxygenation and the healing process is strongly dictated by them.

Amputation was used for over a decade as an exclusive method to study cardiac regeneration in zebrafish. In this injury method, the part of the ventricle is resected and the outcome is a complete regrowth of the missing tissue (Poss et al., 2002).

One of the characteristics of this type of injury is a lack of fibrotic scar due to a complete removal of the apex; i.e. injury does not cause the cell death, and thus the cell debris clearance is not required (González-Rosa et al., 2017).

The first available alternative method to the amputation was to induce cell death using cryoinjury (Chablais et al., 2011; González-Rosa et al., 2011; Schnabel et al., 2011). In this injury type, a metal probe is precooled in the liquid nitrogen and applied to the ventricular surface to freeze part of the apex. The process of fast freezing and thawing of the cells induces necrosis followed by apoptosis of cells surrounding the necrotic area. This method mimics the closest human MI. Here, also the result is a rapid cardiomyocyte enucleation, while the sarcomeric apparatus stays relatively intact for a few days (González-Rosa et al., 2011). Using the cryoinjury method, all cell types are affected, including the epicardium, the endocardium and the coronary vasculature. In general, the cryoinjury compared to the amputation induces a more severe response. The phases of cardiac regeneration in case of the cryoinjury are shown in Fig 4. Fibrosis is transient and fibrotic tissue will be completely resolved and replaced with cardiomyocytes up to 60 days after the injury. Cryoinjured ventricles show signs of cardiac remodelling such as enlargement of the ventricle, thickening of the ventricular wall, and more rounded shape of the ventricle (González-Rosa et al., 2017). The heart function such as pumping is fully recovered after cryoinjury procedure, however, it was reported that regenerated myocardial regions display abnormalities in the wall movement (González-Rosa et al., 2014); Hein et al., 2015).

The third method to induce cardiac injury is the genetic ablation of cardiomyocytes. This strategy relies on the inducible genetic systems to ablate cardiomyocytes using the expression of toxins or enzymes that catalyse the production of cytotoxic metabolites (Curado et al., 2009; Wang et al., 2011). The first approach is based on the method first introduced to the zebrafish field by Curado et al. to genetically ablate cells where bacterial nitroreductase (NTR) is used to catalyse the reduction of the innocuous prodrug metronidazole (MTZ), producing a cytotoxic product that induces cell death (Curado et al. 2009). Another approach was developed by Wang et al. to conditionally express the diphtheria toxin chain A (DTA) specifically in cardiomyocytes. Upon induction of DTA expression, over 60% of cardiomyocytes are ablated. The massive loss of cardiomyocytes is tolerated by zebrafish, however, these animals show signs of heart failure.

Moreover, complete regeneration was reported by day 30, most probably due to no effect of the epicardium and the endocardium by DTA expression.

Due to the nature of the injury, this method resembles more advanced cardiomyopathy than MI, but the studies of cardiomyocyte dedifferentiation and proliferation can be performed using this model (Wang et al., 2011; González-Rosa et al., 2017).

The last model to study zebrafish cardiac regeneration is hypoxia/reoxygenation. This model was introduced by Parente et al. with the aim to better reflect human MI. In this strategy, the whole animal is exposed to hypoxia, thus the lesions and inflammation are not only limited to the heart, but also to other organs. Although hypoxia/reoxygenation induces apoptosis and proliferation in the heart, it does not greatly impact histological changes. After the procedure, fish exhibit a transient reduction in cardiac function, but it is not clear whether cell death or myocardial stunning (term used to describe a state of mechanical cardiac dysfunction that can occur in a position of myocardium without necrosis (Bolli, 1992)) are the reason. (Parente et al., 2013; González-Rosa et al., 2017).

All the aforementioned methods have their advantages and disadvantages, however, currently the method which is closest to human MI, is cryoinjury method (Fig. 5)

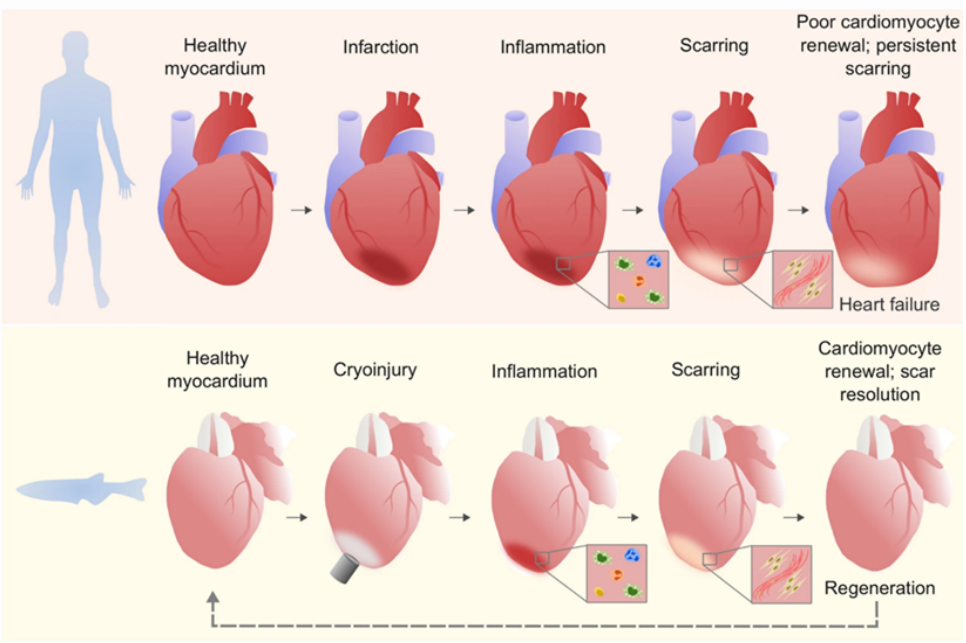

Figure 5: Human and zebrafish heart repair. Phases of repair after MI in humans and cryoinjury in zebrafish. Initial phases of inflammation and scarring are comparable between human and zebrafish. In the final stages, the human heart shows persistent scarring and poor renewal of CMs. Zebrafish heart (after cryoinjury) exhibits transient scarring and proliferation of CMs leading to full regeneration of the cardiac tissue. Adapted from Ryan et al. 2020.

It is known that after cardiac injury such as MI in humans and cryoinjury in zebrafish, the initial phases of repair are comparable (Fig. 5). Both human and zebrafish heart repair involves initial inflammatory phase followed by reparative phase and fibrotic scar deposition. In humans, the collagenous matrix develops to form a permanent fibrotic scar that will never resolve leading to pathological remodelling and potentially to heart failure. In zebrafish, collagenous scar forms and peaks at day 7 after the injury. Importantly, it will be completely resolved at the end of the regeneration process. Additionally, the human heart shows poor cardiomyocyte renewal, which is different for zebrafish where cardiomyocytes will dedifferentiate and proliferate to exchange dead tissue (Ryan et al., 2020).
All these attributes demonstrate the great value of using zebrafish as a model to understand limiting factors of mammalian heart regeneration.

3.3 The welfare of zebrafish

As a general principle, all scientists using experimental animals should follow the 3Rs principle (replace, reduce, refine) in order to ensure animal's welfare. The ability to assess welfare of the experimental animals is a critical element that can inform scientists of the severity of the procedures. Welfare can be defined as the state of the individual as its attempts to cope with the environment (Deakin et al., 2019). It is difficult to accurately determine an animal's welfare state, since it can not communicate its sensation after the procedure. Instead, scientists have to assess animal well-being based on indirect measures such as changes in behaviour and physiology (Deakin et al., 2019).
As described in 3.2.2, cryoinjury method is widely used in zebrafish regeneration studies. The procedure is invasive and requires a surgery on the heart with the outcome of damaging 20% of the zebrafish ventricle (Chablais et al., 2011). Currently, this procedure is performed only under anaesthesia (typically tricaine methanesulfonate is used), and no analgesia is used after the procedure. There is an urgent need for the refinement of current cryoinjury protocols to ensure that welfare of the animals is considered.

3.3.1 Pain perception and welfare evaluation in fish

The concept of pain perception in fish is still under debate (Key, 2015; Rose et al., 2015; Sneddon, 2015; Ohnesorge et al., 2021), however, the mounting body of evidence indicates that fish can perceive and react to noxious stimuli (Pavlidis et al., 2015; Cachat et al., 2010; Deakin et al., 2019). Noxious stimulus is an external or internal physical change that induces afferent input in the nervous system, with or without sensory experience or a behavioural response (Cervero and Merskey, 1996). Noxious stimulus can actually or potentially cause damage to the tissue and is responsible to cause pain, but it does not have to (Cervero and Merskey, 1996). It was also reported that fish including teleost fulfil all the criteria for animal pain perception such as having nociceptors, altered behaviour, responses reduced by analgesic drugs (Sneddon, 2015).

There are several ways to assess the welfare of fish. Fish including zebrafish have an ability to react to harmful stimuli often by changing their behaviour. This may be manifested by the significant reduction in normal activity including the reduction in swimming speed, increased bottom time tank occupancy or the increase in the ventilation rate (Sneddon, 2015; Reilly et al., 2008; Deakin et al., 2019; Nobre Bezerra et al., 2021; Taylor et al., 2017). Another way to investigate discomfort and stress in zebrafish is assessing the changes in the physiology. It was reported that zebrafish in response to acute stress show rapid increase in whole-body cortisol, as well as differences in the expression of several genes involved in the Hypothalamic–Pituitary–Interrenal (HPI) axis (Pavlidis et al., 2015).

3.3.2 Analgesia in zebrafish

Currently, only few systematic studies describing the effect of analgesics and their efficacy to relieve discomfort and pain in fish are available (Chatigny et al., 2018; Martins et al., 2016; Martins et al. 2019; Ohnesorge et al. 2021).

The main focus of the studies on pain-relieving drugs used in fish have been local anaesthetics, NSAID (non-steroidal anti-inflammatory drugs), and opioids in two fish species: rainbow trout *(Oncorhynchus mykiss)* and zebrafish *(Danio rerio).* Local anaesthetics interrupt nerve conduction by inhibiting the influx of sodium ions through voltage-gated sodium channels in axonal membranes (Schwarz et al., 1977).

Fish are routinely treated with the local anaesthetic tricaine methanesulfonate (or MS222) to induce general anaesthesia (Martins et al., 2016; Martins et al., 2019; Sneddon, 2012; Stevens, 2017). Although tricaine methanesulfonate was reported to reversibly block motor as well as sensory neurons, it was not determined how effectively it might be inhibiting the nociceptive transmission, particularly after surgical procedures. (Ramlochansingh et al., 2014; Lelek et al., 2020).

Lidocaine is another local anaesthetic tested as a systemic pain reliever in humans, rodents and fish (Chatigny et al., 2018; Schwarz et al., 1977; Stevens, 2017; Mao and Chen, 2000; Rácz et al., 2021). Lidocaine was also recently reported to be used for adult zebrafish euthanasia either in overdose 1g/L or in combination with another drug such as 5 mg/L of propofol, 150mg/L lidocaine (Jorge et al., 2021; von Krogh et al., 2021). Although lidocaine may improve stress- and/or pain-related behavioural changes in zebrafish adult fish after certain procedures (Deakin et al., 2019), its negative effects have been also reported in embryos as well as in adult fish. Lidocaine was shown to aggravate the symptoms associated with the bipolar disorder in embryos (Ellis and Soanes, 2012), and to cause more sedative-like effects in embryos (Lopez-Luna et al., 2017) as well as in adults through inhibition of acetylcholine activity (Abreu et al., 2018; Lelek et al., 2020).

Opioids are the most common analgesics used in fish. Opioids interact with and block μ, δ, or κ opioid receptors in the central nervous system, where they mimic the actions of endogenous opioid peptides (Chatigny et al., 2018). Opioids increase K^+ efflux or reduce Ca^{2+} influx, leading to impeding nociceptive neurotransmitter release. Morphine similar to lidocaine treatment seems to also induce contrasting effects (Lopez-Luna et al., 2017). On one hand, a low dosage of morphine led to hyperactivity in zebrafish embryos, while a high dosage reduced their swimming activity. However, in adult fish, morphine alleviated noxious effects across a range of concentrations, from as low as 1 mg/mL to high doses of 48 mg/mL (Deakin et al., 2019; Bezerra, 2021). In addition, morphine treatment may cause a number of potential side effects, including those associated with the cardiovascular and respiratory system (Chatigny et al., 2018; Lelek et al., 2020). Another concern in using morphine is its effect on regeneration, especially inflammation and immune response.

Morphine treatment was reported to be both proinflammatory (Wang et al., 2012; Loram et al., 2012; Feehan and Zadina, 2019) and antiinflammatory (Plytycz and Natorska, 2002; Charbaji et al., 2013; Fecho et al., 2007). Also, the aspect of the effect of morphine on regeneration is not clear, depending on the study the outcome can differ. It was shown by Barlass et al. in the mouse model, that morphine treatment increases the severity and prevents pancreatic regeneration by delaying macrophage infiltration and sonic Hedgehog pathway activation and expression of *pdx-1* and *ptf-1* (Barlass et al., 2018). However, it was shown that morphine treatment may improve the wound healing (Charbaji et al., 2013).

Importantly, for the pain treatment of acute myocardial infarction (AMI) in patients, morphine has been used since the 1960s (Thomas et al., 1965; Timmis et al., 1980; Parodi, 2016). The current guidelines from American College of Cardiology/American Heart Association (O'gara et al., 2013) and European Society of Cardiology (Van de Werf et al., 2008) for management of ST segment elevation myocardial infarction (STEMI) recommends that in the absence of a history of hypersensitivity, IV morphine sulphate is the preferred drug for pain relief. STEMI is a clinical syndrome described as symptoms of myocardial ischemia in association with persistent electrocardiographic ST elevation and subsequent release of biomarkers of myocardial necrosis (O'gara et al., 2013; AbuRuz 2016). Thus it is important to remember that pain is associated with higher mortality after AMI and morphine is a medication of choice to relieve the pain in this situation (AbuRuz, 2016).

The variability in the effects of the analgesics seems to be context dependent and could be caused by a difference in dose used or in the time period of the treatment creating a great demand for systematic testing of analgesics after noxious stimuli (Lelek et al., 2020).

3.4 The cellular composition of the heart

Human heart is composed of four morphologically and functionally distinct chambers, which need an exact orchestration of all heterogeneous cell types to ensure proper function. The proper function of the hearts is determined by a spatiotemporal pattern of gene regulation and cell-cell communication, which when altered by disease state, leads to significant phenotypic changes and imbalanced intercellular communication (Schoger et al., 2022).

The cellular composition of the heart was an important topic long before the single-cell RNA-sequencing (scRNA-seq) method was available. The first studies were carried out as early as the first half of the 20th century (Roberts and Wearn, 1941), using stereological and morphometric methods in adult rats. The main focus of this and many following studies were cardiomyocytes and their number in the heart (Zak, 1973; Anversa et al., 1980; Nag, 1980; Banerjee et al., 2007) using either mouse or rat as a model. The techniques used in these studies comprised stereological and morphometric methods, as well as, flow cytometry and immunohistochemistry and the results showed that cardiomyocytes cover 75% of total volume of the heart and they represent ca. 30% of total cardiac cells (Roberts and Wearn, 1941; Anversa et al., 1980; Nag, 1980; Banerjee et al., 2007; Walsh et al., 2010; Bergmann et al., 2015).

Interestingly, at that point not many studies focused on non-myocytes and the available results were not conclusive. In order to further characterize cells in the cardiac tissue, various cell lineage tracing techniques combined with other methods were used such as use of carbon particles to auto-radiographic tattooing and advanced fluorescent dyes or replication-defective retroviruses (Castro-Quezada et al., 1972; Thompson et al.,1987; Patwardhan et al., 2000; Mikawa and Fischman, 1992). Another advancement in the studying of the cellular landscape of the heart was a use of transgenic mouse lines tagging cardiovascular cells (Fadel et al.,1999; Didié et al., 2013). The key improvements for the genetic lineage tracing were use of Cre/LoxP (Soriano, 1999) or Tet OFF (Harding et al., 1998) genetic tools. Genetic lineage tracing enabled us to investigate cell heart composition, structure and response to pathological stimuli and the methods are still significant in nowadays research (Moses et al., 2001; Engleka et al., 2012; Ruiz-Villalba et al., 2015). Many studies using genetic tools in combination with other techniques such as FACS sorting were able to determine the origin of cardiac cells (Red-Horse et al., 2010; Zeisberg et al., 2007) and also characterize and quantify cardiac cell composition as cardiomyocytes representing 35% of total cardiac cells, endothelial cells 60% and <20% fibroblasts (Pinto et al., 2016; Marín-Sedeño et al., 2021).

One of the greatest recent advances to understand the composition of healthy and diseased hearts was development of several-single cell sequencing platforms to profile transcriptomes of all cells. The use of this method for heart studies stayed challenging for some time due to large and elongated cardiomyocytes.
Recently, many improvements were applied in order to sequence cardiomyocytes including single nuclei sequencing (SNS) (Schoger et al., 2022). Within the last few years many single-cell sequencing studies were carried out on mammalian hearts including human and mice, as well as, other vertebrates like zebrafish, in both healthy and diseased states showing the importance of the transcriptome in all the cell types (Gladka, 2021; Ma et al., 2021).

3.4.1 Single cell transcriptome of the healthy heart

A number of studies provided comprehensive transcriptomic data that can be used to get an insight into the healthy human heart. The study by Litvinuková et al. (Litviňuková et al., 2020) reported an extensive transcriptome data on six distinct heart regions of the healthy adult heart using SNS of cardiomyocytes and single-cell sequencing of enriched fibroblasts, stromal, vascular and immune cell populations. One of the crucial findings in this study was the heterogeneity among the atrial and ventricular compartments. This research shows not only chamber-specific and lineage-specific profiles, but also sex differences of the healthy heart (Litviňuková et al., 2020; Schoger et al., 2021). An important aspect in the composition of healthy heart are mentioned sex differences. Unfortunately, sex differences in the heart composition are relatively understudied. However, in a recent review by Walker et al. data sets from Litvinuková et al. were used to analyze and underline the differences between male and female hearts (Fig. 6) It was shown that even in healthy heart cell distribution differs notably between sexes including a significantly higher percentage of ventricular CMs in female hearts (Walker et al., 2021). The differences in cardiac cell distribution might have an important impact in the clinical studies and disease prevalence for example in ischemia, heart failure or myocardial infarction (Walker et al., 2021).

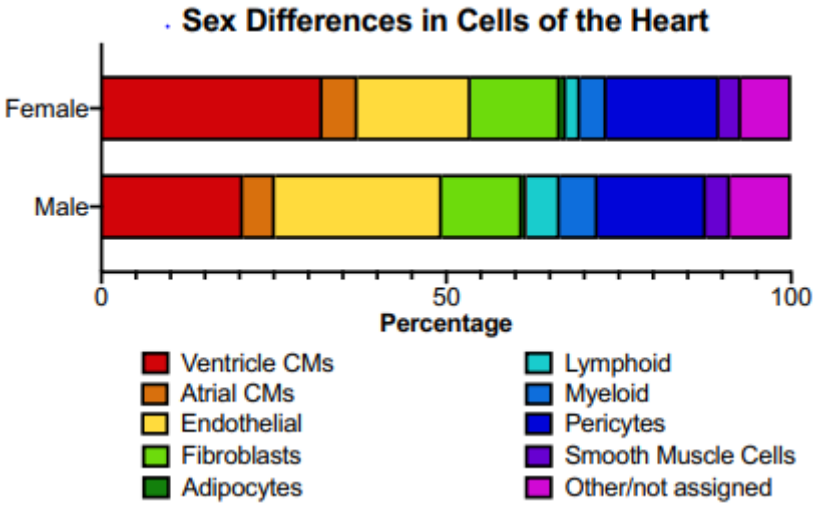

Figure 6: Sex differences in cells distribution of the human heart. Data based on single cell sequencing datasets from the (Litviňuková et al. 2020). Healthy hearts from seven males and seven females with an age range of 40–75 years and collected from North America and the United Kingdom. Adapted from Walker et al. 2021.

The use of single-cell sequencing method was also applied in zebrafish healthy hearts (Spanjaard et al., 2018; Jiang et al., 2021). These studies provide us with the composition of zebrafish adult hearts and with the confirmation that zebrafish is an excellent model to study cardiac disease since its diversity is comparable to the human heart.

3.4.2 Single cell transcriptome of the diseased heart

Single cell transcriptome of the healthy hearts gave us an insight into the homeostatic state of the heart, however, the use of single-cell sequencing in diseased hearts could be a useful resource to understand the pathological conditions.

Several studies were investigating single-cell sequencing of mammalian diseased hearts, mostly focusing on the MI in murine cardiac tissue (Tombor et al., 2021; Farbehi et al., 2019; Gladka et al., 2018). Single-cell sequencing of the interstitial cell population showed comprehensive dynamics of cardiac stromal, vascular and immune cells of healthy and ischemic hearts. Farbehi et al. also showed a novel fibroblasts population characterised by ant-WNT signalling transcriptome signature (Farbehi et al., 2019).

Another interesting finding was reported by Tombor et al. identifying transient phenotypic change upon ischemic injury in murine hearts. In this model, endothelial cells undergo a transient mesenchymal activation within the first days after myocardial damage, however they did not acquire the mesenchymal fate for a longer time (Taylor et al., 2017).

It was concluded that these findings may indicate that the transient mesenchymal state or endocardial cells may facilitate cell migration and clonal expansion to promote regeneration of vasculature (Taylor et al., 2017; Schoger et al., 2022).

The use of single-cell sequencing in diseased hearts is an extremely important tool to identify potential treatment targets for cardiovascular diseases. By looking at the transcriptome and cellular composition of the diseased hearts it is possible to better understand the mechanism behind the pathological condition and tailor more specific therapies.

3.4.3 Responses of cardiomyocytes in zebrafish heart regeneration

Despite zebrafish being widely used as a model for heart development and regeneration until very recently there were no studies looking at the cellular composition of adult zebrafish heart. The first research focusing on the zebrafish ventricle composition was reported by Patra et al. (Patra et al., 2017).

In this study, authors used tissue specific reporter lines, flow cytometry, EdU incorporation assay and immunohistochemical analysis to characterize zebrafish heart composition with the focus on cardiac endothelial cells (cECs). They were able to show that cardiomyocytes account for 39% of the heart cells and 37% account for cECs. Interestingly, it was shown that the relative surface area of the ventricle covered by ECs is larger in zebrafish than in mouse, which could be crucial for the regenerative response. Overall, cell type composition of zebrafish heart is comparable to the mouse heart, however, differences could be an important hint to understand the variety in regenerative capacities between the organisms (Patra et al., 2017). Several recent scRNA-seq studies have determined cell type diversity in the developing and adult heart in different organisms (Paik et al., 2020).

The single-cell sequencing also became a tool to study the composition of zebrafish heart during the regeneration. This is a very useful approach that could potentially improve our understanding for future therapies.

Cardiomyocytes were for a long time in the spotlight of many regeneration studies (Zheng et al., 2021). The majority of adult zebrafish cardiomyocytes are mononucleated diploid cells and retain robust proliferative capacities (Poss et al., 2002; González-Rosa et al., 2018).

Regenerated cardiomyocytes derive from the dedifferentiation and proliferation of pre-existing cardiomyocytes (Kikuchi et al., 2010). On the contrary, human adult cardiomyocytes are mostly polyploid and the level of proliferation in homeostasis or after injury is very low (Bergmann et al., 2009; Zheng et al., 2021). In the regenerating zebrafish heart, a single-cell analysis of sorted cardiomyocytes revealed distinct cluster of border zone cardiomyocytes, that resemble embryonic, proliferating cardiomyocytes and are transcriptionally different from distant non-proliferating cardiomyocytes. Furthermore, Honkoop et al. showed metabolic changes taking place in the border zone cardiomyocytes (in direct contact to the wound) during the regeneration process crucial for the proliferation (Honkoop et al., 2019). In another study by Koth et al. using scRNA-seq identified a transcription factor Runx1, which is expressed by border-zone cardiomyocytes and has a role in reducing cardiomyocyte proliferation and survival following the heart injury (Koth et al., 2020).

3.4.4 Response of non-cardiomyocytes in zebrafish heart regeneration

The non-myocyte cell types including fibroblasts and immune cells in zebrafish heart regeneration have only in recent years attracted much needed attention, and the field is still developing both in tools and knowledge. The analysis of non-cardiomyocytes revealed considerable diversity of cell states among endothelial cells, macrophages and fibroblasts after ventricular amputation in zebrafish (Ma et al., 2021). Also the diversity of epicardial cells was discerned using scRNA-seq (Cao et al., 2016).

Macrophages were reported to have a crucial role in cardiac regeneration as their depletion leads to delayed regeneration (de Preux Charles et al., 2016).

Additionally, using RNA-seq macrophages were found to directly contribute collagen to scar formation during zebrafish heart regeneration and mouse heart repair (Simões et al., 2020). Ma et al. reports diversity of macrophages with five transcriptionally distinct clusters and their dynamics depending on the time after the ventricular resection (Ma et al., 2021).

Epicardial cells after undergoing epithelial to mesenchymal transition (EMT) can form epicardium-derived cells (EPDCs) that migrate into the myocardium through sub-epicardial space (Streef and Smits, 2021). EPDCs can differentiate into various cell types such as fibroblasts, pericytes and smooth muscle cells (Streef and Smits, 2021). One of the recent findings described Cxcl12b-Cxcr4a signalling in epicardium being required to guide coronary revascularization (Marín-Juez et al., 2019). The diversity of epicardial cells using scRNA-seq was first reported by Cao et al. Using *tcf-21* positive sorted cells as a marker of epicardial cells, the authors found that there are at least three epicardial cell subsets after ventricular amputation. All three epicardial clusters express *caveolin 1*, which is reportedly required for cardiomyocyte proliferation and zebrafish heart regeneration (Cao et al., 2016). Another recent study with the use of scRNA-seq method reports that epicardium-derived *pdgfrb*+ cells regulate coronary vessel development and revascularization during cardiac regeneration (Kapuria et al., 2022).

Endocardial cells are a thin layer of specialized endothelial cells covering the luminal surface of the heart that provides a physiological barrier for blood circulation (Zhang et al., 2021). After cardiac injury in the adult mice, endocardial cells were shown to minimally contribute to coronary endothelial cells. However, they serve as an important signalling center for heart regeneration. The activated signalling pathways include: Notch, BMP, Retinoic Acid and IGF signalling (Zhang et al., 2021). In scRNA-seq study, endocardial cells show heterogeneity with a unique activated subtype and their involvement in endocardial angiogenesis (Ma et al., 2021).

3.4.5 Response of fibroblasts in zebrafish heart regeneration

The last non-myocyte cell type, which is crucial for regeneration are fibroblasts. Fibroblasts and fibrosis are central to post-infarction repair and remodelling. Currently, there is a lack of specific and comprehensive markers for fibroblasts, which makes the analysis difficult. Cardiac fibroblasts account for 11% in the healthy mouse heart (Pinto et al., 2016). In response to injury, fibroblasts populations expand and constitute the majority of the cells in the infarcted area during MI repair phase (Talman and Ruskoaho, 2016).

Resident cardiac fibroblasts have distinct developmental origins, which might be important for their function in cardiac disease based on mouse studies (Skelly et al., 2018; Moore-Morris et al., 2014; Ali et al., 2014; Han and Zhou, 2022).

Currently, to understand fibroblasts origin, genetic lineage-tracing based on Cre-loxP recombination system is used to permanently trace labelled cells and follow their fate overtime during tissue repair and regeneration. Using the mouse lines that express Cre, including *Tbx18Cre, Gata5Cre, Sema3DCre, Wt1Cre*, but also inducible CreER, such as $Wt1^{CreERT2}$, $Tcf21^{mCrem}$, and $Tbx18^{CreERT2}$, it was found that the majority of cardiac fibroblasts are originating from epicardium through EMT (Han and Zhou, 2022). Furthermore, scRNA-seq data showed that epicardium-derived fibroblasts express genes associated with cell migration and cell metabolism and comprise the majority of cardiac fibroblasts (Skelly et al., 2018).

As the second source to epicardium, few studies reported that fibroblasts derive also from embryonic endothelium. Using *Tie2Cre* for endothelial genetic lineage-tracing, it was shown that around 10% of fibroblasts in the left ventricle and around 65% of fibroblasts in the interventricular septum derive from endothelial progenitor cells (Ali et al., 2014; Moore-Morris et al., 2014). Moreover, scRNA-seq data endothelium-derived fibroblasts express genes associated with valve leaflets and account for a small population of cardiac fibroblasts in mice (Skelly et al., 2018).

Additionally to epicardial and endocardial origin, it was reported that a small population of cardiac fibroblasts derive from neural crest cells using mouse as a model (Jiang et al., 2000; Han and Zhou, 2022).

Upon the MI, fibroblasts can show differentiated states in order to respond to the wound healing and to be able to participate in the scar formation.

In a recent mouse study, four different states of fibroblasts were identified specifically, resident fibroblasts, active fibroblasts, myofibroblasts, and matrifibrocytes based on genetic lineage tracing (Fu et al., 2018). It was shown that proliferation and activation of fibroblasts are the highest within 2-4 days after MI. Activated fibroblasts become myofibroblasts that express smooth muscle α-actin (αSMA), contain extensive endoplasmic reticulum, and secrete ECM proteins to fill the injury area within 3-7 days after the injury. Moreover, both activated fibroblasts and myofibroblasts reach the proliferation potential by 7 days after MI. Until day 7-10 after MI, the myofibroblasts enter an alternative differentiated state without proliferation ability and no αSMA expression, while the scar completely matures accompanied by ECM deposition. The final stage of fibroblasts are matrifibrocytes, with weak contractile and secretory abilities but still expressing increased ECM genes (Fu et al., 2018; Han and Zhou, 2022).

Recent scRNA-seq studies reported diversity and heterogeneity of cardiac fibroblasts in both humans and mice (Yamada and Nomura, 2020). The heterogeneity of cardiac fibroblasts was also shown by Ren et al. in a pressure overload-induced cardiac injury model and grouped them in six clusters (Ren et al., 2020). In another scRNA-seq research using uninjured hearts, a new fibroblast cluster was identified that could express both fibroblast and immune cell markers (Skelly et al., 2018). McLellan et al. reported two new fibroblast subpopulations, fibroblast-*Clip* and fibroblast-*Thbs4*, after tissue stress and accelerated fibrosis (McLellan et al., 2020).

Very recently, zebrafish became a model to investigate the fibroblasts diversity using scRNA-seq. The most comprehensive study until now was done by Ma et al. using ventricular resection injury method. It was reported that four distinct clusters of fibroblasts are present in zebrafish hearts and their amount changes in the course of the regeneration process. These four subpopulations were expressing unique ECM gene signatures from distinct anatomical sites that confer differential roles in maintaining cardiac structural integrity and modulating cell behaviours.

Additionally, a unique subcluster was identified that exhibited a transformed phenotype likely induced by its interactions with macrophages (Ma et al., 2021).

In the scRNA-seq data reported by de Bakker et al., FACS sorted cells for epicardial origin showed as well the heterogeneity of zebrafish cardiac fibroblasts with ten transcriptionally distinct clusters after cryoinjury.

They further classified the clusters into four groups, belonging to: remote epicardium, injury epicardium, epicardial-derived fibroblasts and epicardial derived-pericytes. In this study de Bakker et al. identified transcriptional factor Prrx1b to be activated in epicardial-derived cells where it restricts TGFβ ligand expression and collagen production and its role in fibrosis and regeneration of zebrafish injured heart (de Bakker et al., 2021).

In recent years technological advances such as scRNAseq and lineage tracing enabled us to discover the great heterogeneity and diversity of non-myocyte cell types. It is necessary to conduct more basic research to understand non-myocytes biology in depth and discover more therapeutic targets for potential treatments.

3.5 Signalling pathways in zebrafish heart regeneration

Many signalling pathways known to be crucial for development are also involved in organ regeneration. Currently, the most common tool to study the signalling pathways of interest is generating a transgenic line overexpressing a core gene of a particular pathway in a temporal or tissue specific manner. Additionally, generation of a mutant line of a gene involved in a certain pathway is a widely used approach (Marques et al., 2019). Another strategy could be pharmacological treatments with known inhibitors and agonists of pathways of interest (Taylor et al., 2010; Zhao et al., 2019). Many pathways have been identified to play a role during zebrafish heart regeneration (González-Rosa et al., 2017).

Retinoic acid (RA) signalling was found to stimulate cardiomyocyte proliferation, likely in paracrine manner (Kikuchi et al., 2011). The fibroblasts growth factor (FGF) and bone morphogenic protein (BMP) signalling are known to be crucial for regeneration. FGF was shown to promote EMT and revascularization thus facilitating muscle regeneration (Lepilina et al., 2006). Wu et al. reported that BMP pathway is required for cardiomyocyte dedifferentiation and proliferation (Wu et al., 2016).

PDGF signalling was shown to be important for stimulation of epicardial proliferation and EMT. Also, it was reported that it is significant for revascularization and cardiomyocyte proliferation (Kim et al., 2010; Lien et al., 2006).

TGFβ signalling has a role in ECM production and cardiomyocyte proliferation (Chablais and Jaźwińska, 2012; Choi et al., 2013). Martin-Juez et al. reported that VEGF is required for early revascularization of the injured area and later supports cardiomyocyte proliferation (Marín-Juez et al., 2016). Insulin-like growth factor (IGF) stimulates cardiomyocyte proliferation (Choi et al., 2013). Hedgehog signalling (Hh) is crucial for epicardial proliferation, directional migration and cardiomyocyte proliferation (Choi et al., 2013). The correct balance of Notch signalling is important for cardiomyocyte proliferation, endocardial maturation, restricting inflammation at the wound edge and both overexpression and inhibition impair heart regeneration (Raya et al., 2003; Zhao et al., 2019; Münch et al., 2017). Nrg1 signalling was found to be required and sufficient for cardiomyocyte proliferation and triggering of regenerative program in the absence of the injury (Gemberling et al., 2015). Cxcl12-Cxcr4 pathway is involved in the integration of cardiomyocytes in the injured area and revascularization (Itou et al., 2012; Marín-Juez et al., 2019).

Jak/stat signalling was reported to be required for cardiomyocyte proliferation (Fang et al., 2013). Karra et al. showed that NF-κB signalling is required for epicardial regeneration, cardiomyocyte proliferation and dedifferantation (Karra et al., 2015). Hippo-Yap/TAZ pathway, which is known to be involved in the control of cell cycle was shown to be required for scar formation during zebrafish heart regeneration (Flinn et al., 2019). There are also several additional factors playing a role in zebrafish heart regeneration such as miRNAs (Yin et al., 2012), inflammation (Huang et al., 2013), hypoxia (Jopling et al., 2012) or matrix metalloproteinases (MMPs) (Gamba et al., 2017; González-Rosa et al., 2017; Marques et al., 2019).

3.5.1 Wnt/β-catenin signalling pathway

One of the most universally required pathways in tissue regeneration in various animals is Wnt signalling (Slack, 2017). Wnt signalling is known to have a crucial role in cell fate determination, cell migration, cell polarity, neural patterning, and organogenesis during embryonic development (Komiya and Habas, 2008). Wnt proteins are a large family of glycoproteins.

There are three branches of Wnt signalling pathway downstream of Fz receptor, namely canonical Wnt/β-catenin signalling and noncanonical Wnt signalling, which can be further divided into Planar Cell Polarity (PCP) and Wnt/Ca2+ pathways (Komiya and Habas, 2008).

The canonical Wnt/tβ-catenin signalling is known to play a role both in cardiac development and cardiac regeneration (Gesser and Kuhl, 2010; Zhao et al., 2019; Duan et al., 2012). The pathway is well established and it takes its name from the downstream effector molecule β-catenin (Fig.7). If the pathway is inactive, β-catenin is phosphorylated by the destruction complex including kinases casein kinase-1 (CK1) glycogen synthase kinase-3 (GSK3)-β, axin and adenomatous polyposis coli (APC) and degraded by the ubiquitin-proteasome pathway in the cytoplasm. In the active state, if Wnt ligand is present, Frizzled (Fz) receptor and Low-density lipoprotein receptor-related proteins 5/6 (Lrp5/6) co-receptor are becoming activated and Lrp5/6 becomes phosphorylated by (GSK3)-β and CK1. The phosphorylation of Lrp5/6 recruits Dvl and Axin to the receptor complex resulting in inhibition of the destruction complex. In consequence β-catenin is stabilized in the cytoplasm and can be translocated to the nucleus by the complex including Fam53b/Smp.

This regulates target gene expression with the Tcf/Lef transcription factors (Fig. 7). Many modulators including the inhibitors sFrps and Wif are known to tightly regulate the signalling cascade (Blankesteijn, 2020; Ozhan and Weidinger, 2015; Komiya and Habas, 2008).

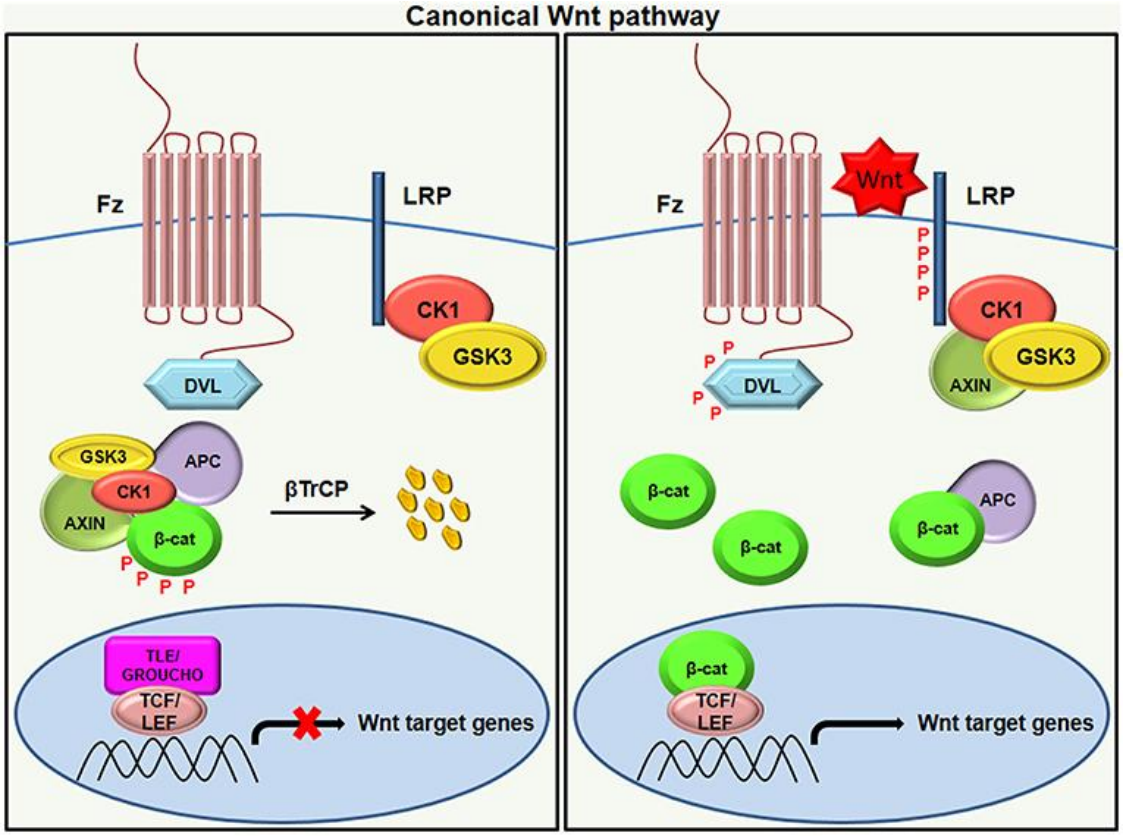

Figure 7: Wnt/β-catenin signalling pathway. In the absence of active Wnt ligands, β-catenin is phosphorylated by the destruction complex (Gsk3, Ck1, Axin, and Apc) and degraded by the ubiquitin-proteasome pathway. Active Wnt ligands interact with the Fz receptors and the Lrp5/6 coreceptor. Phosphorylation of Lrp5/6 by Gsk3 and Ck1 recruits Dvl and Axin to the receptor complex and consequently inhibits the destruction complex. Next, β-catenin phosphorylation is inhibited and β-catenin is stablilized in the cytoplasm. β-catenin is then translocated into the nucleus, by a complex including Fam53b/Smp, and regulates target gene expression with the Tcf/Lef transcription factors. Many modulators including the inhibitors sFrps and Wif are known to tightly regulate the signalling cascade. Adapted from Patel et al. 2019.

3.5.2 Wnt signalling in zebrafish heart regeneration

Many signalling pathways, which play a crucial role in organ development were shown to be also critical for organ regeneration (Stabler and Morrisey, 2018; Nejak-Bowen and Singh Monga, 2015; Gao et al., 2021; Zhou et al., 2016).

Wnt/β-catenin signalling with its known role in cardiac development also got necessary attention in the field of regeneration. Many studies reported that Wnt components are upregulated in response to injury in the mouse heart (Aisagbonhi et al., 2011; Duan et al., 2012; Barandon et al., 2003).

In the mammalian hearts after MI, Wnt signalling was reported to play a role in inflammation, fibrosis, angiogenesis and also that Wnt inhibitors are a class of potential drugs for treating MI (Fu et al., 2019).

Recently, the role of Wnt/β-catenin signalling in zebrafish heart regeneration became a topic of research. Zhao et al. used a ventricular resection model to show that inhibition of endocardial Notch signalling results in reduction of cardiomyocyte proliferation and stimulates fibrosis. Moreover, it was found that the secreted Wnt antagonists, Wif1 and Notum1b, are significantly downregulated in Notch-inhibited hearts, suggesting that Notch-mediated Wnt pathway suppression is necessary for cardiomyocyte renewal. In this study they reported that hyperactivation of Wnt signalling imapired cardiomyocyte proliferation and inhibited heart regeneration. Furthermore, the Wnt/β-catenin signalling inhibition partially rescued the myocardial proliferation in endocardial-specific Notch-suppressed hearts (Zhao et al., 2019). In another study by Peng et al., using the cardiac amputation method, it was shown that inhibition of injury induced myocardial *wnt2bb* and *jnk1/creb1/c-jun* signalling impeded heart regeneration. In this study, the authors also reported that the antagonism of Wnt canonical and non-canonical pathways are crucial to regulate heart regeneration and that non-canonical Wnt is necessary for cardiomyocyte proliferation (Peng et al., 2020).

Zebrafish embryo is a well established model for various pharmacological screens. Xie et al. used embro-based screen and cardiomyogenic assays to discover small molecule Wnt inhibitors that promote heart regeneration. They identified Cardiomogen 1 and 2 (CDMG1 and CDMG2), to be able to promote myocardial hyperplasia through expansion of the cardiac progenitor cell population. CDMG inhibits Wnt by targeting β-catenin and reducing Tcf/Lef-mediated transcription in cultured cells. CDMG treatment of amputated zebrafish hearts decreases nuclear β-catenin in injured hearts, improves cardiomyocyte proliferation, and promotes wound healing. In this study Wnt/β-catenin inhibition results in improved zebrafish heart regeneration (Xie et al., 2020).

In a study by Peng et al. using ventricular amputation as a model, also showed induction of secreted Wnt inhibitors such as Dickkopf 1 (Dkk1), Dkk3, secreted Frizzled-related protein 1 (sFrp1), and sFrp2, in cardiac tissue close to injury area.

It was reported that inhibition of Wnt by Dkk1 overexpression increased cardiomyocyte proliferation and heart regeneration, although ectopic activation of Wnt 8 signalling dampends cardiomyocytes dedifferentiation and proliferation after the injury. Moreover, it was found that Wnt signalling is decreased upon the injury, however the cytoplasmic β-catenin is increased in sarcomeres of cardiomyocytes in myocardial wound edges. During regeneration, Pak2 kinase (p21-activated kinase) is induced at the injured heart, where it increases β-catenin Ser 675 phosphorylation and stability, enhancing CM dedifferentiation and proliferation. This study demonstrated that Wnt/β-catenin signalling is restricted upon cardiac injury and that there is an interaction between Pak2 and Wnt signalling in order to regulate cardiomyocyte renewal after the heart injury (Peng et al., 2021). In the most recent paper published by Bertozzi et al., data reported is contradictory with the previous studies. Here, the cryoinjury of the zebrafish ventricle was used as a model to induce myocardial damage. In this research both pharmacological and genetic tools were used to disrupt the destruction complex of Wnt/β-catenin signalling and in both cases it was shown that Wnt/β-catenin activity is required for cardiomyocyte proliferation and dedifferentiation, furthermore it was also crucial for the maturation of the scar tissue during cardiac regeneration. Bertozzi at al. discovered that cardiomyocyte-specific conditional inhibition of the Wnt/β-catenin pathway promotes cardiomyocyte proliferation in a cell-autonomous manner (Bertozzi et al., 2022).

The Wnt/β-catenin pathway is certainly crucial for cardiac regeneration, however the contradictory data and the complexity of this signalling requires more studies to fully understand the mechanism and the role of Wnt/β-catenin pathway.

4. Aims

CVDs are a leading cause of death worldwide (WHO). Four out of five deaths related to CVDs are caused by either heart attack or a stroke. Currently, the treatment for CVDs focus mostly on reducing the symptoms caused by cardiac functional deterioration and do not include regenerative therapies due to the inability of the human heart to fully repair.

Zebrafish heart can regenerate completely upon myocardial infarction (MI), regaining the functionality of the cardiac tissue (González-Rosa et al., 2014). Zebrafish heart can be injured using cryoinjury technique as one of the methods damaging 20% of the zebrafish ventricle (Chablais et al., 2011). Currently, this procedure is performed only under anaesthesia (typically tricaine methanesulfonate is used), and no analgesia is used after the cryoinjury. Fish, similarly to higher vertebrates also possess nociceptive machinery and they fulfil all the criteria for animal pain perception (Sneddon, 2015). In order to assess animal welfare indirect measures such as behaviour observation are commonly used (Sneddon, 2015; Reilly et al., 2008; Deakin et al., 2019). The first aim of this study is to determine whether cryoinjury affects zebrafish welfare and in what way it can be efficiently ameliorated. To that end, behavioural tests including swimming speed and tank occupancy up to 48h after the procedure will be analyzed. To assess whether morphine or lidocaine can alleviate distress related to cryoinjury, behavioural tests after the treatments with the analgesics will be used. Furthermore, the study aims to ensure that the regeneration process is not affected by analgesics by looking at different hallmarks of regeneration including histological techniques and gene analysis on the single cell level.

Many pro-regenerative factors and signalling pathways are known to be crucial for zebrafish heart regeneration. Until very recently, however, studies focusing on the cellular composition and the cellular drivers of zebrafish heart regeneration are scarse (González-Rosa et al., 2015; Patra et al., 2017). Hence, the second aim of this study is to systematically identify cell types present in adult zebrafish healthy and cryoinjured heart. The goal is to determine cell types and states, which are crucial for the regeneration process and validate their pro-regenerative role in the zebrafish heart. Additionally, the complex role of Wnt signalling, which was previously reported to be crucial for cardiac regeneration (Bertozzi et al., 2022; Peng et al., 2021) will be further characterized using the power of single cell transcriptomics and functional experiments.

The outcome of this study will improve the welfare of the fish used in the cryoinjury procedure. Moreover, it will uncover novel pro-regenerative factors crucial for zebrafish heart regeneration, with the aim towards improving our understanding of mammalian cardiac repair.

5. Materials and methods

Materials and methods were described in Lelek et al. 2020 and Hu et al. 2022 (Lelek et al., 2020; Hu et al., 2022).

5.1 Materials

5.2.1 Equipment and software

Table 1: Overview of the equipment used.

Equipment	Manufacturer
Centrifuge 5427 R	eppendorf
Centrifuge 5920 R	eppendorf
Hybridization Oven, HB-1000 Hybridizer	UVP
M165 Fluorescent Microscopy	Leica
Zeiss LSM880	Zeiss
Zeiss LSM700	Zeiss
MD G33 Brightfield Microscopy	Leica
Keyence Microscope BZX800	Keyence
NanoDrop ND-1000 Spectrophotometer	peqLAB
ViiA™ 7 Real-Time PCR System	Life Technologies
Microtome	Leica
Cryostat microtome	Leica
Tapestation	Agilent Technologies
Illumina NextSeq 500	Illumina
Illumina NovaSeq 6000	Illumina
HiSeq 2500 platform	Illumina
Steamer	WMH

Table 2: Overview of the software used.

Software	Vendor/URL
ImageJ	https://imagej.nih.gov/ij/
idTracker	http://www.idtracker.es/
Adobe Illustrator 2021 26.2	Adobe Systems, Inc. (San Jose, US)
Adobe Photoshop 2021 22.4.3	Adobe Systems, Inc. (San Jose, US)
A Plasmid Editor (APE) by M. Wayne Davis	http://biologylabs.utah.edu/jorgensen/wayned/ape/
GraphPad Prism 9 for Mac OS X, Version 9.0	GraphPad Software, Inc. (La Jolla, US)
Microsoft® Excel for Mac	Microsoft
ViiA™ 7 RUO software	ThermoFisher Scientific
CellRanger version 3.0.2/4.0.0	10x Genomics
SCTransform	https://genomebiology.biomedcentral.com/articles/10.1186/s13059-019-1874-1
Canonical Correlation Analysis	https://www.cell.com/cell/fulltext/S0092-8674(19)30559-8
Seurat version 3.0/4.0.4	https://satijalab.org/seurat/
Harmony	https://www.nature.com/articles/s41592-019-0619-0
ZEN Blue	Zeiss
In-Fusion Cloning Primer Design Tool	www.takarabio.com

5.1.2 Critical Commercial Assays

Table 3: List of critical commercial assays.

Kits	Source	Cat#
AFOG	Gennova	AP0351
cDNA Reverse Transcription Kit	Applied Biosystems, Life Technologies	4368814
RNAscope Multiplex	Advanced Cell	323110

Fluorescent v2 Kit	Diagnostics	
Gateway® LR Clonase® II Plus Enzyme	ThermoFisher Scientific	12538120
GoTaq Long PCR Mastermix	Promega	M4021
Chromium Single Cell 3' kit	10X Genomics	PN-1000075

5.1.3 Chemicals and Reagents

Unless otherwise stated standard chemicals, enzymes, markers, and oligonucleotides were purchased from Ambion, Applied Biosystems, Biorad, Biozym, Calbiochem, Life Technologies, New England Biolabs, Qiagen, Promega, Roche, Roth, R&D Systems, Sigma-Aldrich, Stratagene, Thermo-Scientific, and VWR.

Table 4: List of essential chemicals and reagents.

Chemical/Reagent	**Source**	**Cat#**
Methyl Blue	Sigma-Aldrich	319112
Orange G	Sigma-Aldrich	861286
HCl	Roth	9277.2
Bouin's Solution	Sigma-Aldrich	HT10132
Phosphomolybdic Acid	Sigma-Aldrich	HT153
Acid Fuchsin	Sigma-Aldrich	F8129
Lidocaine hydrochloride monohydrate	Sigma-Aldrich	L5647
Heparin sodium salt	Sigma-Aldrich	H3393
Collagenase D	Sigma-Aldrich	11088858001
TRIzol LS reagent	ThermoFisher Scientific	10296028
Morphine	Lipomed	
Tricaine	PharmaQ	
TaqMan™ Gene Expression Master Mix	Applied Biosystems	10525395

Dream*Taq* DNA Polymerase (5 U μl^{-1})	ThermoFisher Scientific	EP0701
GlycoBlue™ Coprecipitant (15 mg ml–1)	Invitrogen	AM9515
ProLong™ Gold Antifade Mountant	Invitrogen	P36934
ProLong™ Gold Antifade Mountant with 4’,6-diamidino-2-phenylin dole (DAPI)	Invitrogen	P36935
Liberase enzyme mix	Sigma-Aldrich	5401119001
Hank's Balanced Salt Solution (HBSS)	ThermoFisher Scientific	14025092
Pluronic F-68	ThermoFisher Scientific	24040032
Paraformaldehyde 16%	ThermoFisher Scientific	28908
Tissue-Tek O.C.T Compound	Sakura	12351753
Xylol	Sigma-Aldrich	534056
Entellan mounting medium	Merck	107961
TSA Plus Fluorescein	PerkinElmer	NEL741001KT
TSA Plus Cyanine 3	PerkinElmer	NEL744001KT
TSA Plus Cyanine 5	PerkinElmer	NEL745001KT
Antigen Unmasking Solution	Vector Laboratories, Inc.	H-3300
IWR-1	Sigma-Aldrich	I0161-5MG
Dimethylsulfoxid (DMSO)	Sigma-Aldrich	D8418
Metronidazol	Sigma-Aldrich	M1547
(Z)-4-Hydroxytamoxifen	Sigma-Aldrich	H7904

5.1.4 Buffers and Solutions

Table 5: Overview of buffers and solutions.

Name	Composition
Blocking Solution (BS)	3%BSA, 5% goat serum, 0.2% TritonX100 in PBS
E3 Embryo Medium	5 mM NaCl, 0.17 mM KCl, 0.33 mM CaCl2, 0.33 mM $MgSO_4$; pH 7.4
PBST	1× PBS, 0.1% Triton X-100
AFOG	Methyl Blue, Orange G, Acid Fuchsin in PBS; ph 7.4

5.1.5 Antibodies

5.1.5.1 Primary Antibodies

Table 6: List of primary antibodies.

Primary Antibody	Dilution	Source	Identifier
anti-EGFP	1:500	Sigma-Aldrich	G1544
anti-Mef2C	1:200	Santa Cruz Biotechnology	sc-313
anti-PCNA	1:500	Dako	M0879
anti-PCNA	1:500	Santa Cruz Biotechnology	sc-56
anti-RFP	1:200	Rockland	600-401-379

5.1.5.2 Secondary Antibodies

Table 7: List of secondary antibodies.

Secondary Antibody	Dilution	Source	Identifier
AlexaFluor 488 goat anti-rabbit IgG	1:500	ThermoFisher Scientific	A-11008
AlexaFluor 633 goat anti-mouse IgG	1:500	ThermoFisher Scientific	A-21050
AlexaFluor 488 goat anti-mouse IgG	1:500	ThermoFisher Scientific	A-11029
AlexaFluor 647 goat anti-rabbit IgG	1:500	ThermoFisher Scientific	A-21244

5.1.6 RNAscope probes

Table 8: List of RNAscope probes.

Probe	Source	Cat#
Dr-*col1a1a*; Accession No: NM_199214.1 Target Region :3809 - 5244	Advanced Cell Diagnostics	409499-C2
Dr-*vhmc*; Accession No:NM_001112733.1 Target Region :3796 - 5991	Advanced Cell Diagnostics	496241
Dr-*pcna*; Accession No:NM_131404.2 Target Region :216 - 1165	Advanced Cell Diagnostics	574931-C3
Dr-*col1a1a*; Accession No :NM_199214.1	Advanced Cell Diagnostics	409491
Dr-*col11a1a*; Accession No: XM_005162814.1	Advanced Cell Diagnostics	803311-C3
Dr-*col12a1a*; Accession No: XM_002665259.6	Advanced Cell Diagnostics	556481-C2

Dr-*nppc*; Accession No: NM_001109940.1	Advanced Cell Diagnostics	556501-C3
Dr-*cxcl12a*; Accession No: NM_178307.2	Advanced Cell Diagnostics	406481-C2
Dr-*s100a10a*; Accession No: NM_001005961.2	Advanced Cell Diagnostics	556491-C2
Dr-*itm2cb*; Accession No: NM_199980.1	Advanced Cell Diagnostics	556521-C3
Dr-*ttn.2*; Accession No: XM_021479070	Advanced Cell Diagnostics	810421
Dr-*mpeg1.1*; Accession No: NM_212737.1	Advanced Cell Diagnostics	536171-C3
Dr-*pdgfrb*; Accession No: NM_001190933.1	Advanced Cell Diagnostics	493921-C2
Dr-*angptl7*; Accession No: NM_001006073	Advanced Cell Diagnostics	845191-C3
Dr-*cyp26b1*; Accession No: NM_212666.1	Advanced Cell Diagnostics	571281-C2
Dr-*aldh1a2*; Accession No: NM_131850.1	Advanced Cell Diagnostics	455681-C3
mCherry; Accession No:N/A	Advanced Cell Diagnostics	513201
Dr-*cxcl19*; Accession No: NM_001113651.1	Advanced Cell Diagnostics	803671
Dr-*il4*; Accession No: NM_001170740.1	Advanced Cell Diagnostics	803291

5.1.7 TaqMan Probes for Quantitative PCR (qPCR)

All TaqMan probes are designed to analyze gene expression in *Danio rerio* (Dr). TaqMan probe for *eef1α1l1* was labelled with the covalently bound fluorophore VIC™, all other probes were tagged with the reporter dye FAM (6-carboxyfluorescein). The *eef1α1l1* was used as internal control within the same well as the gene of interest.

Table 9: List of TagMan Probes.

TaqMan Probe	Source	Cat#
gata4; Dr03443262_g1	ThermoFisher Scientific	4331182
postnb ; Dr03438569_m1	ThermoFisher Scientific	4448892
aldh2; Dr03131682_m1	ThermoFisher Scientific	4448892
fn1a; Dr03138345_m1	ThermoFisher Scientific	4448892
col1a1a; Dr03150834_m1	ThermoFisher Scientific	4448892
eef1α1l1; Dr03432748_m1	ThermoFisher Scientific	4448892

5.1.8 Oligonucleotides

Table 10: Overview of oligonucleotides used.

Target gene	Sequence
col12a1a fwd	5’-GAGAGAGAGAAAGCACCATTCTG-3’
col12a1a rev	5’-GTTTACACACACACAGTCAGCAG-3’
Minimal *insulin* promoter fwd	(5’-TTTTACGGTACCGATCTTCAGCCCACAGTCTAG TTTAG-3’
Minimal *insulin* promoter rev	5’-CTTGCTCACCATGATCGAAGCAGAGGCGAGGA ATG-3’
Deletion primers fwd	5’-GGTACCGTAAAACGACGGCCAGTGAATTATC-3’
Deletion primers rev	5’-GATATCATGGTGAGCAAGGGCGAGGAGCTGTT C-3’

5.1.9 Recombinant DNA

Table 11: Overview of the recombinant DNA.

Recombinant DNA	Source	Identifier
pENTR5′	Invitrogen	K59120
pDestTol2 cryaa:YFP	(Mosimann et al., 2015)	N/A
pME-Gal4VP16	Addgene	Tol2kit #387
p3E-polyA	Addgene	Tol2kit #302
pAM57 (pDestTol2 insulin:YFP)	This study	This study
Tg(-4kbcol12a1a:GAL4VP16)	This study	This study

5.1.10 Zebrafish lines

Table 12: List of zebrafish lines used.

Zebrafish Line	Source	ZFIN-ID
Zebrafish: AB	ZIRC	ZDB-GENO-960809-7
Tg(ubi:zebrabowM)	Pan et al.	ZDB-FISH-150901-15349
Tg(myl7:EGFP)	Huang et al.	ZDB-FISH-150901-212
TgBAC[cryaa:EGFP, tcf21:Cre-ERT2]^{pd4}	Kikuchi, K. *et al.*	ZDB-TGCONSTRCT-110818-8
Tg[-3.5ubi-loxP-EGFP-loxP-mCherry] (ubi:Switch)	Mosimann, C. *et al*	ZDB-TGCONSTRCT-110124-1
Tg(fli1:Cre-ERT2)^{cn9}	Sánchez-Iranzo, H. *et al.*	ZDB-TGCONSTRCT-170711-8
Tg(–1.5hsp70l:loxP-STOP-loxP-EGFP, cryaa:Venus)^{zh701}	Felker, A. *et al.*	ZDB-TGCONSTRCT-171031-4
Tg(UAS:NTR-mCherry)	Davison, J. M. *et al.*	ZDB-ALT-070316-1
Tg(-0.8flt1:RFP)^{hu5333}	Bussmann, J. *et al.*	ZDB-TGCONSTRCT-110504-1
Tg(-4kbcol12a1a:GAL4VP16, ins:YFP)	This study	This study

5.2 Methods

5.2.1 Zebrafish Husbandry

Zebrafish were bred, raised, and maintained in accordance with the guidelines of the Max-DelbrückCenterfor Molecular Medicine and the local authority for animal protection (Landesamt für Gesundheit und Soziales,Berlin, Germany) for the use of laboratory animals, and followed the 'Principles of Laboratory Animal Care'(NIH publication no. 86-23, revised 1985) as well as the current version of German Law on the Protection of Animals. Embryos were kept in E3 embryo medium (5 mM NaCl, 0.17 mM KCl, 0.33mM CaCl2, 0.33 mM MgSO4, pH7.4) under standard laboratory conditions at 28.5 °C. Adult zebrafish of random sex, aged between 4 months and a year, and with a length of at least 3 cm were used in all experiments.

5.2.2 Analgesics treatment

Fish were treated with either 3 mg/l of lidocaine hydrochloride monohydrate (Sigma) or 1.5mg/l morphine sulphate pentahydrate (Lipomed) dissolved in system water. The concentration of the analgesics was based on the previously published reports (Schroeder and Sneddon, 2017; Bezerra, 2021; Khor et al., 2011). Fish were held in individual tanks for the duration of treatment, between 2 to 48 hpi, with exchange of the drug dissolved in fresh system water twice a day.

5.2.3 Analysis of zebrafish swimming activity

Fish, wild type *AB* strain, were monitored by recording their swimming activity with a fixed video camera positioned over the tanks for a 3-minute period at the following time points: 1 hour (H) before the treatment, 2, 6, 24 and 48 H after the treatment. Swimming speed was recorded for each fish individually in the fixed set-up. Fish were placed in the enclosed environment to not be disturbed by any movements. All measurements were taken at exactly the same time of the day with the same feeding status. To ensure that fish were familiar with the environment, they were transported always 1h before the recording for acclimatization.

The swimming speed (mm/sec) was scored using the software idTracker, calculating the change in position in two dimensions (Correia et al., 2011; Pérez-Escudero et al., 2014).

5.2.4 Analysis of zebrafish tank occupancy (bottom line)

Tank occupancy was recorded for each fish individually. All measurements were taken at exactly the same time of the day with the same feeding status. To ensure that fish were familiar with the environment, they were transported always one hour before the recording for acclimatization. The videos were recorded with a video camera positioned right in front of the tanks. Fish vertical positions (depth) were measured from videos. 10-12 images were extracted from each ~1-minute video and the vertical position was expressed on a scale going from 0 (bottom of the tank) to 1 (water surface). This process was repeated for all fishes in each group (treated and untreated controls and fish treated with morphine and lidocaine) at the following time points: 1 hour before the injury -1H; 2H, 6H, 24H and 48H after the injury and treatment.

5.2.5 Cryoinjury procedure

Cryoinjury was performed as previously described (Chablais et al., 2011; González-Rosa et al., 2011; Schnabel et al., 2011). First, fish were pre-sedated in water containing 0.03 mg/ml Tricaine (PHARMAQ, pH 7). Concentration was then increased to 0.168 mg/ml for anaesthesia. Fish were placed with the ventral side facing up into a foam holder under a dissecting scope. To access the heart, a small incision was made through the body wall and the pericardium, using microdissection forceps and scissors. Once the pericardial sac was opened, the heart ventricle was exposed by gently compressing the abdomen. Excess water was carefully removed by blotting with tissue paper, not allowing fish skin to dry. Then, a stainless steel cryoprobe precooled in liquid nitrogen was applied to the ventricular wall for 20 seconds. Fish were then placed in a tank of fresh system water with 1.5mg/l morphine sulphate for 6h[11]; for the analysis of scRNA-seq data presented here, we also included two morphine treated and two control hearts from Lelek et al.[11] (~20,000 cells, about 10% of the total dataset).

Reanimation was enhanced by the gill oxygenation where water around gills was aerated by pipetting for a couple of minutes. To investigate the effects of the cryoinjury depth, fish were injured using the same procedure, but the cryoprobe was applied for 5s, 10s, 15s, 20s and 25s, respectively. Used protocols use 20s of cryoprobe application (Chablais et al., 2011; González-Rosa et al., 2011; Schnabel et al., 2011). In all injuries, a timer was used to assure the reproducible timing of the cryoprobe contact with the heart tissue. Hearts were analyzed 3, 7, 15, 30 days post injury.

5.2.6 Histological staining, analysis and imaging

For the analysis of the injury areas, animals were humanely killed at different times post-injury by placing them in ice cold water of 0-4°C (measured with thermometer) for 20 minutes. Hearts were dissected and incubated in 2U/ml heparin and 0.1KCl in PBS for 30min. Cryo samples were fixed in 4% PFA in PBS overnight at 4°C, washed in PBS for 3 x 10 min, and incubated overnight in 30% sucrose in PBS. Samples were then frozen in Tissue-Tek O.C.T Compound (Sakura) on the dry ice. Tissue was cut at 7µm on a cryostat (Leica) using Superfrost slides (ThermoFisher Scientific). Connective tissue was stained using acid fuchsin orange G (AFOG). In brief, slides were dried for 30 min at RT. Next, slides were incubated at Bouin Solution (Sigma-Aldrich) for 2H at 60°C and left for overnight incubation under the hood. Slides were washed for 30 min under running water and incubated for 7min in 1% phosphomolybdic acid (Sigma-Aldrich). Samples were washed for 3min in running ddH_2O and incubated with AFOG solution (self-made, Sigma-Aldrich) for 3min or AFOG solution (Gennova). Slides were washed until clear with running ddH_2O and rehydrated with 70%, 94%, 2x 100% ethanol and 2x 5min xylol (Sigma-Aldrich). Slides were mounted with xylene mounting medium (Merck) and let dry overnight under the hood. For the analysis of injury size, the total ventricular tissue area and injury area (IA) on multiple sections per heart were measured. Imaging was done using a Keyence Microscope BZX800 and analyzed with ImageJ/Fiji.

5.2.7 Preparation of single-cell suspensions

Adult zebrafish (injured or uninjured) were humanely killed by immersion in the ice-cold water, (0-4°C) for 20 minutes. The heart was dissected from the fish and transferred into cold HBSS. The dissection included the atrium, ventricle and bulbus arteriosus, except for samples in which only the atrium or the ventricle was isolated. A needle and a syringe filled with cold HBSS were used to pierce into the lumen of the heart and thoroughly wash away most of the erythrocytes in the tissue. Afterwards, the tissue was opened carefully with forceps, and the heart tissue was incubated at 37°C for 30 min in 500µl HBSS containing Liberase enzyme mix (Sigma-Aldrich, 0.26 U/mL final concentration) and Pluronic F-68 (Thermo Fisher Scientific, 0.1%), while shaking at 750 r.p.m. with intermittent pipette mixing. After most of the tissue was dissociated, the reaction was stopped by adding 500µl cold HBSS supplemented with 1% BSA. The suspension was centrifuged at 250*g* at 4°C and washed two times with 500µl cold HBSS containing 0.05% BSA, then filtered through a cell strainer of 35µm diameter. The quality of the single cell suspension was then confirmed under the microscope, and cells were counted prior to scRNA-seq library preparation.

5.2.8 Single cell RNA-seq

Single cells were captured using the Chromium Single Cell 3' GEX Kit (10X Genomics, Chemistry v2, v3, and v3.1), according to the manufacturer's recommendations. We aimed for 10,000 cells per library whenever possible. After successful quality control by Bioanalyzer or Tapestation (Agilent Technologies), samples were sequenced on the Illumina NextSeq 500, Illumina NovaSeq 6000, or Illumina HiSeq 2500 platform.

5.2.9 Mapping and clustering of single-cell mRNA data

A zebrafish transcriptome was created with Cell Ranger 3.0.2/4.0.4 from GRCz11, release 92. Alignment and transcript counting of libraries was done using Cell Ranger 3.0.2/4.0.4. Library statistics are summarised in Appendix Table 13. The transcriptome data was filtered, clustered, and visualised using Seurat 3.0 or SCTransform (Hafemeister and Satija, 2019), followed by Canonical Correlation

Analysis before clustering using Seurat version 4.0.4 (Stuart et al., 2019). We excluded the cluster of *mpeg1.1* fibroblasts (Fig. 2C,D) from further analysis, since we cannot rule out that the expression of the macrophage marker *mpeg1.1* in this fibroblast cluster is an artefact caused by e.g. fragmentation of macrophages (Millard et al., 2021). Immune cells were subclustered, integrated using harmony (Korsunsky et al., 2019), and reclustered using Seurat version 4.0.4.

5.2.10 Quantitative Real-Time PCR

Zebrafish hearts were isolated, cut into smaller pieces under the microscope and incubated for 30 min in heparin solution (Sigma) followed by incubation for 2 h at 37°C in 0.25 ml collagenase IV (Sigma). 3 hearts per biological replicate were used. RNA from zebrafish hearts was extracted using 0.75 mL TRIzol LS reagent (Invitrogen, Thermo Fisher). RNA was transcribed to cDNA using the High-Capacity cDNA Reverse Transcription Kit (Applied Biosystems, Life Technologies). qRT-PCR was performed using TaqMan probes and solutions (Applied Biosystems). TaqMan probe information is available in Table 9.

5.2.11 RNAscope Multiplex Fluorescent V2-Immunofluorescence *in situ* hybridization method and imaging

The RNAscope assay (ACD) for fluorescent *in situ* hybridization was used to localize different mRNAs expressed by various cell types during heart regeneration. The technique was performed according to the manufacturer's instructions for fixed frozen tissues (323100-USM) or in combination with antibody staining (MK 51-150). 7µm cryo-sections were dried for 30 min at RT before the experiment. Following changes were made: slides were incubated at 99°C for 15 min with an antigen retrieval solution (ACD) using a steamer (WMH). Signal development was done using TSA plus fluorophores (PerkinElmer) fluorescein, Cyanine3 and Cyanine5 in 1:1000 dilution. Probes used are listed in Table 8. Additionally, anti-EGFP (Sigma-Aldrich, Cat#G1544, 1:500) and secondary antibody AlexaFluor 488 goat anti-rabbit IgG (Thermo Scientific, Cat#A-11008, 1:500) were used in the protocol combining immunohistochemistry with *in situ* hybridization.

The fluorescent *in situ* hybridization for the whole mount embryo was performed according to the manufacturer's instructions (MK 50-016). Imaging was done using Zeiss LSM880 confocal microscopy and analysis was performed using ImageJ/Fiji and Photoshop software.

5.2.12 Quantification and statistical analysis

Sample sizes are indicated in each figure legend. For the measurement of the injury areas at least 3 biological replicates were used for each condition and each sample has been measured using multiple sections and the average has been calculated. To ensure normal distribution of the data, D'Agostino-Pearson or Shapiro-Wilk normality tests were used depending on the number of values. For the analysis of qPCR expression data, all CT values were normalized to that of the reference gene in the same well, fold induction (fold change, FC) was calculated using the ΔΔCT method (Livak and Schmittgen 2001) and plotted as log2(FC) with GraphPad Prism 9. Statistical analysis was performed on the ΔCT values comparing the untreated uninjured control group to the injured untreated and the morphine-treated groups using unpaired t-test with Welch's correction, and were considered significant at $p<0.05$. Injury areas were analyzed by the two-way ANOVA with Sidak's multiple comparison and considered significant at $p<0.05$. Swimming speed was analyzed by two-way ANOVA with Sidak's multiple comparison test and considered significant at $p<0.05$. Outliers were identified using ROUT method, Q=1% and removed from the data analysis. Tank occupancy was analyzed using Kruskal-Wallis test or Mann-Whitney t-test for not normally distributed values and ordinary one-way ANOVA for normally distributed values and considered significant at $p<0.05$.

scRNA-seq expression data were analyzed by unpaired student t-test with Welch's correction. Sample collection andgenomics analysis were performed by two independent experimenters.

5.2.13 Microscopy analysis of cardiomyocyte (CM) proliferation

Zebrafish hearts were extracted and fixed in 4% paraformaldehyde in PBS overnight, washed in PBS for 3 x 10 min and incubated overnight in 30% sucrose in PBS. Samples were then frozen in Tissue-Tek O.C.T Compound (Sakura) on dry ice.

Tissue was cut at 7µm on a cryostat (Leica) using Superfrost slides (ThermoFisher Scientific). For immunofluorescence, samples were washed with PBST (1× PBS, 0.1% Triton X-100) before permeabilization with Antigen Unmasking Solution (Vector Laboratories, Inc. (H-3300), 1:100) at 80°C for 20 min. Samples were then washed twice with PBST and incubated in a blocking solution [3%BSA, 5% goat serum, 0.2% TritonX100 in PBS]. Primary antibodies were incubated overnight at 4 °C, followed by two PBST washes and incubation with secondary antibodies for 2 h at RT. Slides were washed again with PBST, and mounted with mounting medium Vectashield with DAPI (Vector Laboratories, Inc.). Primary antibodies used: anti-Mef2C (Santa Cruz Biotechnology, Cat#sc-313, 1:200) and anti-PCNA (Dako, Cat#M0879, 1:500). Secondary antibodies used: AlexaFluor 488 goat anti-rabbit IgG (Thermo Scientific, Cat#A-11008, 1:500) and AlexaFluor 633 goat anti-mouse IgG (Thermo Scientific, Cat#A-21050, 1:500). Confocal images were taken using the LSM880 microscope (Zeiss). The percentage of proliferating CMs was calculated as a ratio of (PCNA+Mef2C)+ particles over the total number Mef2c+ particles in the injured area and in 200 µm of the injury border zone using the ImageJ. Briefly, the total number of CMs was analyzed in the Mef2c+ channel, as a total number of particles that were segmented and counted using the “Particle analyzer” tool after thresholding and applying a despeckling filter. The number of (PCNA+Mef2C)+ particles were analyzed using the “Particle analyzer” tool after merge (green and red LUTs (look-up-tables) channels) and selecting color threshold for yellow. Thresholding was verified visually with the original image. For each biological replicate, 3 non-consecutive midsagittal sections were used.

5.2.14 Microscopy analysis of revascularization

Zebrafish ventricles were extracted and fixed in 4% paraformaldehyde for 1 hour at RT. Ventricles were embedded in OCT (Tissue-Tek) and sectioned (8 µm). For each biological replicate, 3 non-consecutive midsagittal sections were used. Immunostaining was performed as previously described (Marín-Juez et al. 2016). Primary antibodies used: anti-RFP (Rockland, Cat# 600-401-379, 1:200) and anti-PCNA (Santa Cruz Biotechnology, Cat#sc-56, 1:500).

Secondary antibodies used: AlexaFluor 488 goat anti-mouse IgG (H+L) (Thermo Scientific, Cat#A-11029, 1:500) and AlexaFluor 647 goat anti-rabbit IgG (H+L) (Thermo Scientific, Cat#A-21244, 1:500). Confocal images were taken using the LSM700 microscope (Zeiss). The percentage of proliferating cEC ($PCNA^+$) was calculated as a ratio from the total cECs in the injured area and in 200 µm of the injury border zone using the ZEN Blue software. For fluorescence intensity analysis, percentage fluorescence was calculated from whole mount images as a ratio from background fluorescence in the injured area using the Fiji software.

5.2.15 Wnt inhibition

To investigate the role of Wnt signalling in heart regeneration, the Wnt antagonist IWR-1-endo (Sigma-Aldrich) was used (Zhao et al. 2019). IWR-1 was dissolved in DMSO to prepare a 10mM stock solution. Wild-type fish were injected intraperitoneally with 25µl of 10µM IWR-1 in PBS or DMSO (0.1% in PBS)(Kinkel et al. 2010). The injection was performed at 1 dpi and 2 dpi for the 3 dpi analysis, and for later time points, once every two days from 2 dpi until the day of sacrifice.

5.2.16 Cloning and transgenesis of *-4kbcol12a1a*:GAL4VP16

The possible 5‘-upstream promoter region upstream of the predicted transcription start site of *col12a1a* was identified using *Danio rerio* strain Tuebingen chromosome 17, GRCz11 Primary Assembly NCBI Reference Sequence: NC_007128.7 and served as a target template for primer design. Forward (5’-GAGAGAGAGAAAGCACCATTCTG-3’) and reverse (5’-GTTTACACACACACAGTCAGCAG-3’) primers were designed using ApE (A plasmid Editor) and used to amplify the promoter region by polymerase chain reaction (PCR) from genomic DNA of *Danio rerio*. PCR was carried out in a 25 µl reaction using the GoTaq Long PCR Mastermix (Promega, Cat#M4021) according to the manufacturer’s protocol and TOPO cloned into pENTR5′ (Invitrogen) to create pAM222. *Tg(-4kbcol12a1a:GAL4VP16)* is a MultiSite Gateway assembly of *pAM222,* Tol2kit *#387 (pME- GAL4VP16)*, *#302* (*p3E_SV40polyA*), and pAM57 (*pDestTol2 insulin:YFP*). To obtain pAM57, *crystallin* promoter was exchanged with minimal *insulin* promoter.

First, using site directed mutagenesis, pAM58, the empty pDestTol2 vector containing YFP with an added restriction side for insertion of any promoter of interest, was generated. Deletion primers were engineered by designing standard, non-mutagenic forward and reverse primers that flank the region to be deleted, (5'-GGTACCGTAAAACGACGGCCAGTGAATTATC-3') and (5'-GATATCATGGTGAGCAAGGGCGAGGAGCTGTTC-3'), respectively. In the forward primer, the sequence for the restriction site EcoRV was included. The minimal *insulin* promoter was amplified from genomic DNA and inserted using In-Fusion Cloning technology (TAKARA). The primers were designed using the In-Fusion Cloning Primer Design Tool (www.takarabio.com). Minimal *insulin* promoter forward primer (5'-TTTTACGGTACCGATCTTCAGCCCACAGTCTAGTTTAG-3') and reverse primer (5'-CTTGCTCACCATGATCGAAGCAGAGGCGAGGAATG-3'). PCR was carried out in a 25 µl reaction using Clone Amp HiFi PCR premix. In-Fusion HD cloning reaction was made with cleaned products of *pDestTol2 GATATC-YFP* (*EcoRV*-digested*)* and minimal *insulin* promoter PCR product using the In-Fusion HD enzyme premix. The minimal insulin promoter is ideal as a selection transgenesis marker because of its small size and very early activity (from 24 hpf). For Tol2-mediated zebrafish transgenesis, 25 ng/µL Tol2 mRNA were injected with 25 ng/µL plasmid DNA. F0 founders were screened for specific *insulin*:YFP expression, raised to adulthood, and screened for germline transmission.

5.2.17 Genetic ablation of *col12a1a*-expressing cells using the NTR/MTZ system

To investigate the role of *col12a1a*-expressing fibroblasts in heart regeneration, we used the fish line *Tg(-4kbcol12a1:GAL4VP16; UAS:NTR:RFP)*. To ablate *col12a1a*-expressing cells, MTZ (Sigma-Aldrich) was dissolved in system water with 0.2% DMSO to prepare a 10mM solution (Curado et al., 2009). To ablate *col12a1a*-expressing cells in adult hearts, the second day after the injury, fish were immersed in the system water containing 10mM of MTZ (or 0.2% DMSO as a vehicle control) and kept in the dark. Water with the fresh drug was exchanged twice a day until the day of sacrifice. Fish were treated with MTZ from day 2 until day 6 for the 7 dpi time point, and additionally from day 14 to day 16 for the 30 dpi time point.

We noticed increased mortality in *col12a1a*>NTR:RFP ablated injured fish compared to DMSO-treated controls. Additional experiments would be needed to determine whether this mortality is related to heart regeneration defects.

5.2.18 Cre/lox lineage tracing

For epicardial Cre/lox lineage tracing *TgBAC(cryaa:EGFP, tcf21:CreERT2; -3.5ubi-loxP-EGFP-loxP-mCherry)* transgenic fish were treated with 10μM 4-OHT (Sigma-Aldrich) dissolved in 100ml of water per fish, 4 and 3 days before the cryoinjury for 12h as described (Sánchez-Iranzo et al., 2018). Before the systemic administration, the 10 mM stock (dissolved in ethanol) was heated for 10 min at 65°C. Hearts were harvested at 7 dpi. For endocardial Cre/lox lineage tracing *Tg(fli1:Cre-ERT2; -1.5hsp70l:loxP-STOP-loxP-EGFP,cryaa:Venus)* transgenic fish were treated as embryos at 24 hpf with 5 μM 4-OHT (Sigma-Aldrich) for 24h and heat shocked for 1h at 37°C. Adult fished were injured and hearts were harvested 7 dpi.

6. Results

6.1 The use of analgesia for zebrafish after cryoinjury procedure

6.1.1 Cryoinjury as a noxious stimulus in zebrafish

Cryoinjury method is widely used by scientists to induce MI in zebrafish. The procedure involves damaging 20% of the fish ventricle, which is an invasive and potentially harmful method (Fig. 8) (Chablais et al., 2011; González-Rosa et al., 2011). Up to day no analgesia is used after the cryoinjury procedure and the refinement of the current protocols is required. To assess whether cryoinjury method is a noxious stimulus for the zebrafish, fish behaviour was used as a welfare indicator.

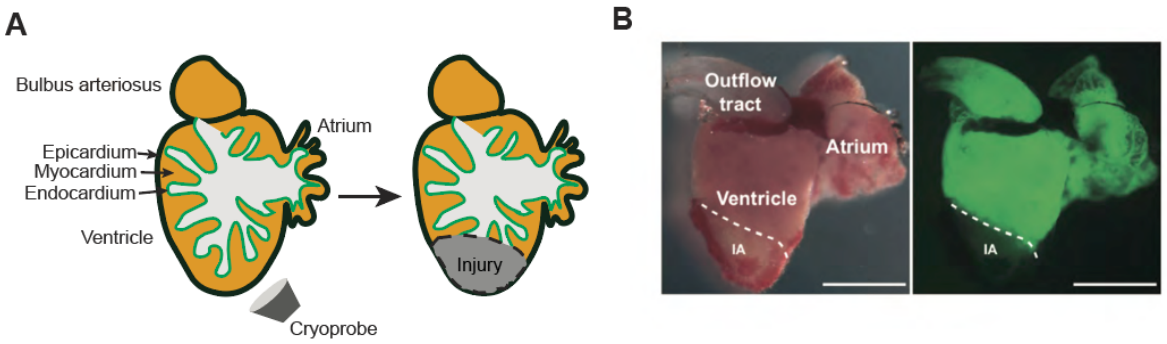

Figure 8: Cryoinjury method used to induce MI. Cryoinjury induces the damage of about 20% of tissue in the heart ventricle. (A) Schematic representation of the injury procedure (B) injured *Tg(myl7:EGFP)* heart at 3 days post injury (dpi). Scale bar, 500µm

6.1.1.1 Cryoinjury affects zebrafish behaviour

Swimming behaviour was reported to be a reliable indirect measure of zebrafish welfare (Sneddon, 2015; Reilly et al., 2008; Deakin et al., 2019; Tilley et al., 2020; Bezerra, 2021; Taylor et al., 2017; Martins et al., 2012). To evaluate the impact of cryoinjury on zebrafish wellbeing, we monitored swimming speed and tank occupancy up to 48H after the procedure.

To visualize what is the standard behaviour of uninjured fish, we monitored them in the same conditions as injured fish (Fig 9A). There was no significant difference in the swimming speed between time points, however, we can observe quite high variability between individuals (Fig. 9A).

High variability in locomotor behaviour between the individuals both, in embryo (Fitzgerald et al., 2019) and adult fish (Tilley et al., 2020; Lange et al., 2013) have been reported previously, highlighting the complexity of behavioural studies and their interpretations in fish. Importantly, there was a significant reduction in swimming speed after cryoinjury procedure (Fig. 9B). Fish were swimming significantly slower 2H after the injury and the tendency was conserved up to 6H after the procedure. After 24H swimming speed improved and 48H after the cryoinjury fish were swimming comparable to the uninjured state (Fig. 9B). Additionally, animals tend to stay significantly more on the bottom of the tank, up to 6H after the procedure, indicating their potential state of distress (Fig 9C).

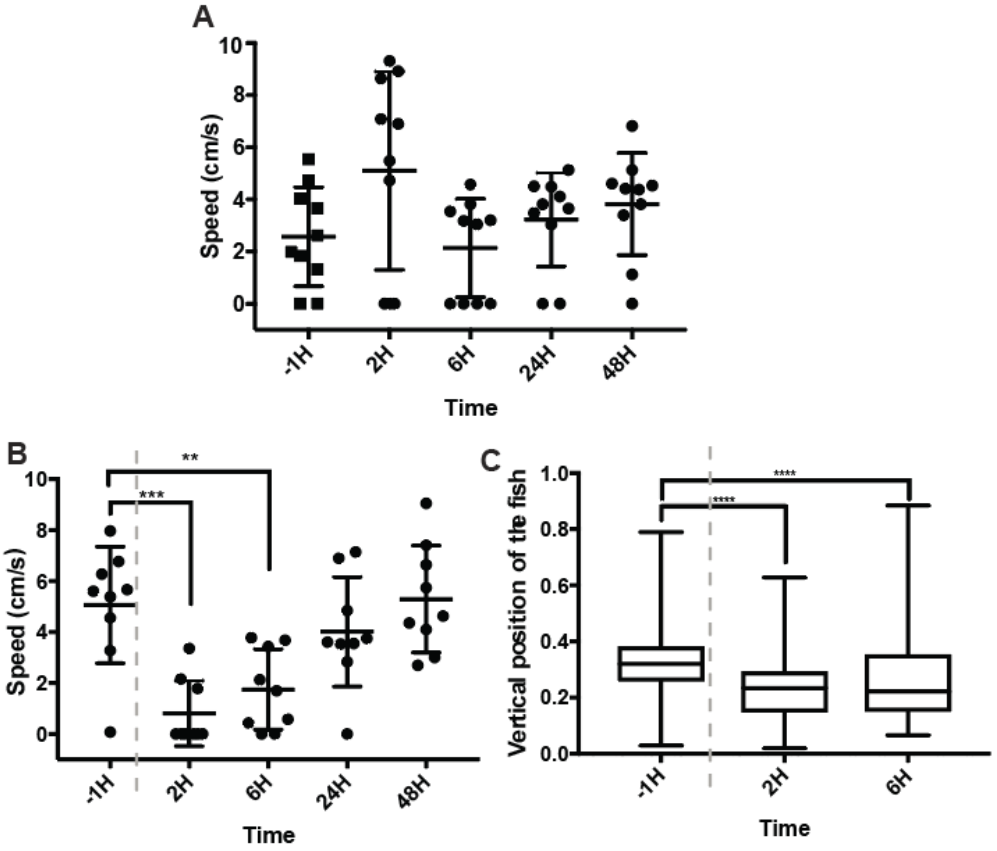

Figure 9: Cryoinjury as a noxious stimulus in zebrafish. (A) Swimming speed of uninjured fish. (B) Effect of the cryoinjury procedure on the swimming behaviour of fish. Swimming speed was assessed in fish one hour prior to cryoinjury (-1H), and at 2, 6, 24, and 48H after cryoinjury (n=9) Mean ±SD. One-way ANOVA with Tukey's multiple comparison test (P>0.05*; P>0.01**). (C) Tank occupancy of the untreated fish after the cryoinjury (n=9).Vertical position of the fish was scored, 0.0 refers to the bottom, 1.0 refers to the top of the tank. Min to Max with median.Kruskal-Wallis test with Dunn's multiple comparison test (P>0.05*). Dashed lines in B and C correspond to the time of cryoinjury procedure.

In summary, zebrafish behaviour is affected by the cryoinjury procedure and thus it should be considered as a noxious stimulus in fish.

6.1.2 Analgesia has an effect on zebrafish behaviour after cryoinjury

Analgesics were reported to have an effect on fish welfare (Deakin et al., 2019; Chatigny et al., 2018). I decided to test two different analgesics lidocaine (3 mg/l) (Schroeder and Sneddon, 2017) and morphine (1.5 mg/l) (Bezerra, 2021; Khor et al., 2011), both of which were previously shown to have a positive effect on zebrafish behaviour after noxious stimuli in different contexts. First, I tested the effect of analgesics on fish behaviour in a control state (i.e., without noxious stimulus). I investigated the swimming speed up to 48H for each treatment (Fig. 10). There were no significant differences in the swimming speed comparing control uninjured, untreated groups with uninjured, lidocaine-treated (Fig. 10A) and uninjured, morphine-treated (Fig. 10A) fish. However, when the test groups are compared individually lidocaine-treated fish swim significantly slower at 6H (Fig. 10B), while the morphine-treated fish swim at 48H significantly faster (Fig. 10C), suggesting their potential sedative and hyperactive effects, respectively.

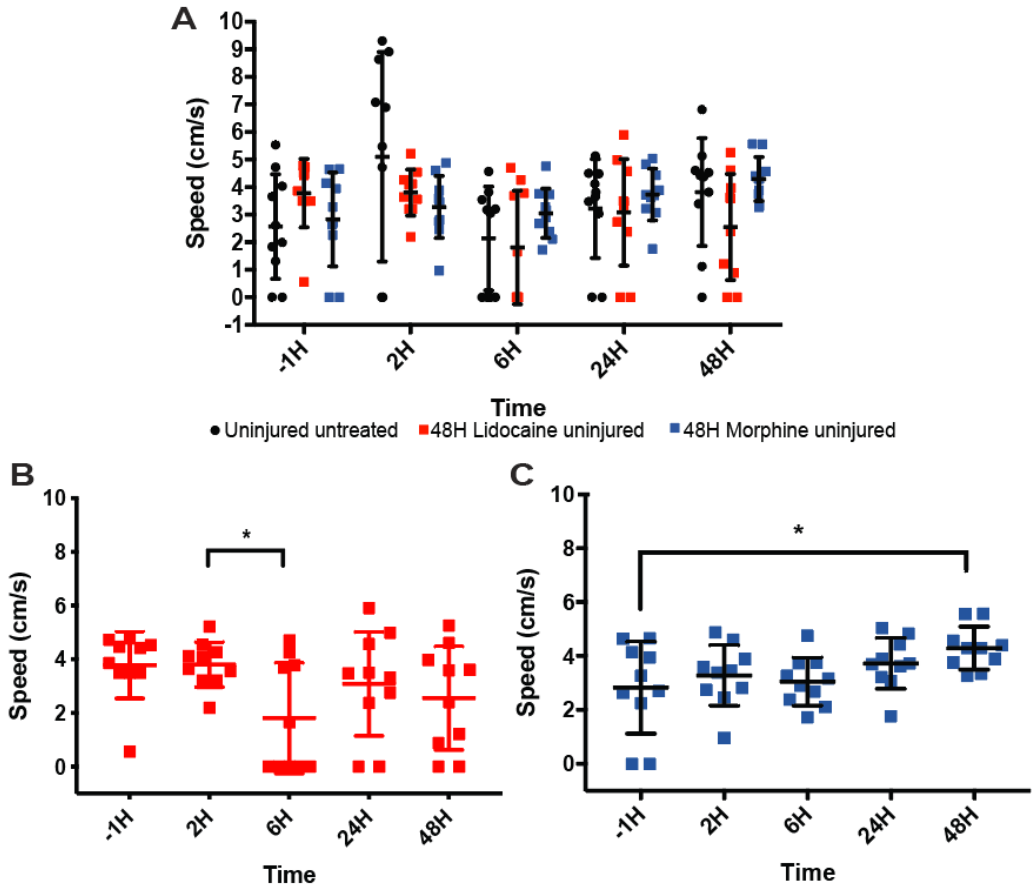

Figure 10: Effect of analgesics on the zebrafish behaviour. (A) Effect of analgesic treatment on the swimming behaviour of the uninjured fish. Swimming speed was assessed in fish one hour prior to analgesic treatments (-1H), and at 2, 6, 24, and 48H of treatment in untreated control fish (n=10, black circles), lidocaine-treated fish (n=10, red squares), and morphine-treated fish (n=10, dark blue squares). (B) Effect of lidocaine treatment on the swimming behaviour of the uninjured fish. Swimming speed was assessed in fish one hour prior to analgesic treatments (-1H), and at 2, 6, 24, and 48H (n=10). Mean ± SEM. One-way ANOVA with Boneroni's multiple comparison test (P >0.05*) (C) Effect of morphine treatment on the swimming behaviour of the uninjured fish. Swimming speed was assessed in fish one hour prior to analgesic treatments (-1H), and at 2, 6, 24, and 48H (n=10). Mean ± SD. One-way ANOVA with Tukey's multiple comparison test (P >0.05*).

6.1.2.1 Morphine improves the zebrafish swimming behaviour after cryoinjury compared to lidocaine

Both, morphine and lidocaine treatments have been shown to be beneficial for alleviating the noxious effects in zebrafish (Deakin et al., 2019; Bezerra, 2021), however, they have not been tested before in the context of cryoinjury.

To determine whether the noxious effect of cryoinjury procedure can be alleviated with the analgesic treatment, I compared the swimming behaviour after the cryoinjury and analgesics treatment up to 48H after the procedure as within this time the wound healing process should be finished (Chablais and Jaźwińska, 2012) (Fig. 11). I performed measurements at different time points: 1H before the procedure and after the cryoinjury 2H, 6H, 24H and 48H. To assess whether there is any difference between the treatments, we compared all three groups together. The swimming speed was notably affected after 2H of analgesics treatment and later all the groups behaved similarly. There was a noticeable but not statistically significant improvement in fish behaviour after treatment with morphine, however there was no detectable effect of lidocaine treatment. These data indicate that morphine (1.5mg/l) might be a potentially suitable candidate for reducing stress/pain effects after the cryoinjury procedure (Fig. 11).

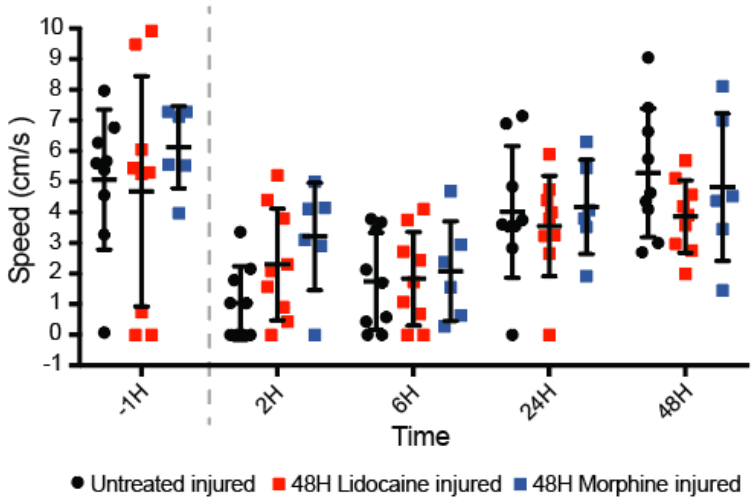

Figure 11: Analgesics affect zebrafish behaviour after cryoinjury. Effect of the analgesic treatment on the swimming behaviour of the cryoinjured fish.Swimming speed was assessed in fish one hour prior to analgesic treatments and cryoinjury (-1H), and at 2, 6, 24, and 48H after cryoinjury in injured untreated control fish (n=9, black circles), in injured lidocaine-treated fish (n=9, red squares), and injured morphine-treated fish (n=6, dark blue squares). Dashed lines indicate injury.

As the effect of analgesics was detectable only after immediate hours after the injury only with morphine use, we decided to repeat the experiment to test the effect of the short morphine treatment with a higher number of fish per group and additionally to consider tank occupancy indicator (Fig. 12).

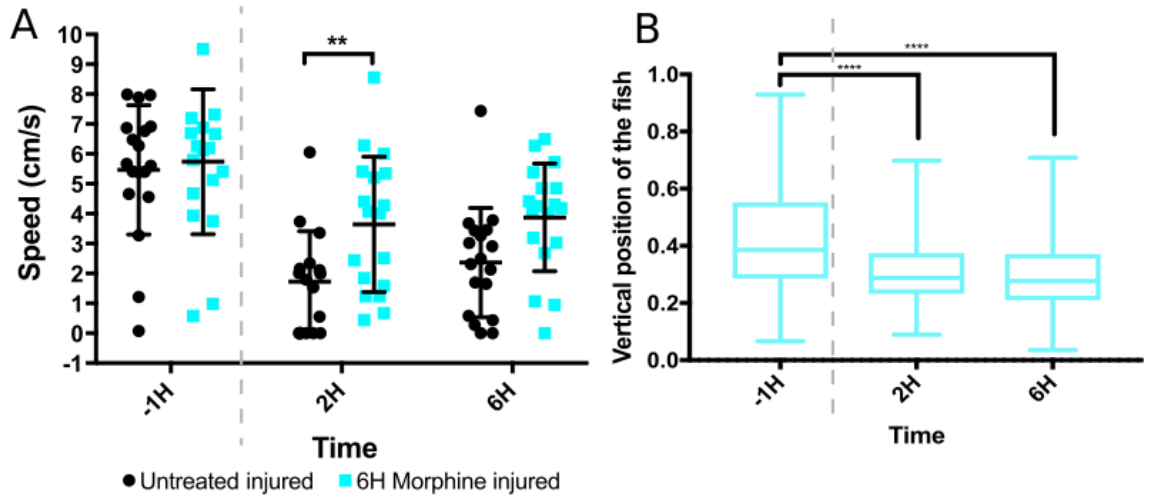

Figure 12: Morphine improves zebrafish behaviour after cryoinjury. (A) Effect of the 6H morphine treatment on the swimming behaviour of the cryoinjured fish. Swimming speed was assessed in injured untreated control fish (n=18, black circles), and in injured morphine-treated fish (n=18, light blue squares). Swimming speed was assessed in fish prior to analgesics treatment and cryoinjury at -1H time point, and at 2, 6H after cryoinjury. Mean±SD. Two-way ANOVA with Sidak's multiple comparison test (P>0.05*). (B) Tank occupancy of the 6H morphine-treated fish after the cryoinjury (n=18, light blue). Vertical position of the fish was scored, 0.0 refers to the bottom,1.0 refers to the top of the tank. Min to Max with median. Kruskal-Wallis test with Dunn's multiple comparison test (P>0.05*). Dashed lines indicate injury.

Interestingly, our data showed the morphine-treated fish swam significantly faster 2H after the injury and the tendency for the improved swimming speed was conserved up to 6H (Fig. 12A). However, morphine treatment did not rescue the tank occupancy. In summary, morphine treatment (1.5mg/l) improved fish behaviour up to 6H after the cryoinjury.

6.1.2.2 Morphine treatment does not delay heart regeneration process in comparison to lidocaine treatment

To assess whether analgesics have an effect on cardiac regeneration, I decided to examine the regenerative capacity after the analgesic treatment using histological analysis as a readout. Zebrafish heart regeneration is a dynamic process with three distinct phases: inflammatory, reparative and regenerative (Chablais et al., 2011). Each of these phases can be characterized by histology. At 7 dpi during the reparative phase there is a collagen and fibrin deposition, at 15dpi extracellular matrix resolves and during the regenerative phase from 30 dpi on, collagen resolves and myocardium replacement takes place. I assessed the regenerative process using the histological dye Acid Fuchsin Orange G (AFOG) staining in untreated (Fig. 13A-A''), injured 48H lidocaine-treated (Fig. 13B-B''), injured 48H morphine-treated (Fig. 13C-C''), injured 6H morphine-treated (Fig. 13D-D'').

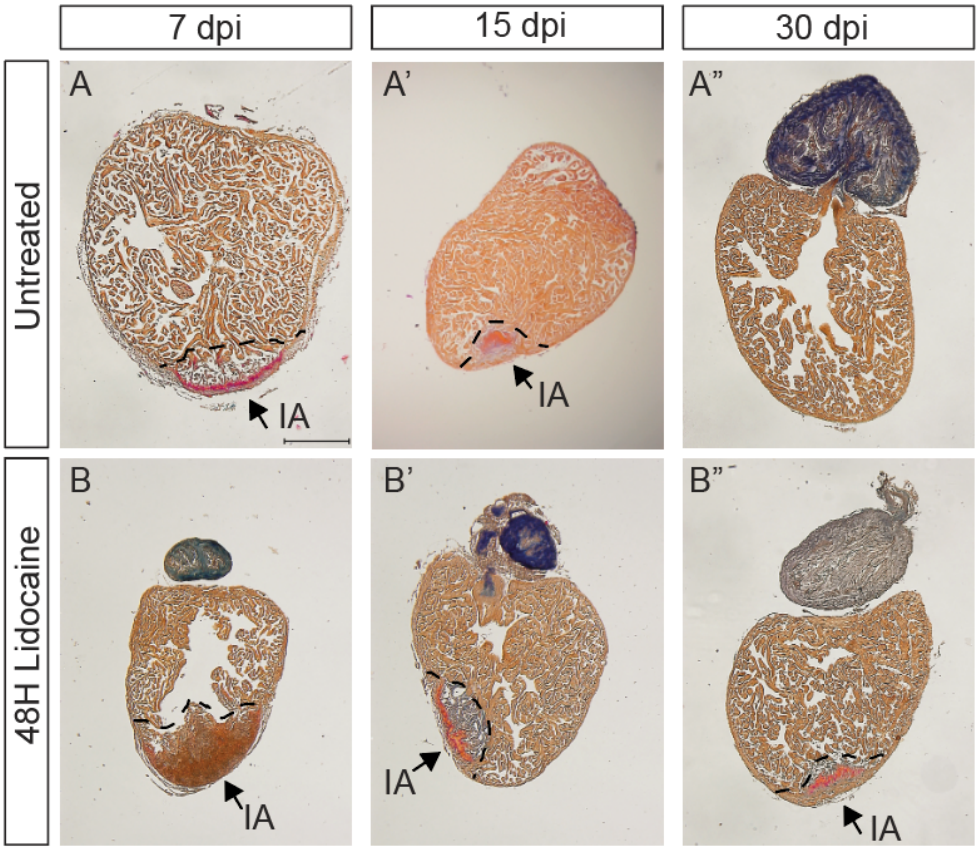

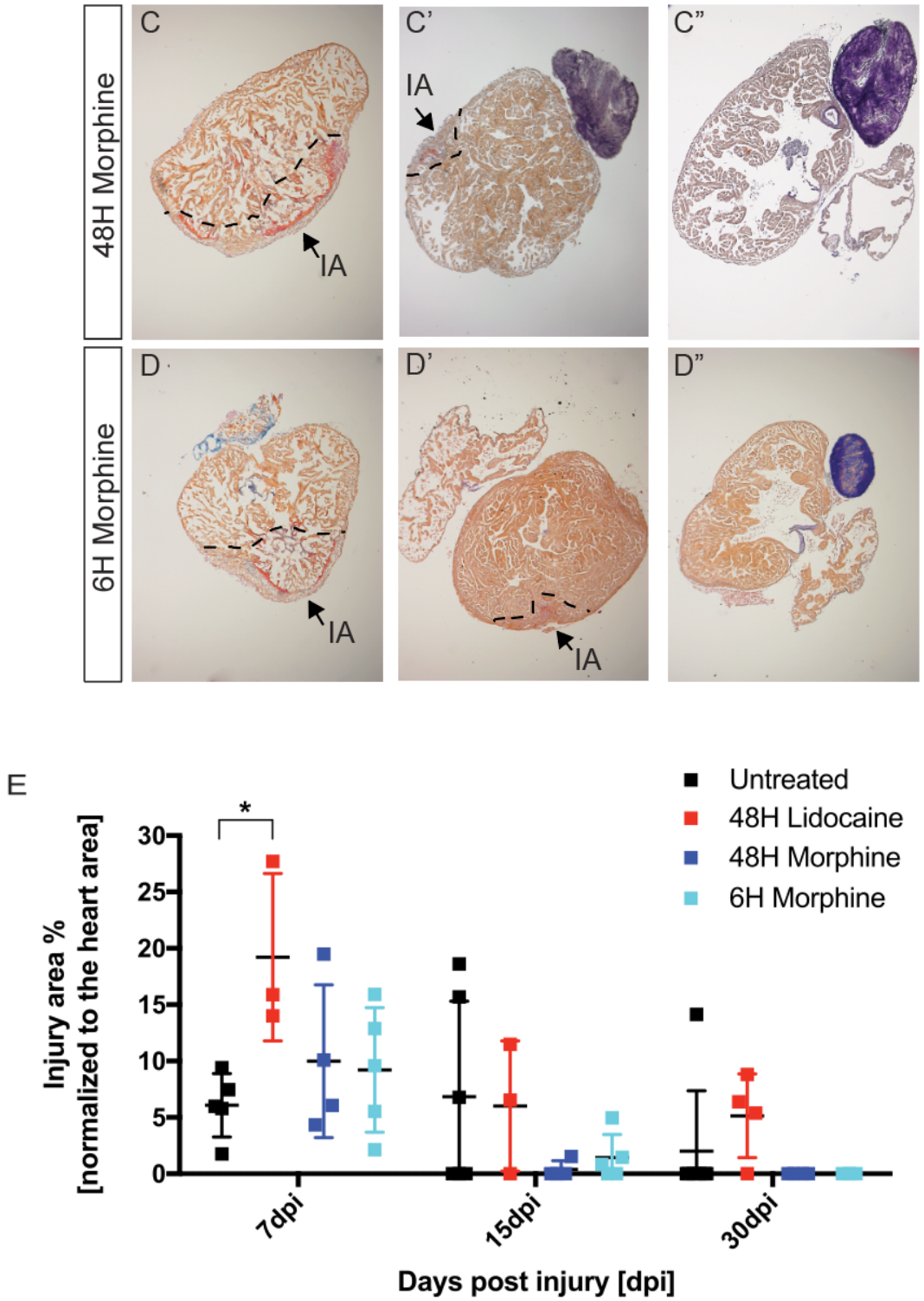

Figure 13: Morphine treatment does not delay heart regeneration. (A-E) Effect of analgesics on the regenerative capacity was compared at 3, 7, 15, and 30 dpi between untreated injured hearts (A-A''), lidocaine-treated (B-B'') and morphine-treated (C-C'') hearts for a 48H, morphine-treated hearts for 6H (D-D''). The histological dye Acid Fuchsin Orange G stains healthy myocardium in orange, fibrin in red, and collagen in blue. IA, injury area. Scale bar, 300 µm. (E) Quantification of the injury area in % normalized to the total ventricular area, n(untreated)=5, n(lidocaine$_{48H}$)=3, n(morphine$_{48H}$)=4, n(morphine$_{6H}$)=5. Two-way ANOVA with Sidak's multiple comparison test (*P*>0.05*).

The regeneration process from both 48H and 6H morphine-treated fish was not affected and was comparable at all assessed time points to the untreated hearts (Fig. 13E). Lidocaine treatment for 48H showed a significant delay in regeneration at 7 dpi with increased injury area (IA) (Fig. 13B-B''). Moreverer, the treatment with lidocaine for 48H revealed a notably visible IA filled with fibrotic and collagen matrix, still present at 30 dpi (Fig. 13).

The quantification of the IA corroborated our initial observation, with the most significant difference in the IA size between 48H lidocaine-treated and untreated hearts detectable at 7 dpi (Fig.13E). These results suggest that lidocaine treatment may interfere with the cardiac regeneration process, while morphine treatment did not have an impact on the regenerative capabilities of zebrafish hearts.

Overall, morphine seems to improve zebrafish welfare after cryoinjury, while not affecting the regeneration process. Therefore, we decided to use only 6H morphine treatment (1.5mg/l) after cryoinjury in all following experiments and refer to this experimental condition as morphine-treated hearts.

6.1.2.3 Morphine treatment does not affect the heart's regenerative capacity

Based on our results from the behaviour tests and histological analysis, morphine seems to be an analgesics of choice in case of improving zebrafish welfare after the cryoinjury and not interfering with the regeneration process. To ensure that the regeneration machinery is not affected by morphine we decided to perform more experiments taking into account transcriptional changes and cell proliferation.

6.1.2.3.1 Transcriptome analysis using single cell RNA-seq and qPCR methods

To gain deeper understanding into the effects of morphine on cardiac regeneration at an early and later stages of the repair process, we deployed single-cell RNA sequencing (scRNA-seq) in collaboration with the lab of Dr. Jan Philipp Junker. Our goal was to determine whether morphine treatment can induce any changes in the cell type diversity and gene expression.

We single-cell sequenced the transcriptomes of the injured hearts isolated at different stages of the regeneration process at 3-, 7- and 15- dpi from untreated and morphine-treated fish and we pooled the data from all the time points for the analysis (Fig. 14).

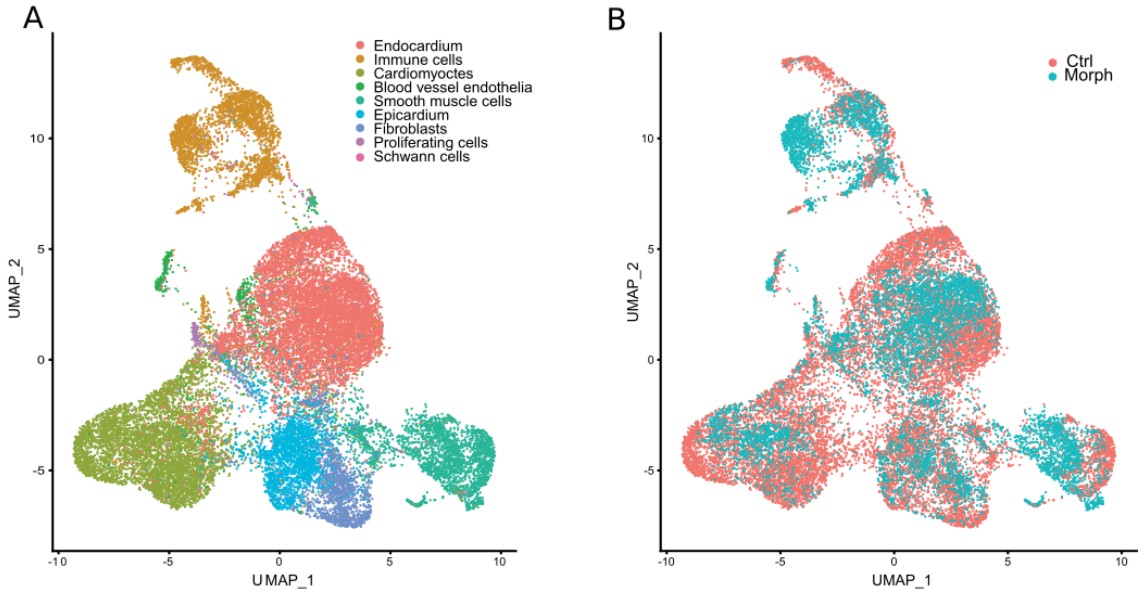

Figure 14: Morphine treatment does not change cell type diversity in regenerating hearts. UMAP of cardiac cells sampled at different timepoints after cryoinjury, grouped by cell type (A) and untreated vs morphine treated (B). Samples were pulled after cryoinjury at 3-, 7-, 15 dpi. Experiments were done by Bo Hu, in collaboration with Junker lab.

The analysis of scRNA-seq transcriptomes revealed that all major cardiac cell types are present in both untreated and morphine-treated hearts (Fig. 14) and that we observed good batch mixing after data integration. The only cell types showing stronger batch effects were cardiomyocytes, however these cells are known to be sensitive to dissociation and exhibit strong batch effects even between replicates (Fig. 14).

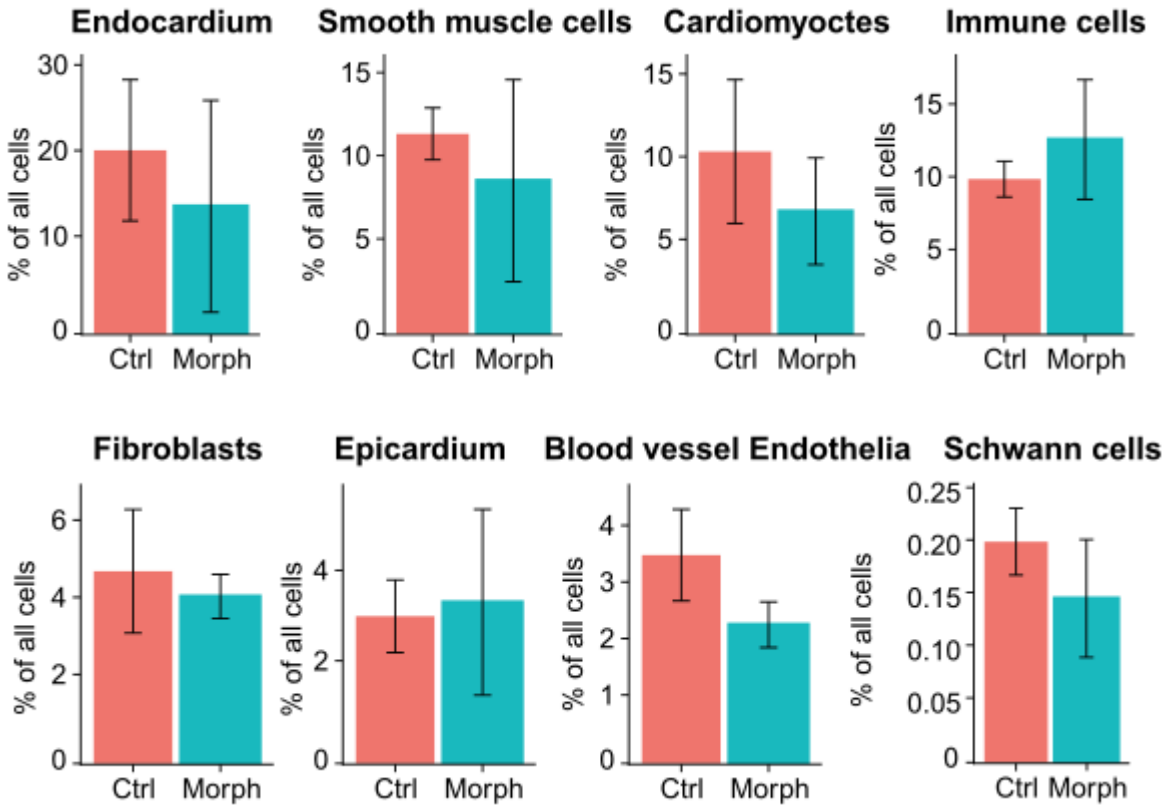

Figure 15: Morphine treatment does not change in the % of individual cell types. Comparison of means of individual cell type groups as % of all cells between untreated hearts and 6H morphine-treated hearts. Unpaired student t-test with Welch's correction (P>0.05).P values show no significant difference. Samples were pulled after cryoinjury at 3-, 7-, 15 dpi. Experiments were done by Bo Hu, in collaboration with Junker lab.

We showed that individual cell types after cryoinjury were not significantly changed by short-term morphine treatment from 3 days up to 15 days after the cryoinjury (Fig. 15). This analysis also included immune cells, since it has been previously suggested that morphine treatment might have an effect on the immune response concerning wound healing (Charbaji et al., 2013) and inflammation (Plytycz and Natorska, 2002; Fecho et al., 2007; Loram et al., 2012; Feehan and Zadina, 2019). However, the earliest time point in the analysis was 3 dpi, which might be too late to assess early immune response and inflammation. This initial finding will require more thorough investigation in future studies including 6- and 24-hpi samples to ensure that in studies focusing on the early immune response morphine-treatment can be used.

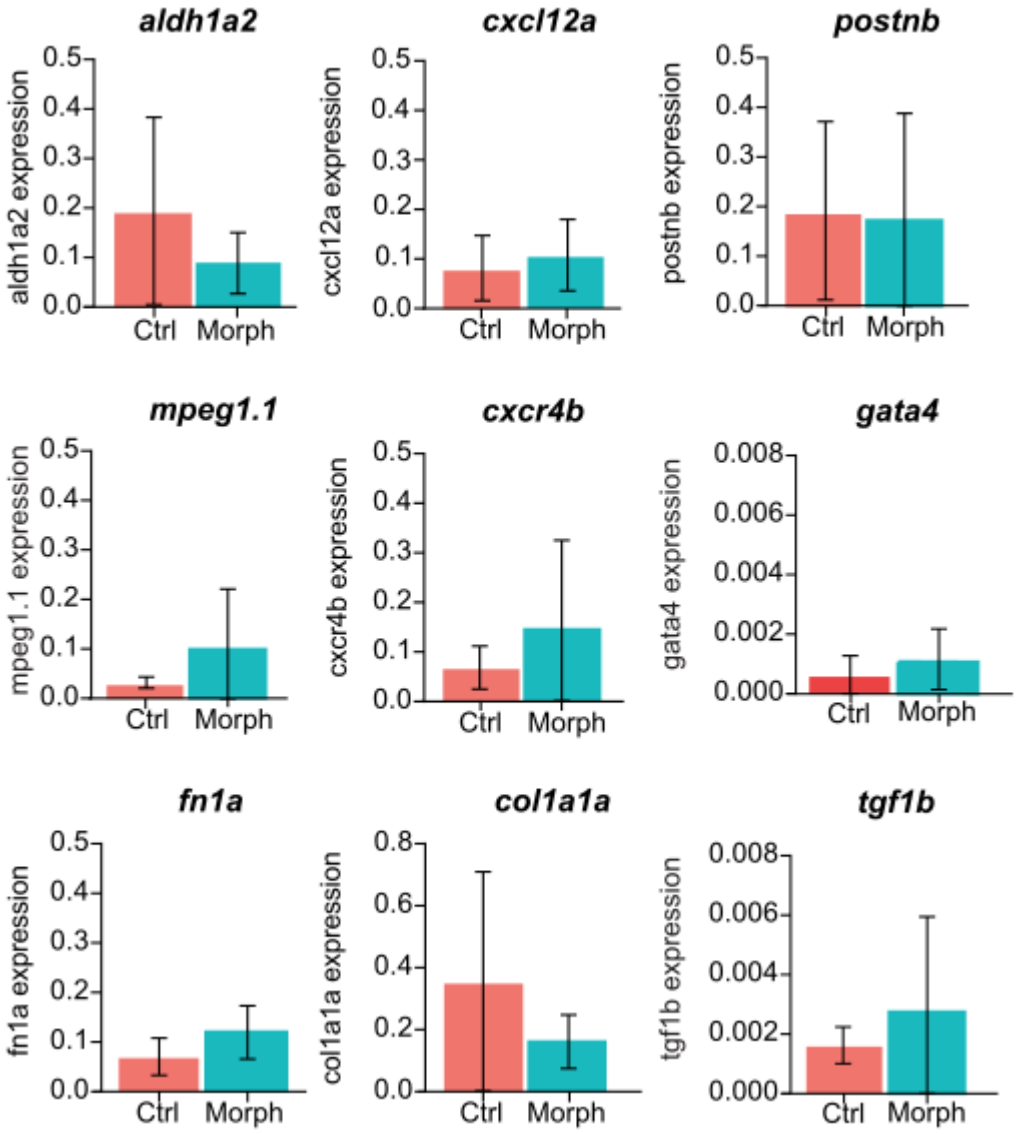

Figure 16: Morphine treatment does not change pro-regenerative gene expression after cryoinjury. Comparison of mean gene expression of selected genes involved in the regeneration between untreated hearts and 6H morphine-treated hearts. Mean ± SEM. Unpaired student t-test with Welch's correction (P>0.05). P values show no significant difference.The data in a-dare pooled over the three time points.

It is reasonable to assume that drug treatments change the gene expression of some genes since their purpose is to have an effect on the treated tissue. In case of morphine the primary effect of this opioid is on the central nervous system (CNS), to relieve moderate to severe pain for example after AMI. Morphine was shown to have beneficial effects and is currently recommended to be administered to the AMI patients (O'gara et al., 2013; Van de Werf et al., 2008).

We therefore decided to compare the gene expression using our sequencing data at 3-, 7- and 15 dpi and mRNA expression using qPCR at 7 dpi (Fig. 16 and 17). The short-term morphine treatment did not affect the gene expression of the individual genes with a known pro-regenerative role including *aldh1a2, cxcl12a, postnb, gata4, cxcr4b, fn1a, col1a1a, tgf1b* and *mpeg1.1* as a marker for macrophages (Bensimon-Brito et al., 2020; Gupta et al., 2013; Itou et al., 2012; Kikuchi et al., 2011; Kim et al., 2010; Liu et al., 2018; Moyse and Richardson, 2020; Sánchez-Iranzo et al., 2018; Wang et al., 2013).

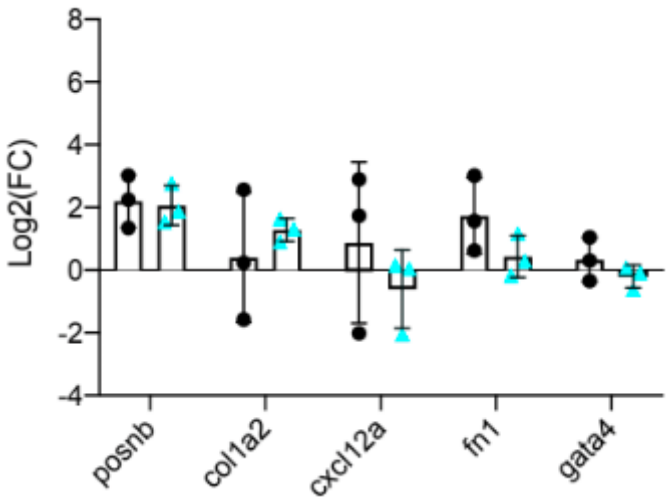

Figure 17: Morphine treatment does not change pro-regenerative gene expression at 7 dpi. Comparison of mean gene expression of selected genes involved in the regeneration between untreated hearts and 6H morphine-treated hearts at 7 dpi. Mean±SD. Unpaired student t-test with Welch's correction (P>0.05). P values show no significant difference.

In conclusion, our systematic analysis of the single cell transcriptomes did not show any major changes on the cellular and the molecular level after 6H morphine treatment of fish after cryoinjury.

6.1.2.3.2 Cell proliferation is not affected by morphine treatment

To further analyze the effect of 6H morphine treatment on the cardiac regeneration process, I focused on cell proliferation as another hallmark of regeneration. I performed RNAscope fluorescent *in situ* hybridization using *pcna* as a marker to visualize proliferative cells at 7 and 30 dpi (Fig. 18).

The IA at 7 dpi is characterized by collagen deposition and induction of cardiomyocyte proliferation at the injury border zone. With the use of appropriate markers such as *collagen I* and *vmhc* (ventricular myosin heavy chain) expression, the proliferation of these cell types can be observed (Fig. 18A). Both untreated and morphine-treated hearts revealed the proliferating cardiomyocytes labelled by the co-localization of *vmhc* and *pcna* (Fig. 18A). In addition, the proliferation of fibroblasts, labelled by co-localization of *collagen I* and *pcna*, was also readily visible (Fig. 18A).

As previously shown the regeneration process was mostly finished at 30 dpi as seen by the absence of the *pcna* marker and low levels of *collagen I* that was present in the epicardial layer in both, untreated and morphine-treated hearts (Fig. 18B).

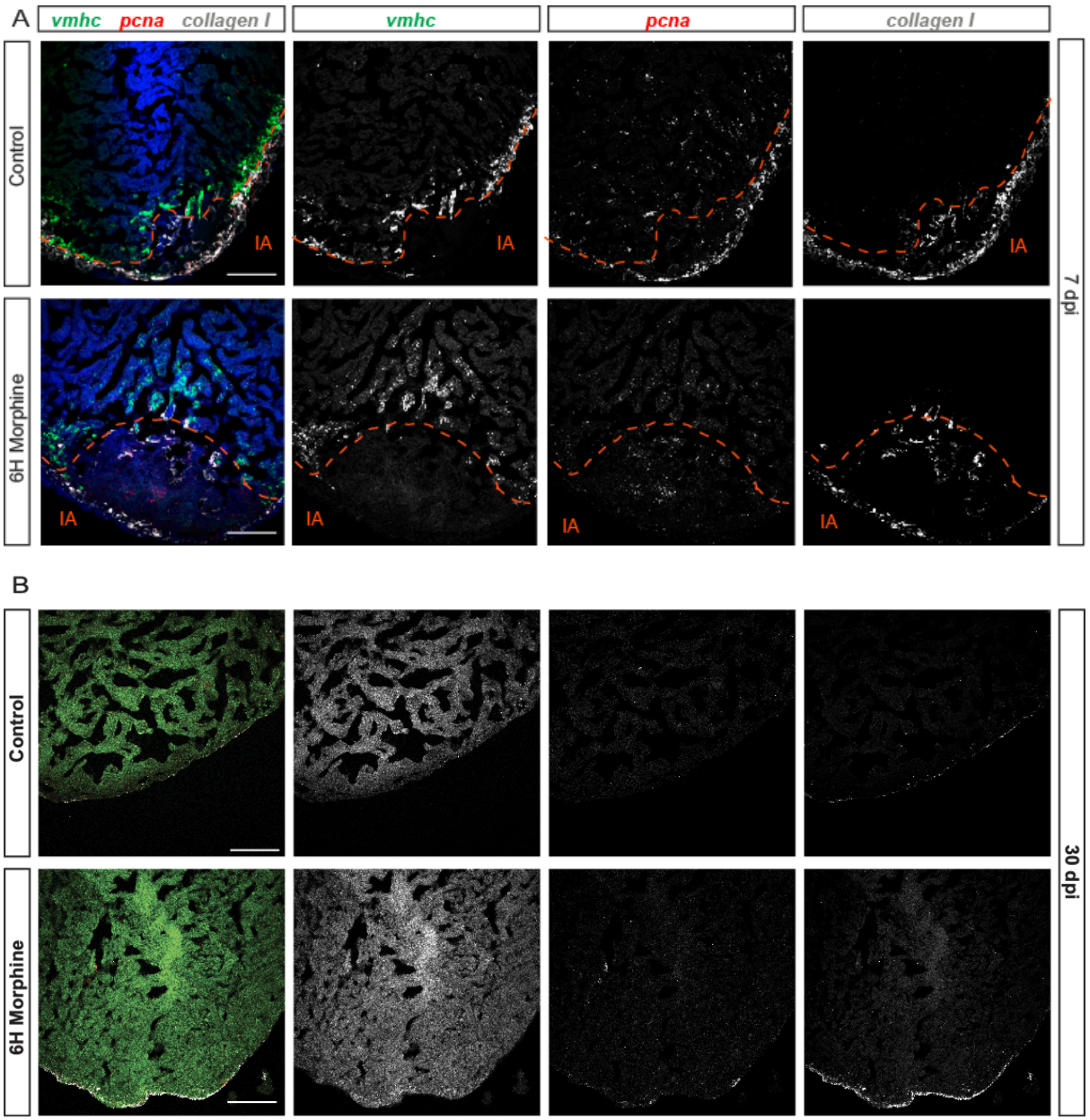

Figure 18: Morphine treatment does not impede cell proliferation after cryoinjury. Using RNAscope fluorescent *in situ* hybridization, the amount of proliferating cells labelled with *pcna* RNAscope probe (red) is comparable between untreated hearts and 6H morphine-treated hearts at 7 and 30 dpi. (A) At 7 dpi IA was detected using *collagen I* (grey), and cardiomyocytes with *ventricular myosin heavy chain*, *vmhc*, (green) probe. (B) At 30 dpi there are not any proliferating cells detected in both untreated hearts and 6H morphine-treated hearts. Scale bar, 100 μm.

Taken together, morphine at the concentration of 1.5 mg/l administered for the first 6H post-cryoinjury improves the zebrafish welfare after the procedure. Furthermore, we could not detect any major changes in the tested parameters used to evaluate heart regeneration between control and morphine-treated hearts after the short-term exposure and at the given concentration (1.5 mg/l), neither at the cellular nor at the molecular level.

6.2.1 The cellular composition of the regenerating heart

Zebrafish heart consists of one ventricle and one atrium (Fig. 19). The croinjury method was used to induce ischemia-like injury (as described in 3.2.2) in zebrafish ventricle to mimic human myocardial infarction (Fig. 19).

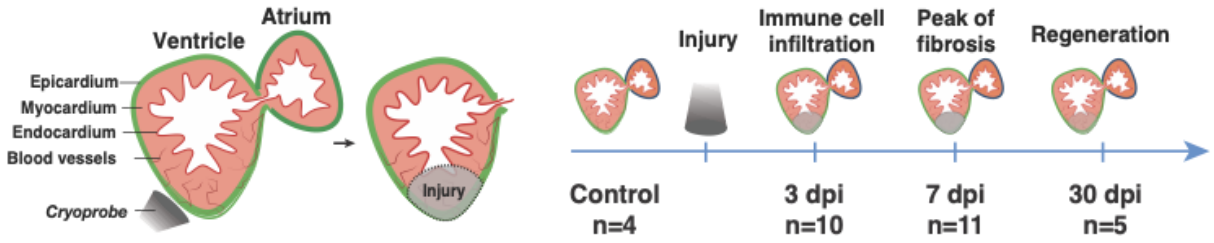

Figure 19: Experimental design of the study. Zebrafish heart was injured using the cryoinjury method. Hearts were harvested either as an uninjured control or at 3, 7 or 30 days post injury (dpi). Experiments were performed in collaboration with Bo Hu, Junker lab.

To systematically identify cardiac cell types in the healthy and regenerating zebrafish heart, we performed scRNA-seq of around 200,000 dissociated cells at different stages pre- and post-injury (Fig. 19). In order to avoid any experimental biases, no sorting procedure was used. All scRNA-seq experiments were performed with Bo Hu and Bastiaan Spaanjard, in collaboration with Junker lab.

First, we assessed cell type diversity in healthy and regenerating hearts (Fig. 20). Clustering of single-cell transcriptomes showed all major cardiac cell types such as immune cells, epicardium, cardiomyocytes, endothelial cells, perivascular cells, endocardium, fibroblasts, valve fibroblasts, smooth muscle, neuron/myelin cells (Fig. 20, Appendix Table 14).

As expected, we observed a strong increase in fibroblasts and immune cells after injury and the composition of the zebrafish heart at 30 dpi resembles the heart of uninjured fish (Fig. 20A). Cells were clustered according to the top differentially expressed genes (Fig. 20B).

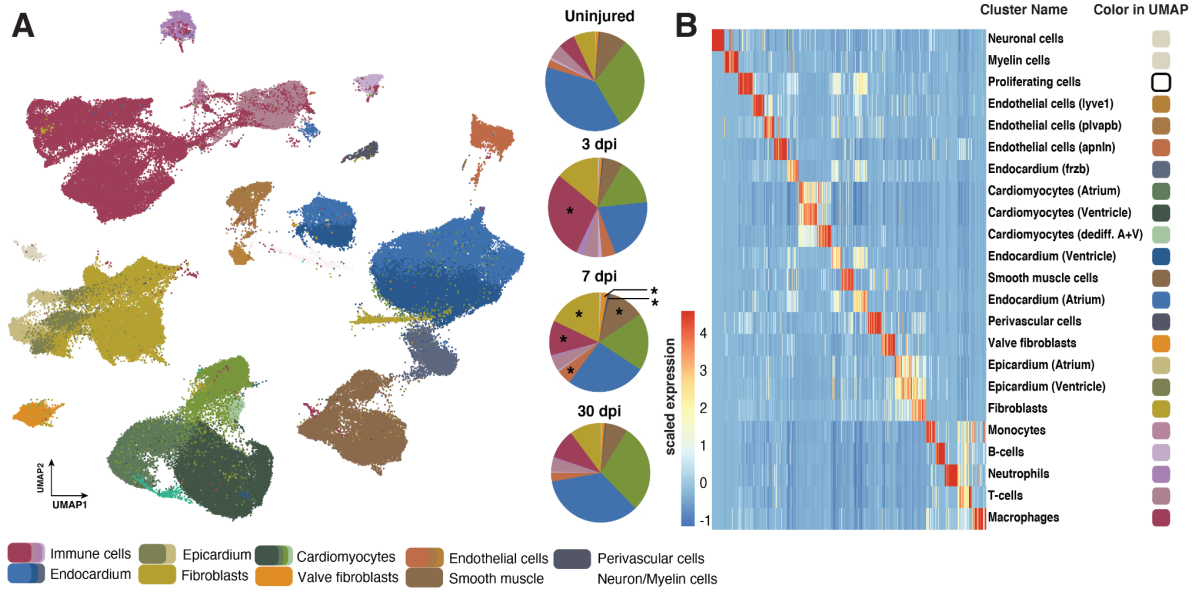

Figure 20: The cellular composition of healthy and regenerating zebrafish hearts. (A) UMAP representation of single-cell RNA-seq data and clustering results. Pie charts show the proportions of different cell types at different time points after injury. In the pie chart representation, similar cell types are grouped and shown by one (representative) colour. Asterisks (*) denote cell types with a statistically significant change in proportions compared to uninjured control. (B) Top differentially expressed genes for each cell type shown in 13A. The genes used in the heatmap can be found in Appendix Table 14. The experiments were done in collaboration with Bo Hu, Junker lab.

6.2.1.2 Cell type diversity of cardiomyocytes after injury

Our scRNA-seq data set allows us to further sub-cluster different cell types that we were able to identify. In combination with RNAscope, fluorescent *in situ* hybridization method we were able to characterize the gene expression in spatiotemporal manner. Similarly to development, the regeneration process requires precise timing and localization of the activation of certain genes to ensure that the process will take place. Therefore, we decided to investigate both dynamics and spatial distribution of distinct genes expressed by various cell types during different phases of zebrafish heart regeneration.

Firstly, we focused on the sub-structure of cardiomyocytes (CMs) (Fig. 21A). Additionally, to the adult cardiomyocytes, which are characterized e.g. by expression of genes involved in ATP synthesis and the tricarboxylic acid cycle (*atp5pd, aldoaa*), another cluster was identified, which is characterized by the expression of genes associated with cardiomyocyte development (*ttn.1, ttn.2, bves, synpo2lb, nppa*) (Fig 21B). *Natriuretic Peptide A* (*nppa)* expression was previously reported to be a marker for dedifferentiated cardiomyocytes in the border zone (Honkoop et al. 2019).

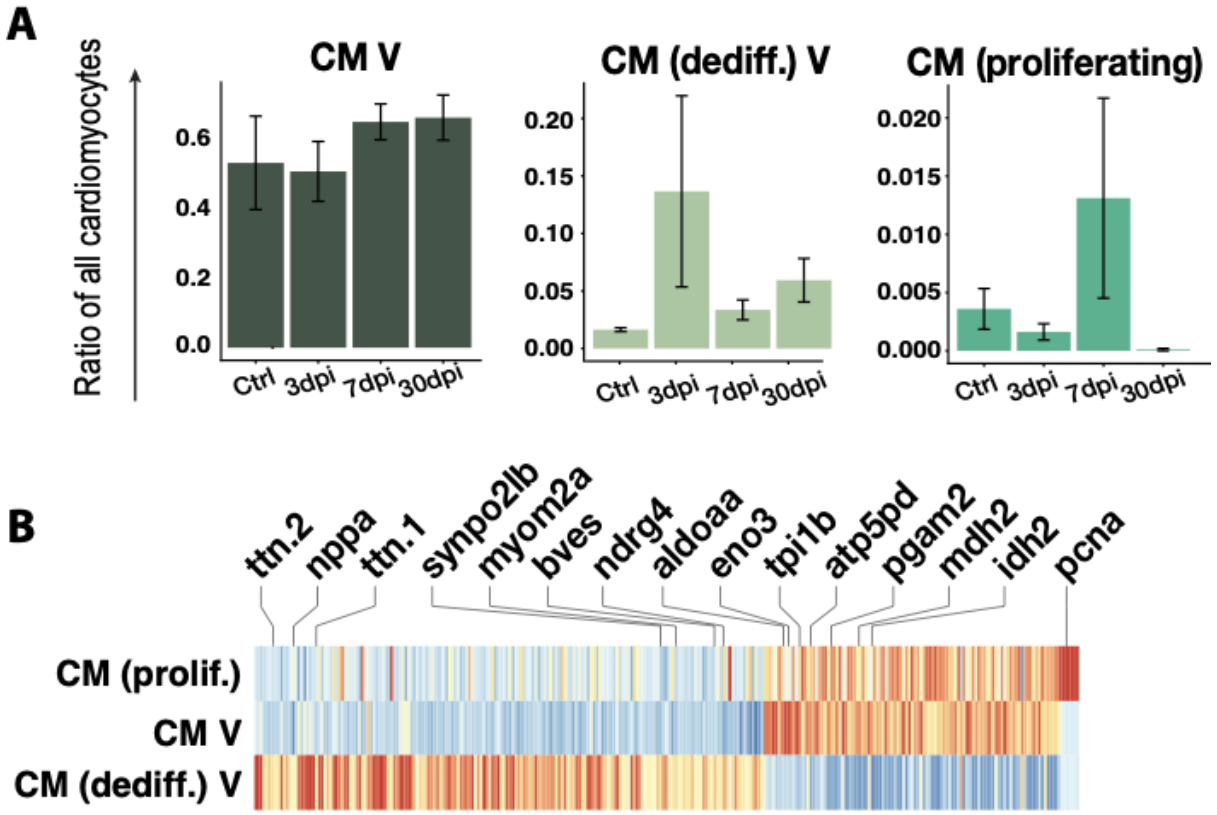

Figure 21: Diversity of cardiomyocytes after zebrafish heart injury. (A) Relative changes of abundance for different subtypes of cardiomyocytes (CMs) across the time points in the ventricle (V) (error bars show standard error of the mean). (B) Differentially expressed genes between subtypes of CMs. The experiments were done in collaboration with Bo Hu, Junker lab.

One of the hallmarks of the zebrafish heart regeneration are dedifferentiated and proliferating cardiomyocytes (CMs). We were able to show that dedifferentiated CMs peak as early as 3 dpi, and proliferating CMs peak at 7 dpi (Fig. 21A). I visualized the dedifferentiated CMs using RNAscope and I could show a partial colocalization of *titin 2* (*ttn.2)* expression with the established marker gene *nppa* (Honkoop et al., 2019) at 7 dpi (Fig. 22).

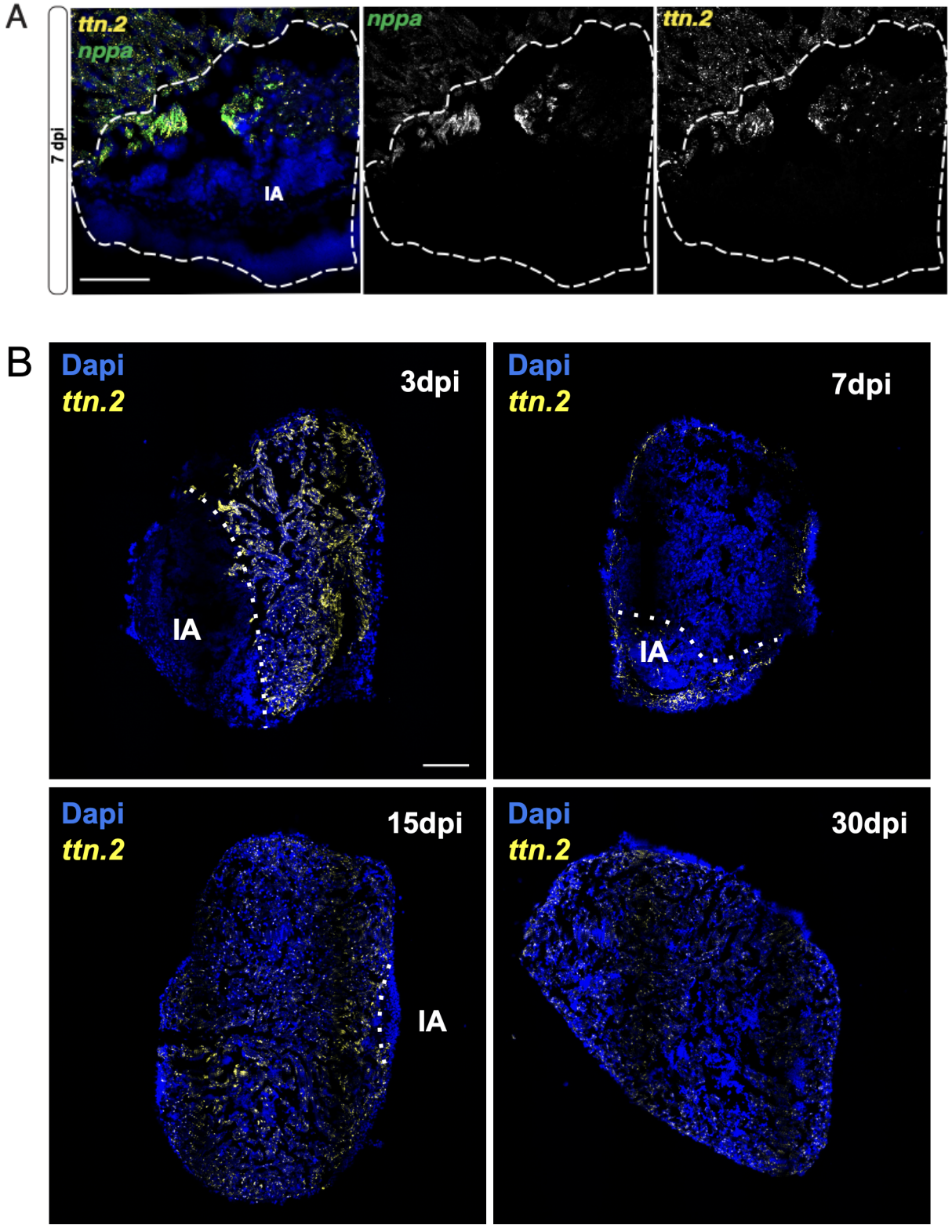

Figure 22: Dedifferentiated cardiomyocytes. (A) Co-localization of *nppa* (green) and *ttn.2* (yellow) markers of differentiated CMs at 7 dpi. (B) Localization of dedifferentiated CMs across different time points after the injury. RNAscope was used to visualize gene expression. White dashed lines indicate the injury area (IA). Scale bar: 100µm.

We showed that dedifferentiated CMs labelled with *ttn.2* are highly expressed in the myocardium at 3 dpi (Fig. 22B). Interestingly, at 7 dpi they localize to the injury area (IA). At 15 dpi dedifferentiated CMs can be found again in the myocardium, but at lower levels than at 3 dpi. Moreover, at this phase they are completely absent from the IA. At 30 dpi, the homeostatic levels of *ttn.2* can be detected in the myocardium in the regenerated hearts (Fig. 22B).

6.2.1.3 Cell type diversity of macrophages after injury

Another diverse cell type that we were able to characterize were immune cells including macrophages (Fig. 23). We were able to identify different clusters of immune cells such as B-cells, monocytes, neutrophils and transcriptionally various T-cells and macrophages (Fig. 23A).

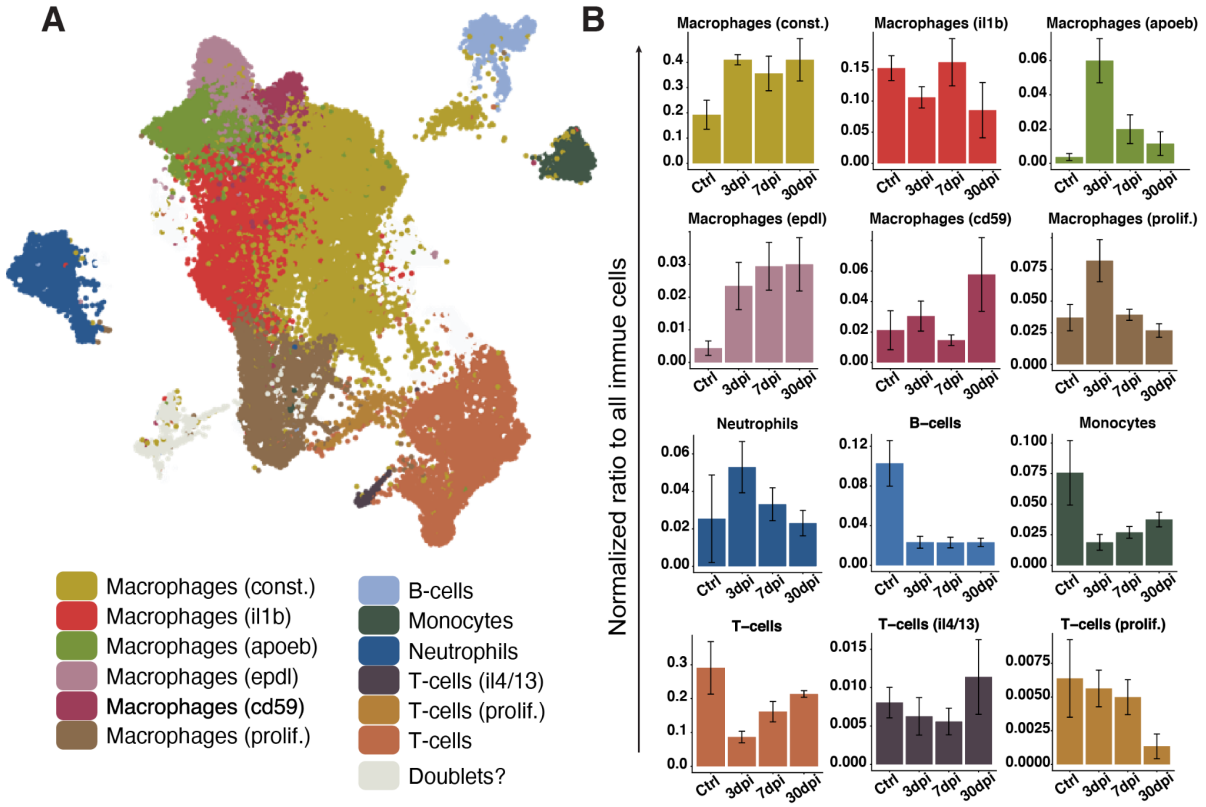

Figure 23: Diversity of immune cells after zebrafish heart injury. (A) UMAP representation of different subclusters of immune cells at different time points after the injury (3-, 7- and 30 dpi). (B) Relative changes of abundance for different subtypes of immune cells. Shown subclusters change significantly in numbers after injury and during regeneration. Mean value across all replicates of the same time point is shown, error bars indicate standard error of the mean. The experiments were done in collaboration with Bo Hu, Junker lab.

Interestingly, different clusters of macrophages showed great dynamics and were present at a certain time point after the injury. We were able to identify 6 transcriptionally distinct macrophage and 3 distinct T-cell clusters (Fig. 23). Constitutive macrophages notably increased in number after the injury and remained elevated until 30 dpi. Macrophages expressing *interleukin-1β* (*il1b)* fluctuated in the amount, first by decrease at 3 dpi, followed by increase at 7dpi and again decrease at 30 dpi. The macrophage subcluster expressing *apolipoprotein Eb* (*apoeb)* peaked at 3 dpi and the amount of these macrophages went down almost to the numbers detectable in the uninjured fish by 30 dpi. Macrophages characterized by the expression of *ependymin-like (epdl)* significantly increased after the injury and stayed highly expressed until 30 dpi. The macrophage subcluster *cd59*, interestingly, increased at 30 dpi. The highest proliferation of macrophages was detected at 3 dpi, indicating the peak of the immune response, which could be also confirmed by the highest numbers of neutrophils (Fig. 23B). There was a significant decrease of B-cells and monocytes after the injury. T-cells did not show such dramatic differences compared to macrophages, however, the general number of T-cells decreased after the injury. T-cell cluster characterized by the expression of *il4/13* increased at 30 dpi and proliferation of T-cells decreased over time after the injury, reaching the lowest levels at 30 dpi (Fig. 23B). The dynamics of the immune cells suggests they are potentially crucial for the regeneration process and warrants further studies (Fig. 23B).

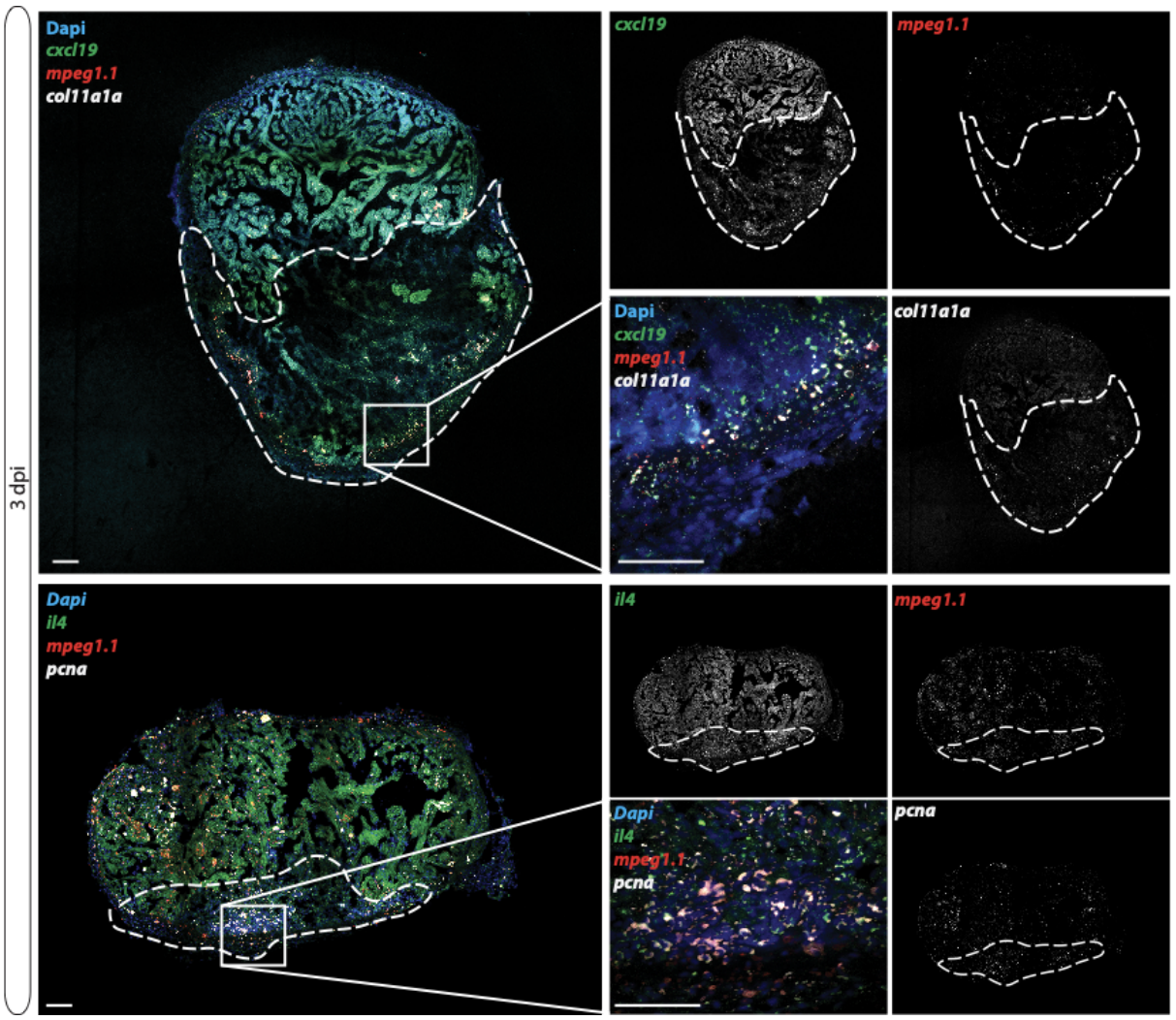

Figure 24: Localization of the immune cells at 3 dpi. Macrophages labelled with *mpeg1.1* (red), *cxcl19* expressing cells (green), *col11a1a* fibroblasts (gray), *il4* expressing cells (green), proliferative cells labelled with *pcna* (gray) visualized using RNAscope at 3 days after the injury. White dashed lines indicate the injury area (IA). Scale bar: 100µm.

Immune cells were highly expressed at 3 dpi (Fig. 24). Macrophages were strongly activated not only in the injury area, but also in the myocardium (in the remote cardiomyocytes from the injury). Some but not all macrophages were expressing *cxcl19*, a chemokine ligand 19, suggesting that it is also expressed by other immune cells for example neutrophils (UniProt, 2008). Interestingly, I could confirm that macrophages were able to express collagens, in our case *col11a1a* (Simões et al., 2020). The expression of *il4* was strongly co-localizing with *macrophage expressed 1, tandem duplicate 1 (mpeg1.1)*, indicating that the majority of *interleukin-1 (il4)* was expressed by the macrophages. There was also high expression of *pcna,* a proliferation marker, that is mostly detectable in the macrophages (Fig. 24).

6.2.1.4 Cell type diversity of cardiac fibroblasts

The scRNA-seq results showed that three well-known pro-regenerative factors in heart regeneration, *aldehyde dehydrogenase 1 family, member A2 (aldh1a2*) (Kikuchi et al., 2011) (the enzyme synthesizing retinoic acid), the cardiomyocyte mitogen *neuregulin 1 (nrg1)* (Gemberling et al., 2015), and the pro-regenerative extracellular matrix (ECM) factor *fibronectin 1a (fn1a)* (Wang et al., 2013), are strongly enriched in fibroblasts (Fig. 25A).

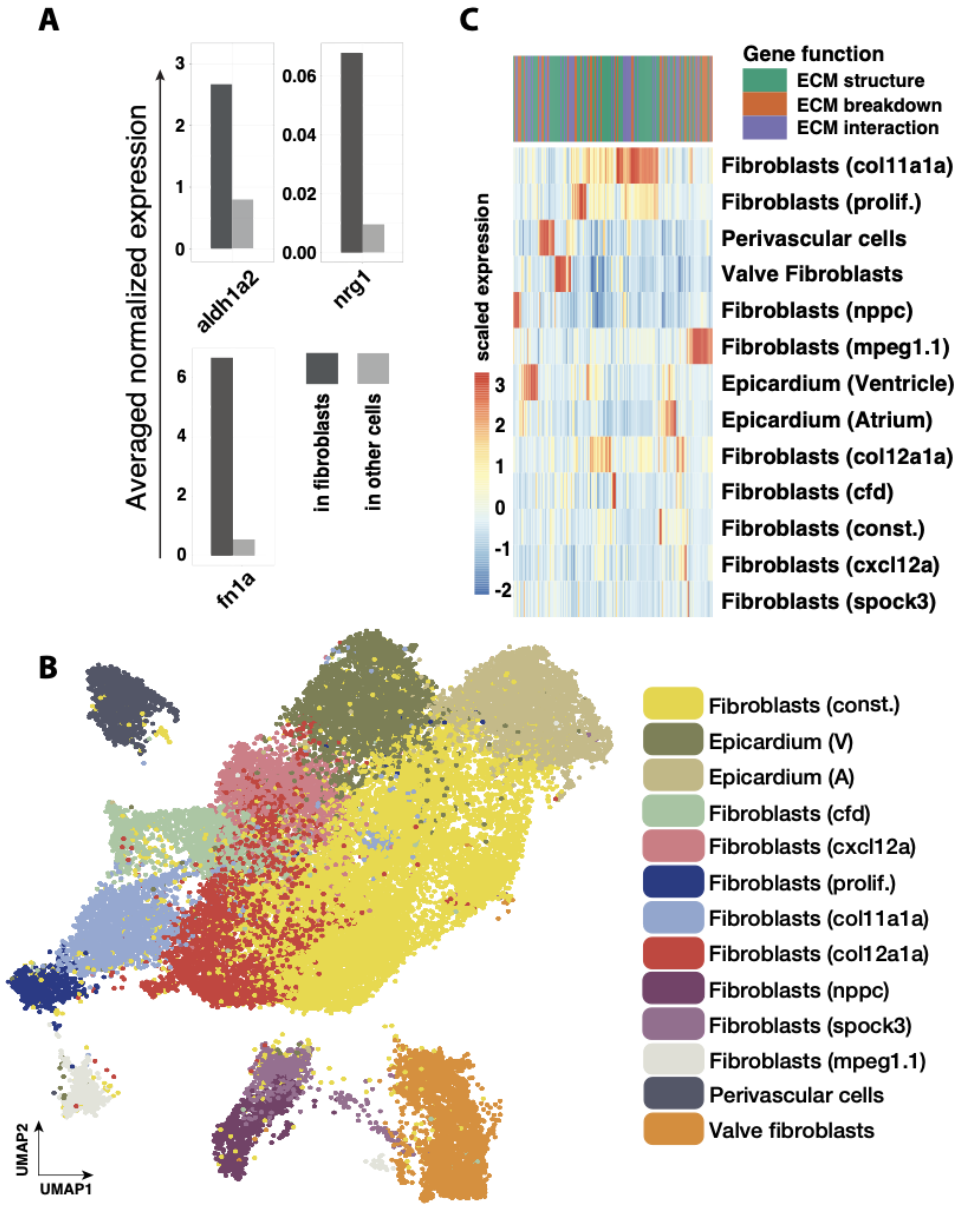

Figure 25: Cell type diversity of cardiac fibroblasts. Comparison of the averaged normalized expression of known pro-regenerative factors in fibroblasts and other cell types. (B) UMAP representation of the subclustering of *col1a1a* expressing cells. (C) Expression of extracellular matrix (ECM) related genes in different fibroblast cell types. The genes are classified according to their contribution to structure, breakdown or interaction of ECM. The experiments were. The experiments were done in collaboration with Bo Hu, Junker lab.

The pro-regenerative factors enriched in fibroblasts motivated us to further analyze the diversity of cardiac fibroblasts. After the sub-clustering of the cardiac fibroblasts we discovered a great diversity with 13 transcriptionally distinct clusters of fibroblasts (Fig. 25B, Appendix Table 15). Interestingly, these 13 clusters show striking differences in their expression profiles of ECM related genes (Fig. 25C). Furthermore the same sub-clusters of fibroblasts can be identified without the inclusion of ECM-related genes, showing their prominent transcriptomic diversity (Fig. 26).

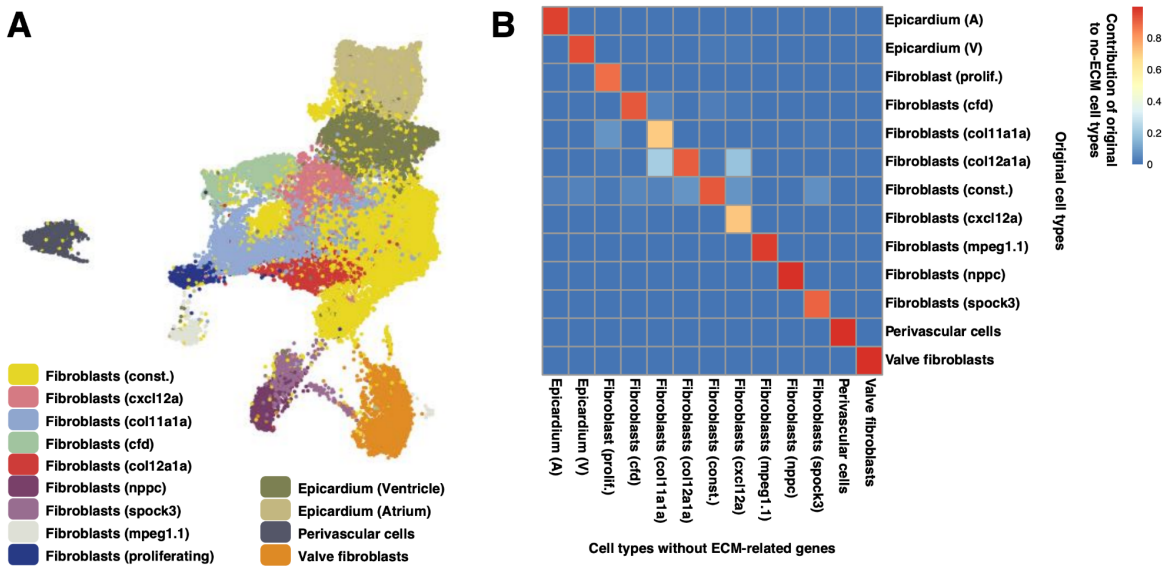

Figure 26: Fibroblast sub-clusters are well defined without inclusion of ECM-related genes. (A) UMAP and clustering of fibroblasts remained distinct even without ECM-related genes. (B) Cell types identified after removal of ECM-related genes mostly overlap with original cell types, although a small fraction of *col12a1a* fibroblasts is found in the *col11a1a* and *cxcl12a* fibroblast subtypes. The experiments were done in collaboration with Bastiaan Spanjaard and Bo Hu, Junker lab.

6.3.1 Identification of pro-regenerative cardiac fibroblasts

The analysis of the dynamics of the fibroblast subtypes revealed that some of the identified clusters are transiently present after the injury. This means that they were transiently present at the peak of regeneration at 3 and/or 7 dpi but almost completely absent in the homeostatic state and after regeneration. Three clusters which stood out were characterized by expression of *collagen, type XI, alpha 1a (col11a1a)*, *collagen, type XII, alpha 1a* (*col12a1a)*, and *natriuretic peptide C (nppc)* respectively (Fig. 27).

Additionally, we discovered that the peak of fibroblasts proliferation was detectable at 3 dpi, which might be crucial for the peak of fibrosis at 7 dpi. The transient nature of these three clusters prompt us to refer to them as states instead of cell types.
One of the identified genes expressed in those clusters, namely *col12a1a,* which is a non-fibrillar collagen that may act as a matrix-bridging component, has already been reported to be expressed in the epicardial and connective tissues upon heart injury (Marro et al., 2016) and is known to be involved in regeneration of other organ systems in zebrafish (Wehner et al., 2017). *Col12a1a* fibroblasts increase after the injury and peak at 7 dpi by later being almost completely absent (Fig. 27).

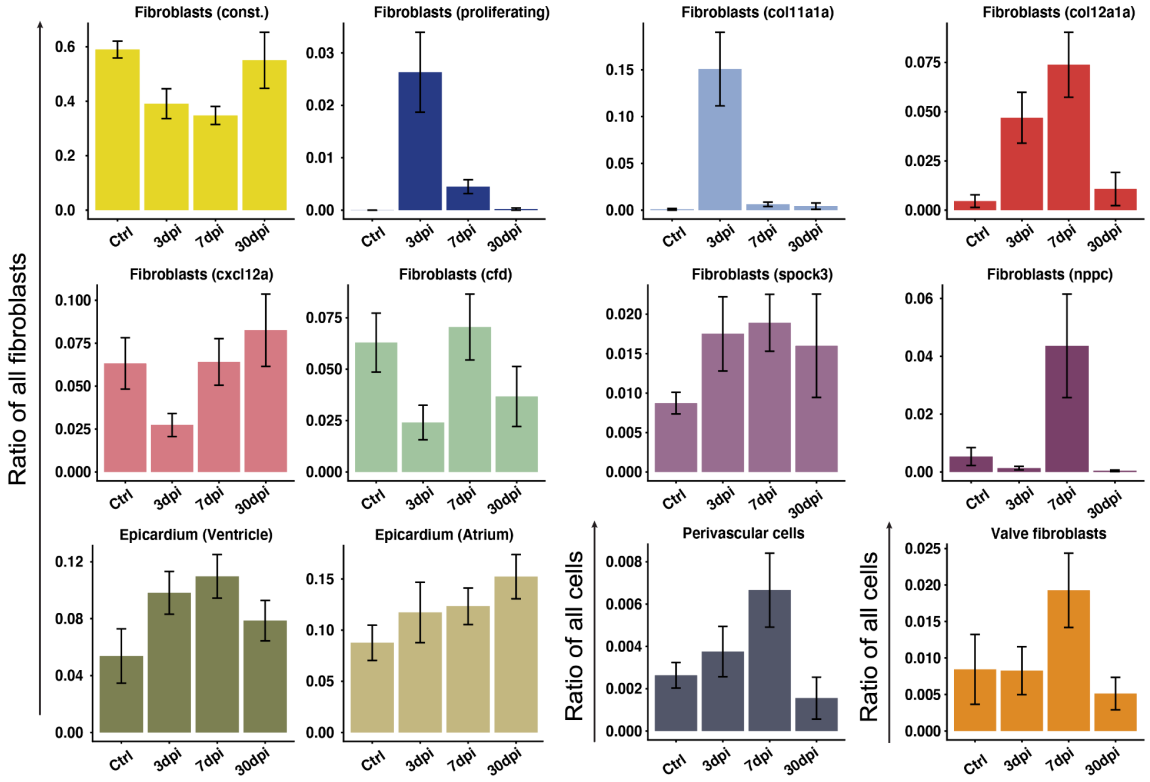

Figure 27: Dynamics of cardiac fibroblasts. Cell number dynamics of all fibroblast subtypes during regeneration. Mean value across all replicates of the same time point is shown, error bars indicate standard error of the mean. The experiments were done in collaboration with Bo Hu, Junker lab.

Two subtypes of transient fibroblasts show similar expression profiles, namely *col12a1a*- and *col11a1a*- expressing subclusters. The expression of *col12a1a* is detectable in both these clusters (Fig. 28), however, *col11a1a*- expressing subclusters peak earlier, namely at 3 dpi. Moreover, mentioned *nppc* fibroblasts peak specifically at 7 dpi and otherwise are virtually absent (Fig. 27).

Other fibroblasts subclusters such as *chemokine (C-X-C motif) ligand 12a- (cxcl12a), complement factor D-(cfd) and SPARC/osteonectin- (spock3)* expressing fibroblasts show their own dynamics after the injury, however the differences are not as dramatic as for other transient fibroblasts and these subclusters are not completely absent before the injury (Fig. 27).

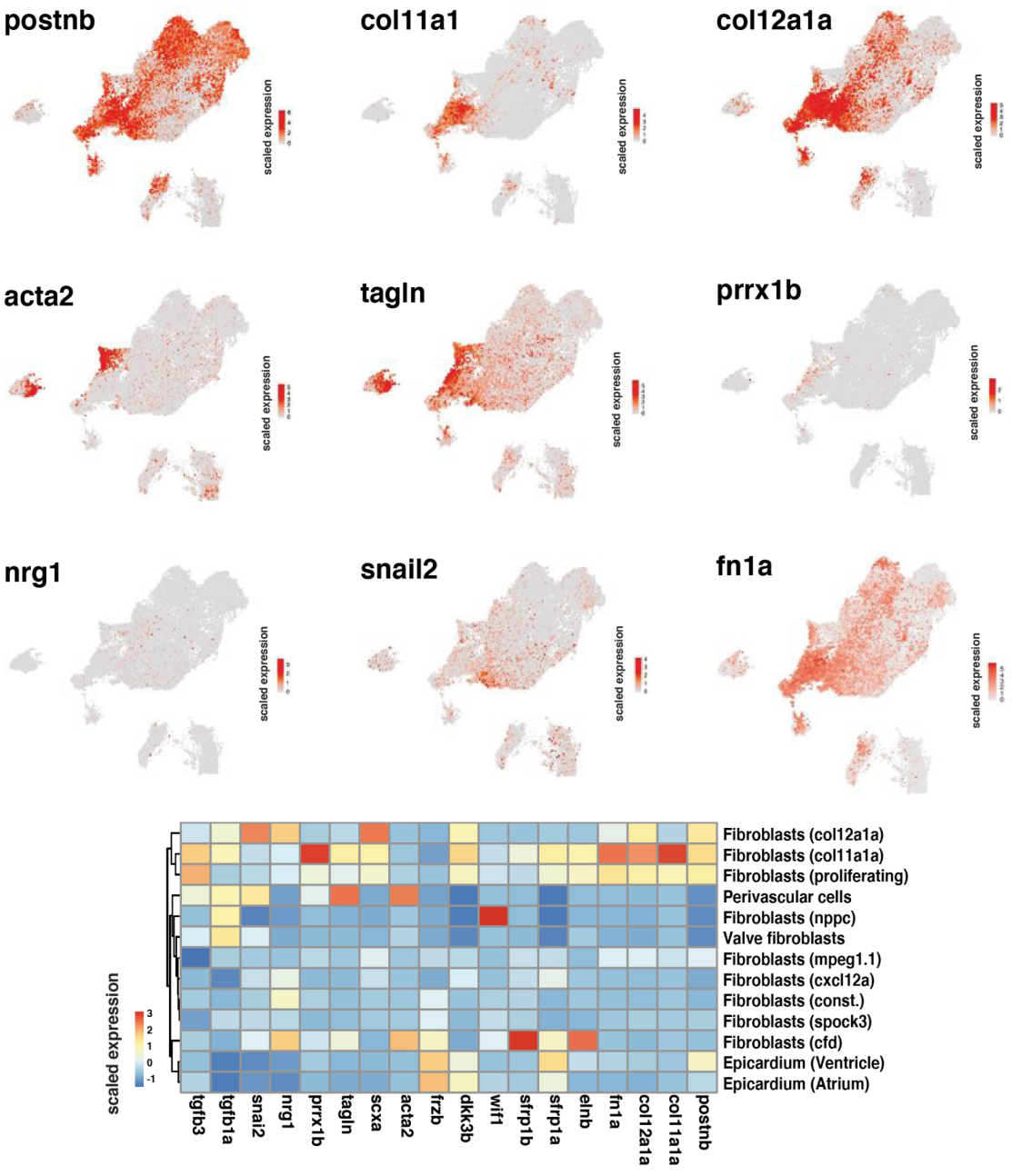

Figure 28: Gene expression in fibroblast subtypes. Expression of selected genes involved in fibroblast function or heart regeneration in the identified fibroblast subclusters. The experiments were done in collaboration with Bo Hu, Junker lab.

The perivascular cells (characterized by the expression of *platelet-derived growth factor receptor, beta polypeptide - pdgfrb*) and valve fibroblasts (characterized by expression of *angiopoietin-like 7 - angptl7*) both having ECM-related function, were also identified as transiently present, peaking at 7 dpi (Fig. 27, Appendix Table 16). The remaining fibroblast cell types did not show significant changes after the injury. Another interesting finding, is that established markers for “activated” fibroblasts like *postnb* (Sánchez-Iranzo et al., 2018) were included in all fibroblast clusters that are present after the injury, and were also expressed in non-fibroblast populations like the epicardial cells (Fig. 28), suggesting that previously the transcriptional diversity of cardiac fibroblasts was strongly underestimated.

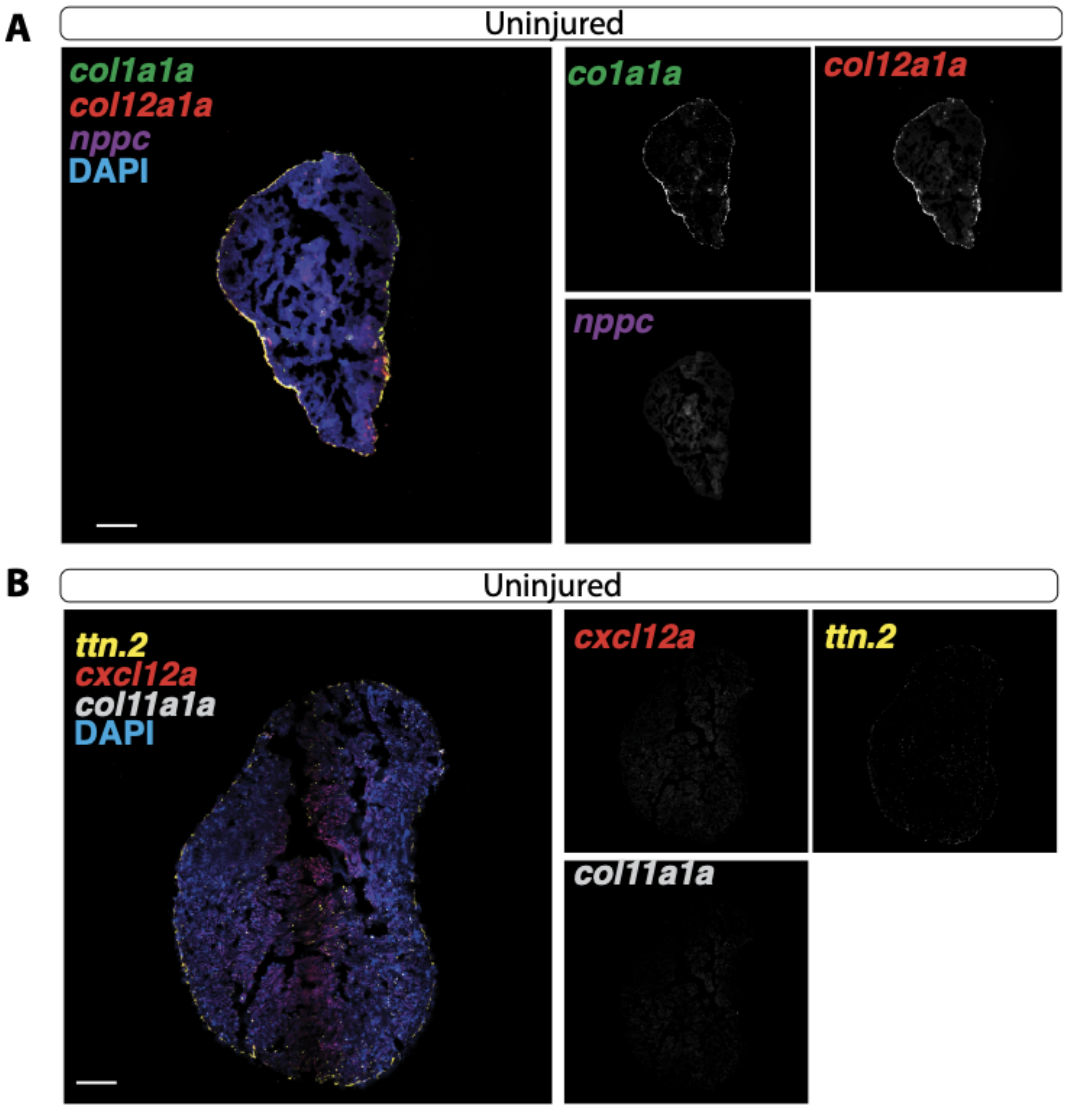

Figure 29: RNAscope marker genes for cell types of interest in uninjured hearts. Markers for transient cell types expression in the ventricle (*col12a1a - red, col11a1a - gray, ttn.2 - yellow* for dedifferentiated cardiomyocytes, *nppc - magenta*). Scale bar: 100 µm.

In order to identify the spatial distribution of different fibroblast cell types, we used the RNAscope method (Fig. 29-32) that allowed us to investigate the localization of transient fibroblasts in uninjured and injured hearts at 3- and 7 dpi. First, we confirmed that in uninjured hearts *col1a1a* and *col12a1a* were co-localizing in the epicardium (Fig. 29A) (Marro et al., 2016). There was no expression of *nppc* detectable in the uninjured hearts (Fig. 29B).

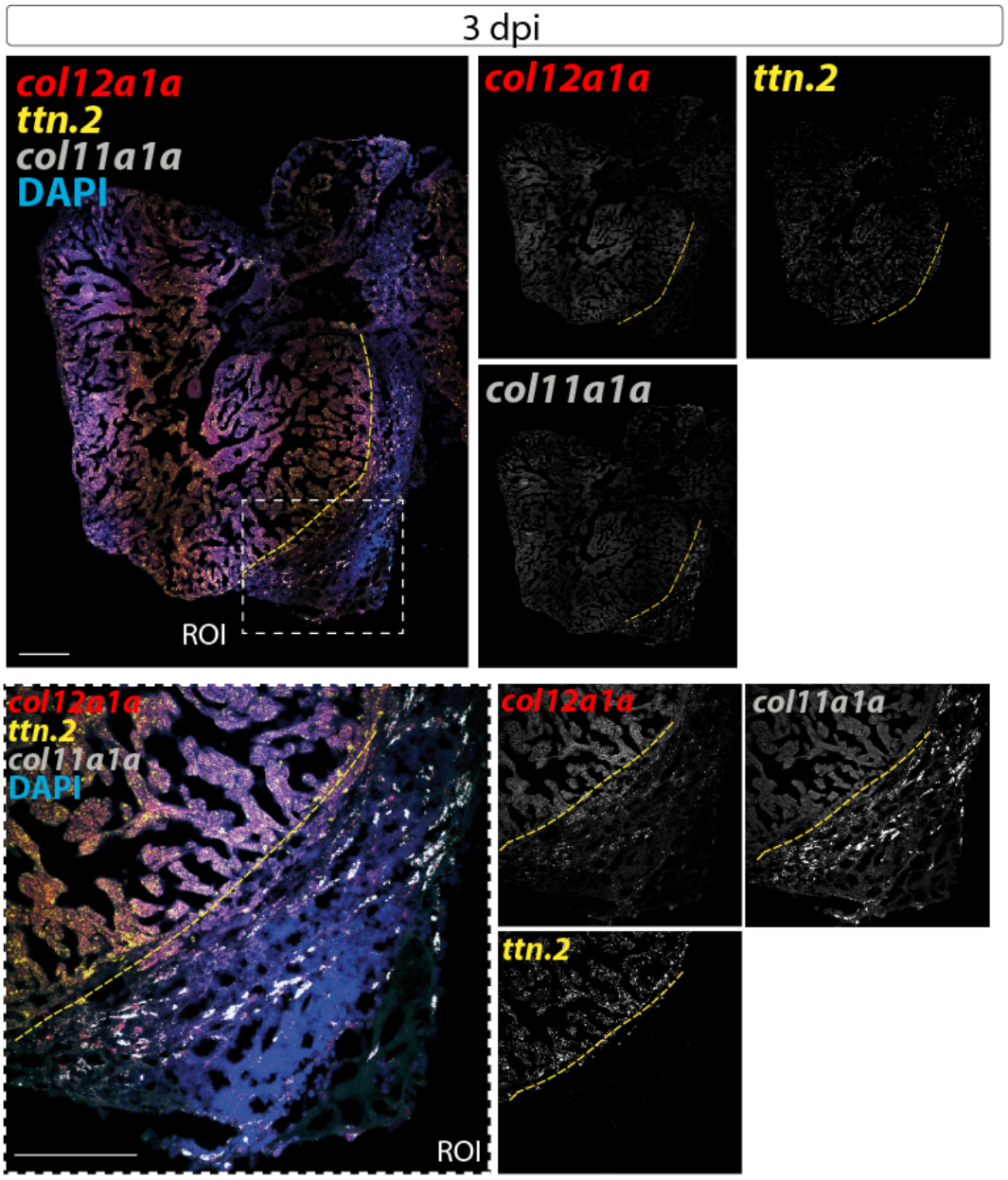

Figure 30: RNAscope marker genes for cell types of interest at 3 dpi. Markers for transient cell types (*col12a1a - red, col11a1a - gray, ttn.2 - yellow* for dedifferentiated cardiomyocytes) are localized at the injury area and myocardium. Yellow dashed lines indicate injury area (IA). ROI: region of interest. Scale bar: 100 µm.

Based on our scRNA-seq analysis, (Fig. 21) I confirmed that at 3 dpi *ttn.2* is highly expressed in the whole myocardium (see also Fig. 22) and *col11a1a* is highly expressed in the injury area (Fig. 30). The expression of *col12a1a* at 3 dpi is barely detectable in the injury (Fig. 30)

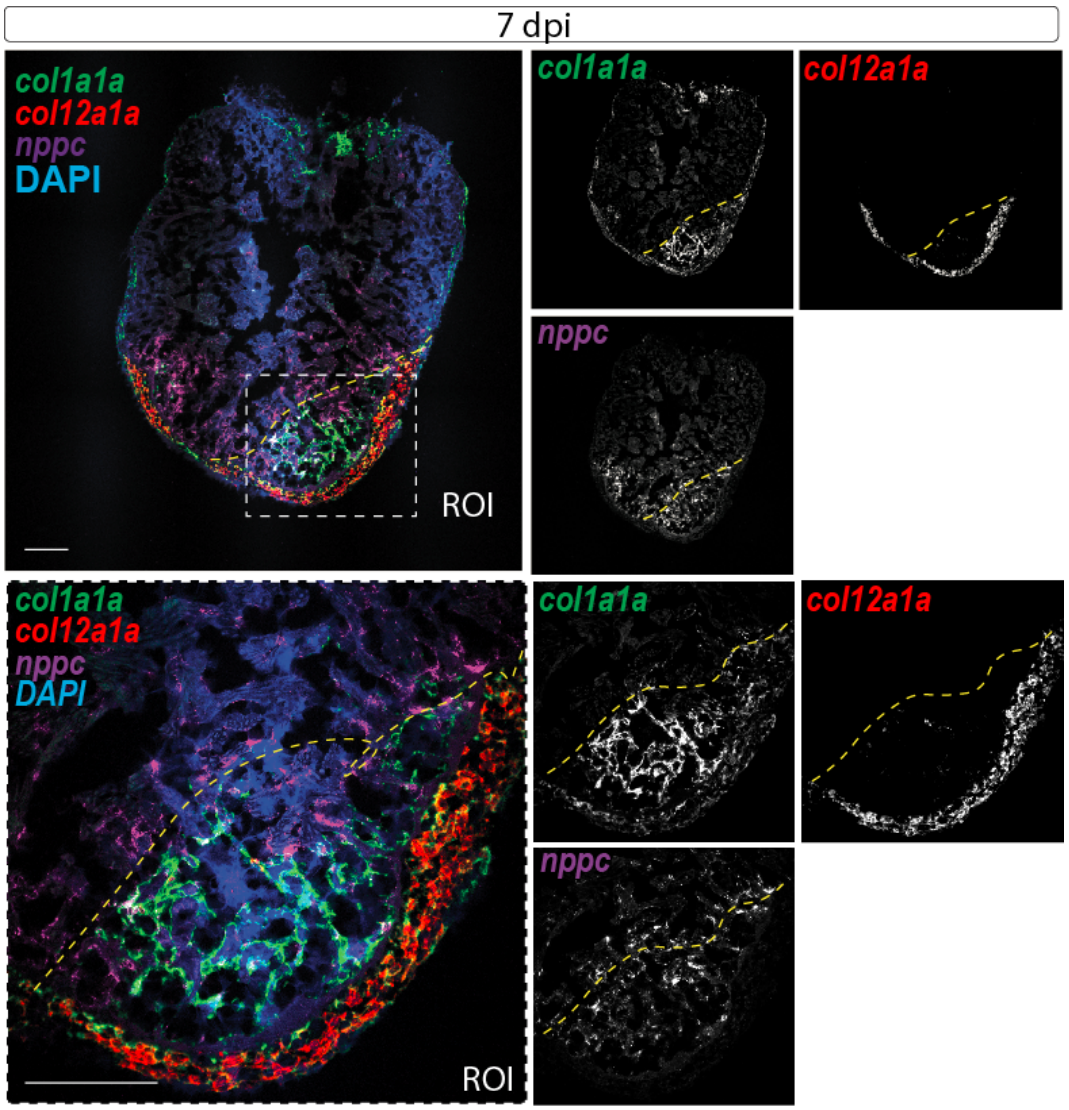

Figure 31: RNAscope marker genes for cell types of interest at 7 dpi. Markers for transient cell types (*col12a1a - red, col11a1a - gray, nppc magenta*) are localized at the injury area. Yellow dashed lines indicate injury area (IA). ROI: region of interest. Scale bar: 100 µm.

The expression of *col12a1a* was detected to peak at 7 dpi (Fig. 27) and I showed that these fibroblasts were localized to the injury area, specifically to the epicardium (Fig. 31). Additionally, high expression of *nppc* was confirmed at 7 dpi (Fig. 27) in the injury border zone (Fig. 31). The marker for fibroblasts *col1a1a* is highly expressed in the injury area, co-localizing partially with *nppc* and *col12a1a* (Fig. 31).

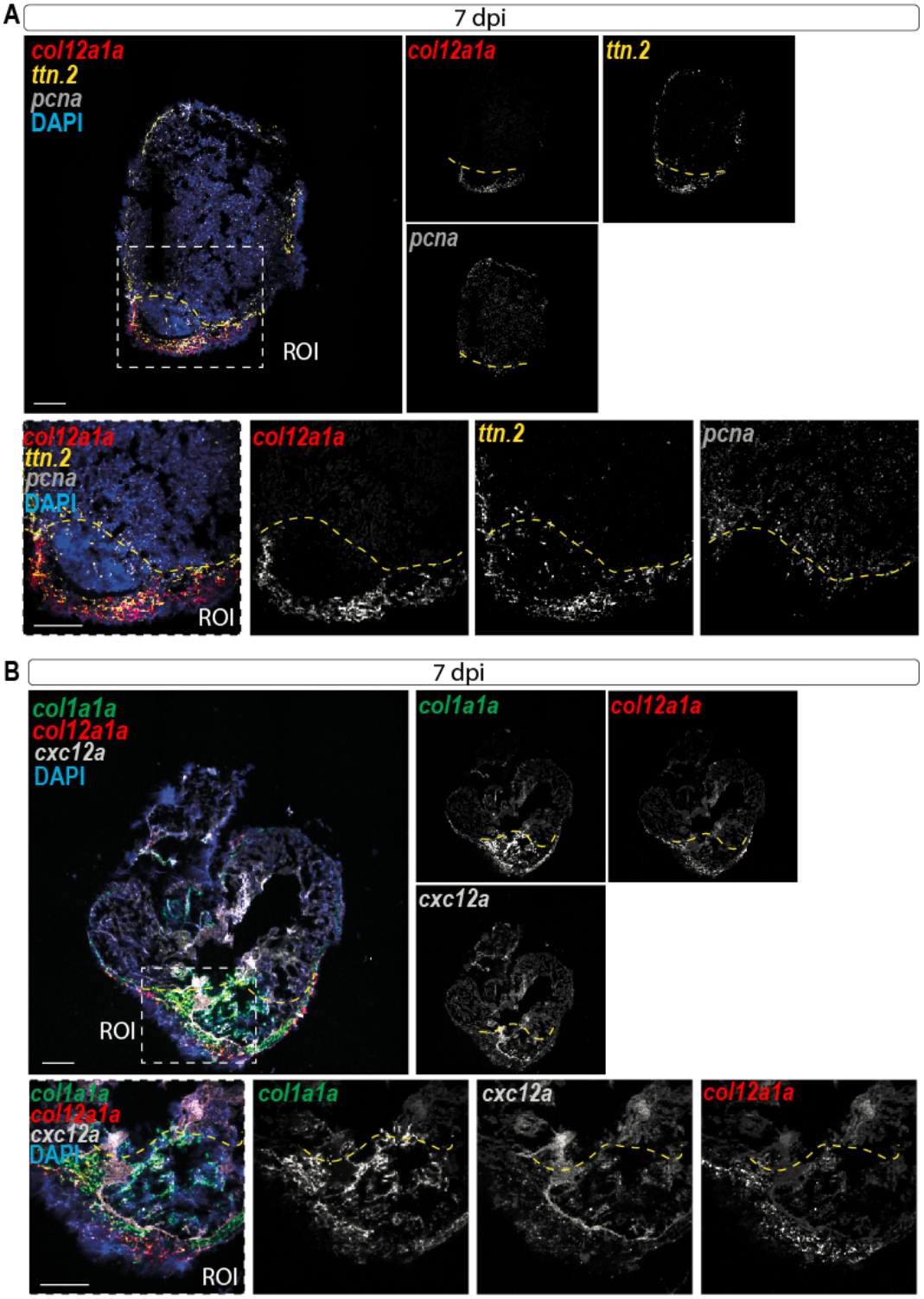

Figure 32: RNAscope marker genes for cell types of interest at 7 dpi. Markers for transient cell types (*col12a1a - red, cxcl12a - gray, ttn.2 - yellow* for dedifferentiated cardiomyocytes, *pcna* - proliferation marker) are localized at the injury area. Yellow dashed lines indicate injury area (IA). Scale bar: 100 µm.

Next, I tested the expression of selected marker genes at 7 dpi (Fig. 32). At 7 dpi *ttn.2* (a marker for dedifferentiated CMs) was detected in the injury area, while proliferating cells are highly expressed in the injury border zone, possibly marking proliferating CMs peaking at 7 dpi (Fig. 32A). Interestingly, *ttn.2* and *col12a1a* strongly co-localize at 7 dpi, suggesting that there might be an interaction between *col12a1a* fibroblasts and dedifferentated CMs (Fig. 32A). Based on our RNA-seq analysis, (Fig. 27) *cxcl12a* fibroblasts should increase in number at 7 dpi. Also, it is known that CXCL12 is improving regeneration in adult mice by re-activation of collateral development (Das et al., 2019). I confirmed the expression of *cxcl12a* fibroblasts at 7 dpi and I localized them in the injury area suggesting their possible role in heart regeneration (Fig. 32B).

To sum up, my RNAscope in situ hybridization analysis confirmed the expression of several transiently peaking genes detected by scRNA-seq. Moreover, I could show specific localization of the transient fibroblast cell states in the border zone as well as injury area, further corroborating our hypothesis that these cells contribute to the regenerative niche and regulate injury response and/or regeneration.

In the next part of the experiment, the expression of known pro-regenerative signalling factors was investigated (Fig. 33A). Our analysis revealed that *fn1a* is expressed mostly in *col11a1a* fibroblasts, that *nrg1* is highly expressed in *col12a1a* fibroblasts and retinoic acid (*aldh1a2*) is highly expressed by *nppc* fibroblasts as well as the epicardium (Fig. 33A). Another important finding was that the retinoic acid readout gene *stra6* (stimulated by retinoic acid 6) (Bouillet et al., 1995; Isken et al., 2008) is produced in high levels in *col11/col12* and proliferating fibroblasts (but not in cardiomyocytes) indicating that there could be a communication between these cell types. Furthermore, we showed a strong interaction between perivascular cells and blood vessel endothelium via Cxcl12b-Cxcr4a chemokine signalling (Fig. 33A). Perivascular cells were reported to have a function in blood-vessel formation (Bergers and Song, 2005), and it was recently shown that Cxcl12b-Cxcr4a signalling is important for revascularization of the regenerating zebrafish heart (Marín-Juez et al., 2019). Moreover, RNAscope showed that *aldh1a2* is highly expressed in the epicardial part of the injury area (but not exclusively), co-localizing with *col1a1a* and *cytochrome P450, subfamily b, polypeptide 1 (cyp261b)* (Fig. 26B). *Cyp26* enzymes were shown to metabolize RA efficiently and they are also inducible by RA in selected systems (Thatcher & Isoherranen, 2009).

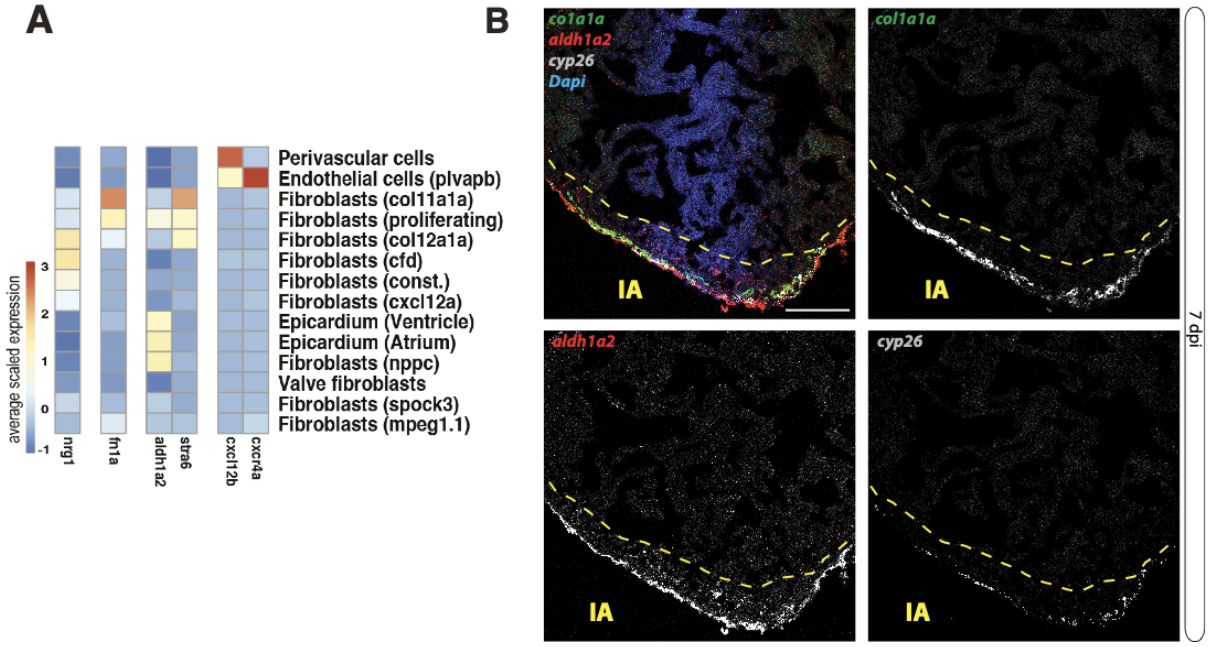

Figure 33: Signalling pro-regenerative factors are expressed by transient fibroblasts. (A) Average expression of selected signalling genes in fibroblast subclusters. Blood vessel endothelial cells were added to show their interaction with perivascular cells via Cxcl12b-Cxcr4a signalling. (B) Retinoic Acid (RA) signalling at 7 dpi. Fibroblasts marker *col1a1a* (green), *aldh1a2* (red), *cyp26b1* (gray). Yellow dashed lines indicate injury area (IA). Scale bar: 100 µm. The experiments were done in collaboration with Bo Hu, Junker lab.

In summary, based on their gene expression patterns, their timing of appearance, and their spatial position in the injury area, we identified three fibroblast states that appear to have a pro-regenerative function during heart regeneration: *col11* and *col12* fibroblasts, and *nppc* fibroblasts.

6.3.1.2 Pro-regenerative role of *col12a1a* fibroblasts

The spatiotemporal analysis of single-cell gene expression profiles strongly indicates a pro-regenerative function of transient fibroblasts. To validate this hypothesis, functional experiments are necessary to assess the potential pro-regenerative role of the transient *col11/col12* fibroblasts. I applied targeted genetic cell ablation using the Nitroreductase/metronidazole (NTR/MTZ) system (Curado et al., 2007). In this approach bacterial nitroreductase (NTR) is used to catalyze the reduction of non-toxic prodrug metronidazole (MTZ), resulting in the production of cytotoxic product that induces cell death (Curado et al., 2007).

Based on that principle, NTR was expressed in the transgenic zebrafish line using a tissue-specific promoter. Subsequent exposure to MTZ by adding it to the media induces cell death exclusively within NTR^+ cells.

In this experiment, I generated a transgenic line labelling *col12a1a*-expressing fibroblasts, *Tg(-4kbcol12a1a:GAL4VP16;UAS:NTR:RFP)* with the support of Alexander Meyer from Panakova lab (Fig. 34A*)* I further referred to this line as *col12a1a*>NTR:RFP for the rest of this work (Methods).

We first isolated *cis r*egulatory 4-kb upstream region of zebrafish *col12a1a* using sequence specific primers and genomic DNA as a template prepared from pooled zebrafish embryos between 24-72 hours post fertilization (hpf), and generated *col12a1a*>NTR:RFP transgenic line. I then verified whether the activity of this 4-kb upstream region of zebrafish *col12a1a* corresponded to the endogenous *col12a1a* expression in embryos of various stages (Fig. 34B). Using RNAscope *in situ* hybridization, I confirmed that the endogenous *col12a1a* expression colocalized with the *col12a1a*>NTR:RFP transgene. Next, to verify the functionality of the cell ablation approach, I treated *col12a1a*>NTR:RFP embryos at 48 hpf with MTZ. Importantly, I observed RFP+ aggregates after 24 hours of MTZ treatment, which are indicative of cell death as previously reported (Curado et al., 2007), (Fig. 34C).

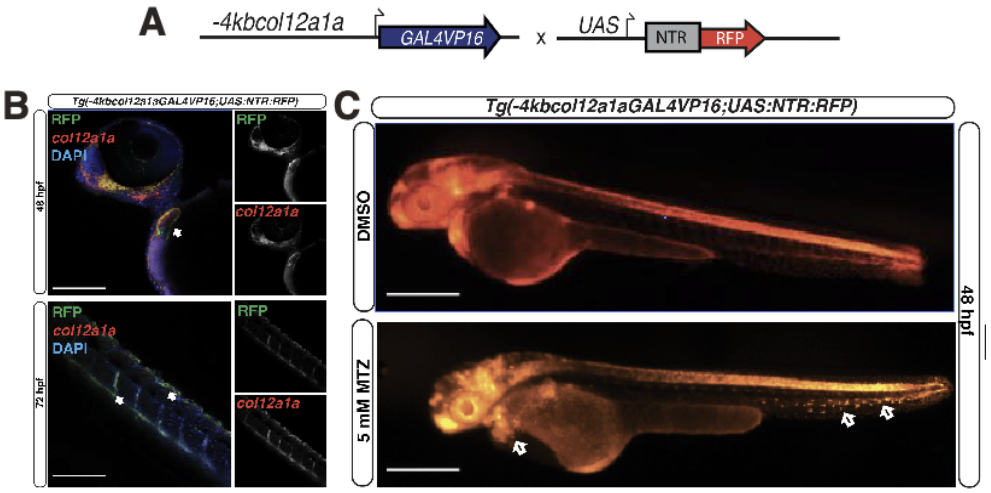

Figure 34: Characterization of *Tg(-4kbcol12a1aGAL4VP16;UAS:NTR:RFP) line* in zebrafish embryos. (A) Transgenic line with 4-kb upstream region of zebrafish *col12a1a*, GAL4VP transcriptional activator crossed to UAS:NTR:RFP reporter line. (B) Embryos at 48 hpf and 72 hpf showing expression of *col12a1a* in developing embryos (arrows: heart, somites) co-localizing with RFP signal. Scale bar: 100 µm. (C) Fluorescent images of embryos at 48 hpf treated with 0.1% DMSO or 5 mM of MTZ. Arrows point to aggregates of RFP in *Tg(-4kbcol12a1aGAL4VP16;UAS:NTR:RFP)* embryo after treatment with MTZ. Scale bar: 500 µm.

In uninjured adult hearts, RFP expression in *col12a1a*>NTR:RFP labelled cells colocalized with endogenous *col12a1a* expression in the epicardium (Fig. 35A). As anticipated, cryoinjury transiently induced both endogenous *col12a1a* as well as RFP expression in the injury area (Fig. 35B). This increase in the expression of *col12a1a*>NTR:RFP further indicates that all important *cis* regulatory elements were amplified and are encoded within the 4kb region. I then proceeded with the genetic ablation of the *col12a1a*-expression fibroblasts using MTZ treatment in adult fish. I treated adult *Tg(-4kbcol12a1aGAL4VP16;UAS:NTR:RFP)* fish with MTZ from day 2 after the injury until day 6 and investigated the hearts at 7 dpi time point.

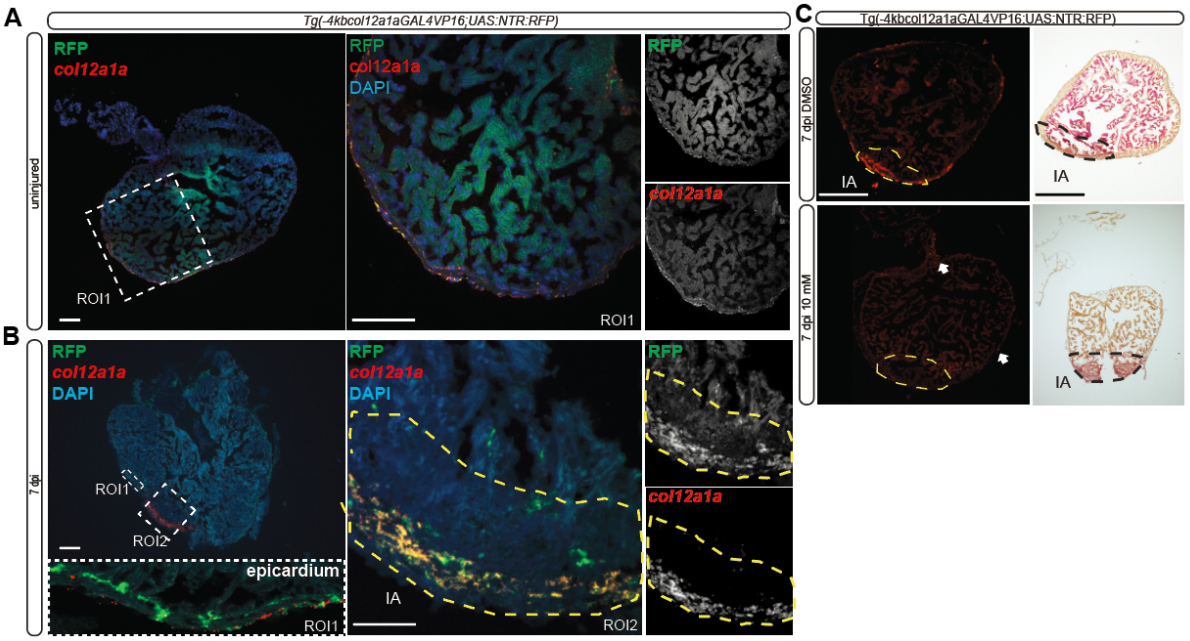

Figure 35: Characterization of *Tg(-4kbcol12a1aGAL4VP16;UAS:NTR:RFP) line* in adult fish. (A) Uninjured adult heart showing the relatively low expression of *col12a1a* in the epicardium (*col12a1a* in red, RFP in green). Region of interest (ROI) in the left panel as white dashed rectangle is shown at higher magnification in the panels on the right. Scale bar: 100 µm. (B) Expression of *col12a1a* in the injury area and the epicardium at 7dpi co-localizes with RFP signal (*col12a1a* in red, RFP in green). Regions of interest (ROI 1 & 2) in the upper left panel (white dashed rectangles) are shown at higher magnification in the panels below and on the right. Yellow dashed lines indicate injury area (IA). Scale bar: 100 µm. (C) Fluorescent images of 0.2% DMSO- and 10mM MTZ-treated hearts at 7dpi. Arrows point to *col12a1a* aggregates. Yellow dashed lines indicate injury area. Histological comparison of the injury area at 7 dpi with or without MTZ treatment. Scale bar: 300µm.

Additionally, I treated the fish with the second pulse from 14 dpi to 16 dpi when I analyzed the 30 dpi time point (Fig. 36A). At 7dpi, MTZ-treated *col12a1a*>NTR:RFP fish displayed a marked reduction in RFP expression, in line with our experimental design (Fig. 35C). While the injured area in *col12a1a*-depleted hearts at 7 dpi overall looked histologically without any abnormalities (Fig. 35C, 36B), 5/6 hearts displayed a reduction in cardiomyocyte proliferation upon depletion of *col12a1a* expressing cells compared to vehicle control (Fig. 36C,D).

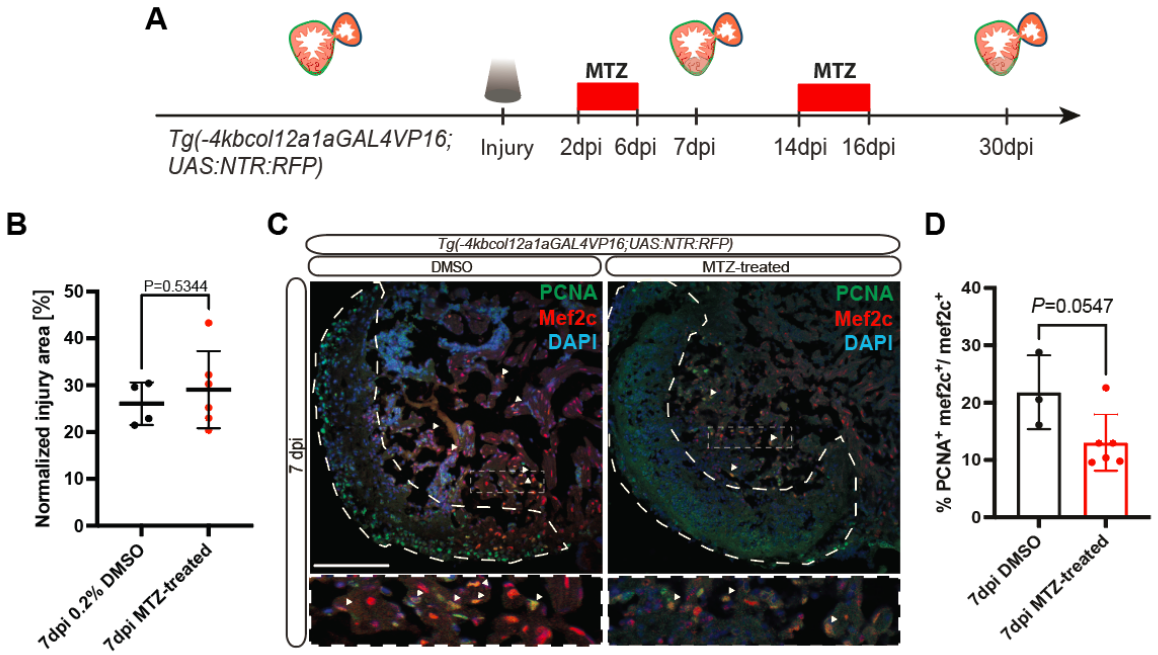

Figure 36: Pro-regenerative role of *col12a1a* fibroblasts at 7 dpi.
(A) Experimental design of NTR/MTZ ablation of *col12a1a* fibroblasts. *Tg(-4kbcol12a1aGAL4VP16;UAS:NTR:RFP)* fish were treated with MTZ from 2 dpi to 6 dpi when analyzed at 7 dpi or additionally with the 2nd pulse from 14 dpi to 16 dpi when analyzed at 30 dpi. (B) Relative size of the injury area across all histological replicates at 7 dpi in 0.2% DMSO- (n=4), and MTZ-treated (n=6) hearts, mean and standard deviation are shown. Student's t-test. (C) Immunostaining of sections of cryoinjured hearts of *Tg(-4kb-col12a1aGAL4VP16;UAS:NTR:RFP)* zebrafish treated with DMSO and MTZ at 7 dpi; sections stained for Mef2c (CMs, red), PCNA (proliferation marker, green), and DNA (DAPI, blue). Arrowheads point to PCNA+ CMs, white dashed lines indicate injury area. Scale bar: 100 µm.(H) Percentage of PCNA+ CMs in DMSO-treated fish (n=3) and MTZ-treated fish (n=6) at 7 dpi. Student's t-test.

When assessed hearts at 30 dpi, I found that heart regeneration was impaired upon *col12a1a*+ cell ablation (Fig. 37), suggesting that transiently activated *col12a1a*-expressing fibroblasts contribute to the regenerative capacity of the zebrafish heart.

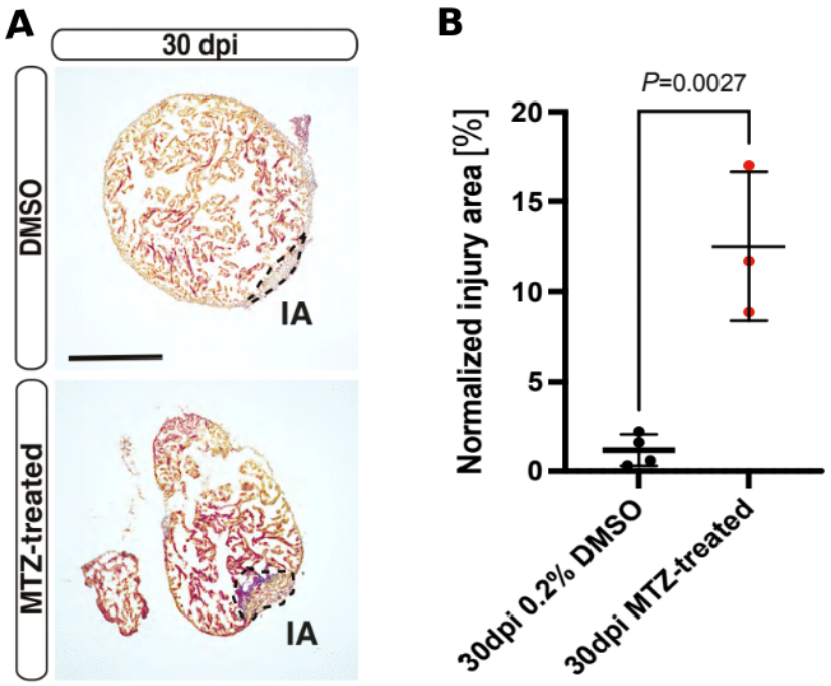

Figure 37: Pro-regenerative role of *col12a1a* fibroblasts at 30 dpi. (A) Histological comparison of the injury area (IA) at 30 dpi with or without MTZ treatment. Scale bar: 300µm. (J) Relative size of the injury area across all histological replicates at 30 dpi in 0.2% DMSO (n=4), MTZ-treated (n=3), mean and standard deviation are shown. Student's T-test.

Important to note, I could not fully confirm that ablation of *col12a1a* expressing cells could potentially result in additional tissue degradation of the ventricle not being related to the regeneration process alone. However, due to lack of *col12a1a* reporter expression in the uninjured ventricle (Fig. 35A) and due to lack of any visible degeneration outside the injury site (Fig. 35C) I believe that this effect would not be significant.

Altogether, the ablation of *col12a1a* expressing cells during the regeneration process led to significant delay in regeneration suggesting the pro-regenerative role for *col12* fibroblasts.

6.4.1 Identification of the origin of pro-regenerative fibroblasts

To understand more the mechanism of activation of transient pro-regenerative fibroblasts, we decided to uncover their origin. As shown in our publication (Hu et al., 2022) we deployed the computational analysis performed by Baastian Spanjaard (Junker lab). He could show a clear distinction between the fibroblasts origin; in zebrafish, the fibroblasts after cryoinjury are derived either from epicardium or endocardium.

In order to validate the lineage origin of the transient fibroblasts, I performed a genetic lineage tracing experiment based on Cre-*loxP* approach in regenerating hearts. The Cre-*loxP* approach is used for genetic lineage tracing by cell marking via genetic recombination. Here, a Cre recombinase enzyme is expressed in a cell- or tissue- specific manner to iniciate the expression of a conditional reporter gene resulting in constant genetic labelling of all progeny of all marked cells (Kretzschmar and Watt, 2012). Gene of interest is flanked with the *loxP* sites, which enables the gene to be excised or inverted based on the orientation of the *loxP* sites. To control the time and space of the recombination a tissue-specific promoter, the heat-shock-induced Cre recombinase expression or the addition of 4-hydroxy tamoxifen (4-OHT) to translocate a Cre–estrogen receptor fusion protein (Cre–ER) to the nucleus can be applied (Brown et al., 2018). In this study we chose *tcf21* and *fli1* tissue-specific promoters and the expression was activated by use of 4-OHT in combination with the heat-shock.

Transgenic line *Tg(tcf21:CreERT2; ubi:Switch)* was used to determine fibroblasts originating from epicardium and *Tg(fli1:CreERT2; hsp70l:Switch)* to mark endocardial fibroblasts.

6.4.1.2 Identification of pro-regenerative epicardial fibroblasts

The computational analysis indicated that perivascular cells, *cxcl12a*, *cfd*, *col11a1a* and *col12a1a* fibroblasts arise from the epicardium. To corroborate the computational approach, I performed a genetic lineage tracing experiment in regenerating hearts using the transgenic line *Tg(tcf21:CreERT2; ubi:Switch)*. Our scRNA-seq data showed that *tcf21* is expressed in epicardial cells, constitutive fibroblasts and other fibroblast types of the epicardial cluster (Fig. 38A).

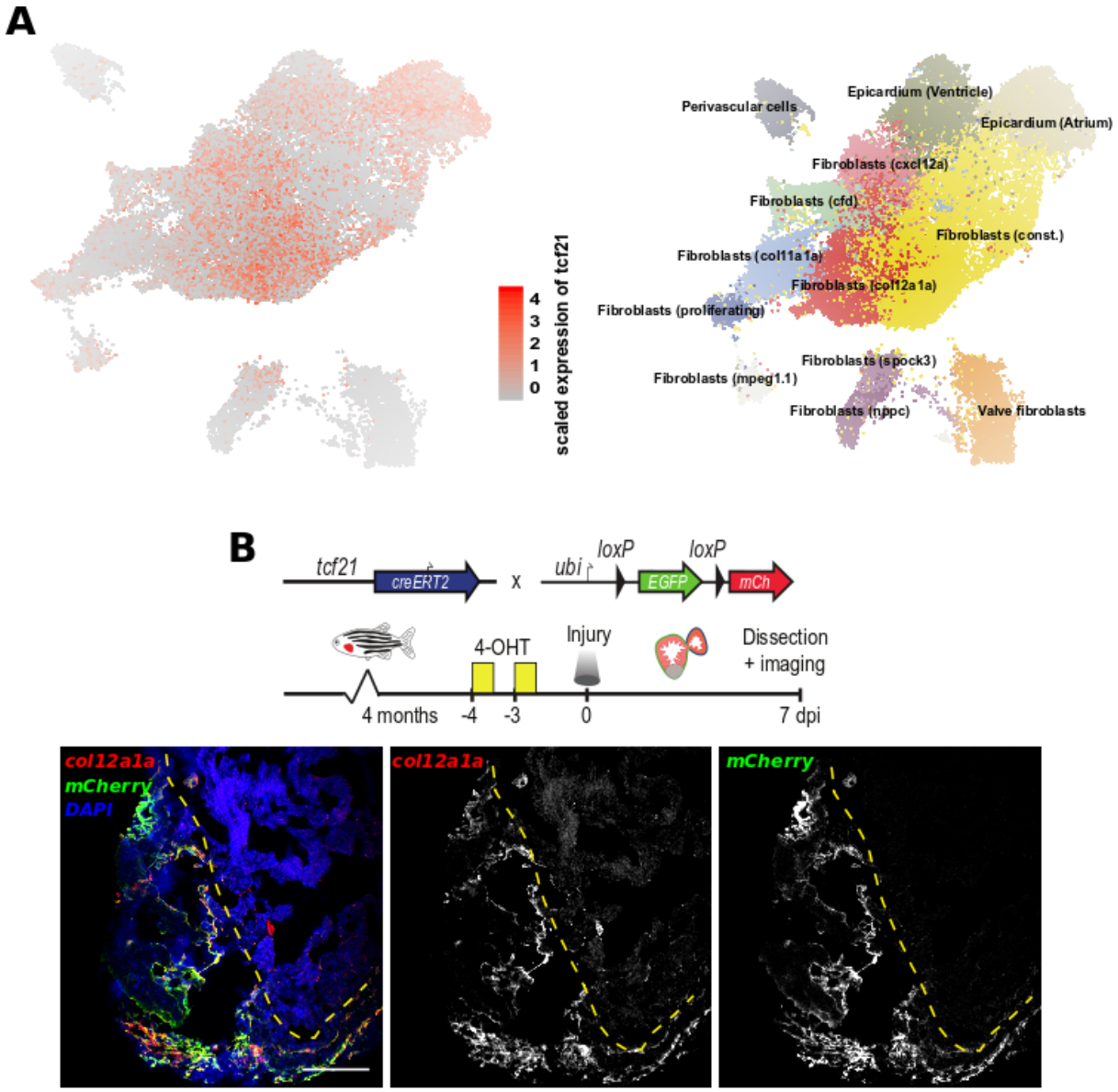

Figure 38: Epicardial origin of *col12a1a* fibroblasts. (A) Expression pattern of *tcf21*. *Tcf21* is expressed in epicardial cells, constitutive fibroblasts and other fibroblast types of the epicardial cluster. (B) Cre-lox lineage tracing at 7 dpi confirms epicardial origin of *col12a1a*-expressing cells. Scale bar: 100µm. The experiments were done in collaboration with Bastiaan Spanjaard, Junker lab.

To activate the labelling of the epicardial and epicard-derived cells in response to the injury, adult fish were treated with 4-OHT from four to three days before the injury. Genetic lineage tracing was assessed at 7 dpi, when expression of *col12a1a* peaks after the injury (Fig. 38B). It would have been also possible to induce the recombination in embryos, which would give us information about epicard-derived cells from the beginning of the development not only injury-induced.

After recombination, expression of mCherry at 7 dpi colocalizes with endogenous expression of *col12a1a* (Fig. 38B), corroborating the origin of the transient *col11a1a* and *col12a1a* fibroblasts from the epicardium, or from epicardial-derived fibroblasts.

6.4.1.3 Identification of pro-regenerative endocardial fibroblasts

Epicardium is known to be the main source of the cardiac fibroblasts. Cardiac fibroblasts, however, can also originate from endocardium (Talman and Ruskoaho, 2016). Up to today, the research has focused only on epicard-derived fibroblasts in the regenerating zebrafish hearts. Whether the fibroblasts can be derived also from the endocardium is not resolved. Moreover, whether such fibroblasts play a role during zebrafish heart regeneration needs to be investigated (Sánchez-Iranzo et al., 2018). Our computational approach identified that fibroblasts after cryoinjury can originate also from the endocardium (Hu et al. 2022). These fibroblasts were characterised by expression of *nppc*, *spock3* and *angptl7.* To confirm the endocardial origin of *nppc* cardiac fibroblasts, we performed genetic lineage tracing using the transgenic line *Tg(fli1:CreERT2; hsp70l:Switch)* to mark endocardial cells. Fli1 promoter was used for the identification of endocardial and endothelial-derived cells and the recombination was activated in the embryo using 4-OHT and heat-shock.
I focused on *nppc* fibroblasts due to their transient expression, peaking at 7dpi and potential pro-regenerative role. These fibroblasts additionally to expressing *nppc* and ECM genes such as *col1a1a*, also were expressing endothelial markers (e.g.*vwf, fli1a*), which could have a potential role in angiogenesis. In this study, zebrafish embryos were treated with 4-OHT from 24 hpf to 48 hpf, heat-shocked for 1h at 37°C and the genetic lineage tracing was assessed in the adult fish 7 days after the injury (Fig. 39, schematic). After embryonic recombination, expression of EGFP at 7 dpi colocalized with endogenous expression of *nppc* (Fig. 39), corroborating the endocardial origin of the transient *nppc* fibroblasts.

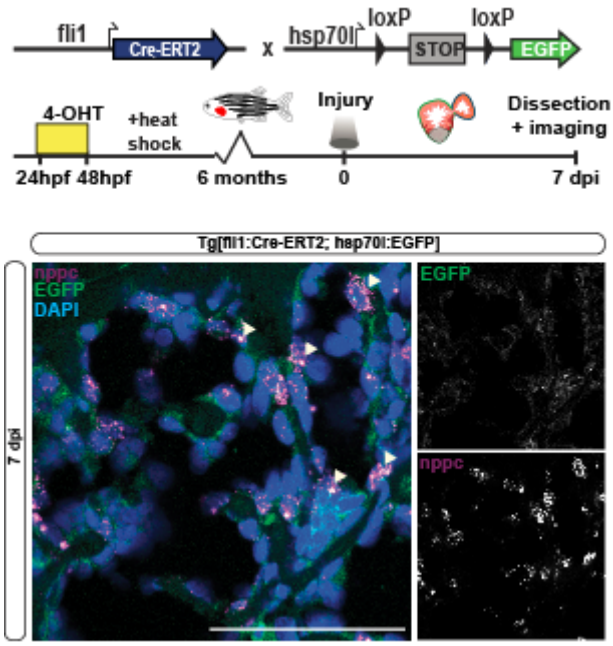

Figure 39: Endocardial origin of *nppc*-expressing fibroblasts. Cre-lox lineage tracing confirms endocardial origin of *nppc*-expressing fibroblasts in cryoinjured hearts at 7 dpi. Sections stained for GFP (green), and *nppc* (magenta). Arrowheads point to *nppc* and EGFP colocalization. Asterisks point to *nppc*-positive delaminating cells. Scale bar: 100µm.

As mentioned before, *nppc*-expressing fibroblasts were clustered as fibroblasts due to high expression of many ECM-related factors. Moreover, these fibroblasts also upregulate *twist1b* and express *snail2* (Hu et al. 2022), which are the markers of epithelial to mesenchymal transition. In the previous study, Sánchez-Iranzo et al. reported that endocardium does not give rise to fibroblasts using *kdrl/fli1* lineage tracing, however their finding was based mostly on the morphology and bulk RNA-seq of sorted endocardial-cells. Thus, this sequencing data corresponds to the combination of activated endocardium and *nppc* fibroblasts, which could have been a reason for less pronounced fibroblasts expression profile compared to our study. Sánchez-Iranzo et al. mentioned that "endocardial cells close to the IA became more rounded'', and it is possible that this sub-population corresponds to our *nppc* fibroblasts (Sánchez-Iranzo et al., 2018). Additionally, in this study *nppc*+ appeared to be delaminating (Fig. 39, asterisks) suggesting that nppc fibroblasts can undergo at least partial transition into mesenchymal state. However, we hypothesize that *nppc*-expressing fibroblasts do not acquire full mesenchymal state due to no clear downregulation of *VE-cadherin* (*cdh5*) or an upregulation of *N-cadherin* (*cdh2*).

To provide an additional proof for *nppc* endocardial origin, we performed an experiment with the increasing time of cryoinjury procedure (Fig. 40).

We hypothesized that only with the deep enough injuries endocardial response can be achieved and *nppc*-fibroblasts would be present. Hearts were injured from 5s to 25s and the injury area, together with *nppc* expression were analyzed. We showed that longer contact of the cryoprobe with the heart resulted in a bigger injury area and led to much stronger *nppc* expression beyond the border zone, compared to the shorter injuries (Fig. 40)

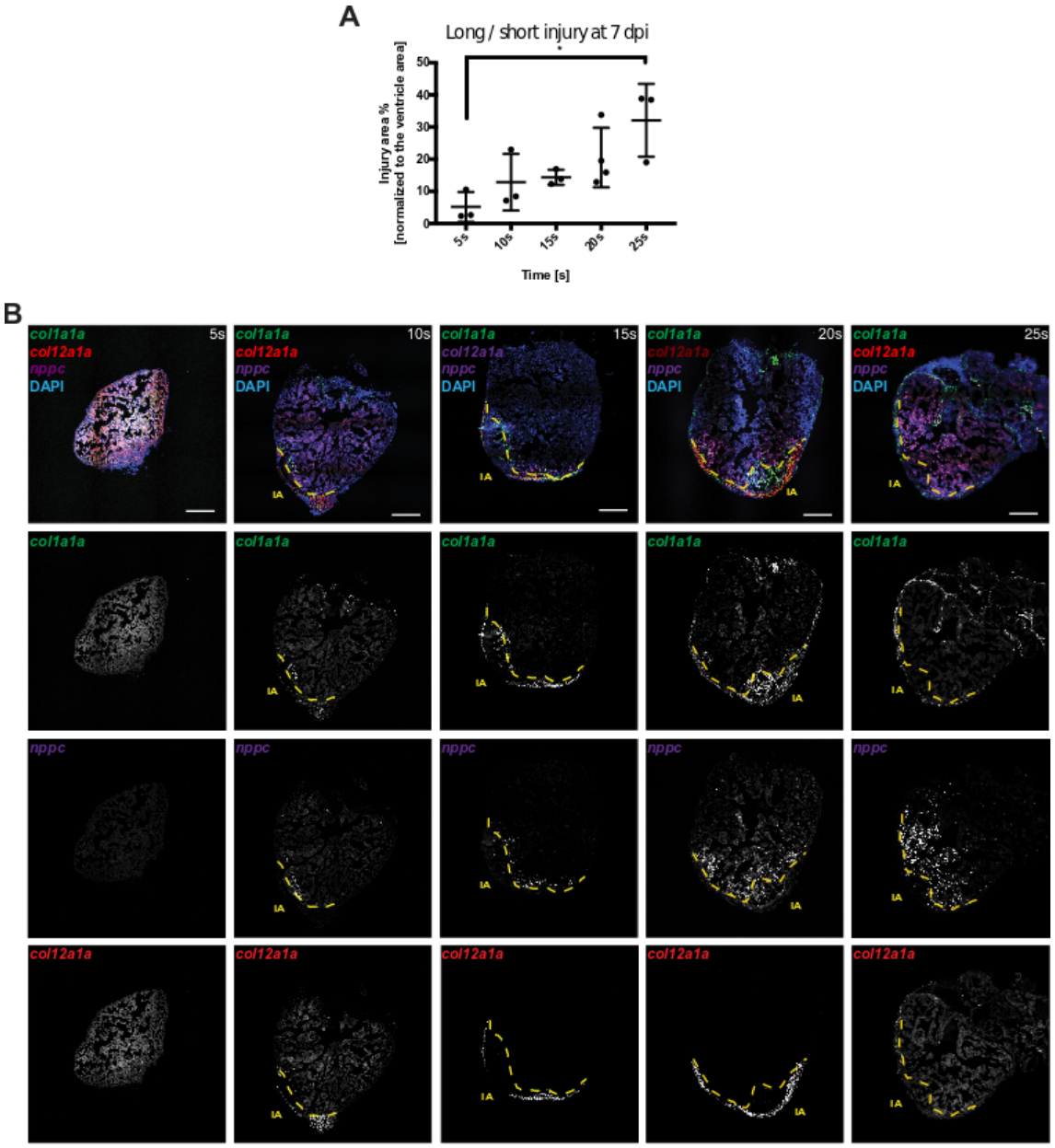

Figure 40: Longer injuries cause higher nppc expression. (A) Quantification of long and short injuries at 7 dpi. Injury areas (IA) in % were normalized to the ventricular area. (n_{5s}=3, n_{10s}=3, n_{15s}=3, n_{20s}=4, n_{25s}=3). Mean ± SD. *One-way ANOVA with Tukey's multiple comparison test. *P=0.0128. (B) Injuries of 20s (standard procedure) and 25s penetrate deeper through heart cell layers and generate *nppc* expression in the endocardium. Scale bar: 100 µm.

In summary I was able to show that cardiac fibroblasts such as *nppc*-fibroblasts can also originate from endocardium after cryoinjury. Furthermore, the internal position of the endocardium, as well as the transient nature of the *nppc* fibroblasts, might mean that these cells are only generated from damaged endocardium with the deep enough injury.

6.4.2 Cellular dissection of the role of canonical Wnt signalling

We were able to identify the origin of *col11, col12* and *nppc* fibroblasts using genetic lineage analysis. It remains uncertain, however, which signalling pathways are necessary to generate these transient cell states upon injury.

To assess the mechanisms of fibroblasts activation, inhibition of the signalling pathway can be used. Moreover, these perturbation experiments can show whether cells with a shared lineage origin exhibit similar changes after a stimulus, i.e. whether lineage relationship is predictive for perturbation response.

Based on our scRNA-seq data set, fibroblasts express many components of the Wnt signalling pathway (ligands, receptors, modulators) upon the injury (Fig. 41), which motivated us to dissect the role of canonical Wnt signalling in the zebrafish heart regeneration.

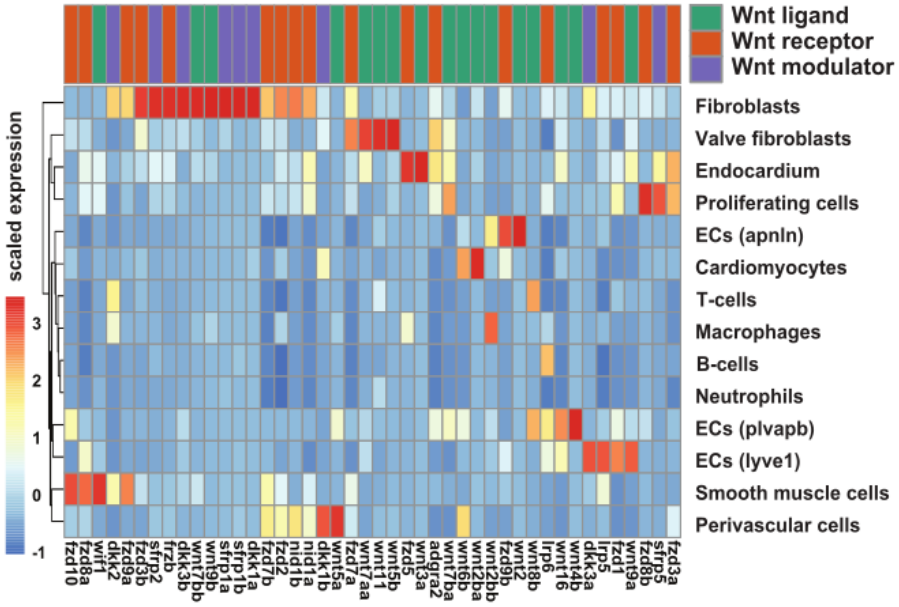

Figure 41: Expression of Wnt signalling components in the different cell types of the zebrafish regenerating heart. Heatmap presents different Wnt ligands, receptors, modulators expression in different cell types upon the injury. The experiments were done in collaboration with Bo Hu, Junker lab.

The role of Wnt signalling in heart regeneration is still not fully understood (Ozhan and Weidinger, 2015): Wnt is generally considered a pro-proliferative factor, and Wnt activation has been shown to be crucial for zebrafish heart regeneration by promoting cardiomyocyte regeneration (Bertozzi et al., 2022) Further, Wnt signalling was also reported to be beneficial for fin and spinal cord regeneration (Wehner et al., 2017; Chen et al., 2009). Other studies, however, showed that activation of Wnt signalling suppressed cardiomyocyte dedifferentiation and proliferation in regenerating zebrafish hearts (Zhao et al., 2019; Peng et al., 2021). Clearly, the role of Wnt signalling in cardiac regeneration is extremely complex and has to be further investigated to parse out the actual mechanisms of the pro-regenerative effects as well as its role in suppression of CM proliferation. Based on our previous findings of cardiac cell types and their characteristics including the origin, location and dynamics upon the injury, I, together with Junker lab, have decided to analyze Wnt signalling on the cellular level.

In order to inhibit canonical Wnt signalling after the cryoinjury, IWR-1 Wnt/β-catenin-dependent signalling inhibitor was used. IWR-1 is a tankyrase inhibitor, which promotes β-catenin phosphorylation by stabilizing Axin-scaffolded destruction complexes. Fish were injured and intraperitoneally injected (IP) each second day with the drug (both days for 3 dpi time point) and observed its effects at 3, 7, 15, and 30 dpi (Fig. 42).

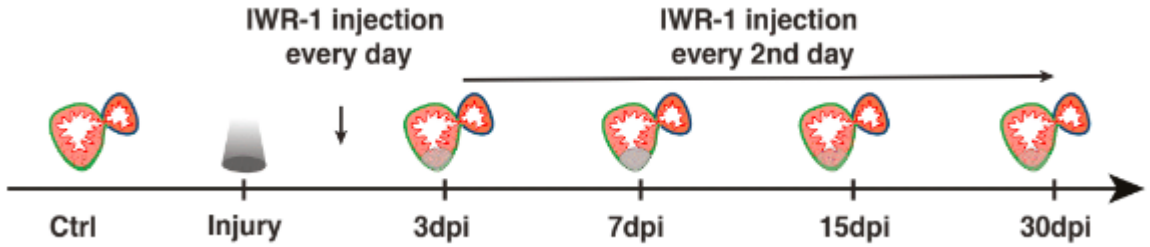

Figure 42: Experimental design of Wnt inhibition experiment. Fish were cryoinjured and IP injected with IWR-1 Wnt inhibitor every day for 3 dpi time point and each second day for 7, 15, and 30 dpi analysis.

6.4.2.1 Effect of Wnt/β-catenin signalling inhibition on heart regeneration process

First, I observed the regeneration process after the Wnt/β-catenin inhibition using histology, namely AFOG staining. Using this method, I can observe healthy myocardium in orange, collagen in blue and fibrin in red. Wnt/β-catenin signalling inhibition led to a significant delay in heart regeneration, with prolonged fibrosis and increased injury area compared to the control 30 days after the injury (Fig. 43).

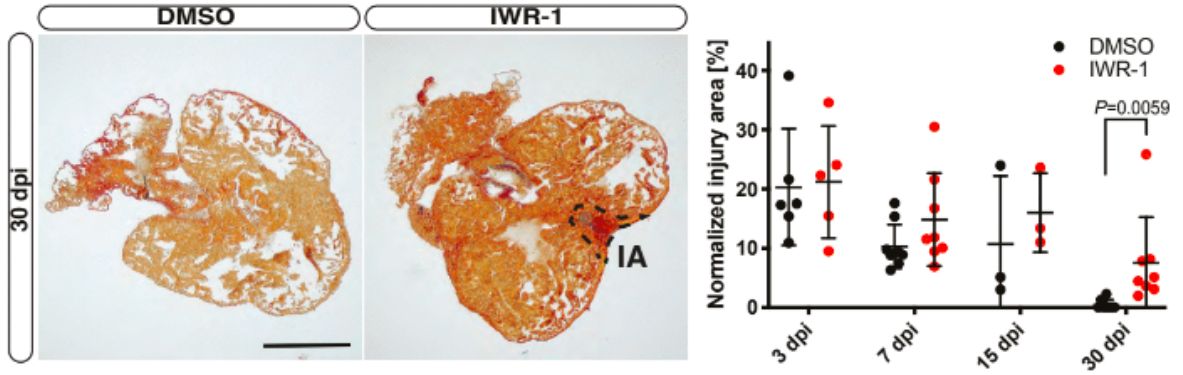

Figure 43: Delay in regeneration process after Wnt/β-catenin signalling inhibition. Left: Histological comparison of the injury area (IA) at 30 dpi with IP injections of IWR-1 or DMSO as a control. The paraffin sections were stained with AFOG staining, myocardium in orange, fibrin in red, and collagen in blue are clearly visible in IA in IWR-1-treated, but not in DMSO-treated hearts at 30 dpi. Scale bar: 300µm. Right: Normalized IA across all histological replicates, mean and standard deviation are shown. Student's t-test.

6.4.2.2 Effect of Wnt/β-catenin signalling inhibition on different cell types during regeneration

In order to uncover how Wnt/β-catenin signalling inhibition effects different cell types that we have initially identified as being crucial for regeneration, we used scRNA-seq approach. We perform single-cell analysis at 3- and 7 dpi. First, we characterized the differences in differentiated cardiomyocytes (Fig. 44)

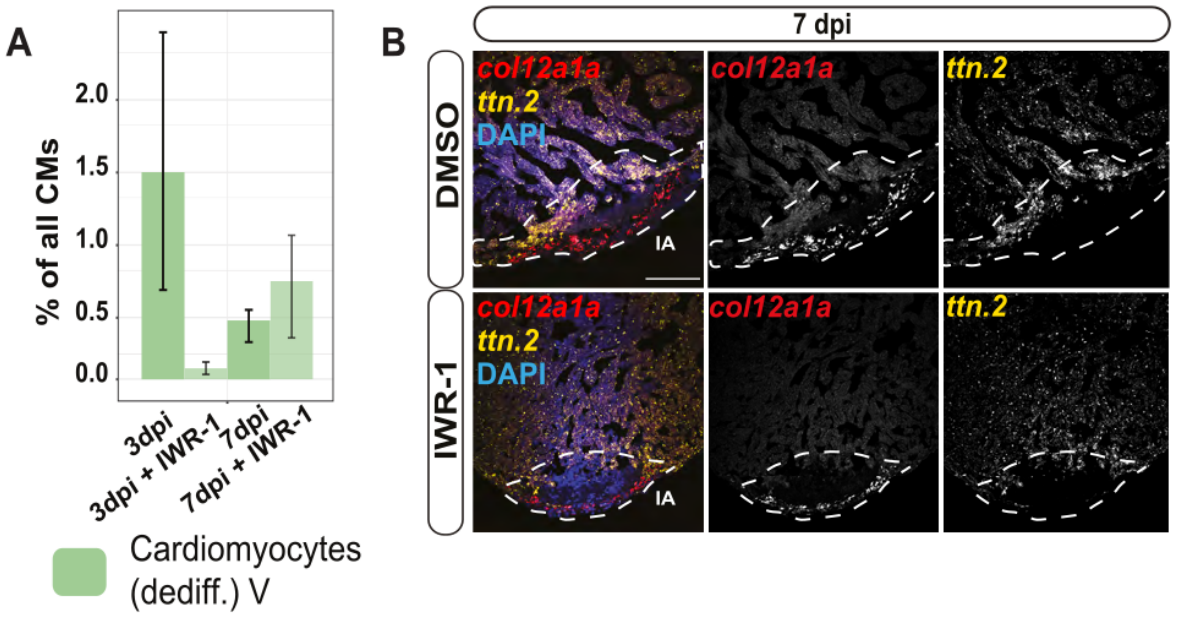

Figure 44: Effect of Wnt/β-catenin signalling inhibition on dedifferentiated cardiomyocytes. (A) Changes in the number of dedifferentiated cardiomyocytes at 3 and 7 dpi between Wnt inhibited (IWR-1) and control (DMSO) hearts. (B) Localization of dedifferentiated (ttn.2) cardiomyocytes (yellow) at 7 dpi in the injured heart with or without Wnt inhibition. Error bars show standard error of the mean. Scale bar:100µm. White dashed lines indicate the injury area. The experiments were done in collaboration with Bo Hu, Junker lab.

The results of scRNA-seq of IWR-1 treated hearts at 3 dpi and 7 dpi showed that cardiomyocyte dedifferentiation was delayed upon Wnt inhibition (Fig. 44A). At 3 dpi the number of dedifferentiated CMs from Wnt inhibited hearts were reduced, however, they increased at 7 dpi. Additionally, dedifferentiated CMs at 7 dpi do not localize to the injury area compared to the control (Fig. 44B), Indicating that the migration of dedifferentiated CMs could have been impared after Wnt inhibition.

Next, we investigated the effect of canonical Wnt inhibition on non-cardiomyocyte cell types. We focused on the fibroblasts due to their potential pro-regenerative function. Interestingly, only epicardial-derived fibroblast cluster decreased, was perivascular cells. In addition, all endocardium-derived fibroblasts including *nppc, spock3 and* valve fibroblasts were strongly reduced upon Wnt inhibition (Fig. 45A) . All other transiently expressed fibroblasts overall remained at similar levels (Fig. 46). Interestingly, the overall abundance of *col11a1a* and *col12a1a* fibroblasts remain the same (Fig. 46), however *col12a1a* fibroblast numbers peaked earlier upon Wnt inhibition (at 3 dpi instead of 7 dpi), which could be caused by an indirect effect due to the observed impairment of heart regeneration.

Cfd and *cxcl12a* fibroblast abundance is transiently reduced in untreated hearts at 3 dpi (Fig. 46), and this transient depletion seems to be extended to 7 dpi upon IWR-1 treatment. I corroborated these results by RNAscope looking both at perivascular cell (using *pdgfrb* as a marker) originating from epicardium and *nppc* fibroblasts as an example of endocardial-derived fibroblast affected by the Wnt inhibition (Fig. 45B). I could show that there was a significant decrease of *pdgfrb* and *nppc* expression after canonical Wnt inhibition at 7 dpi and there was no detectable difference in *col1a1a* expression.

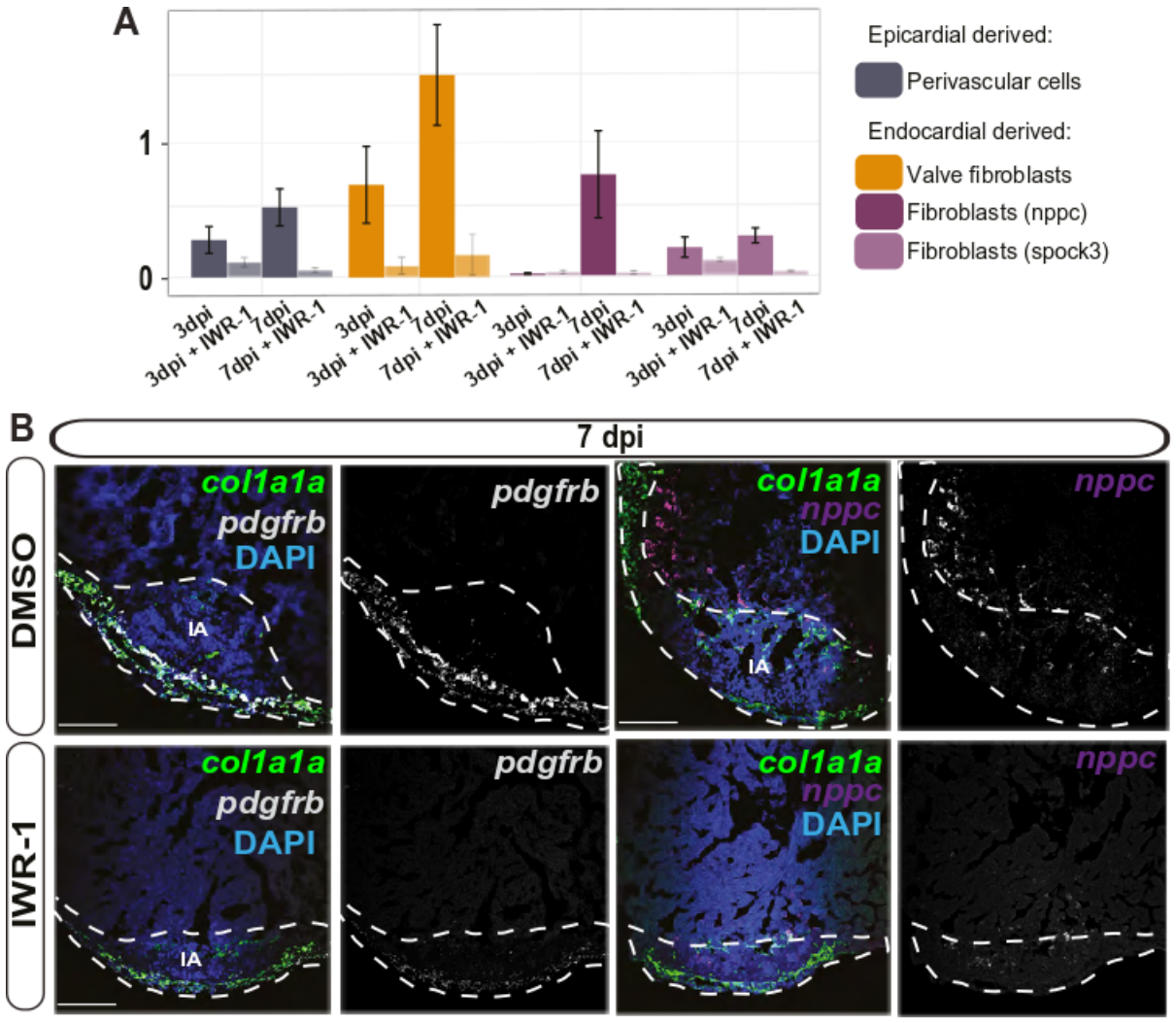

Figure 45: Effect of Wnt/ -catenin signalling inhibition on fibroblasts. (A) Changes in abundance of fibroblasts upon Wnt inhibition at 3 and 7 dpi. Error bars show standard error of the mean. (B) RNAscope of perivascular cells (*pdgfrb*, white) and fibroblasts (*nppc*, purple) in cryoinjured hearts at 7 dpi with or without Wnt inhibition. Scale bar: 100µm. White dashed lines indicate the injury area.The experiments were done in collaboration with Bo Hu, Junker lab.

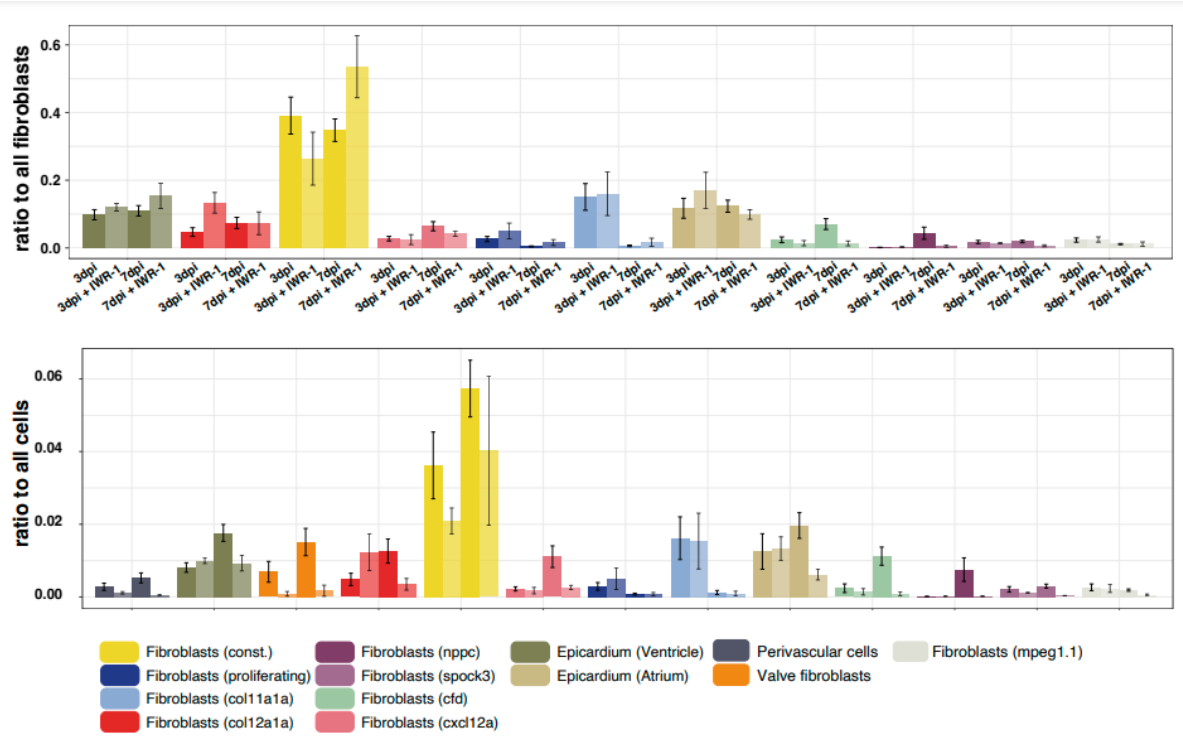

Figure 46: Comparison of cell type abundance for all fibroblast subtypes at 3 and 7 dpi with or without Wnt inhibition. Two types of normalization are shown: either cell numbers were normalized to total number of fibroblasts, or to total number of cells. Mean value across all replicates of the same treatment and time point is shown, error bars indicate standard error of the mean. The experiments were done in collaboration with Bo Hu, Junker lab.

These results indicate that Wnt signalling is necessary for the activation of endocardial fibroblasts, similar to the reported data of Wnt role in endothelial-to-mesenchymal transition in mice (Aisagbonhi et al., 2011; Duan et al,. 2012).

6.4.2.3 Effect of Wnt/β-catenin signalling inhibition on revascularization

To understand how the missing cell types could mediate the observed delay in regeneration we decided to perform more functional experiments. It was reported that perivascular cells have a pro-angiogenic role via signalling and mechanical stabilization of nascent vasculature (Carmeliet, 2000). We observed high expression of the chemokine *cxcl12b* in perivascular cells in our data set (Fig. 26A), which is an additional confirmation for pro-angiogenic function of these cells. It was previously shown that cxcl12b-cxcr4a signalling regulates superficial revascularization in zebrafish heart (Marín-Juez et al., 2019).

Recently, also NPPC signalling was found to have a role in the cardiovascular system including pro-angiogenic function (Moyes and Hobbs, 2019). It was reported that NPPC is a crucial regulator of angiogenesis and vascular remodelling after ischemia in cells and mice (Bubb et al., 2019). The study by Zhang et al. showed that *nppc* is essential for zebrafish angiogenesis by controlling the endothelial cell proliferation and migration (Zhang et al., 2017). Moreover, NPPC signalling was also reported to be important for zebrafish fin regeneration (Shi et al., 2021). All this information suggests that Wnt inhibition might delay heat regeneration via reduced revascularization upon injury.

In order to evaluate revascularization after the cryoinjury and Wnt inhibition, together with Hadil el Sammal (Stainier lab) we designed the study and Hadil el Sammak performed the experiments. First, we quantified the proliferation of coronary endothelial cells (cECs) at 4 dpi. The experiment was done using *Tg(-0.8flt1:RFP)* zebrafish line to label coronaries in RFP signal. Next, the proliferation using PCNA as a marker was analyzed using co-localization of RFP+/PCNA+ cells at 4 dpi and compared between uninhibited and Wnt inhibited hearts. Treatment with IWR-1 resulted in notable but not significant reduction of cEC proliferation at 4 dpi (Fig. 47A,B).

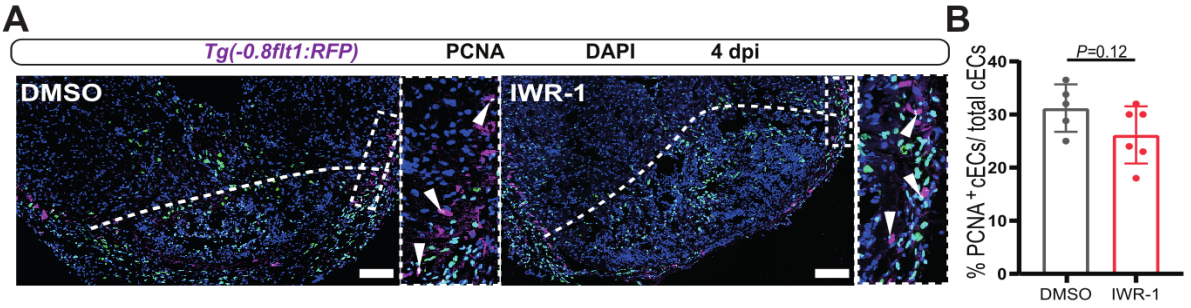

Figure 47: Effect of Wnt inhibition on the proliferation of coronary endothelial cells (cECs) at 4 dpi. (A) Immunostaining of sections of cryoinjured hearts of *Tg(0.8flt1:RFP)* zebrafish after intraperitoneal (IP) injections with DMSO and IWR-1 at 4 dpi; sections stained for RFP (coronaries, magenta), PCNA (proliferation marker, green). Arrowheads point to PCNA+ cECs, white dashed lines indicate injury area. (B) Percentage of PCNA+ cECs in DMSO-injected fish (n=5) and IWR-1-injected fish (n=6) at 4 dpi. Student's t-test. The experiments were done in collaboration with Hadil el Sammak, Stainier lab.

Next, we decided to investigate the effect of Wnt inhibition on the coverage of coronaries in the injury area at 7 dpi. *Tg(-0.8flt1:RFP)* zebrafish line was used to label coronaries with RFP signal. The fluorescent intensity of coronaries was analyzed at 7 dpi and compared between untreated and Wnt inhibited hearts. Interestingly, the coverage of coronary vessels at 7 dpi was significantly reduced after IWR-1 treatment, suggesting the effect of Wnt inhibition on revascularization (Fig. 48A,B).

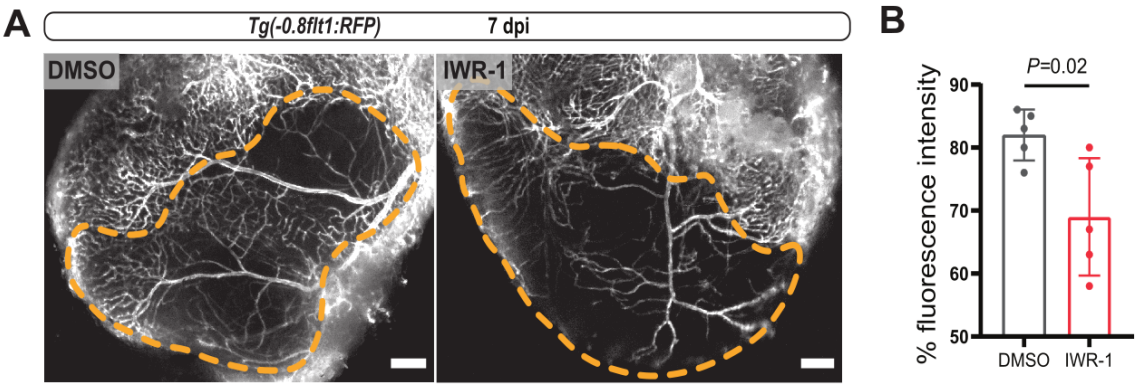

Figure 48: Effect of Wnt inhibition on coverage of coronary vessels in the injury area. (A) Whole mount images of 7 dpi *Tg(0.8flt1:RFP)* zebrafish after IP injections with DMSO and IWR-1. Orange dashed lines indicate the injury area. (B) Percentage of RFP fluorescence intensity in the injured tissue of 7 dpi *Tg(-0.8-flt1:RFP)* ventricles after IP injections with DMSO (n=5) and IWR-1 (n=5). Student's t-test. The experiments were done in collaboration with Hadil el Sammak, Stainier lab.

In summary, these results indicate that impairment in revascularization after inhibition of canonical Wnt could be at least partially responsible for the reported delay in regeneration. Importantly, the observed perturbation of regeneration was not caused by the reduced proliferation of cECs. One possible explanation is that other aspects of revascularization such as migration of coronaries or their interactions with perivascular cells are impaired in the hearts with inhibited Wnt canonical signalling. Together with recent work showing an effect of Wnt signalling on cardiomyocyte dedifferentiation and proliferation (Peng et al., 2021; Zhao et al., 2019; Bertozzi et al., 2022), these results highlight the importance of coordinated Wnt activity within the homeostatic signalling range.

7. Discussion

7.1 Zebrafish as a model to study cardiac regeneration

Zebrafish is an excellent model to study zebrafish cardiac regeneration due to multiple advantages that this small fish can provide. Firstly, it was shown that 71% of human genes have at least one zebrafish orthologue with 84% of known human disease-causing genes having a zebrafish counterpart (Howe et al., 2013). This similarity in genetic structure makes zebrafish a great model to study vertebrate gene function in many different fields including regeneration. Second, it has the same major organs and tissues as humans including brain, blood, gut, eyes and heart with highly conserved physiological functions (Gut et al., 2017). Third, the histological composition of the zebrafish heart is comparable to other vertebrates (González-Rosa et al., 2017). Additionally, zebrafish hearts compared to mammalian hearts can fully regenerate throughout their life even after multiple insults (Bise et al., 2020), although the efficiency of the regeneration decreases after repeated rounds of regeneration. To mimic the best human myocardial infarction, cryoinjury method was established (Chablais et al., 2011; González-Rosa et al., 2011; Schnabel et al., 2011) where necrosis followed by apoptosis takes place, affecting all cell types in the heart. Moreover, zebrafish maintenance is easier and cheaper than traditional rodent models. (Avdesh et al., 2012). In addition, the genetic manipulation in zebrafish is relatively easy compared to other models and the available genetic tools are making zebrafish increasingly appealing for regeneration studies. Transgenesis techniques are well-established and high fecundity of transparent embryos provides advantage when generating required tools.

To sum up, zebrafish have a great number of advantages as a model for cardiac regeneration studies and its similarity to higher vertebrates makes it an excellent translational model, in which the findings can be utilized in further translational models including human induced pluripotent stem cells with the aim to improve future treatments of human heart repair.

7.2 Morphine improves zebrafish welfare after cryoinjury procedure

All the advantages of zebrafish as a model for cardiac regeneration made them popular in the last 20 years in this research field (González-Rosa et al., 2017). The widely used cryoinjury procedure is generally well-tolerated by animals, with a high survival rate of 95% (Chablais and Jaźwińska, 2012). Nevertheless, until now there were no studies, which would assess the adverse effects associated with stress and/or pain in fish after this invasive method.

The primary goal of the first part of my study was to establish whether cryoinjury elicits a noxious stimulus in the fish. I used a broadly accepted indirect measure to assess zebrafish welfare including behaviour tests. (Sneddon, 2015; Reilly et al., 2008; Deakin et al., 2019; Nobre Bezerra et al., 2021; Taylor et al., 2017). My data showed significant changes in zebrafish behaviour after cryoinjury procedure. Fish swam significantly slower and stayed at the bottom of the tank up to 6H after the cryoinjury (6hpi). To confirm that zebrafish are affected by the cryoinjury procedure, a second line of evidence could be tested in the future experiments. It was reported that cortisol is expressed in response to stress in teleost fish and its release is coordinated by the hypothalamic-pituitary-interrenal axis (HPI-axis) (Tudorache et al., 2018; Cachat et al., 2010). The whole body cortisol can be isolated and measured using ELISA method, however, the reported fluctuations of cortisol dependent on the fish circadian rhythm have to be taken into consideration in the study design (Tudorache et al., 2018). There are several genes in HPI-axis reported to be affected by the stress and/or pain in fish including zebrafish such as *prl, crf, hcrt or c-fos* (Pottinger et al., 1992; Pavlidis et al., 2015), which could be measured by quantitative RNA expression analysis in the future studies.

Altogether, behavioural tests indicate that cryoinjury is a noxious stimulus for the fish and requires revising current protocols, assuring any possible pain and discomfort of animals can be reduced to the minimum.

Currently, there are no measures to minimize pain after heart injury procedures in adult zebrafish. However, the effectiveness of analgesia in fish was reported in multiple studies investigating the effect after different stressors including fish farming, fin clipping or chemical stimuli (Chatigny et al., 2018; Martins et al., 2016; Sneddon, 2015; Nobre Bezerra et al., 2021).

Here, I tested the effects of two different analgesics with distinct modes of action, lidocaine (3mg/l) and morphine (1.5mg/l). I opted for testing only one concentration of each drug based on the published literature (Schroeder and Sneddon, 2017; Khor et al., 2011). As a variable, I tested different durations of treatments instead (up to 48H). The use of lidocaine as a systemic pain reliever is relatively common (Mao and Chen, 2000). However, in my experimental setup lidocaine-treated fish did not improve behaviour both, in the aspect of swimming speed and tank occupancy. On the contrary, morphine, which was also shown to have beneficial effects on zebrafish welfare (Chatigny et al., 2018; Nobre Bezerra et al., 2021), significantly improved swimming speed of the fish up to 2 hpi after the cryoinjury and the tendency was conserved up to 6hpi. The tank occupancy indicator was not rescued by the morphine treatment, suggesting that morphine might reduce some but not all adverse effects triggered by the cryoinjury underlying the need for more research to be conducted in this area of fish physiology. In summary, lidocaine treatment did not improve zebrafish behaviour after cryoinjury as a noxious stimulus, while morphine significantly alleviated the stress and/or pain resulting from the cryoinjury procedure.

7.2.1 Pain perception in fish

Mounting evidence indicates that fish can perceive pain, however, the field still did not reach a consensus on this highly disputed topic (Key, 2015; Rose et al., 2015; Sneddon, 2015; Ohnesorge et al., 2021). The definition of pain can be a complex issue, especially when animals can not communicate their feelings. The basic sensory ability to respond to potentially harmful stimuli is called nociception and can be found even in bacteria (Berg, 1975). Yet, there is a differentiation between pain and nociception (Allen, 2011). Pain is described as a subjective experience of anguish, despair and other negative affective states (Allen et al., 2005). There is no simple way to assess mental stress in other species, which makes the evaluation of pain perception in animals so difficult (Broom, 1998). It is clear that animal pain behaviour differs from the one that we can see in humans, however, animals including fish react to harmful stimuli both by behavioural changes and physiological responses (Sneddon, 2015; Reilly et al., 2008; Deakin et al., 2019; Nobre Bezerra et al., 2021; Taylor et al., 2017; Pavlidis et al., 2015). Here arises the question: should we use humans as an ultimate determinant of animal pain?

Also, when are the differences between humans and other species important? Several reviews came to the conclusion that animals from different phyla experience pain beyond reasonable doubt since they fulfil all the criteria for animal pain perception (Shriver, 2006; Sneddon et al., 2014). Nociceptors have been identified in fish for the first time by Sneddon et al. in 2002 in teleost fish and in 2003 also in rainbow trout using electrophysiology and neuroanatomical approaches (Sneddon, 2002; Sneddon, 2003). Previous studies also showed that a jawless fish, the lamprey has receptors responsive to noxious stimuli (Matthews and Wickelgren, 1978). The rainbow trout nociceptors were found to be two fibre types, C fibres and small diameter myelinated A-delta fibres. Three classes of nociceptors were reported in fish including polymodal (nociceptors, which are responsive to mechanical, thermal and chemical stimuli), mechanothermal (nociceptors, which have no response to chemicals) and mechanochemical (nociceptors, which have no response to temperature) (Sneddon, 2003; Ashley et al., 2006; Ashley et al., 2007; Mettam et al., 2012). Importantly, the electrophysiological properties of the trout nociceptors are similar to those identified in mammals (Sneddon, 2004; Sneddon, 2012). It was shown by anatomical and electrophysiological research that a small amount of fish nociceptors (4–5%) are innervated by C fibres as (Sneddon, 2002; Roques et al., 2010), in comparison to terrestrial vertebrates where C fibres accounts for ca 50% of nociceptors (Young, 1977). It is known that C fibres in mammals are responsible for dull, ‘thudding’ pain while A fibres are conducting faster and are believed to signal ‘first’ pain to the CNS. These differences made some researchers arrive at the conclusion that fish do not experience pain (Rose et al., 2012). Another reason for scientists to doubt fish pain perception is lack of neocortex (cerberal cortex), where it is believed that the electrical signals are processed into the sensation of pain (Rose et al., 2012). However, we should keep in mind that fish differ in lifestyle, morphology, neuroanatomy and environment that they live in and we should not expect identical structure of nociceptors. Additionally, it was shown that trout A-delta fibres respond in the same way as mammalian C fibres in response to noxious stimuli (Sneddon, 2002; Sneddon, 2003; Ashley et al., 2006; Ashley et al., 2007; Roques et al., 2010; Mettam et al., 2012). Moreover, several studies have reported that fish have highly conserved neuroanatomical pathways from peripheral areas to the brain (Kitchener et al., 2010; Sneddon, 2015).

As aforementioned, opioid receptors as well as the action of non-steroidal anti-inflammatory drugs (NSAIDs) on cyclo-oxygenase enzymes (COX1 and COX2) are also highly conserved between fish and mammals (Malafoglia et al., 2013). In summary, the pain neural apparatus in fish is directly comparable with the mammalian system and works in the equivalent way (Sneddon, 2015).

One of the main indicators of fish pain perception is change in the behaviour after the noxious stimulus. There is a great amount of evidence showing that fish modify their behaviour according to the stressor including my study (Cachat et al., 2010; Schroeder and Sneddon, 2017; Deakin et al., 2019; Bozi et al., 2021). It was reported that teleost fish respond to electric shock, they learned to avoid them, however food deprived fish risked entering electric shock zone to obtain food (Sneddon, 2012). Zebrafish was shown to increase its opercular beat rate (ventilation of the gills) in response to injecting a potentially harmful chemical (Sneddon, 2009). Other behavioural changes in zebrafish after injecting a noxious chemical included decrease in swimming speed and tail beating (Maximino, 2011). My study confirms that fish after cryoinjury procedure, which is a potential noxious stimulus, swam significantly slower and they tended to stay at the bottom of the tank.

Another indicator of fish pain perception is their reaction to analgesia. Zebrafish were shown to respond to analgesia after harmful stimuli (Chatigny et al., 2018; Martins et al., 2016; Martins et al., 2019; Ohnesorge et al., 2021). Moreover, zebrafish, given the choice after the painful treatment prefered to spend most of their time in an unfavourable environment with analgesia present (Sneddon, 2012). In my study I confirmed that analgesia, namely morphine (1.5mg/l), did significantly improve zebrafish behaviour after cryoinjury procedure using swimming speed as a readout.

In summary, a great number of studies including the research from this thesis, prove that fish comprising zebrafish, can perceive pain. The pain perception in fish is not necessarily equal to humans due to the differences in neuroanatomy and environment that fish live in. However, fish fulfil all the criteria for animal pain perception including having nociceptors comparable to mammalian and responding to analgesia. The fish pain perception should be considered for all future experiments and current protocols should be revised to ensure the wellbeing of the animals. Thus, analgesia use in case of cryoinjury procedure in zebrafish should be incorporated into the current protocols.

7.2.2 Effect of morphine on the tissue repair

I showed that morphine treatment alleviates zebrafish pain after cryoinjury procedure, however it is also important to make sure that analgesic of choice does not interfere with the process that is investigated, which in this case is cardiac regeneration.

Morphine is a pain medication from the opiate family and it acts on the central nervous system to relieve the pain. In zebrafish morphine have been reported to be effective analgesics (Chatigny et al., 2018). To this date, however, no studies have reported the potential effect of morphine on the zebrafish cardiac repair. Morphine has been shown to be both beneficial and detrimental for tissue repair (Barlass et al., 2018; Charbaji et al., 2013). In this study, I examined the main hallmarks of regeneration after analgesia treatments. First, I used histological analysis to assess the regeneration process. The results indicated that 48H lidocaine treatment seems to delay heart regeneration due to delayed collagen deposition followed by delayed collagen resolution and bigger injury areas (IA) at 30 dpi. On the contrary, morphine treatment did not have an impact on the regeneration process and hearts fully regenerated, in comparable manner as the control untreated hearts. Additionally, I showed that there was no visible difference in proliferative capacity of cardiac cells as assessed by co-localization of *pcna* with *vmhc* or *col1a1a* using the RNAscope *in situ* hybridization method.

Although I could not observe any visible differences in the cardiac regeneration in zebrafish with the use of 1.5mg/l of morphine, the effect of morphine on tissue repair and wound healing have been described in the literature. The effect of morphine on wound healing has been tested in cell culture, animal studies, and clinical trials (Charbaji et al., 2012; Bigliardi-Qi et al., 2006; Stein et al., 1991; Stein and Küchler, 2013). Morphine treatment was shown to induce cell migration of oral epithelial cells (Charbaji et al., 2012) or human keratinocytes (Bigliardi et al., 2002). The latter study reported that opioid peptides released in wound tissue were essential for re-epithelialization and tissue regeneration (Bigliardi et al., 2002). It was shown by Küchler et al. that in a 3D model of wound healing opioid application resulted in thicker layers of viable keratinocytes covering the wound area (Küchler et al., 2010). Moreover, Bigliardi-Qi et al. reported that mice lacking δ-opioid receptors show delayed wound healing (Bigliardi-Qi et al., 2006).

Additionally, few small clinical trials took place and morphine treatment was shown to be advantageous for pain relief and healing after arthroscopic knee surgery and chronic cutaneous lesions (Stein et al., 1991; Farley, 2011). There were also few studies showing contradictory results; however, the initial delay in wound closure seemed not to have an impact on the final speed of the wound healing (Rook et al., 2011; Rook and McCarson, 2007; Stein and Küchler, 2013).

The effect of morphine on heart repair and recovery is not yet fully understood. Currently, the guidelines from American College of Cardiology/American Heart Association and European Society of Cardiology recommends morphine sulphate as the preferred drug for pain relief (O'gara et al., 2013; AbuRuz, 2016). There were several studies showing that morphine treatment after myocardial infarction (MI) in humans improved patients recovery based on myocardial performance index (MPI), other studies investigated reduction of myocardial and microvascular damage (Stiermaier et al., 2021; Murphy et al., 2006; Murphy et al., 2009). Nevertheless the morphine's mode of action is not completely understood, thus the question whether benefits outweigh the possible risks coming from morphine treatment remains (Caspi and Aronson, 2020; Agewall, 2017).

In summary, morphine can have an impact on tissue repair where concentration and timing of the treatment is crucial. Morphine is advised to be used after human MI where it may have even beneficial effects. I was able to show that morphine can be effectively used in zebrafish after cryoinjury since it did not impact the regeneration outcome while alleviating zebrafish pain.

7.2.2.1 Possible effect of morphine on the immune response

In the last part of this study I decided to investigate changes in gene expression after 6H morphine-treatment after the cryoinjury procedure. To have a systems view on the impact of morphine, I teamed up with the lab of Dr. Jan Philipp Junker to detect the differences in transcriptome on the single cell level using scRNA-sequencing. In addition, I tested the expression of genes with known roles in zebrafish heart regeneration using qPCR analysis.

Morphine is a pain relieving drug, thus it is expected the treatment would lead to differences at the transcriptional level.

Several studies have reported the effect of morphine on the brain gene expression using different animals models including zebrafish embryos (Ammon-Treiber and Höllt, 2005; Loguinov et al., 2001; Herrero-Turrión et al., 2014; McClung et al., 2005). It is understandable that most of the studies focus on the brain since morphine mode of action is on the central nervous system (CNS). There were only few studies reported where morphine treatment was assessed in the context of heart gene expression.

However, most of these publications are using chronic morphine uptake in their study design combined with the withdrawal to mimic opioids addictions (Drastichova et al., 2012; Drastichova et al., 2011; González-Cuello et al., 2003). González-Cuello et al. showed that morphine withdrawal in rats induced c-fos expression, which might be a marker for changes in cardiac excitability (González-Cuello et al., 2003), while the proteomic analysis reported by Drastichova et al. found that long morphine treatment or withdrawal led to alteration of the expression levels of 237 proteins, significantly of the heat shock proteins (Drastichova et al., 2012). Another study using rat as a model, showed that morphine pretreatment reduces myocardial ischemia-reperfusion injury in heart failure rats via GSK-3β/Cx43 signalling proteins and apoptosis-related gene, Bcl-2/Bax (Zhu et al., 2020).

In this study, I was able to show using scRNA-seq that short-time morphine treatment (6H) after cryoinjury procedure did not impact the cellular composition of the zebrafish heart. All cell clusters were detected in 6H morphine-treated hearts compared to untreated control and no cell clustered were missing, indicating that short-term morphine treatment did not cause any significant changes on the cellular level. The previous data indicates that morphine can have an impact on the immune response, especially inflammation (Plytycz and Natorska, 2002; Fecho et al., 2007; Loram et al., 2012; Feehan and Zadina, 2019). Inflammation is a natural reaction to the injury, however it can also contribute to many diseases. Inflammation is essential for the induction of tissue repair and is a crucial part of the immune response after the injury (Stein and Küchler, 2013). Opioids including morphine were reported to interfere at different stages in the inflammatory cascade and can be considered as pro- and anti- inflammatory depending on the concentration, timing or *in vivo* versus *in vitro* studies (Stein and Küchler, 2013).

In my study we looked at the transcriptional level as early as 3 days after cryoinjury procedure.

At this time point, there were no significant differences detectable in the amount of the immune cell present or in the gene expression for example of *mpeg1.1* gene, which is a known macrophage marker. The effect of morphine-treatment of the early immune response have been previously reported (Barlass et al., 2018; Clark et al., 2007; Wang et al., 1998). Barlass et al. showed that morphine worsens the severity of acute pancreatitis and delays resolution and regeneration in mice. One of the main findings was increased pancreatic neutrophilic infiltration and necrosis after morphine treatment in acute pancreatitis (Barlass et al., 2018). Another study in mice also reported reduction in neutrophil infiltration after acute morphine administration after skin incision (Clark et al., 2007). Additionally, Wang et al. reported that morphine preconditioning attenuates neutrophil activation in rat models of myocardial infarction (Wang et al., 1998). Therefore, more studies to characterize early immune response in zebrafish heart regeneration would be needed to fully understand the inflammation and neutrophil infiltration after the use of opioids. Groups working specifically with early time points after cryoinjury (up to 6H) should be cautious with using morphine after the procedure.

In the last part of this study I showed that after 6H morphine treatment genes known for their role in regeneration *aldh1a2, cxcl12a, postnb, gata4, cxcr4b, fn1a, col1a1a, and tgf1b* were not affected by 6H morphine-treatment (Bensimon-Brito et al., 2020; Gupta et al., 2013; Itou et al., 2012; Kikuchi et al., 2011; Kim et al., 2010; Liu et al., 2018; Moyse and Richardson, 2020; Sánchez-Iranzo et al., 2018; Wang et al., 2013).

In summary, morphine was reported to have an impact on gene expression and immune response in multiple organs including heart. We were able to show that short-term morphine treatment (6H) after the cryoinjury did not affect cellular composition of the heart, gene expression of genes known to play a role in regeneration, however the early immune response could be affected by morphine and more studies are necessary to further characterize this phenomenon.

7.3 Cellular composition of zebrafish heart

In this part of the study I used in collaboration a combination of single-cell transcriptomics and functional experiments to identify and characterize pro-regenerative cell states in the adult zebrafish heart. This approach allowed us to identify all cell types present in zebrafish heart in the healthy and cryoinjured state in most detailed way reported so far (Patra et al., 2017). Firstly, we showed the diversity of cardiomyocytes (CMs) after zebrafish heart injury. CMs have been so far the most studied cell type in regeneration research (Zheng et al., 2021; Poss et al., 2002; González-Rosa et al., 2018) understandably due to the fact that zebrafish CMs can dedifferentiated, proliferate and fully replace the dead tissue. We confirmed the dynamics of dedifferentiating CMs peaking at day 3 and proliferating CMs peaking at day 7 after injury . Dedifferentiated CMs are one of the most studied cell types, since they revert their state from partially or terminally differentiated into a less differentiated stage, and they switch their expression pattern from mature CMs to a more immature state, which is a prerequisite for the CMs proliferation (Yao and Wang, 2020). Additionally, we identified a gene signature for these clusters of CMs and determined a new marker for dedifferentiated CMs, *ttn.2* with its expression pattern after the injury.

We also identified non-myocyte cell types. Focusing on immune cells including macrophages, we were able to show diversity of the macrophages and the transient nature of the different clusters. Macrophages are known to play a crucial role in the immune response after the injury (de Preux Charles et al., 2016). However, their ability to also contribute collagen to scar formation in both mouse and zebrafish models (Simões et al., 2020) makes them an even more interesting cell type. More detailed studies on the specific macrophage clusters with their possible pro-regenerative role should be carried out to fully understand their pro-regenerative function. The zebrafish model has great advantages with its available tools thus experiments such as specific macrophage subtypes ablation using NTR-MTZ or mutant line generation, which was done for example by generating zebrafish lacking the *CSF1R* gene (Kuil et al., 2020) or overexpression of the specific macrophage subtypes using heat-shock can be rather easily used.

In summary, we showed the complete composition of the zebrafish heart in healthy and regenerating hearts at different stages of regeneration.

Our study provides a resource for future studies including cell types and gene expression of the cardiac cells crucial for the regeneration process.

7.3.1 Great diversity of cardiac fibroblasts after cryoinjury

The expression of known pro-regenerative factors such as *aldh1a2* (Kikuchi et al., 2011) (the enzyme synthesizing retinoic acid), the cardiomyocyte mitogen *nrg1* (Gemberling et al., 2015), and the pro-regenerative extracellular matrix (ECM) factor *fn1a* (Wang et al., 2013) by fibroblasts prompt us to further characterize this cell type after cryoinjury in zebrafish.

Fibroblasts have been reported to be crucial for zebrafish heart regeneration. (Sánchez-Iranzo et al., 2018). Using the cryoinjury method, we were able to identify thirteen transcriptionally different clusters of cardiac fibroblasts based on our single-cell data. Fibroblasts were identified as cells expressing *col1a1a* and further subclustered based on 50 top differentially expressed genes. Importantly, clusters remained separate even after removal of ECM-related genes, although a small fraction of *col12a1a* fibroblasts is found in the *col11a1a* and *cxcl12a* fibroblast subtypes. One of the most important findings was the identification of dynamics of different clusters of fibroblasts. Some of the fibroblasts but not all were transiently expressed at the specific point after the cryoinjury. To gain spatial information, we used RNAscope, *in situ* hybridization and visualized that transient fibroblasts are localizing to the injury area suggesting their pro-regenerative function. These approaches allowed us to identify three transient cell states with fibroblast characteristics (*col11*, *col12*, and *nppc* fibroblasts) that are major sources of known pro-regenerative genes and also express additional secreted factors with a potential pro-regenerative function.

It was shown that the ablation of *col1a2*-expressing cells impaired cardiomyocyte proliferation, which indicates that fibroblasts can have a pro-regenerative role additionally to ECM production (Sánchez-Iranzo et al., 2018) and more studies are necessary to further characterize pro-regenerative role of fibroblasts.

7.3.2 Fibrosis and the role of pro-regenerative fibroblasts

Fibrosis is an outcome of the tissue repair response after different types of injury including MI. The formation of the fibrotic tissue is associated with excessive accumulation of ECM components such as collagens or fibronectin. It is important to note that fibrosis is a normal and important process of tissue repair in all organs (Henderson et al., 2020).

After MI, fibrosis takes place (fibrotic scar formation); this process is crucial in preventing ventricular wall from rupturing. In addition, mechanical stress and hormonal changes also result in the formation of the connective tissue in the areas remote from the border zone of the injury, which will also lead to the pathological remodelling (Talman and Ruskoaho, 2016). The main players of fibrosis are fibroblasts, which become activated after the injury, they increase their motility, secretion of inflammatory mediators, and synthesis of ECM components (Henderson et al., 2020). Thus studying transient zebrafish fibrosis and fibroblasts characteristics is extremely important, and this topic has only recently gained attraction in the field (Sánchez-Iranzo et al., 2018; Ma et al., 2021; de Bakker et al., 2021).

In order to characterize further the pro-regenerative role of transient fibroblasts, we investigated the origin of the cardiac fibroblasts after the cryoinjury. We combined computational methods (not described in this thesis, study performed by Baastian Spanjaard from Junker lab)(Hu et al. 2022) with genetic lineage tracing to confirm that fibroblasts after cryoinjury originate from epicardium such as *col12a1a* fibroblasts. However, we also discovered that fibroblasts can also originate from endocardium as for example *nppc* fibroblasts. In agreement, examining the effect of deeper vs shallow injuries, I showed that only deep enough cryoinjury is necessary to induce all cell type responses including endocardium.

To confirm the pro-regenerative role of one of the fibroblasts that we have identified, we generated a new transgenic zebrafish line to specifically ablate *col12a1a*-expressing cells. Similarly, ablation of *col1a2*-expressing cells led to the notable decrease of CMs proliferation at 7 dpi, but did not impair the regeneration process as no quantifiable difference between control and *col1a2*-ablated fibroblasts at 30 dpi was detected (Sánchez-Iranzo et al., 2018). In contrast, depletion of *col12a1a*-expressing cells after cryoinjury impaired heart regeneration at 30 dpi.

The reason for a difference in the extent of the regeneration impairment compared to the ablation of *col1a2* and *col12a1a*-expressing cells could be explained by different MTZ regimen in the experimental setup. In our study, *col12a1a* was depleted earlier due to our knowledge when exactly epicard-derived fibroblasts are present (not described in this thesis, study performed by Baastian Spanjaard from Junker lab)(Hu et al., 2022), also *col12a1a* could have been a more specific target for the regeneration process. One more explanation for this variation in the experimental outcome could be that *col1a2* promoter was a weaker promoter and did not result in the high enough expression of NTR, while our results showed that isolated *col12a1a* cis regulatory element responded to the injury in a similar manner as an endogenous promoter, with marked increase in *col12a1a* expression. This shows that NTR was expressed in very high levels in those cells leading to efficient ablation by the MTZ treatment.

In summary, we have shown that transient fibroblasts states can have a pro-regenerative role. In addition to the ECM production, they have an impact on the CMs proliferation and specific ablation of *col12a1a*-expressing cells led to significant delay in regeneration at 30 dpi. In the future it would be interesting to investigate further other identified pro-regenerative fibroblast clusters such as *nppc* with gain and loss of function experiments. Also, heart-specific ablation of *col12* fibroblasts would have been a significant improvement in the experimental setup to ensure that the effect of the cell ablation can be related only to the loss of the cells in the heart as *col12* is expressed also in other organs including the brain. Additionally, it was described by Sánchez-Iranzo et al. that fibroblasts are not fully eliminated during fibrosis regeneration but become inactivated (Sánchez-Iranzo et al., 2018). Future studies could investigate whether these pro-regenerative fibroblast clusters could also transition into other cell types such as CMs. Currently, newly formed CMs are reported to arise from dedifferentiated CMs as a main source (D'Uva et al., 2015; Bersell et al., 2009).

Overall, this study shows the importance of transient fibroblasts in zebrafish cardiac regeneration and gives a great possibility for new studies, which hopefully will advance the field of heart repair.

7.4 Complexity of Wnt signalling in zebrafish heart regeneration

Wnt/β-catenin signalling is known to be crucial for organ development and regeneration including heart (Gesser and Kuhl, 2010; Zhao et al., 2019; Duan et al., 2012). The role of Wnt/β-catenin signalling has been previously described in cardiac regeneration in different models including cell culture, mouse, rat or zebrafish (Ozhan and Weidinger, 2015). However, the current data show that the role of the canonical Wnt signalling is complex since the results are often contradictory. It seems that this pathway can either enhance (Bertozzi et al., 2022) or delay (Zhao et al., 2019; Peng et al., 2020) heart regeneration focusing mostly on its effect on CMs.
In this study, we used the advantage of the scRNA-seq method to systematically identify transcriptional differences at the single-cell level and further characterize it with the functional experiments. We were able to confirm that Wnt/β-catenin signalling components are re-expressed upon zebrafish heart injury (Bergmann and Kühl, 2010) and after Wnt inhibition the cell type diversity is changed.
Firstly, in our experimental setup, Wnt signalling inhibition led to the significant delay in heart regeneration. Using our single-cell data we were able to see that dedifferentiated CMs are notably decreased at 3 dpi and increased at 7 dpi suggesting the delay in regeneration that we can observe at 30 dpi. Interestingly, dedifferentiated CMs at 7 dpi do not localize to the injury area (IA) as shown in the controls. This could be explained by the impairment of the migration of the dedifferentiated CMs. Another effect of Wnt inhibition was detected on fibroblast cell clusters. First of all, perivascular cells, labelled with *pdgfrb* were significantly decreased. Importantly, all endocardial-derived fibroblasts were significantly decreased including *nppc* fibroblasts. Both perivascular cells and NPPC signalling were described to have a role in angiogenesis (Carmeliet, 2000; Bubb et al., 2019; Moyes and Hobbs, 2019; Zhang et al., 2017). Additionally, Wnt signalling has been described to be crucial for vascular and angiogenic development (Bergmann and Kühl, 2010). However, the role of Wnt signalling in angiogenesis was not clear due to contradictory effects reported similar to those from regeneration (Bergmann and Kühl, 2010). One of the possible reasons could be the biphasic control of Wnt signalling is essential for a beneficial effect where Wnt activation promotes proliferation of the vasculogenic precursors, while Wnt inhibition is crucial for mobilization, homing, and differentiation (Bergmann and Kühl, 2010).

In our study, inhibition of Wnt resulted in the significant decrease of coronary arteries' coverage at 7 dpi. However, we did not detect a significant difference in the proliferation of coronaries suggesting that the impaired revascularization is probably an outcome of another aspect of revascularization such as migration of coronaries or interactions with perivascular cells.

In summary, Wnt/β-catenin signalling is undoubtedly crucial for cardiac regeneration as it was previously shown for heart development. The use of scRNA-see enabled us to investigate in detail the effect of Wnt inhibition of specific cell types and will provide an important resource for future studies. Wnt/β-catenin signalling is known to have a stage-specific, at least biphasic, role in heart development. One of the explanations for the contradictory data could be that Wnt signalling is required to be activated at the specific time point and stage of the regeneration process as it is described for the development. Another important consideration is the experimental model and set up. It was reported both for murine models as well as for zebrafish that the kind of the heart injury (i.e. amputation vs cryoinjury) has an impact on the outcome of the experiments including the role of Wnt signalling (Ozhan and Weidinger, 2015).

Taken together, we showed that Wnt signalling is a key-regulator of endocardial response and its inhibition led to impairment of revascularization followed by significant delay in regeneration.

8. References

Abreu, M. (2018). . Effects of lidocaine on adult zebrafish behavior and brain acetylcholinesterase following peripheral and systemic administration. *Neuroscience letters*, *692*, 181–186.

AbuRuz, M. E. (2016). The Effect of Pain and Morphine Use on Complication Rates after Acute Myocardial Infarction. *Health Science Journal*.

Agewall, S. (2017). Morphine in acute heart failure. *Journal of Thoracic Disease*, *9*(7).

Aisagbonhi, O., Rai, M., Ryzhov, S., Atria, N., Feoktistov, I., & Hatzopoulos, A. K. (2011). Experimental myocardial infarction triggers canonical Wnt signaling and endothelial-to-mesenchymal transition. *Dis Model Mech.*, *4*(4), 4469-83.

Ali, S., Ranjbarvaziri, S., Talkhabi, M., Zhao, P., Subat, A., & Hojjat, A. (2014). Developmental heterogeneity of cardiac fibroblasts does not predict pathological proliferation and activation. *Circulation Research*, *115*(7), 625–35.

Allen, C. (2011). Animal Consciousness. *Stanford Encyclopedia of Philosophy*, 1-63.

Allen, C., Fuchs,, P., Shriver, A., & Wilson, H. D. (2005). Deciphering Animal Pain. *American Psychological Association*, 351–366.

Ammon-Treiber, S., & Höllt, V. (2005). Morphine-induced changes of gene expression in the brain. *Addiction biology.*, *10*(1), 81-9.

Antos, C. L., McKinsey, T. A., Frey, N., Hill, J. A., & Olson, E. N. (2002). Activated glycogen synthase-3β suppresses cardiac hypertrophy in vivo. *Proc Natl Acad Sci U S A*, *99*(2), 907–912.

Anversa,, P., Olivetti, G., Melissari, M., & Loud, A. V. (1980). Stereological measurement of cellular and subcellular hypertrophy and hyperplasia in the papillary muscle of adult rat. *J. Mole. .Cell. Cardiol.*, *12*, 781–795.

Ashley, P. J., Sneddon, L. U., & McCrohan, C. R. (2006). Properties of corneal receptors in a teleost fish. *Neuroscience Letters*, *410*(3), 165-168.

Ashley, P. J., Sneddon, L. U., & McCrohan, C. R. (2007). Nociception in fish: stimulus–response properties of receptors on the head of trout Oncorhynchus mykiss. *Brain Research*, *1166*, 47-54.

Avdesh, A., Chen, M., Martin-Iverson, M. T., Mondal, A., Ong, D., Rainey-Smith, S., Taddei, K., Lardelli, M., Groth, D. M., Verdile, G., & Martins, R. N. (2012). Regular Care and Maintenance of a Zebrafish (Danio rerio) Laboratory: An Introduction. *J Vis Exp.*, *69*.

Azevedo, P. S., & Zornoff, L. A.M. (2016). Cardiac Remodeling: Concepts, Clinical Impact, Pathophysiological Mechanisms and Pharmacologic Treatment. *Arquivos Brasileiros de Cardiologia*, *106*(1), 62-69. Retrieved 01 19, 2022, from https://www.ncbi.nlm.nih.gov/pmc/articles/PMC4728597/#:~:text=Cardiac%20remodeling%20is%20defined%20as,ventricular%20dysfunction%20and%20malignant%20arrhythmias.

Banerjee, I., Fuseler, J. W., Price, R. L., Borg, T. K., & Baudino, T. A. (2007). Determination of cell types and numbers during cardiac development in the neonatal and adult rat and mouse. *Am. J. Physiol. Heart Circul. Physiol.*, *293*, 1883–1891.

Barandon, L., Couffinhal, T., Ezan, J., Dare, D., & Duplàa, C. (2003). Reduction of infarct size and prevention of cardiac rupture in transgenic mice overexpressing FrzA. *Circulation*, *108*(18), 2282-9.

Barlass, U., Dutta, R., Cheema, H., George, J., Roy, S., & Saluja, A. K. (2018). Morphine worsens the severity and prevents pancreatic regeneration in mouse models of acute pancreatitis. *Gut .*, *67*(4), 600-602.

Baurand, A., Zelarayan, L., Betney, R., Birchmeier, W., Dietz, R., & Bergmann, M. W. (2007). Beta-catenin downregulation is required for adaptive cardiac remodeling. *Circ Res .*, *100*(9), 1353-62.

Becker, T., Wullimann, M. F., Becker, C. G., Bernhardt, R. R., & Schachner, M. (1997). Axonal regrowth after spinal cord transection in adult zebrafish. *The Journal of comparative neurology*, *1096-9861*.

Bensimon-Brito, A., Ramkumar, S., Boezio, G. L. M., Guenther, S., Kuenne, C., Helker, C. S. M., Sánchez-Iranzo, H., Iloska, D., Piesker, J., Pullamsetti, S., Mercader, N., Beis, D., & Stainier, D. Y. R. (2020). TGF-β Signaling Promotes Tissue Formation during Cardiac Valve Regeneration in Adult Zebrafish. *Dev Cell .*, *52*(1).

Berg, H. C. (1975). Chemotaxis in Bacteria. *Annual Review of Biophysics and Bioengineering*, *4*, 119-136.

Bergers, G., & Song, S. (2005). The role of pericytes in blood-vessel formation and maintenance. *Neuro-oncology.*, *7*(4), 452-64.

Bergmann, M. W., & Kühl, M. (2010). WNT signaling in adult cardiac hypertrophy and remodeling: lessons learned from cardiac development. *Circulation Research*, *107*(10), 1198–1208.

Bergmann, O., Bhardwaj, R. D., Bernard, S., Zdunek, S., Barnabé-Heider, F., Walsh, S., Zupicich, J., Alkass, K., Buchholz, B. A., Druid, H., Jovinge, S., & Frisén, J. (2009). Evidence for cardiomyocyte renewal in humans. *Science*, *324*, 98-102.

Bergmann, O., Zdunek, S., Felker, A., Salehpour, M., Alkass, K., & Bernard, S. (2015). Dynamics of Cell Generation and Turnover in the Human Heart. *Cell*, *161*, 1566–1575.

Bersell, K., Arab, S., Haring, B., & Kühn, B. (2009). Neuregulin1/ErbB4 Signaling Induces Cardiomyocyte Proliferation and Repair of Heart Injury. *Cell*, *138*(2), 257-270.

Bertozzi, A., Wu, C.-C., Hans, S., Brand, M., & Weidinger, G. (2022). Wnt/β-catenin signaling acts cell-autonomously to promote cardiomyocyte regeneration in the zebrafish heart. *Dev Biol .*, *481*, 226-237.

Bezerra, A. J.N. (2021). Antinociceptive effect of triterpene acetyl aleuritolic acid isolated from Croton zehntneri in adult zebrafish (Danio rerio). *Biochemical and biophysical research communications*, *534*, 478–484.

Bigliardi, P. L., Büchner, S., Rufli, T., & Bigliardi-Qi, M. (2002). Specific stimulation of migration of human keratinocytes by mu-opiate receptor agonists. *J Recept Signal Transduct Res.*, *22*(1-4), 191-9.

Bigliardi-Qi, M., Gaveriaux-Ruff, C., Zhou, H., Hell, C., Bady, P., Rufli, T., Kieffer, B., & Bigliardi, P. (2006). Deletion of delta-opioid receptor in mice alters skin differentiation and delays wound healing. *Differentiation .*, *74*(4), 174-85.

Bise, T., Sallin, P., Pfefferli, C., & Jaźwińska, A. (2020). Multiple cryoinjuries modulate the efficiency of zebrafish heart regeneration. *Scientific Reports*, *10*.

Blankesteijn, W. M. (2020). Interventions in WNT Signaling to Induce Cardiomyocyte Proliferation: Crosstalk with Other Pathways. *Molecular Pharmacology*, *97*(2), 90-101.

Bolli, R. (n.d.). Myocardial “stunning” in man. *Circulation Research*, *86*, 1671-1691.

Bouillet, P., Oulad-Abdelghani, M., Vicaire, S., Garnier, J. M., Schuhbaur, B., Dollé, P., & Chambon, P. (1995). Efficient cloning of cDNAs of retinoic acid-responsive genes in P19 embryonal

carcinoma cells and characterization of a novel mouse gene, Stra1 (mouse LERK-2/Eplg2). *Developmental biology.*, *170*(2), 420-33.

Bozi, B., Rodrigues, J., Lima-Maximino, M., Siqueira-Silva, D. H. d., Candeias Soares, M., & Maximino, C. (2021). Social Stress Increases Anxiety-Like Behavior Equally in Male and Female Zebrafish. *Frontiers in Behavioral Neuroscience*, *15*.

Brand, M. (2011). *Regeneration of the adult zebrafish brain from neurogenic radial glia-type progenitors*. PubMed. Retrieved January 31, 2022, from https://pubmed.ncbi.nlm.nih.gov/22007133/

Broom, D. M. (1998). Welfare, Stress, and the Evolution of Feelings. *Advances in the Study of Behavior*, *27*, 371-403.

Brown, W., Liu, J., Tsang, M., & Deiters, A. (2018). Cell-Lineage Tracing in Zebrafish Embryos with an Expanded Genetic Code. *Chembiochem : a European journal of chemical biology.*, *19*(12), 1244–1249.

Bubb, K. J., Aubdool, A. A., Moyes, A. J., Lewis, S., Drayton, J. P., Tang, O., Mehta, V., Zachary, I. C., Abraham, D. J., Tsui, J., & Hobbs, A. J. (2019). Endothelial C-Type Natriuretic Peptide Is a Critical Regulator of Angiogenesis and Vascular Remodeling. *Circulation*, *139*(13), 1612-1628.

Burkhardt-Holm, P., Oulmi, Y., Schroeder, A., Storch, V., & Braunbeck, T. (1999). Toxicity of 4-Chloroaniline in Early Life Stages of Zebrafish (Danio rerio): II. Cytopathology and Regeneration of Liver and Gills After Prolonged Exposure to Waterborne 4-Chloroaniline. *Archives of Environmental Contamination and Toxicology*, *37*, 85–102.

Cachat, J., Stewart, A., Grossman, L., Gaikwad, S., Kadri, F., Chung, K. M., Wu, N., Wong, K., Roy, S., Suciu, C., Goodspeed, J., Elegante, M., Bartels, B., Elkhayat, S., Tien, D., Tan, J., Denmark, A., Gilder, T., Kyzar, E., … Kalueff, A. V. (2010). Measuring behavioral and endocrine responses to novelty stress in adult zebrafish. *Nature protocols.*, *5*(11), 1786-99.

Cano-Martínez, A., Vargas-González, A., Guarner-Lans, V., Prado-Zayago, E., León-Oleda, M., & Nieto-Lima, B. (2010). Functional and structural regeneration in the axolotl heart (Ambystoma mexicanum) after partial ventricular amputation. *Archivos de cardiología de México*, *80*(2), 79-86.

Canto, J. G. (n.d.). *Number of Coronary Heart Disease Risk Factors and Mortality in Patients With First Myocardial Infarction*. NCBI. Retrieved January 20, 2022, from https://www.ncbi.nlm.nih.gov/pmc/articles/PMC4494683/

Cao, J., Navis, A., Cox, B. D., Dickson, A. L., Gemberling, M., Karra, R., Bagnat, M., & Poss, K. D. (2016). Single epicardial cell transcriptome sequencing identifies Caveolin 1 as an essential factor in zebrafish heart regeneration. *Development*, *143*(2), 232–243.

Carmeliet, P. (2000). Mechanisms of angiogenesis and arteriogenesis. *Nature medicine*, *6*(4), 389-95.

Caspi, O., & Aronson, D. (2020). Morphine in the Setting of Acute Heart Failure: Do the Risks Outweigh the Benefits? *Cardiac Failure Review*, *6*(20).

Castro-Quezada, A., Nadal-Ginard, B., & De La Cruz, M. V. (1972). Experimental study of the formation of the bulboventricular loop in the chick. *J. Embryol. Exp. Morphol.*, *27*, 623–637.

Cervero, F., & Merskey, H. (1996). What is a noxious stimulus? *Pain Forum*, *5*(3), 57-161.

Chablais, F., & Jaźwińska, A. (2012). Induction of myocardial infarction in adult zebrafish using cryoinjury. *J Vis Exp* ., *62*.

Chablais, F., & Jaźwińska, A. (2012). The regenerative capacity of the zebrafish heart is dependent on TGFβ signaling. *Development*, *139*(11), 1921–1930.

Chablais, F., Veit, J., Rainer, G., & Jaźwińska, A. (2011, April 7). *The zebrafish heart regenerates after cryoinjury-induced myocardial infarction*. PubMed. Retrieved February 1, 2022, from https://pubmed.ncbi.nlm.nih.gov/21473762/

Charbaji, N., Rosenthal, P., Schäfer-Korting, M., & Küchler, S. (2013). Cytoprotective effects of opioids on irradiated oral epithelial cells. *Wound Repair Regen*, *21*(6), 883-9.

Charbaji, N., Schäfer-Korting, M., & Küchler, S. (n.d.). Morphine stimulates cell migration of oral epithelial cells by delta-opioid receptor activation. *PLoS One* ., *7*(8), 2012.

Chatigny, F., Creighton, C. M., & Stevens, E. D. (2018). Updated Review of Fish Analgesia. *Journal of the American Association for Laboratory Animal Science : JAALAS*, *1*(57), 5-12.

Chen, B., Dodge, M. E., Chen, C., & Lum, L. (100-7). Small molecule-mediated disruption of Wnt-dependent signaling in tissue regeneration and cancer. *Nat Chem Biol* ., (5), 2.

Choi, W.-Y., Gemberling, M., & Poss, K. D. (2013). In vivo monitoring of cardiomyocyte proliferation to identify chemical modifiers of heart regeneration. *Development*, *140*(3), 660-6.

Clark, J. D., Shi, X., Li, X., Qiao, Y., Liang, D., Angst, M. S., & Yeomans, D. C. (2007). Morphine reduces local cytokine expression and neutrophil infiltration after incision. *Molecular pain*, *3*(28).

Correia, A. D., Cunha, S. R., Scholze, M., & Stevens, E. D. (2011). A Novel Behavioral Fish Model of Nociception for Testing Analgesics. *Pharmaceuticals (Basel)*, *4*(4), 665–680.

Cousineau, A., Midwood, J.D., Stamplecoskie, K., King, G., Suski, C.D., & Cooke, S.J. (2014). Diel patterns of baseline glucocorticoids and stress responsiveness in a teleost fish (bluegill, Lepomis macrochirus). *Canadian Journal of Zoology*, *92*(5).

Curado, S., Stainier, D. Y. R., & Anderson, R. M. (2009). Nitroreductase-mediated cell/tissue ablation in zebrafish: a spatially and temporally controlled ablation method with applications in developmental and regeneration studies. *Nature protocols*, *3*(6), 948–954.

Das, S., Goldstone, A. B., Wang, H., Farry, J., D'Amato, G., Paulsen, M. J., Eskandari, A., Hironaka, C. E., Phansalkar, R., Sharma, B., Rhee, S., Shamskhou, E. A., Agalliu, D., Perez, V. d. J., Woo, Y. J., & Red-Horse, K. (2019). A unique collateral artery development program promotes neonatal heart regeneration. *Cell*, *176*(5), 1128–1142.

Deakin, A. G., Buckley, J., AlZu'bi, H. S., Cossins, A. R., Spencer, J. W., Al'Nuaimy, W., Young, I. S., Thomson, J. S., & Sneddon, L. U. (2019). Automated monitoring of behaviour in zebrafish after invasive procedures. *Scientific Reports*, *9*.

Deakin, A. G., Buckley, J., AlZu'bi, H. S., Cossins, A. R., Spencer, J. W., Al'Nuaimy, W., Young, I. S., Thomson, J. S., & Sneddon, L. U. (2019). Automated monitoring of behaviour in zebrafish after invasive procedures. *Scientific Reports*, *9*.

Deakin, A. G., Spencer, J. W., Cossins, A. R., Young, I. S., & Sneddon, L. U. (2019). Welfare Challenges Influence the Complexity of Movement: Fractal Analysis of Behaviour in Zebrafish. *MDPI fishes*, *4*(1).

de Bakker, D. E. M., Bouwman, M., Dronkers, E., Simões, F. C., Riley, P. R., Goumans, M.-J., Smits, A. M., & Bakkers, J. (2021). Prrx1b restricts fibrosis and promotes Nrg1-dependent cardiomyocyte proliferation during zebrafish heart regeneration. *Development*, *148*(19).

de Preux Charles, A.-S., Bise, T., Baier, F., Marro, J., & Jaźwińska, A. (2016). Distinct effects of inflammation on preconditioning and regeneration of the adult zebrafish heart. *Open biology*, *6*(7).

Didié, M., Christalla, P., Rubart, M., Muppala, V., Döker, S., & Unsöld, B. (2013). Parthenogenetic stem cells for tissue-engineered heart repair. *J. Clin. Investig.*, *123*, 1285–1298.

Drastichova, Z., Skrabalova, J., Jedelsky, P., Neckar, J., Kolar, F., & Novotny, J. (2012). Global Changes in the Rat Heart Proteome Induced by Prolonged Morphine Treatment and Withdrawal. *Plos One*.

Drastichova, Z., Skrabalova, J., Neckar, J., Kolar, F., & Novotny, J. (2011). Prolonged morphine administration alters protein expression in the rat myocardium. *Journal of Biomedical Science*, *18*(89).

Duan, J., Gherghe, C., Liu, D., Hamlett, E., Srikantha, L., Rodgers, L., Regan, J. N., Rojas, M., Willis, M., Leask, A., Majesky, M., & Deb, A. (2012). Wnt1/βcatenin injury response activates the epicardium and cardiac fibroblasts to promote cardiac repair. *EMBO J .*, *31*(2), 429-42.

D'Uva, G., Aharonov, A., Lauriola, M., Kain, D., Yahalom-Ronen, Y., Carvalho, S., Weisinger, K., Bassat, E., Rajchman, D., Yifa, O., Lysenko, M., Konfino, T., Hegesh, J., Brenner, O., Neeman, M., Yarden, Y., Leor, J., Sarig, R., Harvey, R. P., & Tzahor, E. (2005). ERBB2 triggers mammalian heart regeneration by promoting cardiomyocyte dedifferentiation and proliferation. *Nature Cell Biology*, *17*, 627–638.

Ellis, L. D., & Soanes, K. H. (2012). A larval zebrafish model of bipolar disorder as a screening platform for neuro-therapeutics. *Behavioural brain research*, *233*, 450–457.

Engleka, K. A., Manderfield, L. J., Brust, R. D., Li, L., Cohen, A., & Dymecki, S. M. (2012). Islet1 Derivatives in the Heart Are of Both Neural Crest and Second Heart Field Origin. *Circulat. Res.*, *110*, 922–926.

Ernst, A., Alkass, K., Bernard, S., Salehpour, M., Perl, S., Tisdale, J., Possnert, G., Druid, H., & Frisén, J. (2014). Neurogenesis in the Striatum of the Adult Human Brain. *Cell*, *156*(5), 1072-1083.

Fadel, B., Boutet, S. C., & Quertermous, T. (1999). Octamer-dependent in Vivo Expression of the Endothelial Cell-specific TIE2 Gene. *J. Biol. Chem.*, *274*, 20376–20383.

Fang, Y., Gupta, V., Karra, R., Holdway, J. E., Kikuchi, K., & Poss, K. D. (2013). Translational profiling of cardiomyocytes identifies an early Jak1/Stat3 injury response required for zebrafish heart regeneration. *PNAS*, *110*(33), 13416-21.

Farbehi, N., Patrick, R., Dorison, A., Xaymardan, M., Janbandhu, V., & Wystub-Lis, K. (2019). Single-cell expression profiling reveals dynamic flux of cardiac stromal, vascular and immune cells in health and injury. *eLife*, *8*.

Farley, P. (2011). Should topical opioid analgesics be regarded as effective and safe when applied to chronic cutaneous lesions? *J Pharm Pharmacol.*, *63*(3), 747-56.

Fecho, K., Manning, E. L., Maixner, W., & Schmitt, C. P. (2007). Effects of carrageenan and morphine on acute inflammation and pain in Lewis and Fischer rats. *Brain, Behavior, and Immunity*, *21*(1), 68-78.

Feehan, A. K., & Zadina, J. E. (2019). Morphine immunomodulation prolongs inflammatory and postoperative pain while the novel analgesic ZH853 accelerates recovery and protects against latent sensitization. *Journal of neuroinflammation*, *16*(100).

Fitzgerald, J. A., Tulasi Kirla, K., Zinner, C. P., & vom Berg, C. M. (2019). Emergence of consistent intra-individual locomotor patterns during zebrafish development. *Scientific Reports*, *9*.

Flinn, M. A., Jeffery, B. E., O'Meara, C. C., & Link, B. A. (2019). Yap is required for scar formation but not myocyte proliferation during heart regeneration in zebrafish. *Cardiovascular Research*, *115*(3), 570–577.

Fu, W., Wang, W. E., & Zeng, C. (2019). Wnt signaling pathways in myocardial infarction and the therapeutic effects of Wnt pathway inhibitors. *Acta pharmacologica sinica*, *40*, 9–12.

Fu, X., Khalil, H., Kanisicak, O., Boyer, J., Vagnozzi, R., & Maliken, B. (2018). Specialized fibroblast differentiated states underlie scar formation in the infarcted mouse heart. *J Clin Invest.*, *128*(5), 2127–43.

Furutani-Seik, M., Jiang, Y. J., Brand, M., Heisenberg, C. P., Houart, C., Beuchle, D., van Eeden, J. F., Granato, M., Haffter, P., Hammerschmidt, M., Kane, D. A., Kelsh, R. N., Mullins, M. C., Odenthal, J., & Nüsslein-Volhard, C. (1996). *Neural degeneration mutants in the zebrafish, Danio rerio*. PubMed. Retrieved January 31, 2022, from https://pubmed.ncbi.nlm.nih.gov/9007243/

Gamba, L., Amin-Javaheri, A., & Lien, C.-L. (2017). Collagenolytic Activity Is Associated with Scar Resolution in Zebrafish Hearts after Cryoinjury. *J Cardiovasc Dev Dis.*, *4*(1).

Gao, J., Fan, L., Zhao, L., & Su, Y. (2021). The interaction of Notch and Wnt signaling pathways in vertebrate regeneration. *Cell Regeneration*, *10*.

Gemberling, M., Karra, R., Dickson, A. L., & Poss, K. D. (2015). Nrg1 is an injury-induced cardiomyocyte mitogen for the endogenous heart regeneration program in zebrafish. *Elife*.

Gesser, S., & Kuhl, M. (2010). The Multiple Phases and Faces of Wnt Signaling During Cardiac Differentiation and Development. *Circulation Research*, *107*(2), 186-99.

Gladka, M. M. (2021). Single-Cell RNA Sequencing of the Adult MammalianHeart—State-of-the-Art and Future Perspectives. *Current Heart Failure Reports*, *18*, 64–70.

Gladka, M. M., Molenaar, B., de Ruiter, H., van der Elst, S., Tsui, H., & Versteeg, D. (2018). Single-cell sequencing of the healthy and diseased heart reveals cytoskeleton-associated protein 4 as a new modulator of fibroblasts activation. *Circulation*.

González-Cuello, A., Milanés, M. V., Castells, M. T., & Laorden, M. L. (2003). Activation of c-fos expression in the heart after morphine but not U-50,488H withdrawal. *British journal of pharmacology.*, *138*(4), 626-33.

González‐Rosa, J. M., Burns, C. E., & Burns, C. G. (2017). Zebrafish heart regeneration: 15 years of discoveries. *Regeneration (Oxford, England)*, *4*(3), 105–123.

González-Rosa, J. M., Guzmán-Martínez, G., João Marques, I., Sánchez-Iranzo, H., Jiménez-Borreguero, L. J., & Mercader, N. (2014). Use of echocardiography reveals reestablishment of ventricular pumping efficiency and partial ventricular wall motion recovery upon ventricular cryoinjury in the zebrafish. *PLoS One*, *12*.

González-Rosa, J. M., Martín, V., Peralta, M., Torres, M., & Mercader, N. (2011, March 23). *Extensive scar formation and regression during heart regeneration after cryoinjury in zebrafish*. PubMed. Retrieved February 1, 2022, from https://pubmed.ncbi.nlm.nih.gov/21429987/

González-Rosa, J. M., Sharpe, M., Field, D., Soonpaa, M. H., Field, L. J., Burns, C. E., & Burns, C. G. (2018). Myocardial Polyploidization Creates a Barrier to Heart Regeneration in Zebrafish. *Developmental Cell*, *26*, 433-446.

Gupta, V., Gemberling, M., Karra, R., Rosenfeld, G. E., Evans, T., & Poss, K. D. (2013). An injury-responsive gata4 program shapes the zebrafish cardiac ventricle. *Curr Biol .*, *23*(13), 1221-7.

Gut, P., Reischauer, S., Stainier, D. Y. R., & Arnaout, R. (2017). Little Fish, Big Data: Zebrafish as a Model for Cardiovascular and Metabolic Disease. *Physiological reviews.*, *889–938*(97), 3.

Hafemeister, C., & Satija, R. (2019). Normalization and variance stabilization of single-cell RNA-seq data using regularized negative binomial regression. *BMC Genome Biology*, *20*.

Han, M., & Zhou, B. (2022). Role of Cardiac Fibroblasts in Cardiac Injury and Repair. *Current Cardiology Reports*, *154*.

Harding, T. C., Geddes, B. J., Murphy, D., Knight, D., & Uney, J. B. (1998). Switching transgene expression in the brain using an adenoviral tetracycline-regulatable system. *Nat. Biotechnol.*, *16*, 553–555.

Harris, J. A., Cheng, A. G., Cunningham, L. L., MacDonald, G., Raible, D. W., & Rubel, E. W. (2003). *Neomycin-induced hair cell death and rapid regeneration in the lateral line of zebrafish (Danio rerio)*. PubMed. Retrieved January 31, 2022, from https://pubmed.ncbi.nlm.nih.gov/12943374/

Heallen, T., Zhang, M., Wang, J., Bonilla-Claudio, M., Klysik, E., Johnson, R. L., & Martin, J. F. (2011). Hippo pathway inhibits Wnt signaling to restrain cardiomyocyte proliferation and heart size. *Science*, *332*, 458-61.

Hein, S. J., Lehmann, L. H., Kossak, M., Juergensen, L., Fuchs, D., Katus, H. A., & Hassel, D. (2015). Advanced echocardiography in adult zebrafish reveals delayed recovery of heart function after myocardial cryoinjury. *PLoS One*, *4*.

Henderson, N. C., Rieder, F., & Wynn, T. A. (2020). Fibrosis: from mechanisms to medicines. *Nature*, *587*, 555–566.

Herrero-Turrión, M. J., Rodríguez-Martín, I., López-Bellido, R., & Rodríguez, R. E. (2014). Whole-genome expression profile in zebrafish embryos after chronic exposure to morphine: identification of new genes associated with neuronal function and mu opioid receptor expression. *BMC Genomics*, *15*(874).

Honkoop, H., de Bakker, D. E., Aharonov, A., Kruse, F., Shakked, A., Poss, K. D., van Oudenaarden, A., Tzahor, E., & Bakkers, J. (2019). Single-cell analysis uncovers that metabolic reprogramming by ErbB2 signaling is essential for cardiomyocyte proliferation in the regenerating heart. *eLife*, *8*.

Howe, K., Clark, M. D., Torroja, C. F., Crollius, H. R., Rogers, J., & Stemple, D. L. (2013). The zebrafish reference genome sequence and its relationship to the human genome. *Nature*, *496*, 498–503.

Hu B., Lelek S., Spanjaard B., El-Sammak H., Guedes Simões M., Mintcheva J., Aliee H., Schäfer R., Meyer A.M., Theis F., Stainier D.Y.R., Panáková D., Junker J.P., (2022); **“Origin and function of**

activated fibroblasts states during zebrafish heart regeneration"; accepted ***Nature Genetics***, pre-print on bioRxiv; attached with this thesis

Huang, W.-C., Yang, C.-C., & Chuang, Y.-J. (2013). Treatment of Glucocorticoids Inhibited Early Immune Responses and Impaired Cardiac Repair in Adult Zebrafish. *PLoS One*, *8*(6).

Isken, A., Golczak, M., Oberhauser, V., Hunzelmann, S., Driever, W., Imanishi, Y., Palczewski, K., & von Lintig, J. (2008). RBP4 disrupts vitamin A uptake homeostasis in a STRA6-deficient animal model for Matthew-Wood syndrome. *Cell metabolism.*, *7*(3), 258-68.

Itou, J., Oishi, I., Kawakami, H., Glass, T. J., Richter, J., Johnson, A., Lund, T. C., & Kawakami, Y. (2012). Migration of cardiomyocytes is essential for heart regeneration in zebrafish. *Development*, *139*(22), 4133-42.

Jiang, M., Xiao, Y., & Guo, G. (2021). Characterization of the Zebrafish Cell Landscape at Single-Cell Resolution. *Frontiers in Cell and Developmental Biology*.

Jiang, X., Rowitch, D., Soriano, P., McMahon, A., & Sucov, H. (2000). Fate of the mammalian cardiac neural crest. *Development*, *127*(8), 1607–16.

Jopling, C., Suñé, G., Faucherre, A., Fabregat, C., & Izpisua Belmonte, J. C. (2012). Hypoxia induces myocardial regeneration in zebrafish. *Circulation*, *125*(25), 3017-27.

Jorge, S., Ferreira, J. M., Olsson, I. A. S., & Valentim, A. M. (2021). Adult Zebrafish Anesthesia: A Study of Efficacy and Behavioral Recovery of Different Anesthetics. *Zebrafish*, *18*(5).

Kan, N. G., Junghans, D., & Izpisua Belmonte, J. C. (2009). Compensatory growth mechanisms regulated by BMP and FGF signaling mediate liver regeneration in zebrafish after partial hepatectomy. *Federation of American Societies for Experimental Biology*.

Kapuria, S., Bai, H., Fierros, J., Harrison, M. M. R., & Lien, C.-L. (2022). Heterogeneous pdgfrβ+ cells regulate coronary vessel development and revascularization during heart regeneration. *Development*.

Karra, R., Knecht, A. K., Kikuchi, K., & Poss, K. D. (2015). Myocardial NF-κB activation is essential for zebrafish heart regeneration. *PNAS*, *112*(43), 13255-60.

Key, B. (2015). Fish do not feel pain and its implications for understanding phenomenal consciousness. *Biology & philosophy*, *30*(2), 149–165.

Khor, B.-S., Jamil, M. F. A., Adenan, M. I., & Shu-Chien, A. C. (2011). Mitragynine attenuates withdrawal syndrome in morphine-withdrawn zebrafish. *PLoS One*, *6*(12).

Kikuchi, K., Holdway, J. E., Major, R. J., Dahn, R. D., Begemann, G., & Poss, K. D. (2011). Retinoic Acid Production by Endocardium and Epicardium Is an Injury Response Essential for Zebrafish Heart Regeneration. *Developmental Cell*, *20*(3), 397-404.

Kikuchi, K., Holdway, J. E., Werdich, A. A., Anderson, R. M., Fang, Y., Egnaczyk, G. F., Evans, T., Macrae, C. A., Stainier, D. Y. R., & Poss, K. D. (2010). Primary contribution to zebrafish heart regeneration by gata4(+) cardiomyocytes. *Nature*, *464*, 601-5.

Kim, J., Wu, Q., Zhang, Y., Starnes, V. A., & Lien, C.-L. (2010). PDGF signaling is required for epicardial function and blood vessel formation in regenerating zebrafish hearts. *Proceedings of the National Academy of Sciences of the United States of America*, *107*(40), 17206-10.

Kinkel, M. D., Eames, S. C., Philipson, L. H., & Prince, V. E. (2010). Intraperitoneal injection into adult zebrafish. *Journal of visualized experiments : JoVE*, *42*.

Kitchener, P. D., Fuller, J., & Snow, P. J. (2010). Central Projections of Primary Sensory Afferents to the Spinal Dorsal Horn in the Long-Tailed Stingray, Himantura fai. *Brain, Behavior and Evolution*, *76*, 60–70.

Komiya, Y., & Habas, R. (2008). Wnt signal transduction pathways. *Organogenesis.*, *4*(2), 68–75.

Korsunsky, I., Millard, N., Fan, J., Slowikowski, K., Zhang, F., Wei, K., Baglaenko, Y., Brenner, M., Loh, P., & Raychaudhuri, S. (2019). Fast, sensitive and accurate integration of single-cell data with Harmony. *Nature Methods*, *16*, 1289–1296.

Koth, J., Wang, X., Killen, A. C., Stockdale, W. T., & Mommersteeg, M. T. M. (2020). Runx1 promotes scar deposition and inhibits myocardial proliferation and survival during zebrafish heart regeneration. *Development*, *147*(8).

Kretzschmar, K., & Watt, F. M. (2012). Lineage Tracing. *Cell*, *148*(1-2), 33-45.

Küchler, S., Wolf, N. B., Heilmann, S., Weindl, G., Helfmann, J., Yahya, M. M., Stein, C., & Schäfer-Korting, M. (2010). 3D-wound healing model: influence of morphine and solid lipid nanoparticles. *J Biotechnol* ., *148*(1), 24-30.

Kuil, L. E., Oosterhof, N., Ferrero, G., Mikulášová, T., Hason, M., Dekker, J., Rovira, M., van der Linde, H. C., van Strien, P. M., de Pater, E., Schaaf, G., Bindels, E. M., Wittamer, V., & van Ham, T. J. (2020). Zebrafish macrophage developmental arrest underlies depletion of microglia and reveals Csf1r-independent metaphocytes. *eLife*, *9*.

La Manno, G., Soldatov, R., Zeisel, A., Braun, E., Hochgerner, H., Petukhov, V., Lidschreiber, K., Kastriti, M. E., Lönnerberg, P., Furlan, A., Fan, J., Borm, L. E., Liu, Z., van Bruggen, D., Guo, J., He, X., Barker, R., Sundström, E., Castelo-Branco, G., … Kharchenko, P. V. (2018). RNA velocity of single cells. *Nature*, *560*, 494-498.

Lange, M., Neuzeret, F., Fabreges, B., Froc, C., Bedu, S., Bally-Cuif, L., & Norton, W. H. J. (2013). Inter-Individual and Inter-Strain Variations in Zebrafish Locomotor Ontogeny. *Plos One*.

Lázár, E., Sadek, H. A., & Bergmann, O. (2017). Cardiomyocyte renewal in the human heart: insights from the fall-out. *European heart journal.*, *38*(30), 2333–2342.

Lelek, S., Guedes Simões, M., Hu, B., Alameldeen, A. M.A., Czajkowski,, M. T., Ferrara, F., Meyer, A. M., Junker, J. P., & Panáková, D. (2020). Morphine alleviates pain after heart cryoinjury in zebrafish without impeding regeneration. *bioRxiv*. Retrieved 02 02, 2022, from https://www.biorxiv.org/content/10.1101/2020.10.01.322560v1

Lepilina, A., Coon, A. N., Kikuchi, K., Holdway, J. E., Roberts, R. W., Burns, C. G., & Poss, K. D. (2006). A dynamic epicardial injury response supports progenitor cell activity during zebrafish heart regeneration. *Cell*, *127*(3), 607-19.

Lien, C.-L., Schebesta, M., Makino, S., Weber, G. J., & Keating, M. T. (2006). Gene expression analysis of zebrafish heart regeneration. *PLoS Biology*, *4*(8).

Litviňuková, M., Talavera-López, C., Maatz, H., Reichart, D., Worth, C. L., Lindberg, E. L., Kanda, M., Polanski, K., Heinig, M., Lee, M., Nadelmann, E. R., Roberts, K., Tuck, L., Fasouli, E. S., DeLaughter, D. M., McDonough, B., Wakimoto, H., Gorham, J. M., Samari, S., … Teichmann, S. A. (2020). Cells of the adult human heart. *Nature*, *588*, 466-472.

Liu, F.-Y., Hsu, T.-C., Choong, P., Lin, M.-H., Chuang, Y.-J., Chen, B.-S., & Lin, C. (2018). Uncovering the regeneration strategies of zebrafish organs: a comprehensive systems biology study on heart, cerebellum, fin, and retina regeneration. *BMC Syst Biol .*, *12*.

Livak, K. J., & Schmittgen, T. D. (2001). Analysis of relative gene expression data using real-time quantitative PCR and the 2(-Delta Delta C(T)) Method. *Methods*, *25*(4), 402-8.

LOGUINOV, A. V., ANDERSON, L. M., CROSBY, G. J., & YUKHANANOV, R. Y. (2001). Gene expression following acute morphine administration. *Physiological Genomics*, *6*(3), 169-181.

Lopez-Luna, J., Al-Jubouri, Q., Al-Nuaimy, W., & Sneddon, L. U. (2017). Reduction in activity by noxious chemical stimulation is ameliorated by immersion in analgesic drugs in zebrafish. *J Exp Biol*, *220*, 1451–1458.

Loram, L. C., Grace, P. M., Strand, K. A., Taylor, F. R., Ellis, A., Berkelhammer, D., Bowlin, M., Maier, B. S. S. F., & Watkins, L. R. (2012). Prior exposure to repeated morphine potentiates mechanical allodynia induced by peripheral inflammation and neuropathy. *Brain, behavior, and immunity.*, *26*(8), 1256-64.

Ma, H., Liu, Z., Yang, Y., Feng, D., Dong, Y., Garbutt, T. A., Hu, Z., Wang, L., Luan, C., Cooper, C. D., Li, Y., Welch, J. D., Qian, L., & Liu, J. (2021). Functional coordination of non-myocytes plays a key role in adult zebrafish heart regeneration. *EMBO Reports*, *22*.

Ma, H., Liu, Z., Yang, Y., Feng, D., Dong, Y., Garbutt, T. A., Hu, Z., Wang, L., Luan, C., Cooper, C. D., Li, Y., Welch, J. D., Qian, L., & Liu, J. (2021). Functional coordination of non-myocytes plays a key role in adult zebrafish heart regeneration. *EMBO Reports*, *22*.

Malafoglia, V., Bryant, B., Raffaeli, W., Giordano, A., & Bellipanni, G. (2013). The zebrafish as a model for nociception studies. *Journal of Cellular Physiology*, *228*(10), 1956-1966.

Mao, J., & Chen, L. L. (2000). Systemic lidocaine for neuropathic pain relief. *Pain*, *87*, 7–17.

Marín-Juez, R., El-Sammak, H., Poss, K. D., & Stainier, D. Y. R. (2019). Coronary Revascularization During Heart Regeneration Is Regulated by Epicardial and Endocardial Cues and Forms a Scaffold for Cardiomyocyte Repopulation. *Developmental Cell*, *51*(4), 503-515.

Marín-Juez, R., Marass, M., Gauvrit, S., & Stainier, D. Y. R. (2016). Fast revascularization of the injured area is essential to support zebrafish heart regeneration. *PNAS*, *113*(40), 11237-11242.

Marín-Sedeño, E., Martínez de Morentin, X., Pérez-Pomares, J. M., Gómez-Cabrero, D., & Ruiz-Villalba, A. (2021). Understanding the Adult Mammalian Heart at Single-Cell RNA-Seq Resolution. *Frontiers in Cell and Developmental Biology*, *12*.

Marques, I. J., Lupi, E., & Mercader, N. (2019). Model systems for regeneration: zebrafish. *Development*, *146*(18). Retrieved 01 31, 2022, from https://journals.biologists.com/dev/article/146/18/dev167692/224198/Model-systems-for-regeneration-zebrafish

Marro, J., Pfefferli, C., de Preux Charles, A.-S., Bise, T., & Jaźwińska, A. (2016). Collagen XII Contributes to Epicardial and Connective Tissues in the Zebrafish Heart during Ontogenesis and Regeneration. *PLOS ONE*.

Martins, C. I. M., Galhardo, L., Noble, C., Damsgård, B., Spedicato, M. T., Zupa, W., Beauchaud, M., Kulczykowska, E., Massabuau, J.-C., Carter, T., Rey Planellas, S., & Kristiansen, T. (2012). Behavioural indicators of welfare in farmed fish. *Fish Physiol Biochem.*, *38*(1), 17–41.

Martins, T., Valentim, A., & Marques Antunes, L. (2019). Anaesthetics and analgesics used in adult fish for research: A review. *Laboratory Animal Science Association*, *57*(4), 325-341.

Martins, T., Valentim, A. M., Pereira, N., & Antunes, L. M. (2016). Anaesthesia and analgesia in laboratory adult zebrafish: a question of refinement. *aboratory Animal Science Association*, *50*(6), 476-488.

Matthews, G., & Wickelgren, W. O. (1978). Trigeminal sensory neurons of the sea lamprey. *Journal of comparative physiology*, *123*, 329–333.

Maximino, C. (2011). Modulation of nociceptive-like behavior in zebrafish (Danio rerio) by environmental stressors. *Psychology & Neuroscience*, *4*(1), 149-155.

McClung, C. A., Nestler, E. J., & Zachariou, V. (2005). Regulation of Gene Expression by Chronic Morphine and Morphine Withdrawal in the Locus Ceruleus and Ventral Tegmental Area. *The Journal of Neuroscience*, *25*(25), 6005-6015.

McLellan, M., Skelly, D., Dona, M., Squiers, G., Farrugia, G., & Gaynor, T. (2020). High-Resolution Transcriptomic Profiling of the Heart During Chronic Stress Reveals Cellular Drivers of Cardiac Fibrosis and Hypertrophy. *Circulation*, *142*(15), 1448–63.

Meier, C. K., & Oyman, M. A. (2009). *Chapter 41 - Myocardial Infarction*. Elsevier. Retrieved 01 19, 2022, from https://doi.org/10.1016/B978-1-4160-2591-7.10041-4

Mettam, J. J., McCrohan, C. R., & Sneddon, L. U. (2012). Characterisation of chemosensory trigeminal receptors in the rainbow trout, Oncorhynchus mykiss: responses to chemical irritants and carbon dioxide. *Journal of Experimental Biology*, *215*(4), 685–693.

Mikawa, T., & Fischman, D. A. (1992). Retroviral analysis of cardiac morphogenesis: discontinuous formation of coronary vessels. *PNAS*, *89*, 9504–9508.

Millard, S. M., Heng, O., Opperman, K. S., Sehgal, A., Irvine, K. M., Kaur, S., Sandrock, C. J., Wu, A. C., Magor, G. W., Batoon, L., Perkins, A. C., Noll, J. E., Zannettino, A. C. W., Sester, D. P.,

Levesque, J.-P., Hume, D. A., Raggatt, L. J., Summers, K. M., & Pettit, A. R. (n.d.). Fragmentation of tissue-resident macrophages during isolation confounds analysis of single-cell preparations from mouse hematopoietic tissues. *Cell Reports*, *37*(8), 2021.

Moore-Morris, T., Guimaraes-Camboa, N., Banerjee, I., Zambon, A., Kisseleva, T., & Velayoudon, A. (2014). Resident fibroblast lineages mediate pressure overload-induced cardiac fibrosis. *J Clin Invest.*, *127*(4), 2921–34.

Moses, K. A., DeMayo, F., Braun, R., Reecy, J. L., & Schwartz, R. J. (2001). Embryonic expression of anNkx2-5/Cre gene usingROSA26 reporter mice. *Genesis*, *31*, 176–180.

Mosimann, C., Panáková, D., Werdich, A. A., Musso, G., Burger, A., Lawson, K. L., Carr, L. A., Nevis, K. R., Sabeh, M. K., Zhou, Y., Davidson, A. J., DiBiase, A., Burns, C. E., Burns, C. G., MacRae, C. A., & Zon, L. I. (n.d.). Chamber identity programs drive early functional partitioning of the heart. *Nature Communications*, *6*(8146).

Moyes, A. J., & Hobbs, A. J. (2019). C-type Natriuretic Peptide: A Multifaceted Paracrine Regulator in the Heart and Vasculature. *International journal of molecular sciences.*, *20*(9), 2281.

Moyse, B. R., & Richardson, R. J. (2020). A Population of Injury-Responsive Lymphoid Cells Expresses mpeg1.1 in the Adult Zebrafish Heart. *Immunohorizons .*, *4*(8), 464-474.

Münch, J., Grivas, D., González-Rajal, Á., & de la Pompa, J. L. (2017). Notch signalling restricts inflammation and serpine1 expression in the dynamic endocardium of the regenerating zebrafish heart. *Development*, *144*(8), 1425-1440.

Murphy, G. S., Szokol, J. W., Marymont, J. H., Avram, M. J., & Vender, J. S. (2006). Opioids and cardioprotection: the impact of morphine and fentanyl on recovery of ventricular function after cardiopulmonary bypass. *J Cardiothorac Vasc Anesth*, *20*(4), 493-502.

Murphy, G. S., Szokol, J. W., Marymont, J. H., Greenberg, S. B., Avram, M. J., Vender, J. S., Sherwani, S. S., Nisman, M., & Doroski, V. (2009). Morphine-based cardiac anesthesia provides superior early recovery compared with fentanyl in elective cardiac surgery patients. *Anesth Analg.*, *109*(2), 311-9.

Nag, A. (1980). Study of non-muscle cells of the adult mammalian heart: a fine structural analysis and distribution. *Cytobios.*, *28*, 41–61.

Nejak-Bowen, K. N., & Singh Monga, S. P. (2015). Chapter 6 - Developmental Pathways in Liver Regeneration-I. *Liver Regeneration*, 77-101.

Nesan, D., & Vijayan, M. M. (2016). Maternal Cortisol Mediates Hypothalamus-Pituitary-Interrenal Axis Development in Zebrafish. *Scientific Reports*, *6*.

Nobre Bezerra, A. N. J., Oliveira Silva, F. C., & Dos Santos, H. S. (2021). Antinociceptive effect of triterpene acetyl aleuritolic acid isolated from Croton zehntneri in adult zebrafish (Danio rerio). *Biochemical and biophysical research communications*, *1*, 478-484.

O'gara, P. T., Kushner, F. G., Ascheim, D. D., Casey, D. E., & Chung, M. K. (2013). 2013 ACCF/AHA Guideline for the Management of ST-Elevation Myocardial Infarction: A Report of the American College of Cardiology Foundation/American Heart Association Task Force on Practice Guidelines. *Journal of the American College of Cardiology*, *61*(4), 78-140.

Ohnesorge, N., Heinl, C., & Lewejohann, L. (2021). Current Methods to Investigate Nociception and Pain in Zebrafish. *Frontiers in Neuroscience*.

Ohnesorge, N., Heinl, C., & Lewejohann, L. (2021). Current Methods to Investigate Nociception and Pain in Zebrafish. *Frontiers in Neuroscience*.

Ozhan, G., & Weidinger, G. (2015). Wnt/β-catenin signaling in heart regeneration. *Cell Regen.*, *4*(3).

Paik, D. T., Cho, S., Tian, L., Chang, H. Y., & Wu, J. C. (2020). Single-cell RNA sequencing in cardiovascular development, disease and medicine. *Nature Reviews Cardiology*, *17*, 457–473.

Parente, V., Balasso, S., Pompilio, G., Verduci, L., Colombo, G. I., Milano, G., Guerrini, U., Squadroni, L., Cotelli, F., Pozzoli, O., & Capogrossi, M. C. (2013). Hypoxia/reoxygenation cardiac injury and regeneration in zebrafish adult heart. *PLoS One*, *8*(1).

Parodi, G. (2016). Chest pain relief in patients with acute myocardial infarction. *European Heart Journal - Acute Cardiovascular Care*, *5*(3).

Patel, S., Alam, A., Pant, R., & Chattopadhyay, S. (2019). Wnt Signaling and Its Significance Within the Tumor Microenvironment: Novel Therapeutic Insights. *Frontiers in Immunology*.

Patra, C., Kontarakis, Z., Kaur, H., Rayrikar, A., Mukherjee, D., & Stainier, D. Y. R. (2017). The zebrafish ventricle: A hub of cardiac endothelial cells for in vitro cell behavior studies. *Scientific Reports*, *7*.

Patwardhan, V., Fernandez, S., Montgomery, M., & Litvin, J. (2000). The rostro-caudal position of cardiac myocytes affect their fate. *Devel. Dynam.*, *218*, 123–135.

Pavlidis, M., Theodoridi, A., & Tsalafouta, A. (2015). Neuroendocrine regulation of the stress response in adult zebrafish, Danio rerio. *Progress in Neuro-Psychopharmacology & Biological Psychiatry*, *60*, 121-131.

Peng, X., Fan, S., Tan, J., Cai, W., & Tang, W. H. (2020). Wnt2bb Induces Cardiomyocyte Proliferation in Zebrafish Hearts via the jnk1/c-jun/creb1 Pathway. *Frontiers in Cell and Developmental Biology*.

Peng, X., Lai, K. S., She, P., Kang, J., Wang, T., Li, G., Zhou, Y., Sun, J., Jin, D., Xu, X., Liao, L., Liu, J., Lee, E., Poss, K. D., & Zhong, T. P. (2021). Induction of Wnt signaling antagonists and p21-activated kinase enhances cardiomyocyte proliferation during zebrafish heart regeneration. *J Mol Cell Biol.*, *13*(1), 41–58.

Pérez-Escudero, A., Vicente-Page, J., Hinz, R. C., Arganda, S., & de Polavieja, G. G. (2014). idTracker: tracking individuals in a group by automatic identification of unmarked animals. *Nature Methods*, *11*, 743–748.

Pinto, A. R., Ilinykh, A., Ivey, M. J., Kuwabara, J. T., D'antoni, M. L., & Debuque, R. (n.d.). Revisiting cardiac cellular composition. *Circulat. Res.*, *118*(400–409), 2016.

Plytycz, B., & Natorska, J. (2002). Morphine attenuates pain and prevents inflammation in experimental peritonitis. *Trends in immunology.*, *23*(7), 345-6.

Porrello, E. R., Mahmoud, A. I., Simpson, E., Hill, J. A., Richardson, J. A., Olson, E. N., & Sadek, H. A. (2011). Transient Regenerative Potential of the Neonatal Mouse Heart. *Science*, *331*(1078).

Poss, K. D., WILSON, L. G., & KEATING, M. T. (2002). Heart Regeneration in Zebrafish. *Science*, *298*(5601), 2188-2190.

Pottinger, T. G., Prunet, P., & Pickering, A. D. (1992). The effects of confinement stress on circulating prolactin levels in rainbow trout (Oncorhynchus mykiss) in fresh water. *Gen Comp Endocrinol .*, *88*(3), 454-60.

Rácz, A., Allan, B., Dwyer, T., Thambithurai, D., Crespel, A., & Killen, S. S. (2021). Identification of Individual Zebrafish (Danio rerio): A Refined Protocol for VIE Tagging Whilst Considering Animal Welfare and the Principles of the 3Rs. *Animals (Basel).*, *11*(3), 616.

Ramlochansingh, C., Branoner, F., Chagnaud, B., & Straka, H. (2014). Efficacy of Tricaine Methanesulfonate (MS-222) as an Anesthetic Agent for Blocking Sensory-Motor Responses in Xenopus laevis Tadpoles. *Plos One*, *9*.

Raya, A., Koth, C. M., Büscher, D., Kawakami, Y., & Izpisúa-Belmonte, J. C. (2003). Activation of Notch signaling pathway precedes heart regeneration in zebrafish. *PNAS*, *100*, 1889-95.

Red-Horse, K., Ueno, H., Weissman, I. L., & Krasnow, M. A. (2010). Coronary arteries form by developmental reprogramming of venous cells. *Nature*, *464*, 549–553.

Reilly, S. C., Quinn, J. P., Cossins, A. R., & Sneddon, L. U. (2008). Behavioural analysis of a nociceptive event in fish: Comparisons between three species demonstrate specific responses. *Applied Animal Behaviour Science*, *114*(1-2), 248-259.

Reimschuesse, R. I. (2001). A Fish Model of Renal Regeneration and Developmen. *ILAR*, *42*(4), 285–291.

Ren, Z., P, Y., Li, D., Li, Z., Liao, Y., & Wang, Y. (2020). Single-Cell Reconstruction of Progression Trajectory Reveals Intervention Principles in Pathological Cardiac Hypertrophy. *Circulation*, *141*(21), 1704–19.

Roberts, J. T., & Wearn, J. T. (1941). Quantitative changes in the capillary-muscle relationship in human hearts during normal growth and hypertrophy. *Heart J.*, *21*, 617–633.

Rook, J. M., Hasan, W., & McCarson, K. E. (2008). Morphine-induced early delays in wound closure: involvement of sensory neuropeptides and modification of neurokinin receptor expression. *Anesthesiology*, *77*(11), 1747-55.

Rook, J. M., & McCarson, K. E. (2007). Delay of cutaneous wound closure by morphine via local blockade of peripheral tachykinin release. *Biochem Pharmacol*, *74*(5), 752-7.

Roques, J. A.C., Abbink, W., Geurds, F., van de Vis, H., & Flik, G. (2010). Tailfin clipping, a painful procedure: Studies on Nile tilapia and common carp. *Physiology & Behavior*, *101*(4), 533-540.

Rose, J. D., Arlinghaus, R., Cooke, S. J., Diggles, B. K., Sawynok, W., Stevens, E. D., & Wynne, C. D. L. (2012). Can fish really feel pain? *Fish and Fisheries*, *15*(1), 97-133.

Ruiz-Villalba, A., Simón, A. M., Pogontke, C., Castillo, M. I., Abizanda, G., & Pelacho, B. (2015). Interacting resident epicardium-derived fibroblasts and recruited bone marrow cells form myocardial infarction scar. *J. Am. College Cardiol.*, *65*, 2057–2066.

Ryan, R., Moyse, B. R., & Richardson, R. J. (2020). Zebrafish cardiac regeneration—looking beyond cardiomyocytes to a complex microenvironment. *Histochemistry and cell biology*, *154*(5), 533–548.

Sánchez-Iranzo, H., Galardi-Castilla, M., Sanz-Morejón, A., & Mercader, N. (2018). Transient fibrosis resolves via fibroblast inactivation in the regenerating zebrafish heart. *PNAS*, *115*(16), 4188-4193.

Schnabel, K., Wu, C.-C., Kurth, T., & Weidinger, G. (2011, April 12). *Regeneration of cryoinjury induced necrotic heart lesions in zebrafish is associated with epicardial activation and cardiomyocyte proliferation*. PubMed. Retrieved February 1, 2022, from https://pubmed.ncbi.nlm.nih.gov/21533269/

Schoger, E., Lelek, S., Panáková, D., & Zelarayán, L. C. (2022). Tailoring Cardiac Synthetic Transcriptional Modulation Towards Precision Medicine. *Frontiers in Cardiovascular Medicine*. Retrieved 01 19, 2022, from https://doi.org/10.3389/fcvm.2021.783072

Schroeder, P. G., & Sneddon, L. U. (2017). Exploring the efficacy of immersion analgesics in zebrafish using an integrative approach. *Applied Animal Behaviour Science*, *187*, Applied Animal Behaviour Science.

Schwarz, W., Palade, P. T., & Hille, B. (1977). Local anesthetics. Effect of pH on use-dependent block of sodium channels in frog muscle. *Biophys J*, *20,*, 343–368.

Shi, L., Chen, C., Yin, Z., Wei, G., Xie, G., & Liu, D. (2021). Systematic profiling of early regulators during tissue regeneration using zebrafish model. *Wound Repair Regen*, *29*(1), 189-195.

Shriver, A. (2006). Minding Mammals. *Philosophical Psychology*, *19*(4).

Simões, F. C., Cahill, T. J., Kenyon, A., Sauka-Spengler, T., & Riley, P. R. (2020). Macrophages directly contribute collagen to scar formation during zebrafish heart regeneration and mouse heart repair. *Nature Communications*, *11*.

Simon, A., & Tanaka, E. M. (2012). Limb regeneration. *WIREs Developmental Biology*, *2*(2). Retrieved 01 31, 2022, from https://wires.onlinelibrary.wiley.com/doi/10.1002/wdev.73

Singer, F. (1981). *Production of clones of homozygous diploid zebra fish (Brachydanio rerio)*. PubMed. Retrieved January 31, 2022, from https://pubmed.ncbi.nlm.nih.gov/7248006/

Skelly, D., Squiers, G., McLellan, M., Bolisetty, M., Robson, P., & Rosenthal, N. (2018). Single-Cell Transcriptional Profiling Reveals Cellular Diversity and Intercommunication in the Mouse Heart. *Cell Reports*, *22*(3), 600–10.

Slack, J. M. (2017). Animal regeneration: ancestral character or evolutionary novelty? *EMBO Reports*, *18*, 1497-1508.

Smith, A., Avaron, F., Guay, D., Padhi, B. K., & Akimenko, M. A. (2006). Inhibition of BMP signaling during zebrafish fin regeneration disrupts fin growth and scleroblast differentiation and function. *Developmental Biology*, *299*(2), 438-454.

Sneddon, L. U. (2002). Anatomical and electrophysiological analysis of the trigeminal nerve in a teleost fish, Oncorhynchus mykiss. *Neuroscience Letters*, *319*(3), 167-171.

Sneddon, L. U. (2003). The evidence for pain in fish: the use of morphine as an analgesic. *Applied Animal Behaviour Science*, *83*(2), 153-162.

Sneddon, L. U. (2003). Trigeminal somatosensory innervation of the head of a teleost fish with particular reference to nociception. *Brain Research*, *972*(1-2), 44-52.

Sneddon, L. U. (2004). Evolution of nociception in vertebrates: comparative analysis of lower vertebrates. *Brain Research Reviews*, *46*(2), 123-130.

Sneddon, L. U. (2009). Pain Perception in Fish: Indicators and Endpoints. *ILAR Journal*, *50*(4), 338–342.

Sneddon, L. U. (2012). Clinical Anesthesia and Analgesia in Fish. *Journal of Exotic Pet Medicine*, *21*, 32–43.

Sneddon, L. U. (2015). Pain in aquatic animals. *Journal of Experimental Biology*, *218*(7), 967–976.

Sneddon, L. U., Elwood, R. W., Adamo, S. A., & Leach, M. C. (2014). Defining and assessing animal pain. *Animal Behaviour*, *97*, 201-212.

Soriano, P. (1999). Generalized lacZ expression with the ROSA26 Cre reporter strain. *Nat. Genet.*, *21*, 70–71.

Spanjaard, B., Hu, B., Mitic, N., Olivares-Chauvet, P., Janjuha, S., Ninov, N., & Junker, J. P. (2018). Simultaneous lineage tracing and cell-type identification using CRISPR/Cas9-induced genetic scars. *Nature Biotechnology*, *36*(5), 469–473.

Stabler, C. T., & Morrisey, E. E. (2018). Developmental pathways in lung regeneration. *Cell Tissue Res.*, *367*(3), 677–685.

Stein, C., Comisel, K., Haimerl, E., Yassouridis, A., Lehrberger, K., Herz, A., & Peter, K. (1991). Analgesic effect of intraarticular morphine after arthroscopic knee surgery. *N Engl J Med* ., *325*(16), 1123-6.

Stein, C., & Küchler, S. (2013). Targeting inflammation and wound healing by opioids. *Trends in Pharmacological Sciences*, *34*(6), 303-312.

Stevens, F. (2017). Uses and Doses of Local Anesthetics in Fish, Amphibians, and Reptiles. *J Am Assoc Laboratory Animal Sci Jaalas*.

Stiermaier, T., Schaefer, P., Meyer-Saraei, R., Saad, M., de Waha-Thiele, S., Pöss, J., Fuernau, G., Graf, T., Kurz, T., Frydrychowicz, A., Barkhausen, J., Desch, S., Thiele, H., & Eitel, I. (2021). Impact of Morphine Treatment With and Without Metoclopramide Coadministration on Myocardial and Microvascular Injury in Acute Myocardial Infarction: Insights From the Randomized MonAMI Trial. *Journal of the American Heart Association logo*, *10*(9).

Streef, T. J., & Smits, A. M. (2021). Epicardial Contribution to the Developing and Injured Heart: Exploring the Cellular Composition of the Epicardium. *Frontiers in Cardiovascular Medicine*.

Stuart, T., Butler, A., Hoffman, P., Stoeckius, M., Smibert, P., & Satija, R. (2019). Comprehensive Integration of Single-Cell Data. *Cell*, *177*(7), 1888-1902.

Talman, V., & Ruskoaho, H. (2016). Cardiac fibrosis in myocardial infarction—from repair and remodeling to regeneration. *Cell and Tissue Research*, (365), 563–581. Retrieved 01 19, 2022, from https://link.springer.com/article/10.1007/s00441-016-2431-9#citeas

Talman, V., & Ruskoaho, H. (2016). Cardiac fibrosis in myocardial infarction—from repair and remodeling to regeneration. *Cell and Tissue Research*, *365*, 563–581.

Taylor, J. C., Dewberry, L. S., & Sorge, R. E. (2017). A novel zebrafish-based model of nociception. *Physiology & Behavior*, *174*, 83-88.

Taylor, K. L., Grant, N. J., Temperley, N. D., & Patton, E. E. (2010). Small molecule screening in zebrafish: an in vivo approach to identifying new chemical tools and drug leads. *Cell Communication and Signaling*, *8*.

Thatcher, J. E., & Isoherranen, N. (2009). The role of CYP26 enzymes in retinoic acid clearance. *Expert Opinion on Drug Metabolism & Toxicology*, *5*(8), 875-886.

Thomas, M., Malmcrona, R., Fillmore, S., & Shillingford, J. (1965). Haemodynamic effects of morphine in patients with acute myocardial infarction. *British heart journal.*, *27*(6), 863-75.

Thompson, R. P., Abercrombie, V., & Wong, M. (1987). Morphogenesis of the truncus arteriosus of the chick embryo heart: Movements of autoradiographic tattoos during septation. *Anatom. Rec.*, *218*, 434–440.

Tilley, C. A., Carreño Gutierrez, H., Sebire, M., Obasaju, O., Reichmann, F., Katsiadaki, I., Barber, I., & Norton, W. H. J. (2020). Skin swabbing is a refined technique to collect DNA from model fish species. *Scientific Reports*, *10*.

Timmis, A. D., Rothman, M. T., Henderson, M. A., Geal, P. W., & Chamberlain, D. A. (1980). Haemodynamic effects of intravenous morphine in patients with acute myocardial infarction complicated by severe left ventricular failure. *British Medical Journal*, *280*(6219), 980-2.

Tombor, L. S., John, D., Glaser, S. F., Luxan, G., Forte, E., & Furtado, M. (2021). Single cell sequencing reveals endothelial plasticity with transient mesenchymal activation after myocardial infarction. *Nature Communications*, *12*(681).

Tseng, A.-S., Engel, F. B., & Keating, M. T. (2006). The GSK-3 inhibitor BIO promotes proliferation in mammalian cardiomyocytes. *Chem Biol .*, *13*(9), 957-63.

Tudorache, C., Slabbekoorn, H., Robbers, Y., Hin, E., Meijer, J. H., Spaink, H. P., & Schaaf, M. J. M. (2018). Biological clock function is linked to proactive and reactive personality types. *BMC Biology*, *16*.

UniProt. (2008). *cxcl19 - Chemokine (CXC motif) ligand 19 - Danio rerio (Zebrafish) - cxcl19 gene & protein*. UniProt. Retrieved 03 1, 2022, from https://www.uniprot.org/uniprot/A9ZPF1

Van de Werf, F., Bax, J., Betriu, A., Blomstrom-Lundqvist, C., Crea, F., Falk, V., Filippatos, G., Fox, K., Halvorsen, S., Kaufmann, P., Kornowski, R., Lip, G. Y. H., & Rutten, F. (2008). Management of acute myocardial infarction in patients presenting with persistent ST-segment elevation: The Task Force on the management of ST-segment elevation acute myocardial infarction of the European Society of Cardiology. *European Heart Journal*, *29*(23), 2909–2945.

Vihtelic, T. S., & Hyde, D. R. (2000). *Light-induced rod and cone cell death and regeneration in the adult albino zebrafish (Danio rerio) retina*. PubMed. Retrieved January 31, 2022, from https://pubmed.ncbi.nlm.nih.gov/10942883/

von Krogh, K., Higgins, J., Torres, Y. S., & Mocho, J.-P. (2021). Screening of Anaesthetics in Adult Zebrafish (Danio rerio) for the Induction of Euthanasia by Overdose. *Biology (Basel) .*, *10*(11), 1133.

Walker, C. J., Schroeder, M. E., Aguado, B. A., Anseth, K. S., & Leinwand, L. A. (2021). Matters of the heart: Cellular sex differences. *Journal of Molecular and Cellular Cardiology*, *160*, 42-55.

Walsh, S., Pontén, A., Fleischmann, B. K., & Jovinge, S. (2010). Cardiomyocyte cell cycle control and growth estimation in vivo-An analysis based on cardiomyocyte nuclei. *Cardiovasc. Res.*, *86*, 365–373.

Wang, J., Karra, R., Dickson, A. L., & Poss, K. D. (2013). Fibronectin is deposited by injury-activated epicardial cells and is necessary for zebrafish heart regeneration. *Dev Biol .*, *382*(2), 427-35.

Wang, J., Panáková, D., Kikuchi, K., Holdway, J. E., Gemberling, M., Burris, J. S., Singh, S. P., Dickson, A. L., Lin, Y.-F., Sabeh, M. K., Werdich, A. A., Yelon, D., Macrae, C. A., & Poss, K. D. (2011). The regenerative capacity of zebrafish reverses cardiac failure caused by genetic cardiomyocyte depletion. *Development*, *138*(16), 3421-30.

Wang, T.-L., Chang, H., Hung, C.-R., & Tseng, Y.-Z. (1998). Morphine preconditioning attenuates neutrophil activation in rat models of myocardial infarction. *Cardiovascular Research*, *40*, 557–563.

Wang, X., Loram, L. C., Ramos, K., de Jesus, A. J., Thomas, J., Cheng, K., Reddy, A., Somogyi, A. A., Hutchinson, M. R., Watkins, L. R., & Yin, H. (2012). Morphine activates neuroinflammation in a manner parallel to endotoxin. *PNAS*, *109*(16).

Wehner, D., Tsarouchas, T. M., Michael, A., Haase, C., Weidinger, G., Reimer, M. M., Becker, T., & Becker, C. G. (2017). Wnt signaling controls pro-regenerative Collagen XII in functional spinal cord regeneration in zebrafish. *Nature communications*, *8*(1), 126.

White, J. A., Boffa, M. B., Jones, B., & Petkovich, M. (1994). A zebrafish retinoic acid receptor expressed in the regenerating caudal fin. *Development*, *120*(7), 1861-72.

WHO, 2017. (2017). *Cardiovascular diseases*. WHO | World Health Organization. Retrieved January 19, 2022, from https://www.who.int/health-topics/cardiovascular-diseases#tab=tab_1

Wu, C.-C., Kruse, F., Dalvoy Vasudevarao, M., Junker, J. P., Weidinger, G., & Bakkers, J. (2016). Spatially Resolved Genome-wide Transcriptional Profiling Identifies BMP Signaling as Essential Regulator of Zebrafish Cardiomyocyte Regeneration. *Developmental Cell*, *36*(1), 36-49.

Xiao, J., & Rosenzweig, A. (2021). *Exercise and cardiovascular protection: Update and future*. Science Direct.

Xie, S., Fu, W., Yu, G., Hu, X., Zeng, C., Wang, W. E., & Zhong, T. P. (2020). Discovering small molecules as Wnt inhibitors that promote heart regeneration and injury repair. *J Mol Cell Biol .*, *12*(1), 42-54.

Yamada, S., & Nomura, S. (2020). Review of Single-Cell RNA Sequencing in the Heart. *Int J Mol Sci.*, *21*(21).

Yao, Y., & Wang, C. (2020). Dedifferentiation: inspiration for devising engineering strategies for regenerative medicine. *npj Regenerative Medicine*, *5*.

Yin, V. P., Lepilina, A., Smith, A., & Poss, K. D. (2012). Regulation of zebrafish heart regeneration by miR-133. *Developmental Biology*, *365*(2), 319-27.

Young, B., O'Dowd, G., & Woodford, P. (2014). *Wheater's Functional Histology: A Text and Colour Atlas*. Churchill Livingston/Elsevier.

Young, R. F. (1977). Fiber spectrum of the trigeminal sensory root of frog, cat and man determined by electron microscopy. *In Pain in the Trigeminal Region, Elsevier*, 137-160.

yourgenome. (2021, July 21). *Why use the zebrafish in research? | Facts | yourgenome.org*. YourGenome. Retrieved April 8, 2022, from https://www.yourgenome.org/facts/why-use-the-zebrafish-in-research

Zak, R. (1973). Cell proliferation during cardiac growth. *Am. J. Cardiol.*, *31*, 211–219.

Zeisberg, E. M., Tarnavski, O., Zeisberg, M., Dorfman, A. L., McMullen, J. R., & Gustafsson, E. (2007). Endothelial-to-mesenchymal transition contributes to cardiac fibrosis. *Nat. Med.*, *13*, 952–961.

Zelarayán, L. C., Noack, C., Sekkali, B., Balligand, J.-L., & Bergmann, M. W. (2008). β-Catenin downregulation attenuates ischemic cardiac remodeling through enhanced resident precursor cell differentiation. *Proc Natl Acad Sci U S A*, *150*(50), 19762–19767.

Zhang, J.-J., Wang, X., & Liu, D. (2017). Natriuretic peptide precursor C coding gene contributes to zebrafish angiogenesis. *Acta physiologica Sinica*, *69*(1), 11-16.

Zhang, R., Han, P., Yang, H., Ouyang, K., Lee, D., Lin, Y.-F., Ocorr, K., Kang, G., Chen, J., Stainier, D. Y. R., Yelon, D., & Chi, N. C. (2013). In vivo cardiac reprogramming contributes to zebrafish heart regeneration. *Nature*, *27;498*((7455)), 497-501.

Zhang, W., Liang, J., & Han, P. (2021). Cardiac cell type-specific responses to injury and contributions to heart regeneration. *Cell Regeneration*, *10*(4).

Zhao, L., Ben-Yair, R., Burns, C. E., & Burns, C. G. (2019). Endocardial Notch Signaling Promotes Cardiomyocyte Proliferation in the Regenerating Zebrafish Heart through Wnt Pathway Antagonism. *Cell Reports*, *26*(3), 546-554.

Zheng, L., Du, J., Wang, Z., Zhou, Q., Zhu, X., & Xiong, J.-W. (2021). Molecular regulation of myocardial proliferation and regeneration. *Cell regeneration*, *10*(13).

Zhou, Q., Li, L., Zhao, B., & Guan, K.-L. (2016). The Hippo pathway in heart development, regeneration, and diseases. *Circ Res*, *116*(8), 1431–1447.

Zhu, X., Geng, Z., Han, X., & Xin, X. (2020). Morphine pretreatment reduces myocardial ischemiareperfusion injury in heart failure rats via GSK-3β/Cx43 signaling proteins and apoptosis-related gene, Bcl-2/Bax. *Tropical Journal of Pharmaceutical Research*, *19*(6), 1173-1178.

9. Appendix

Table 13: Library statistics of scRNA-seq data in the project - cellular drivers of heart repair.

Library name	Days post injury (dpi)	Average nUMI per cell	Average nGene per cell	Number of cells	Atrium/Ventricle	10x Chemistry	Wnt-inhibition
H5	0	4053	813	2095	Whole heart	V2	none
H6	0	2512	617	3444	Whole heart	V2	none
H7	0	3226	680	8526	Whole heart	V2	none
H8a	0	2286	608	5245	Atrium	V2	none
H8v	0	2812	682	3728	Ventricle	V2	none
Hr1	0	4035	837	13027	Whole heart	V2	none
Hr2a	0	3247	725	10832	Whole heart	V2	none
Hr2b	0	3347	730	11183	Whole heart	V2	none
Hr3	30	3991	793	8575	Whole heart	V2	none
Hr4	30	3313	731	7367	Whole heart	V2	none
Hr6a	7	4656	938	2851	Atrium	V2	none
Hr6v	7	4145	897	7854	Ventricle	V2	none
Hr7a	7	3159	730	4332	Atrium	V2	none
Hr7v	7	3411	783	5511	Ventricle	V2	none
Hr8	7	2934	830	5604	Whole heart	V2	none

Hr9	7	4361	993	8829	Whole heart	V2	none
Hr10	3	1985	608	10063	Whole heart	V2	none
Hr11	3	1019	347	9887	Whole heart	V2	none
Hr12	3	3044	676	6869	Whole heart	V2	none
Hr13	7	1737	534	3835	Whole heart	V2	none
Hr14	7	2035	518	5449	Whole heart	V2	none
Hr15	7	1319	432	5207	Whole heart	V2	none
Hr19	30	2061	546	414	Whole heart	V2	none
Hr20	30	1910	533	419	Whole heart	V2	none
Hr21	30	2128	556	457	Whole heart	V2	none
Hr22	3	6364	1279	2140	Whole heart	V3	none
Hr23	3	6942	1343	2689	Whole heart	V3	none
Hr24	3	5894	1092	4560	Whole heart	V3	none
Hr25	3	6164	979	1140	Whole heart	V3	none
Hr26	3	6873	1208	8150	Whole heart	V3	none
Hr27	3	6119	1132	5861	Whole heart	V3	none
Hr28	3	5619	1038	3739	Whole heart	V3	DMSO
Hr29	3	5101	922	1829	Whole heart	V3	IWR-1
Hr30	7	4703	972	3345	Whole heart	V3	DMSO

Hr31	7	4680	693	1768	Whole heart	V3	IWR-1
Hr32	7	6394	1169	1422	Whole heart	V3	IWR-1
Hr33	7	5695	1057	1145	Whole heart	V3	IWR-1
Hr34	3	8753	1571	5639	Whole heart	V3	IWR-1
Hr35	3	8475	1625	7225	Whole heart	V3	IWR-1

Table 14: All cell types present in zebrafish heart.

	B-cells	Endothelial cells (apnln)	Endothelial cells (lyve1)	Endothelial cells (plvapb)	Cardiomyocytes (dediff.)	Cardiomyocytes (Atrium)	Cardiomyocytes (Ventricle)	Endocardium (Atrium)	Endocardium (frzb)
1	ighv1-4	hbegfb	cxcl12a	wu:fj16a03	nppa	tnnc1b	tnni4a	zgc:158343	vwf
2	CU571382.1	admb	CU929150.1	cxcl12b	nppb	myh6	CR926459.1	spock3	si:ch211-153b23.5
3	igic1s1	apln	thy1	rbp2a	hsp90aa1.1	si:ch211-270g19.5	fabp3	im:7152348	c2cd4a
4	si:dkey-234i14.9	si:ch211-195b11.3	lyve1a	plvapb	ttn.2	tcap	myl7	ptgs2a	edn2
5	CU896602.1	sele	selenop	cldn5b	ttn.1	tnni1b	ak1	ptgs2b	cfd
6	zgc:153659	itga2b	cdh6	rgcc	myh6	aldoab	cmlc1	id2b	frzb
7	igl3v5	thbs1b	si:dkey-203a12.9	fabp11a	atp2a2a	tnnt2a	actc1a	vcam1b	ecscr

8	zgc:194275	fgl2a	lyve1b	id1	xirp1	smtnl1	acta1b	aqp8a.1	glulb
9	CR318588.1	FO681357.1	id1	tmsb1	si:ch211-131k2.3	cmlc1	myh7l	mycb	efemp2b
10	mgst3b	pim2	si:ch211-105c13.3	ldb2a	hspb11	gapdh	ndufa4	her6	calm1a
11	ccr9a	gp1bb	arl4aa	tcima	her4.1	tnnc1a	gapdh	krt18	cyr61
12	BX571825.5	cldn5b	si:ch211-152c2.3	cavin1b	mybpc3	nppa	ckma	grb10a	nr4a2b
13	cxcr4b	gcnt4a	hapln3	rgs5b	lmo7a	ddx54	eno3	clic2	cpamd8
14	ccl35.1	il11b	stab1	hopx	si:ch211-270g19.5	ckma	tnnt2a	si:ch211-248e11.2	nr4a1
15	CR936442.1	si:ch211-105j21.9	loxl1	cdh5	unc45b	zgc:101840	atp5pd	gpr182	cdh5
16	cxcr4a	tln1	ramp2	kdrl	tcap	mybphb	cox5b2	klf2a	s100v2
17	si:busm1-266f07.2	si:ch211-214p13.9	etv2	scarb2a	ryr2b	myl7	cox7a1	cxcl18b	appa
18	grap2b	f5	hsd3b7	gig2j	tnnc1b	tpm4a	aldoaa	fosl1a	cyr61l2
19	rgs13	si:ch211-214p16.2	ctsla	bcl6b	synpo2lb	actc1a	tnnc1a	tmem88b	hbegfa
20	cd74b	si:ch211-153b23.5	rgcc	bsg	ldb3a	acta1b	tnni1b	dusp5	si:ch211-248e11.2
21	CT573342.2	si:ch211-214p16.1	akap12a	podxl	pla1a	idh2	tpm4a	glulb	entpd8
22	CT573231.1	rap1b	tppp3	mcamb	sorbs1	cox5b2	cox4i1l	si:ch73-335l21.4	her9

23	si:dkey-24p1.1	blf	tcima	pdgfbb	bves	mpc1	mdh2	akap12b	klf2a
24	cd74a	Sep-12	ch25h	jam2a	flnca	mdh2	ppdpfa	ctsla	ptmaa
25	b2m	myh9a	fabp11a	ecscr	ACTC1	uqcrfs1	mustn1b	fosb	ptgs2a
26	dapp1	fam212ab	CR762483.1	si:dkey-126g1.9	slc8a1a	mdh1aa	atp5mc1	ackr4b	krt15
27	zgc:171713	plek	plvapb	krt18	ndrg4	ldhba	idh2	igf2b	ehd2b
28	tspan2a	lpp	sox7	ptprb	trdn	ak1	nme2b.2	bzw1b	crip2
29	BX005450.1	srgn	gstt1b	epas1b	myh7l	ptp4a3	tbpms2b	si:ch211-153b23.5	spock3
30	si:ch1073-220m6.1	pfn1	pde4ba	si:ch211-156j16.1	pdk2a	nmrk2	pgam2	tmem88a	lmo2
31	ponzr6	hsp70l	lgmn	si:dkey-262k9.2	pabpc4	atp5mc3b	ldb3b	zfp36l1b	junba
32	BX571825.3	hacd3	plk2b	CABZ01030107.1	myom1b	atp5mc1	hspb11	ramp2	s100a10b
33	si:ch211-150o23.2	si:ch211-250g4.3	hyal2b	plvapa	cox7c	calm3a	cox6b1	errfi1a	id2b
34	si:busm1-194e12.11	fermt3b	mrc1b	sox7	hspb8	atp5pd	atp5meb	ponzr1	clec14a
35	ncf1	blvrb	rab11bb	cav1	cited4b	atp5meb	cox6a2	fosab	icn
36	hspbp1	atp2b1a	gpm6ab	ch25h	ATP5MD	atp5f1b	ATP5MD	si:ch211-145b13.6	clic2
37	hspa4a	cbx7a	stab2	plpp3	desma	chchd10	mpc1	btg2	cav1

38	rplp2l	hsp70.1	dab2	col4a1	cox6a2	adprhl1	gamt	junba	gpd1b
39	si:ch211-119e14.1	hsp70.2	myct1a	CABZ01075125.1	zgc:101840	fhl2a	atp5po	cyp2ad2	fosl2
40	cd83	crema	zfp36l1b	gpm6ab	mt-co1	ckbb	atp5mc3b	nppc	tie1
41	blnk	zgc:171686	ponzr1	fgd5a	bag3	atp5mc3a	zgc:193541	lpl	gadd45ba
42	DNAJA4	mpl	flt4	pecam1	TGB1BP2	lmod2b	tpi1b	slc22a31	errfi1a
43	rps17	tpte	clec14a	ca16b	kcnh6a	si:dkey-51e6.1	uqcr10	sat1a.2	BX663503.3
44	dusp2	lmo2	ebf3a.1	gpm6aa	tnni1b	cox5aa	slc25a5	jun	sox7
45	si:ch211-195b13.1	arpc1b	s1pr1	cavin2b	tnnt2a	ndufb10	csrp3	junbb	net1
46	atp11a	grasp	carhsp1	TCIM (1 of many)	laptm4b	mybpc3	atp5if1b	tmem2	ackr4b
47	bcl6a	hsp70.3	fxyd6l	limch1b	smtnl1	zgc:85722	atp5f1d	vwf	serpine1
48	coro1a	myh11a	cldn11a	igfbp1a	aldoab	slc25a3b	atp5f1e	kctd12.2	sult2st3
49	pdcd4b	si:ch211-222l21.1	ms4a17a.8	clec14a	pygmb	atp5if1b	cox7b	spint2	CABZ01030107.1
50	syk	bmp16	igf2a	oaz2a	cox7a1	hbaa1	mdh1aa	pim1	efnb2a

	Endocardium (Ventricle)	Epicardium (Atrium)	Epicardium (Ventricle)	Valve Fibroblasts	Fibroblasts	Macrophages	Monocytes	Myelin cells	Neuronal cells
1	si:ch73-86n18.1	gstm.3	si:ch211-106h4.12	zgc:153704	col1a2	grn1	ccl35.1	scn4ab	vipb
2	aqp8a.1	s100a10a	gstm.3	abi3bpb	mdka	grn2	epdl1	cd59	elavl4
3	spock3	fn1b	krt15	krt4	col1a1a	ccl35.1	si:ch211-214p16.1	mbpa	stmn1b
4	mb	krt15	postnb	angptl7	col1a1b	cd74a	si:busm1-266f07.2	mpz	syt1a
5	fabp11a	mmp2	s100a10a	igfbp5b	col5a1	c1qb	si:ch211-214p16.2	mbpb	tuba1c
6	epas1b	si:ch211-105c13.3	fn1b	cyp26b1	dpt	ctsd	ccl35.2	plp1b	gap43
7	ramp2	krt4	endouc	tnfaip6	fn1b	c1qc	CU459094.3	BX936284.1	snap25a
8	si:ch211-145b13.6	frzb	mmp2	mgp	ccl25b	lygl1	cd74a	anxa13l	stmn2a
9	f8	mmel1	tfa	rspo1	sparc	lgals3bpb	arpc1b	apoeb	sncga
10	her6	anxa2a	krt4	fibinb	clu	si:ch211-147m6.2	cd74b	si:rp71-19m20.1	rtn1b
11	cdh5	ppdpfa	krt94	aif1l	dcn	marco	tmsb1	sncga	mllt11
12	fosab	krt94	frzb	krt91	mfap5	fcer1gl	anxa3b	nrgna	crhbp
13	si:ch211-248e11.2	rbp4	si:ch211-105c13.3	bhmt	postnb	ctss2.2	sftpbb	stmn1b	slc5a7a

14	eppk1	si:ch211-286o17.1	cldnc	gyg1b	c4	mfap4	id2a	itgb4	anxa13l
15	socs3a	anxa1a	tmsb1	si:dkey-4p15.3	fn1a	NPC2 (1 of many)	mpeg1.1	scn1ba	zgc:65894
16	tmem88b	CR318588.3	si:ch211-198c19.3	serpinh1b	col12a1a	si:ch211-147m6.1	mhc2dab	fstl3	stmn2b
17	podxl	dkk3b	adh8a	si:dkey-205h13.1	c6.1	cd74b	cxcr4b	cldnk	ddc
18	cyp1b1	tcf21	si:ch1073-459j12.1	tuft1a	si:ch1073-459j12.1	grna	si:dkey-33i11.9	sox10	chata
19	grb10a	postnb	mdka	f13a1b	htra1b	si:busm1-266f07.2	zgc:92066	CABZ01068367.1	gng3
20	si:ch73-335l21.4	slc29a1b	c6.1	ITGB1BP2	pmp22a	ctss2.1	pfn1	pdgfbb	FO907089.1
21	lpl	tmsb1	anxa2a	crip1	hapln1a	atp6v0ca	hspbp1	si:ch211-286c4.6	phox2a
22	jun	phactr4a	col1a2	carhsp1	ckba	hmox1a	DNAJA4	nanos1	pcsk1nl
23	si:ch211-160j14.3	podxl	podxl	uchl1	col6a3	zgc:174904	si:dkey-27i16.2	entpd3	scg2b
24	spon1b	c6.1	si:ch211-137i24.10	fbln5	gstm.3	si:dkey-5n18.1	stip1	timd4	atp1b2a
25	tmem88a	myh10	col1a1a	krt15	col6a1	ctsba	cxcl11.6	lim2.2	cpe
26	akap12b	tuba1a	spaca4l	rbp5	tnfaip6	rasgef1ba	aif1l	foxd3	nsg2
27	klf2b	f3b	igfbp5b	gch2	tfa	lgmn	hspa4a	acbd7	vip
28	id2b	timp2a	col1a1b	pcolcea	mmp2	c1qa	nr4a3	pou3f1	vgf

29	zgc:64106	tbx18	rbp4	irs2b	f3b	psap	syngr3b	cldn19	npcal4
30	egfl7	endouc	eppk1	cbx7a	rbp4	sqstm1	sqstm1	ugt8	atp1a3a
31	ecscr	cxcl14	sparc	snorc	col5a2a	CR855311.1	zgc:152863	gldn	cplx2
32	tspan4b	ckba	anxa1a	hspb8	CR936442.1	ctsz	rhbdd1	si:ch211-197g15.7	phox2bb
33	fam174b	aldh1a2	dkk3b	rpl22l1	ifitm1	pfn1	hspe1	fabp2	prph
34	kdrl	col6a1	cygb1	thbs1b	sostdc1a	atp6v1g1	BX004816.2	znf536	synpr
35	junba	c1qtnf5	col6a3	ptx3a	anxa2a	si:ch211-212k18.7	pdcd4b	ninj2	map1b
36	ackr4b	hsd11b2	tgm2b	timp4.3	pcolcea	tspan36	zgc:103700	depdc7	maptb
37	zgc:152791	c7a	si:dkey-8k3.2	csrp2	olfml3b	ctsc	chchd2	si:ch211-137a8.4	rab6bb
38	si:dkey-261h17.1	si:ch211-156j16.1	sostdc1a	laptm4b	tmsb2	si:dkey-27i16.2	actb2	tlcd1	tuba2
39	si:dkeyp-97a10.2	id2a	mgp	cebpd	si:ch211-105c13.3	mrc1b	zdhhc18b	elovl1a	syt11a
40	junbb	rn7sk	aldh1a2	crip2	si:ch211-137i24.10	cd9b	psap	si:ch211-234p6.5	chrna3
41	nppc	acvrl1	c4	mmp2	c1qtnf5	zgc:92066	rasgef1ba	col15a1b	stxbp1a
42	slc22a31	spaca4l	crip1	dcn	ppib	ccl34a.4	ctss2.2	egr2b	si:ch73-119p20.1

43	klf6a	mxra8b	zgc:123068	sec61g	si:ch211-106h4.12	tppp	zgc:64051	gpm6ab	ret
44	clic2	mfap5	ppdpfa	rps27.2	col6a2	cotl1	spi1b	fstb	vamp2
45	appa	s100a10b	hsd11b2	tgm2l	mgp	ncf1	zgc:136870	nr4a2b	cplx2l
46	flt1	c4	fn1a	GSTZ1	cxcl12a	cfp	coro1a	dhrs3b	cntnap2a
47	tfpia	lxn	col5a1	matn4	edil3a	laptm5	hspa8	phlda2	sypa
48	ier2b	flnb	col6a1	hmgb3a	dkk3b	coro1a	hsp90aa1.2	calm1a	eef1a1a
49	im:7152348	olfml3b	colec12	MYO1D	si:ch211-198c19.3	si:ch211-194m7.4	wbp2	cd9b	stx1b
50	ccdc187	cav1	si:ch211-286o17.1	fxyd6l	fstl1b	scpep1	ckbb	vwa1	elavl3

	Neutrophils	**Perivascular cells**	**Proliferating cells**	**Smooth muscle cells**	**T-cells**
1	lyz	TCIM (1 of many)	pcna	rgs5a	si:ch211-214p16.1
2	lect2l	cxcl12b	stmn1a	acta2	ccl34b.4
3	BX908782.2	pdgfrb	hmgb2b	TPM1 (1 of many)	ccl36.1
4	npsn	rasl12	DUT	C11orf96	ccl38.6
5	si:ch211-117m20.5	BX901920.1	sumo3b	tagln	DNAJA4
6	mmp13a.1	kcne4	rrm2.1	myh11a	ccr9a

7	si:ch211-9d9.1	rgs5b	si:ch211-288g17.3	krt91	CR936442.1
8	scpp8	rgs4	rpa3	itih1	cxcr4b
9	si:ch1073-67j19.1	agtr2	banf1	myl6	hspbp1
10	mmp9	TPM1 (1 of many)	rpa2	myl9a	zgc:64051
11	pnp5a	si:ch211-198c19.3	lig1	BX663503.3	rgs13
12	mpx	ifitm1	fen1	vim	pfn1
13	ncf1	fxyd6l	sfrp5	si:dkey-164f24.2	nkl.1
14	fcer1gl	slc20a1a	dnajc9	ctgfa	pdcd4b
15	pfn1	calm2b	rbbp4	lmod1b	hspa4a
16	scinlb	notch3	tyms	flna	sla2
17	cfl1l	cd248a	rrm1	cfd	cebpb
18	cotl1	tagln	top2a	tpm2	cyb5a
19	plekhf1	si:ch73-193i22.1	nutf2l	si:busm1-57f23.1	coro1a
20	cpa5	col18a1b	cks1b	zgc:77517	stip1
21	illr4	mcamb	hells	mdkb	b2m
22	myh9a	atp1a1b	chaf1a	tns1b	si:dkey-27i16.2
23	adam8a	stk17al	selenoh	si:ch211-1a19.3	si:dkey-109a10.2
24	si:dkey-102g19.3	rgs5a	mki67	mylka	si:ch211-202a12.4

25	lta4h	mustn1a	zgc:110540	gch2	chchd2
26	timp2b	myh11a	mcm5	slmapb	hsp90aa1.2
27	il6r	pcdh18a	mcm6	cyr61	rhbdd1
28	si:ch73-54b5.2	plp1b	ubr7	lpp	cxcr4a
29	cfbl	fhl3b	si:ch211-156b7.4	dnajb4	tnfb
30	vsir	sh3d21	smc2	CR855337.1	calm1b
31	alox5ap	ccdc3b	si:ch211-66k16.27	fhl1a	tnfrsf9b
32	nccrp1	prx	mcm4	fhl3b	ptprc
33	arg2	snai1a	mcm3	fbln5	si:ch211-105j21.9
34	si:ch211-284o19.8	sparc	rrm2	alcama	dusp2
35	CU499336.2	si:ch211-251b21.1	cdk1	tmsb4x	arpc1b
36	si:ch1073-443f11.2	si:ch211-270g19.5	dek	c2cd4a	sh2d1ab
37	s1pr4	slc7a2	rpa1	htra1a	FP236356.1
38	arpc1b	myo1b	h2afx	phlda2	wasb
39	DNAJA4	jam3a	mcm2	anxa1a	BX120005.1
40	antxr2a	arhgap36	nasp	cav2	capgb
41	si:ch211-136m16.8	AL954322.2	cks2	cst3	si:dkey-262k9.2
42	tmsb1	BX908750.1	gins2	zgc:92162	si:ch211-165d12.4

43	si:ch73-343l4.8	atp1b4	asf1ba	f3a	BX005105.1
44	srgn	en1b	dhfr	sort1a	laptm5
45	zgc:77112	CABZ01068367.1	prim2	cald1b	oser1
46	coro1a	oscp1a.1	rfc5	kng1	mcl1a
47	stip1	ppp1r14aa	rnaseh2a	epas1a	wbp2
48	cd7al	rftn2	chtf8	wfdc2	fkbp4
49	si:ch73-248e21.5	rassf4	si:dkey-6i22.5	tpm4b	scinlb
50	CT030188.1	spdya	dctd	fhl2a	si:dkey-177p2.6

Table 15: Marker genes for fibroblasts subclusters.

	Epicardium (Atrium)	**Epicardium (Ventricle)**	**Fibroblasts (const.)**	**Fibroblasts (cfd)**	**Fibroblasts (col11a1a)**	**Fibroblasts (col12a1a)**	**Fibroblasts (cxcl12a)**	**Fibroblasts (mpeg1.1)**	**Fibroblasts (nppc)**
1	s100a10a	si:ch211-106h4.12	hapln1a	cfd	tnc	col12a1a	adh8a	grn1	nppc
2	CR318588.3	cldnc	myl7	ccl25b	fn1a	serpine1	si:dkey-8k3.2	ccl35.1	si:ch211-248e11.2
3	mmel1	eppk1	cmlc1	si:ch1073-406l10.2	col11a1a	mdka	clu	cd74a	aqp8a.1
4	ppdpfa	tmsb1	fgl2b	sfrp1b	col12a1a	serpinh1b	ccl25b	grn2	nppb

5	gstm.3	podxl	si:ch211-5k11.8	rgs5a	col5a1	mfap2	slco2b1	fcer1gl	serpine1
6	CR318588.1	krt15	hbba1.1	ccl20b	col1a2	postnb	cxcl12a	c1qb	clic2
7	slc29a1b	endouc	NC-002333.4	pcolcea	col1a1b	lgals2a	dhrs3a	c1qc	sele
8	podxl	gstm.3	dpt	clu	timp2b	timp2b	rbp4	cd74b	vwf
9	tmsb1	krt94	mt-nd3	plpp1a	col11a1b	col5a1	c4	lgals3bpb	spock3
10	si:ch211-286o17.1	s100a10a	hbaa1	C11orf96	col1a1a	sparc	selenop	si:ch211-147m6.2	cdh5
11	phactr4a	cavin1b	hbba1	mfap5	tnfaip6	si:busm1-57f23.1	tfa	ctss2.2	zgc:158343
12	myh10	krt91	mfap5	ifitm1	fkbp9	col11a1b	hsd11b2	si:busm1-266f07.2	lepb
13	frzb	adh8a	htra1b	cxcl12a	lrrc17	lum	pcolcea	si:ch211-147m6.1	si:ch211-153b23.5
14	krt94	aldh1a2	CR936442.1	si:dkey-164f24.2	col5a2a	nupr1	bhmt	ctss2.1	ptgs2a
15	CR318588.4	frzb	hbba2	cyp2ad2	vmp1	col1a2	vmo1a	marco	rhoca
16	cav1	krt8	gapdh	cyp1c2	adam8a	CR753876.1	lxn	grna	zfand2a

17	zgc:158404	tmem88b	tnnt2a	lmod1b	col12a1b	col1a1a	dpt	mfap4	ctsla
18	anxa1a	spaca4l	CR753876.1	mylka	pcolce2b	col12a1b	tmem176	zgc:64051	DNAJA4
19	itm2cb	postnb	si:dkey-261h17.1	dpt	zgc:85975	vwa1	rspo3	NPC2 (1 of many)	vmp1
20	tuba1a	cav1	sostdc1a	acta2	asph	DNAJA4	CR855311.1	c1qa	krt18
21	aldh1a2	ppdpfa	si:ch211-137i24.10	ccl19a.1	cthrc1a	ppib	c6.1	zgc:174904	kcne4
22	krt15	sost	NC-002333.17	lum	ckba	fn1a	cemip	coro1a	crlf1a
23	si:ch211-66e2.3	cfl1l	pmp22a	rbp4	tagln	col1a1b	si:ch1073-291c23.2	cxcr4b	tfpia
24	id2a	anxa1a	actc1a	mdkb	mdka	CR936442.1	steap4	si:dkey-5n18.1	fabp11a
25	calm1a	si:ch211-198c19.3	hbaa2	osr1	fkbp7	hspa5	ponzr1	laptm5	hspb8
26	cxcl14	c3a.1	tnnc1a	ponzr1	cygb1	sulf2b	pmp22a	ncf1	edn2
27	zgc:152791	cygb1	phlda2	si:ch1073-459j12.1	efemp2a	edil3a	cpn1.1	rac2	hspa5
28	cavin2b	si:ch211-105c13.3	atf5b	ctgfa	cxcl12a	aebp1	mgst1.2	ptprc	sat1a.2

29	arvcfb	slc43a3b	nppa	mgst1.2	serpinh1a	rgcc	stmn1b	cfp	ramp2
30	tmem98	tmem98	tnni1b	rasl11b	postnb	si:dkey-12l12.1	ntn1a	mrc1b	dusp5
31	si:ch211-105c13.3	gpx1a	tnnc1b	vmo1a	fkbp11	clu	c6	csf3b	errfi1a
32	ecm1b	cemip	ckma	tnfsf12	lgals2a	nid1b	si:ch211-106h4.12	si:dkey-102g19.3	id2b
33	krt4	si:ch211-286o17.1	fam107b	tagln	rcn3	tnfaip6	cxcl18b	mpeg1.1	hspb1
34	mao	zgc:110182	myh7l	c6.1	kdelr2b	col5a2a	stmn1a	tppp	hsp90aa1.2
35	gata5	CR925728.1	acta1b	dcn	ssr3	pcolce2b	aldh9a1a.1	si:ch211-194m7.4	pnp5a
36	tcf21	bnc2		tsc22d3	tuba8l3	zgc:92161	tsc22d3	zgc:153317	tspan36
37	sox6	mmp2		thbs4b	calua	fstl1b	prss23	mafbb	glulb
38	atoh8	cyp2ad3		glula	loxa	col6a1	cebpd	ccl34a.4	egfl7
39	si:ch211-250c4.4	eps8l3b		olfml3b	ddost	snai2	serpinf1	mhc2dab	arl4ab
40	cavin1b	si:ch211-137i24.10		si:busm1-57f23.1	eif5a2	col6a2	soul5	zgc:173915	hspbp1

41	smad6a	efna1b		TPM1 (1 of many)	ssr2	tmsb2	mfap2	pglyrp5	sult2st3
42	gcga	phactr4a		myh11a	tubb5	hsp90b1	thbs3a	si:ch211-102c2.4	si:ch211-160j14.3
43	si:dkey-188i13.7	si:ch211-250c4.4		si:ch211-132p1.3	txn	mxra8a	fabp11a	spi1b	ahsa1b
44	wnt11r	krt4		arl5c	eno1a	ctsk	gchfr	slc2a6	sox7
45	lrrc15	igfbp5b		b2m	rrbp1b	si:dkey-27i16.2	mdkb	ms4a17a.10	atp1b1a
46	tbx18	cotl1		cd74b	cox7a2a	zgc:85975	rgs5b	zgc:103700	hspa4a
47	si:ch211-156j16.1	CR318588.3		saa	hint1	plxdc2	ifitm1	slc7a7	prelid3b
48	frmd8	CR318588.4		zgc:195173	gapdhs	col8a1b	ptgdsb.2	stoml3b	sik1
49	igfbp2a	aldh9a1a.1		tpm2	dad1	dpt		tcirg1b	srgn
50	zgc:110182	scarb2a		si:busm1-266f07.2	p4hb	ckba		sftpbb	fosl2

	Fibroblasts (proliferating)	**Fibroblasts (spock3)**	**Valve Fibroblasts**	**Perivascular cells**
1	ube2c	spock3	zgc:153704	TCIM (1 of many)
2	kpna2	aqp8a.1	abi3bpb	cxcl12b

3	top2a	epas1b	angptl7	TPM1 (1 of many)
4	cdk1	si:ch211-145b13.6	rspo1	BX901920.1
5	mki67	cdh5	cyp26b1	rgs5a
6	pcna	si:ch211-248e11.2	aif1l	rasl12
7	cks1b	grb10a	si:dkey-205h13.1	si:ch211-270g19.5
8	cenpf	vwf	igfbp5b	myh11a
9	col11a1a	zgc:64106	si:ch211-131k2.3	rgs4
10	stmn1a	ecscr	f13a1b	agtr2
11	DUT	fam174b	gyg1b	pdgfrb
12	mad2l1	egfl7	gch2	kcne4
13	aspm	gpr182	bhmt	fabp11a
14	rrm2.1	clec14a	ITGB1BP2	marcksl1b
15	zgc:194627	f8	krt4	slc20a1a
16	ccnb1	yrk	si:dkey-4p15.3	oaz2a
17	si:ch211-69g19.2	lpl	cbx7a	cd248a
18	cdc20	fli1a	carhsp1	notch3
19	nusap1	id2b	fibinb	mcamb
20	si:ch211-266i6.3	sox7	fbln5	stk17al
21	rpa2	tmem88a	irs2b	si:ch73-193i22.1

22	cks2	mb	snorc	atp1a1b
23	anln	errfi1a	tuft1a	plp1b
24	plk1	fabp11a	nr4a3	pcdh18a
25	tp53inp2	edn2	itih1	mylka
26	tpx2	dll4	nr4a2b	sh3d21
27	marcksb	marcksl1b	hsp90aa1.2	ccdc3b
28	lmnb2	slc22a31	DNAJA4	slc7a2
29	si:dkey-30c15.10	si:ch211-153b23.5	rps27.2	BX908750.1
30	kif23	ackr4b	eef2l2	jam3a
31	cdca8	si:ch73-86n18.1	mcl1a	arhgap36
32	rpa3	nrarpa	csrp2	cdkn1ca
33	birc5a	nr4a1	matn4	atp1b4
34	si:ch211-156b7.4	ramp2	CR855337.1	en1b
35	kif20a	ponzr1	sec61g	ppp1r14aa
36	ccna2	fosab	vcanb	oscp1a.1
37	prdx1	im:7152348	tgm2l	rassf4
38	smc2	appa	pnrc2	sorbs2b
39	aurkb	dusp5	hsp70l	spdya
40	spc24	hsp70l	si:ch211-200p22.4	pkib

41	kif11	fosl1a	si:dkey-19b23.8	ndufa4l2a
42	dek	her6	cyr61l2	ncaldb
43	cenpx	clic2	slc38a4	tagln
44	tyms	vcam1b	MYO1D	prx
45	CABZ01058261.1	fosb	rpl22l1	acta2
46	prc1b	mycb	wwp2	rftn2
47	tacc3	glulb	rsl24d1	calm2b
48	chaf1a	klf2a	si:ch211-152c2.3	rasgef1ba
49	fen1	si:ch73-335l21.4	timp4.3	rbpms2a
50	cenpe	zgc:158343	rps26	atp2a3

Table 16:Cell type counts in the individual sequencing libraries.

Condition	**0 dpi**	**0 dpi**	**0 dpi**	**0 dpi**	**0 dpi**	**0 dpi**	**30 dpi**	**30 dpi**	**7 dpi**
Library	H5	H6	H7	Hr1	Hr2a	Hr2b	Hr3	Hr4	Hr8
B-cells	49	42	80	26	76	78	29	5	20
Bl.ves.EC (apnln)	84	178	46	188	250	303	55	35	53
Bl.ves.EC (lyve1)	6	0	20	111	207	197	34	75	43
Bl.ves.EC (plvapb)	16	18	55	254	120	128	71	139	125
Cardiomyocytes (Atrium)	438	238	1623	667	178	179	218	480	224

Cardiomyocytes (Ventricle)	267	943	1774	1879	1104	1379	1272	1203	763
Cardiomyocytes (proliferating)	3	9	2	5	4	4	0	1	31
Cardiomyocytes (ttn.2)	101	32	471	113	90	93	1250	241	122
Endocardium (Atrium)	230	256	1058	950	1237	1186	1309	1101	450
Endocardium (Ventricle)	195	709	983	1294	943	898	1129	1904	742
Endocardium (frzb)	85	76	169	541	663	678	175	161	225
Epicardium (Atrium)	10	33	81	209	305	330	156	190	141
Epicardium (Ventricle)	17	9	32	323	186	175	68	82	161
Fibroblasts (cfd)	16	22	27	265	282	270	65	65	107
Fibroblasts (col11a1a)	0	0	2	17	6	5	3	17	4
Fibroblasts (col12a1a)	0	1	8	396	97	133	38	10	24
Fibroblasts (const.)	112	178	486	808	516	503	350	312	374
Fibroblasts (cxcl12a)	17	13	44	276	80	89	105	119	79
Fibroblasts (mpeg1.1)	0	0	7	51	35	28	13	9	12
Fibroblasts (nppc)	2	0	4	135	189	196	1	1	13

Fibroblasts (proliferating)	0	0	0	37	11	8	0	1	8
Fibroblasts (spock3)	2	2	7	57	39	46	23	27	10
Macrophages	204	220	407	1601	1336	1336	1013	338	503
Monocytes	28	13	115	37	72	96	33	16	19
Myelin cells	1	5	28	28	34	41	42	7	18
Neuronal cells	0	0	5	7	5	7	7	1	1
Neutrophils	1	36	1	103	73	78	48	18	72
Perivascular cells	3	11	29	151	38	43	27	36	77
Proliferating cells	0	10	3	7	43	32	1	8	81
Smooth muscle cells	150	139	540	2156	1677	1633	617	546	802
T-cells	48	188	393	179	722	776	372	122	167
Valve fibroblasts	10	62	26	146	209	231	47	97	133

Condition	**7 dpi**	**3 dpi**	**3 dpi**	**3 dpi**	**7 dpi**	**7 dpi**	**7 dpi**	**30 dpi**	**30 dpi**
Library	Hr9	Hr10	Hr11	Hr12	Hr13	Hr14	Hr15	Hr19	Hr20
B-cells	20	281	8	18	7	20	0	4	5
Bl.ves.EC (apnln)	185	17	9	47	9	47	8	39	15
Bl.ves.EC (lyve1)	6	51	0	34	5	15	52	1	0

Bl.ves.EC (plvapb)	72	221	113	151	189	126	85	1	11
Cardiomyocytes (Atrium)	520	33	91	145	137	131	53	9	14
Cardiomyocytes (Ventricle)	1400	187	324	630	164	1216	236	91	36
Cardiomyocytes (proliferating)	211	2	1	4	0	1	2	0	0
Cardiomyocytes (ttn.2)	571	118	3852	506	58	321	148	15	14
Endocardium (Atrium)	731	1307	1430	1209	959	927	876	5	17
Endocardium (Ventricle)	103	655	1645	1680	615	1185	1151	40	35
Endocardium (frzb)	145	85	141	195	76	45	133	6	1
Epicardium (Atrium)	112	103	171	149	228	114	108	7	7
Epicardium (Ventricle)	164	142	83	80	75	48	158	5	3
Fibroblasts (cfd)	127	120	3	34	12	18	46	1	0
Fibroblasts (col11a1a)	14	455	0	60	29	2	1	0	0
Fibroblasts (col12a1a)	298	59	58	25	39	42	20	0	0
Fibroblasts (const.)	792	495	1150	237	507	251	329	18	45
Fibroblasts (cxcl12a)	384	3	26	24	57	43	20	4	1
Fibroblasts (mpeg1.1)	29	88	17	7	6	3	7	1	0
Fibroblasts (nppc)	342	0	0	0	0	0	0	0	0

Fibroblasts (proliferating)	5	77	11	8	2	0	1	0	0
Fibroblasts (spock3)	19	27	80	26	28	17	31	1	0
Macrophages	1463	4192	372	576	343	256	458	110	129
Monocytes	103	13	23	2	11	5	4	9	9
Myelin cells	42	43	1	16	2	9	9	1	0
Neuronal cells	7	6	2	1	0	1	0	0	0
Neutrophils	43	99	3	24	4	1	17	0	6
Perivascular cells	135	41	12	29	16	28	8	0	0
Proliferating cells	29	2	8	23	1	3	2	0	0
Smooth muscle cells	449	961	5	754	5	430	1086	3	31
T-cells	217	105	43	109	38	42	83	41	39
Valve fibroblasts	90	75	205	66	213	102	75	2	0

Condition	**3 dpi**	**3 dpi**	**3 dpi**	**3 dpi**	**3 dpi**	**3 dpi, DMSO**	**3 dpi, IWR-1**	**7 dpi, DMSO**	**7 dpi, IWR-1**	**7 dpi, IWR-1**	**7 dpi, IWR-1**	**3 dpi, IWR-1**	**3 dpi, IWR-1**
Library	Hr22	Hr23	Hr24	Hr26	Hr27	Hr28	Hr29	Hr30	Hr31	Hr32	Hr33	Hr34	Hr35
B-cells	5	13	50	67	37	66	44	23	2	2	26	33	196
Bl.ves.EC (apnln)	110	59	119	196	76	142	123	396	114	28	77	211	187

Bl.ves.EC (lyve1)	9	6	10	46	5	19	13	26	7	3	2	24	25
Bl.ves.EC (plvapb)	23	22	128	138	210	58	53	113	49	13	5	71	307
Cardiomyocytes (Atrium)	327	139	62	103	289	142	208	169	138	26	18	201	101
Cardiomyocytes (Ventricle)	227	206	263	558	64	522	77	134	101	120	47	13	71
Cardiomyocytes (proliferating)	0	1	0	5	0	0	0	0	0	0	0	97	35
Cardiomyocytes (ttn.2)	22	35	48	43	137	38	25	28	10	38	14	171	60
Endocardium (Atrium)	16	30	50	249	1328	79	250	63	112	27	56	651	239
Endocardium (Ventricle)	98	193	314	999	726	163	106	126	131	53	43	108	158
Endocardium (frzb)	8	12	32	23	59	42	2	29	25	0	3	51	81
Epicardium (Atrium)	28	16	15	73	345	30	42	45	25	21	24	174	91
Epicardium (Ventricle)	29	22	58	176	29	53	31	131	29	24	60	84	129
Fibroblasts (cfd)	7	0	7	18	3	13	0	21	5	4	0	11	34

Fibroblasts (col11a1a)	7	34	223	271	314	8	8	6	1	1	11	133	323
Fibroblasts (col12a1a)	0	9	57	206	21	17	24	127	2	16	31	68	250
Fibroblasts (const.)	83	77	268	444	142	250	94	475	222	78	113	136	224
Fibroblasts (cxcl12a)	8	3	13	66	11	26	12	28	9	7	15	10	7
Fibroblasts (mpeg1.1)	0	2	30	68	22	9	3	10	2	4	1	15	51
Fibroblasts (nppc)	0	0	4	4	2	1	0	2	0	2	1	4	3
Fibroblasts (proliferating)	2	3	39	102	27	1	3	5	0	3	8	31	119
Fibroblasts (spock3)	0	1	10	15	18	7	3	3	1	2	1	12	14
Macrophages	845	1292	2254	3169	1360	979	574	855	429	563	478	1946	2973
Monocytes	3	53	8	41	35	64	33	22	21	28	6	19	71
Myelin cells	3	8	5	26	19	15	3	19	7	3	1	2	5
Neuronal cells	0	0	0	0	0	0	0	1	1	0	0	0	1

Neutrophils	53	92	105	610	144	55	5	23	7	10	7	112	280
Perivascular cells	0	7	13	59	67	3	4	8	1	4	2	5	19
Proliferating cells	0	0	2	42	8	1	0	1	0	1	0	80	40
Smooth muscle cells	157	109	184	3	1	670	0	339	182	185	4	1049	589
T-cells	66	242	179	208	195	266	87	116	121	154	80	106	482
Valve fibroblasts	3	3	0	52	164	0	0	1	13	0	2	5	23

10. Abbreviations

µg	microgram
µl	microliter
µM	micromole
A	atrium
AMI	acute myocardial infarction
BS	blocking solution
BSA	bovine serum albumin
cDNA	complementary DNA
CM	cardiomyocyte(s)
CRISPR	clustered regularly interspaced short palindromic repeats
CT	cycle threshold
ctl	control
DAPI	4’,6 diamidino-2-phenylindole
DEPC	diethyl pyrocarbonate
DMSO	dimethylsulfoxide
DNA	2-deoxyribonucleic acid
DNase	deoxyribonuclease
dpi	day(s) post injury
FC	fold change
ECM	extracellular matrix
fwd	forward
g	gram(s)
H	hour(s)
hpf	hour(s) post fertilization
hpi	hour(s) post injury
HPI-axis	Hypothalamic Pituitary Adrenal Axis
hsp	heat shock promoter
IA	injury area
Ig	immunoglobulin
KO	knockout
l	litre
M	molar

mg	milligram
MHC	myosin heavy chain
MI	myocardial infarction
min	minute(s)
ml	millilitre
mM	millimolar
mRNA	messenger RNA
MTZ	Metronidazole
myl7	myosin regulatory light chain 7
N/A	not available
NCBI	National Centre for Biotechnology Information
ng	nanogram
NTR	Nitroreductase
PBS	phosphate buffered saline
PCNA	proliferating cell nuclear antigen
PCP	planar cell polarity
PCR	polymerase chain reaction
RNA	ribonucleic acid
scRNA-seq	single-cell RNA sequencing
SD	standard deviation
SEM	standard error of mean
UMAP	Uniform Manifold Approximation and Projection
V	ventricle
vmhc	ventricular myosin heavy chain

11. List of Figures

12. List of Tables

13. Acknowledgements

First of all, I would like to thank my great supervisor Dr. Daniela Panáková for believing in me from the very beginning and giving me the opportunity to join her team. I am grateful for all the years together and all the support I got from her during my PhD. I would like to thank for all the knowledge and expertise she shared with me and that it made me a better and more confident scientist. I hope we will be able to continue working together in the future.

I would like to thank my co-supervisor Prof. Dr. Philipp Junker for the great collaborations we had between our labs and all the support and guidance with my projects. I am also grateful for his optimism, which pushed us through the hard times.

I thank Prof. Dr. Simone Supuler for her interest in my doctoral studies and the supervision at the Freie Universität Berlin. I am thankful for all the guidance during my studies and meetings.

I would like to acknowledge the MDC Fish Facility and MDC Advanced Light Microscopy Facility, for their expert support.

Many thanks to Dr. Bo Hu, Dr. Baastian Spanjaard and Janita Mintcheva, for our successful collaborations and good work.

I would like to thank all my work colleagues for supporting me scientifically but most importantly with their good words and everyday kindness. I would like to thank Dr. Mariana Guedes Simões. Even though practically we did not work together in the lab, we still had a very nice collaboration and I could have always counted on her help with the project. I am grateful to previous and current lab members Laura Bartolini, Nicola V. Müller, Anne Merks, Mai Phan and Motahareh Moghtadaei. Special thanks to Aikaterini Kourpa and Kevin Manuel Mendez Acevedo for many hours of discussions and great atmosphere in the office and all their support.

Many thanks to my family, especially my parents Jerzy and Beata, who gave me the opportunity to study and have always believed in me. I would like to thank my siblings, Dawid, Jakub, Marta and Simon, also my grandparents and my best friend Ania for being my cheerleaders and listening to my boring scientific talks.

In the end I would like to thank the most important person, who was by my side everyday no matter if tears or smiles were there, my husband Peter. I could not imagine doing it without you. You gave me this opportunity, all the help and your heart for which I am most grateful for.

14. Publications

● Sara Lelek*, Mariana Guedes Simões*, Janita Mintcheva, Bo Hu, Ahmed M.A. Alameldeen, Maciej T. Czajkowski, Alexander M. Meyer, Fabienne Ferrara, Claudia Gösele, Jan Philipp Junker, and Daniela Panáková** 2020; **“Morphine alleviates pain after heart cryoinjury in zebrafish without impeding regeneration”**; pre-print on bioRxiv

● Bo Hu ,*, Sara Lelek*, Bastiaan Spanjaard ,*, Hadil El-Sammak, Mariana Guedes Simões, Janita Mintcheva, Hananeh Aliee, Ronny Schäfer, Alexander M. Meyer, Fabian Theis, Didier Y. R. Stainier, Daniela Panáková ,**, Jan Philipp Junker ,** 2021; **“Origin and function of activated fibroblasts states during zebrafish heart regeneration”**; accepted ***Nature Genetics***, pre-print on bioRxiv

● Eric Schoger, Sara Lelek, Daniela Panáková**, Laura Cecilia Zelarayán** 2022; **“Patient-specific cardiac transcriptomes: the future for tailored CRISPR-mediated epigenetic modulation therapies”**; ***Frontiers in Cardiovascular Medicine***

● Anne M. Merks2, Marie Dreher, Sara Lelek, Kevin M. Méndez-Acevedo, Motahareh Moghtadaei, Ahmed M. A. Alameldeen, Séverine Kunz, Alison C. McGarvey, Ronny Schäfer, Jan Philipp Junker, Laura C. Zelarayán-Behrend, and Daniela Panáková,** 2021; **“Vangl2 couples changes in nuclear mechanics to muscle development and heart muscle memory”**; in preparation

*authors contributed equally
**correspondence

15. Abstract and Presentations

● 2019 2nd DZHK Conference on Translational Medicine in Berlin, Germany (poster presentation)
● 2019 Edinfishtech in Edinburgh, Scotland (poster presentation)
● 2019 Cardiovascular Development Meeting in Malaga, Spain (poster presentation)
● 2019 DZHK Retreat in Berlin, Germany (talk, selected from abstract)
● 2019 BSRT Symposium 2019 The Hitchhiker's Guide to Regenerative Therapies (talk, selected from abstract)
● 2020 Zebrafish 2020 Virtual Meeting (poster presentation)
● 2020 Rising from the Ashes: Regeneration at the Single-Cell Level in Berlin, Germany (virtual talk, selected from abstract)
● 2021 CardioAscona Virtual Meeting (virtual poster presentation)
● 2021 International Zebrafish Conference 2021 (virtual talk, selected from abstract)
● 2021 Joint Vascular Biology Meeting in Gottingen, Germany (poster presentation and talk, selected from abstract)
● 2022 Weinstein Cardiovascular Development and Regeneration Conference in Marseilles (talk, selected from abstract), awarded with travel grant